



Ab Razak, Nur Izah (2016) *MicroRNA modulation of aldosterone production in the adrenal gland*. PhD thesis.

<https://theses.gla.ac.uk/7719/>

Copyright and moral rights for this work are retained by the author

A copy can be downloaded for personal non-commercial research or study, without prior permission or charge

This work cannot be reproduced or quoted extensively from without first obtaining permission in writing from the author

The content must not be changed in any way or sold commercially in any format or medium without the formal permission of the author

When referring to this work, full bibliographic details including the author, title, awarding institution and date of the thesis must be given

Enlighten: Theses

<https://theses.gla.ac.uk/>  
[research-enlighten@glasgow.ac.uk](mailto:research-enlighten@glasgow.ac.uk)



# **MicroRNA modulation of aldosterone production in the adrenal gland**

**Nur Izah Ab Razak (MBBS Malaya)**

Thesis submitted for the degree of Doctor of Philosophy to the  
University of Glasgow

Institute of Cardiovascular and Medical Sciences  
College of Medical, Veterinary and Life Sciences  
University of Glasgow

April 2016

© Nur Izah Ab Razak 2016

## Abstract

Hypertension is the major risk factor for coronary disease worldwide. Primary hypertension is idiopathic in origin but is thought to arise from multiple risk factors including genetic, lifestyle and environmental influences. Secondary hypertension has a more definite aetiology; its major single cause is primary aldosteronism (PA), the greatest proportion of which is caused by aldosterone-producing adenoma (APA), where aldosterone is synthesized at high levels by an adenoma of the adrenal gland. There is strong evidence to show that high aldosterone levels cause adverse effects on cardiovascular, cerebrovascular, renal and other systems. Extensive studies have been conducted to analyse the role that regulation of *CYP11B2*, the gene encoding the aldosterone synthase enzyme plays in determining aldosterone production and the development of hypertension. One significant regulatory factor that has only recently emerged is microRNA (miRNA). miRNAs are small non-coding RNAs, synthesized by a series of enzymatic processes, that negatively regulate gene expression at the post-transcriptional level. Detection and manipulation of miRNA is now known to be a viable method in the treatment, prevention and prognosis of certain diseases. The aim of the present study was to identify miRNAs likely to have a role in the regulation of corticosteroid biosynthesis. To achieve this, the miRNA profile of APA and normal human adrenal tissue was compared, as was the H295R adrenocortical cell line model of adrenocortical function, under both basal conditions and following stimulation of aldosterone production. Key differentially-expressed miRNAs were then identified and bioinformatic tools used to identify likely mRNA targets and pathways for these miRNAs, several of which were investigated and validated using in vitro methods. The background to this study is set out in Chapter 1 of this thesis, followed by a description of the major technical methods employed in Chapter 2.

Chapter 3 presents the first of the study results, analysing differences in miRNA profile between APA and normal human adrenal tissue. Microarray was implemented to detect the expression of miRNAs in these two tissue types and several miRNAs were found to vary significantly and consistently between them. Furthermore, members of several miRNA clusters exhibited similar changes in expression pattern between the two tissues e.g. members of cluster miR-29b-1

(miR-29a-3p and miR-29b-3p) and of cluster miR-29b-2 (miR-29b-3p and miR-29c-3p) are downregulated in APA, while members of cluster let-7a-1 (let-7a-5p and let-7d-5p), cluster let-7a-3 (let-7a-5p and let-7b-5p) and cluster miR-134 (miR-134 and miR-382) are upregulated. Further bioinformatic analysis explored the possible biological function of these miRNAs using Ingenuity® Systems Pathway Analysis software. This led to the identification of validated mRNAs already known to be targeted by these miRNAs, as well as the prediction of other mRNAs that are likely targets and which are involved in processes relevant to APA pathology including cholesterol synthesis (*HMGCR*) and corticosteroidogenesis (*CYP11B2*). It was therefore hypothesised that increases in miR-125a-5p or miR-335-5p would reduce *HMGCR* and *CYP11B2* expression.

Chapter 4 describes the characterisation of H295R cells of different strains and sources (H295R Strain 1, 2, 3 and HAC 15). Expression of *CYP11B2* was assessed following application of 3 different stimulants: Angio II, dbcAMP and KCl. The most responsive strain to stimulation was Strain 1 at lower passage numbers. Furthermore, H295R proliferation increased following Angio II stimulation.

In Chapter 5, the hypothesis that increases in miR-125a-5p or miR-335-5p reduces *HMGCR* and *CYP11B2* expression was tested using realtime quantitative RT-PCR and transfection of miRNA mimics and inhibitors into the H295R cell line model of adrenocortical function. In this way, miR-125a-5p and miR-335-5p were shown to downregulate *CYP11B2* and *HMGCR* expression, thereby validating certain of the bioinformatic predictions generated in Chapter 3.

The study of miRNA profile in the H295R cell lines was conducted in Chapter 6, analysing how it changes under conditions that increase aldosterone secretion, including stimulation Angiotensin II, potassium chloride or dibutyryl cAMP (as a substitute for adrenocorticotrophic hormone). miRNA profiling identified 7 miRNAs that are consistently downregulated by all three stimuli relative to basal cells: miR-106a-5p, miR-154-3p, miR-17-5p, miR-196b-5p, miR-19a-3p, miR-20b-5p and miR-766-3p. These miRNAs include those derived from cluster miR-106a-5p/miR-20b-5p and cluster miR-17-5p/miR-19a-3p, each producing a single polycistronic transcript. IPA bioinformatic analysis was again applied to identify experimentally validated and predicted mRNA targets of these miRNAs and the key biological pathways likely to be affected. This predicted several interactions

between miRNAs derived from cluster miR-17-5p/miR-19a-3p and important mRNAs involved in cholesterol biosynthesis: LDLR and ABCA1. These predictions were investigated by in vitro experiment. miR-17-5p/miR-106a-p and miR-20b-5p were found to be consistently downregulated by stimulation of aldosterone biosynthesis. Moreover, miR-766-3p was upregulation throughout. Furthermore, I was able to validate the downregulation of *LDLR* by miR-17 transfection, as predicted by IPA.

In summary, this study identified key miRNAs that are differentially-expressed in vivo in cases of APA or in vitro following stimulation of aldosterone biosynthesis. The many possible biological actions these miRNAs could have were filtered by bioinformatic analysis and selected interactions validated in vitro. While direct actions of these miRNAs on steroidogenic enzymes were identified, cholesterol handling also emerged as an important target and may represent a useful point of intervention in future therapies designed to modulate aldosterone biosynthesis and reduce its harmful effects.

# Table of Contents

ABSTRACT .....	1
PUBLICATIONS .....	14
ACKNOWLEDGEMENTS .....	15
AUTHOR'S DECLARATION .....	17
DEFINITIONS/ABBREVIATIONS .....	18
<b>1 INTRODUCTION.....</b>	<b>24</b>
1.1 HYPERTENSION.....	25
1.2 THE ADRENAL CORTEX.....	27
1.2.1 <i>Structure of the adrenal gland</i> .....	27
1.2.2 <i>The corticosteroids</i> .....	28
1.2.3 <i>Corticosteroid effects and mechanism of action</i> .....	31
<b>1.2.3.1 The steroid receptors: structure function and distribution</b> .....	<b>31</b>
1.3 CHOLESTEROL: ORIGIN AND TRANSPORT .....	38
1.3.1 <i>StAR</i> .....	42
1.3.2 <i>SF-1</i> .....	43
1.3.3 <i>HMGCR</i> .....	43
1.3.4 <i>LDLR</i> .....	44
1.3.5 <i>ABCA1</i> .....	45
1.4 BIOSYNTHESIS OF CORTICOSTEROIDS .....	46
1.4.1 <i>Enzymes</i> .....	46
<b>1.4.1.1 The hydroxysteroid dehydrogenases</b> .....	<b>46</b>
<b>1.4.1.2 The mixed function oxidases</b> .....	<b>47</b>
1.4.2 <i>Control of corticosteroid biosynthesis and secretion</i> .....	52
<b>1.4.2.1 Cortisol</b> .....	<b>52</b>
<b>1.4.2.2 Aldosterone</b> .....	<b>53</b>
<b>1.4.2.3 CYP11B1 and CYP11B2</b> .....	<b>57</b>
1.5 THE ADRENAL CORTEX AND DISEASE .....	60
1.5.1 <i>Adrenal tumours</i> .....	60
<b>1.5.1.1 Aldosterone-producing adenoma (APA)</b> .....	<b>60</b>
<b>1.5.1.2 Gene mutations in APA</b> .....	<b>62</b>
1.6 HYPERTENSION STUDIES.....	66
1.6.1 <i>Monogenic disorders</i> .....	66
1.6.2 <i>Candidate gene analysis</i> .....	68
1.6.3 <i>Linkage analysis</i> .....	68
1.6.4 <i>Genome-wide association studies</i> .....	70
1.7 THE NATURE, SYNTHESIS AND REGULATORY ROLE OF MICRORNA.....	71
1.7.1 <i>microRNA</i> .....	71
1.7.2 <i>miRNA structure</i> .....	71
1.7.3 <i>miRNA biogenesis</i> .....	71
<b>1.7.3.1 In the nucleus</b> .....	<b>72</b>
<b>1.7.3.2 Nucleus-cytoplasm transportation</b> .....	<b>76</b>
<b>1.7.3.3 Cytoplasmic processing</b> .....	<b>76</b>
<b>1.7.3.4 Argonaute Loading</b> .....	<b>77</b>
<b>1.7.3.5 miRNA Target Repression or Destruction</b> .....	<b>78</b>
1.7.4 <i>miRNA Clusters</i> .....	79
1.7.5 <i>miRNA in the Circulation</i> .....	81
1.7.6 <i>miRNA in Adrenal Tumours</i> .....	83
<b>1.7.6.1 miRNA in adrenocortical carcinoma</b> .....	<b>83</b>
<b>1.7.6.2 miRNA in aldosterone regulation and adrenocortical adenoma (ACA)</b> .....	<b>87</b>
1.7.7 <i>miRNA in clinical trials</i> .....	90
<b>1.7.7.1 Miravirsen (miR-122 antagonist) in hepatitis C</b> .....	<b>90</b>
<b>1.7.7.2 MRX-34 (miR-34a mimic) in liver cancer and liver metastases</b> .....	<b>90</b>
1.8 CONCLUSION .....	91
1.9 AIMS.....	92
<b>2 MATERIALS AND METHODS .....</b>	<b>93</b>
2.1 CELL CULTURE.....	94

2.1.1	<i>H295R</i> .....	94
2.1.2	<i>Culturing Technique</i> .....	94
2.1.3	<i>Cryopreservation</i> .....	96
2.1.4	<i>Cell Resuscitation</i> .....	96
2.1.5	<i>Cell Counting</i> .....	96
2.2	STIMULATION OF CELLS.....	97
2.2.1	<i>Angiotensin II (Angio II), 100 nM, Dibutyl-cyclic adenosine monophosphate(dbcAMP), 1mM and Potassium Chloride (KCl), 20mM</i> .....	97
2.3	PRE-MiR™ AND ANTI-MiR™ TRANSFECTION OF CELLS.....	97
2.3.1	<i>Lipofectamine Transfection</i> .....	97
2.3.2	<i>siPORT™ NeoFX Transfection</i> .....	98
2.4	PROLIFERATION ASSAY.....	98
2.4.1	<i>CellTiter 96® Aqueous Non-Radioactive Proliferation Assay Using MTS Promega Assay</i> .....	98
2.4.2	<i>Bromodeoxyuridine Cell Proliferation Assay (BrdU)</i> .....	99
2.5	LYSING CELLS WITH QIAZOL.....	100
2.6	RNA EXTRACTION AND DNASE TREATMENT USING MIRNEASY MINI KIT (QIAGEN, CRAWLEY, UK).....	100
2.7	NUCLEIC ACID QUANTIFICATION.....	101
2.8	AGAROSE GEL ELECTROPHORESIS.....	101
2.9	REVERSE TRANSCRIPTION.....	102
2.10	QUANTITATIVE REAL-TIME POLYMERASE CHAIN REACTION (UNIVERSAL PROBE LIBRARY).....	103
2.11	SYBR GREEN QUANTITATIVE REAL-TIME POLYMERASE CHAIN REACTION.....	104
2.12	ANALYSIS OF QPCR RESULTS.....	105
2.13	MICROARRAY ANALYSIS.....	106
2.14	MIRBASE DATABASE RELEASE 19: AUGUST 2012.....	107
2.15	INGENUITY PATHWAY ANALYSIS (IPA).....	107
2.16	STATISTICAL ANALYSIS.....	108
2.17	ETHICAL BOARD.....	109
<b>3</b>	<b>MICROARRAY ANALYSIS OF MICRORNA IN NORMAL HUMAN ADRENAL (NA) AND ALDOSTERONE-PRODUCING ADENOMA (APA) TISSUES.....</b>	<b>111</b>
3.1	INTRODUCTION.....	112
3.2	AIMS.....	114
3.3	RESULT.....	114
3.3.1	<i>miRNA expression in microarray</i> .....	114
3.3.2	<i>miRNA expression more than 500 Arbitrary Units (AU)</i> .....	116
3.3.3	<i>miRBase analysis of the differentially-expressed miRNAs in NA and APA</i> .....	119
3.3.4	<i>miRNA Clusters Expression in NA and APA Tissues</i> .....	120
3.3.5	<i>Ingenuity® Systems Pathway Analysis (microRNA target Filter)</i> .....	132
3.3.5.1	<b>Experimentally Validated Targets of clustered differentially-expressed miRNAs</b> .....	<b>137</b>
3.3.5.2	<b>HMGCR, a potential miRNA target</b> .....	<b>140</b>
3.4	DISCUSSION.....	146
3.5	CONCLUSION.....	150
<b>4</b>	<b>OPTIMISATION OF H295R CELLS.....</b>	<b>151</b>
4.1	INTRODUCTION.....	152
4.2	AIM.....	152
4.3	RESULTS.....	153
4.3.1	<i>Adrenocortical Cell Characterization</i> .....	153
4.3.1.1	<b>H295R Cell Lines Morphology</b> .....	<b>153</b>
4.3.1.2	<b>CYP11B2 Gene Expression in Angiotensin II Stimulated Cells</b> .....	<b>154</b>
4.3.1.3	<b>Passage number effect to CYP11B2 Gene Expression</b> .....	<b>155</b>
4.3.1.4	<b>CYP11B2 Gene Expression in Angiotensin II dbcAMP and KCl Stimulated Cells</b> .....	<b>156</b>
4.3.1.5	<b>H295R Cell Proliferation in Response to Angiotensin II (100 nM) in MTS and BrdU</b> <b>158</b>	<b>158</b>
4.4	DISCUSSION.....	160
<b>5</b>	<b>VALIDATION OF NA VS APA MICROARRAY STUDY.....</b>	<b>162</b>
5.1	INTRODUCTION.....	163
5.2	AIM.....	163
5.3	RESULT: VALIDATION OF THE MICROARRAY AND BIOINFORMATIC STUDY OF NORMAL ADRENAL VS APA.....	163
5.3.1	<i>miR-125a-5p</i> .....	163

5.3.1.1	miR-125a-5p in Microarray and qRT PCR.....	163
5.3.1.2	miR-125a-5p Expression in Transfected Cells.....	165
5.3.1.3	CYP11B2 Gene Expression in Pre-miR-125a and Anti-miR-125a Transfection .....	166
5.3.1.4	HMGCR Gene Expression in Pre-miR-125a and Anti-miR-125a Transfection.....	168
5.3.2	miR-335-5p.....	169
5.3.2.1	miR-335-5p Expression in Transfected Cells.....	169
5.3.2.2	CYP11B2 Gene Expression in Pre-miR-335 and Anti-miR-335 Transfection .....	170
5.3.2.3	HMGCR Gene Expression in Pre-miR-335 and Anti-miR-335 Transfection.....	171
5.4	DISCUSSION.....	172
5.5	CONCLUSION .....	174
<b>6</b>	<b>ANALYSIS OF MICRORNA IN BASAL, ANGIOTENSIN II-, DBCAMP- AND KCL-STIMULATED H295R CELLS.....</b>	<b>175</b>
6.1	INTRODUCTION.....	176
6.2	AIM .....	177
6.3	MICROARRAY RESULTS.....	177
6.3.1	<i>Differentially Expressed miRNAs in Basal vs Angiotensin II, dbcAMP and KCl; miRBase Annotation.....</i>	<i>181</i>
6.3.2	<i>Consistent miRNAs Expression Throughout the 3 Stimulations (Angio II, dbcAMP and KCl) &amp; The Cluster Involved.....</i>	<i>185</i>
6.4	INGENUITY® SYSTEMS PATHWAY ANALYSIS (MICRORNA TARGET FILTER).....	190
6.5	SYNONYMOUS miRNA, SEED SEQUENCE AND NUMBER OF TARGETED mRNAs (IPA DATABASE). .....	194
6.6	IPA TARGET FILTER ANALYSIS: MRNA TARGETS INVOLVED IN STEROIDOGENESIS, CHOLESTEROL SYNTHESIS AND RELATED PATHWAYS.....	195
6.6.1	CYP11B2, CYP11B1 & CYP17A1 .....	195
6.6.2	HMGCR, ABCA1, LDLR & other related genes.....	195
6.7	IPA TARGET FILTER ANALYSIS: EXPERIMENTALLY-VALIDATED MRNA TARGET BY CLUSTERS. ....	200
6.7.1	Cluster miR-17-5p and miR-19a-3p (Chromosome 13).....	200
6.7.2	Cluster miR-106a-5p and miR-20b-5p (Chromosome X).....	204
6.7.3	IPA Canonical Signalling Involving cluster miR-17-5p/miR-19a-3p. ....	207
6.7.3.1	<b>Genes Targeted by miR-17/ 19 in Aldosterone Signalling in the epithelial cell pathway</b>	<b>207</b>
6.7.3.2	<b>Genes Targeted by miR-17/ 19 in LXR/RXR Activation pathway.....</b>	<b>209</b>
6.7.3.3	<b>Genes Targeted by miR-17/ 19 in t WNT/ <math>\beta</math>-catenin Signalling pathway.....</b>	<b>210</b>
6.7.3.4	<b>Genes Targeted by miR-17/ 19 in Apoptosis Signalling pathway .....</b>	<b>211</b>
6.7.3.5	<b>Genes Targeted by miR-17/ 19 in VEGF Signalling pathway .....</b>	<b>212</b>
6.7.3.6	<b>Genes Targeted by miR-17/ 19 in TGF-<math>\beta</math> Signalling pathway .....</b>	<b>212</b>
6.8	RESULT: VALIDATION OF MICROARRAY AND BIOINFORMATICS STUDY OF miR-17-5P .....	221
6.8.1	miR-17-5p.....	221
6.8.1.1	miR-17-5p in Angio II-Stimulated Cells.....	221
6.8.1.2	miR-17-5p in dbcAMP Stimulated Cells.....	222
6.8.1.3	miR-17-5p in KCl Stimulated Cells.....	223
6.8.2	miR-20b-5p.....	224
6.8.2.1	miR-20b-5p in Angio II Stimulated Cells.....	224
6.8.2.2	miR-20b-5p in dbcAMP Stimulated Cells.....	225
6.8.2.3	miR-20b-5p in KCl Stimulated Cells.....	226
6.8.3	miR-766-3p.....	227
6.8.3.1	miR-766-3p in Angio II Stimulated Cells.....	227
6.8.3.2	miR-766-3p in dbcAMP Stimulated Cells.....	228
6.8.3.3	miR-766-3p in KCl-Stimulated Cells.....	229
6.8.3.4	Validation of other miRNAs in Stimulated H295R Cells.....	230
6.8.3.5	LDLR expression in miR-17 Transfection .....	231
6.9	DISCUSSION.....	232
6.9.1	Microarray.....	232
6.9.2	Validation .....	235
6.10	CONCLUSIONS .....	238
<b>7</b>	<b>GENERAL DISCUSSION.....</b>	<b>239</b>
<b>8</b>	<b>APPENDIX .....</b>	<b>246</b>
	<b>REFERENCES.....</b>	<b>270</b>

## List of Tables

Table 1-1: Adrenal steroid products, their systematic names and their abbreviations. ....	30
Table 1-2: Major differences between Aldosterone Producing Adenoma (APA) and Bilateral Adrenal Hyperplasia (BAH). ACTH: Adrenocorticotrophic Hormone; AVS: A drenal Venous Sampling; PA: Primary Aldosteronism; ZF: Zona Fasciculata; ZG: Zona Reticularis. Modified from (Freel and Connell 2005). ....	61
Table 1-3: Steroidogenic Enzymes that contribute to CAH.....	65
Table 1-4: Summary of Monogenic Loci Associated with BP (Modified from Padmanabhan, Caulfield et al. 2015).....	67
Table 1-5: Selected linkage studies in hypertension .....	69
Table 1-6: Previous studies analysing miRNA expression in ACC and ACA.....	85
Table 1-7: Previous studies analysing miRNA expression in ACC and ACA.....	86
Table 1-8: Previous studies analysing miRNA expression in ACA vs NA. ....	89
Table 2-1: H295R Strains, HAC 15 and their medium specification. ....	95
Table 2-2: Reaction cycle of miScript Reverse-transcription. ....	103
Table 2-3: Taqman reaction components. ....	104
Table 2-4: Reaction cycle of Taqman qRT PCR. ....	104
Table 2-5: SYBR Green reaction components. ....	105
Table 2-6: Reaction cycle of SYBR Green qRT PCR. ....	105
Table 2-7: List of TaqMan Gene Expression Assay .....	110
Table 2-8: List of SYBRGreen miRNA Assay used.....	110
Table 3-1: Synonymous miRNAs expressed in NA (>500 AU) i.e. miRNAs having similar seed sequence and therefore sharing similar mRNA targets (IPA).....	135
Table 3-2: Synonymous miRNAs expressed in APA (>500 AU) i.e. miRNAs having similar seed sequence and therefore sharing similar mRNA targets (IPA).....	136
Table 3-3: Cluster let-7a and let-7b miRNAs share the same experimentally-validated mRNA targets as a result of their synonymous seed sites. ....	138
Table 3-4: Clusters miR-29b-1 and miR-29b-2 miRNAs share the same experimentally-validated mRNA targets as a result of their synonymous seed sites. ....	139
Table 4-1: <i>CYP11B2</i> expression in different strains of H295R cells. ....	157
Table 4-2: <i>CYP11B2</i> expression following stimulation (Angio II, dbcAMP and KCl) of H295R cells (Strain 1).....	157
Table 4-3: <i>CYP11B2</i> expression by passage number in H295R cells (Strain 1). ..	157
Table 5-1: miR-125a-5p expression in Basal vs dbcAMP-stimulated cells (Strain 1). ....	164
Table 5-2: miR-125a-5p expression following precursor-miRNA transfection. ..	165
Table 5-3: miR-125a-5p expression following anti-miRNA transfection. ....	165
Table 5-4: <i>CYP11B2</i> gene expression in H295R cells (Strain 1) transfected with precursor-negative miRNA (Pre-Neg) or precursor-miRNA-125a (Pre-miRNA-125a). ....	166
Table 5-5: <i>CYP11B2</i> gene expression in H295R cells (Strain 1) transfected with <i>CYP11B2</i> anti-negative miRNA (Anti-Neg) or anti-miRNA-125a. ....	167
Table 5-6: <i>HMGCR</i> expression in H295R cells (Strain 1) transfected with precursor-negative miRNA (Pre-Neg) or precursor-miRNA-125a (Pre-miRNA-125a). ....	168
Table 5-7: <i>HMGCR</i> expression in H295R cells (Strain 1) transfected with anti-negative miRNA (Anti-Neg) or anti-miRNA-125a. ....	168
Table 5-8: miR-335-5p expression following precursor-miRNA transfection.....	169
Table 5-9: miR-335-5p expression following anti-miRNA transfection.....	169

Table 5-10: <i>CYP11B2</i> mRNA levels in H295R Strain 1 cells following transfection with precursor-negative miRNA (Pre-Neg) and precursor-miRNA-335 (pre-miR-335).	170
Table 5-11: <i>CYP11B2</i> mRNA levels in H295R Strain 1 cells following transfection with <i>CYP11B2</i> anti-negative miRNA (Anti-Neg) and anti-miRNA-335 (anti-miR-335).	170
Table 5-12: <i>HMGCR</i> mRNA levels in H295R Strain 1 cells following transfection with precursor-negative miRNA (Pre-Neg) and precursor-miRNA-335 (Pre-miR-335).	171
Table 5-13: <i>HMGCR</i> mRNA levels in H295R Strain 1 cells following transfection with <i>HMGCR</i> anti-negative miRNA (Anti-Neg) and anti-miRNA-335 (anti-miR-335).	171
Table 6-1: miRNA expression in Basal vs Angio II-stimulated H295R cells (Strain 1), analysed by realtime qRT-PCR.	221
Table 6-2: miRNA expression in Basal vs dbcAMP-stimulated H295R cells (Strain 1), analysed by realtime qRT-PCR.	222
Table 6-3: miRNA expression in Basal vs KCl-stimulated H295R cells (Strain 1), analysed by realtime qRT-PCR.	223
Table 6-4: miRNA expression in Basal vs Angio II-stimulated H295R cells (Strain 1), analysed by realtime qRT-PCR.	224
Table 6-5: miRNA expression in Basal vs dbcAMP-stimulated H295R cells (Strain 1), analysed by realtime qRT-PCR.	225
Table 6-6: miR-20b-3p levels in Basal vs KCl-stimulated H295R cells (Strain 1), analysed by realtime qRT-PCR.	226
Table 6-7: miRNA levels in Basal vs Angio II-stimulated H295R cells (Strain 1), analysed by realtime qRT-PCR.	227
Table 6-8: miRNA levels in basal vs dbcAMP-stimulated H295R cells (Strain 1), analysed by realtime qRT-PCR.	228
Table 6-9: miRNA levels in Basal vs KCl-stimulated H295R cells (Strain 1), as analysed by realtime qRT-PCR.	229
Table 6-10: miRNA expression in Basal vs Angio II-stimulated cells (Strain 1).	230
Table 6-11: miRNA expression in Basal vs dbcAMP-stimulated cells (Strain 1).	230
Table 6-12: miRNA expression in Basal vs KCl-stimulated cells (Strain 1).	230
Table 6-13: <i>LDLR</i> mRNA levels following pre-miR-17 transfection of H295R cells (Strain 1), analysed by realtime qRT-PCR.	231
Table 6-14: miRNA expression in microarray and qRT PCR.	235
Table 8-1: Highly expressed miRNAs in NA (mir-10a to miR-195).	247
Table 8-2: Highly expressed miRNAs in NA (mir-202* to miR-29c).	248
Table 8-3: Highly expressed miRNAs in NA (mir-30a to miR-376c).	249
Table 8-4: Highly expressed miRNAs in NA (mir-376 to miR-424).	250
Table 8-5: Highly expressed miRNAs in APA (let-7a to let-7d).	251
Table 8-6: Highly expressed miRNAs in APA (miR-103 to miR-149*).	252
Table 8-7: Highly expressed miRNAs in APA (miR-320a to miR-382).	253
Table 8-8: Highly expressed miRNAs in APA (miR-432 to miR-483-5p).	254
Table 8-9: Highly expressed miRNAs in APA (miR-509 to miR-574-5p).	255
Table 8-10: Highly expressed miRNAs in APA (miR-92a to miR-92b).	256
Table 8-11: miRNAs that are differentially expressed in Angio II-stimulated cells (>500 AU).	257
Table 8-12: miRNAs that are differentially expressed in Angio II-stimulated cells (>500 AU).	258
Table 8-13: miRNAs that are differentially expressed in dbcAMP-stimulated cells (>500 AU).	259

Table 8-14: miRNAs that are differentially expressed in dbcAMP-stimulated cells (>500 AU). .....	260
Table 8-15: miRNAs that are differentially expressed in dbcAMP-stimulated cells (>500 AU). .....	261
Table 8-16: miRNAs that are differentially expressed in dbcAMP-stimulated cells (>500 AU). .....	262
Table 8-17: miRNAs that are differentially expressed in dbcAMP-stimulated cells (>500 AU). .....	263
Table 8-18: miRNAs that are differentially expressed in dbcAMP-stimulated cells (>500 AU). .....	264
Table 8-19: miRNAs that are differentially expressed in KCl-stimulated cells (>500 AU). .....	265
Table 8-20: miRNAs that are differentially expressed in KCl-stimulated cells (>500 AU). .....	266
Table 8-21: miRNAs that are differentially expressed in KCl-stimulated cells (>500 AU). .....	267
Table 8-22: miRNAs that are differentially expressed in KCl-stimulated cells (>500 AU). .....	268
Table 8-23: miRNAs that are differentially expressed in KCl-stimulated cells (>500 AU). .....	269

## List of Figures

Figure 1-1: The anatomy of the adrenal gland.....	28
Figure 1-2: The basic carbon structure present in all steroid hormones. ....	29
Figure 1-3: The chemical structures of aldosterone and cortisol. ....	29
Figure 1-4: Chemical structure of cholesterol. ....	31
Figure 1-5: Intracellular action of glucocorticoid from cytoplasm to nucleus....	34
Figure 1-6: Intracellular action of mineralocorticoid (aldosterone) from membrane to cytoplasm into nucleus. ....	37
Figure 1-7: Cholesterol synthesis pathway. ....	38
Figure 1-8: Pathway of cholesterol biosynthesis and its relation with LDLR, HMGCR and CYP11B2. ....	41
Figure 1-9: Mitochondrial and microsomal P450 redox partners. ....	48
Figure 1-10: Chemical structure of steroid hormones in aldosterone and cortisol biosynthesis. Red indicates CYP11B2- and CYP11B1-mediated conversions. ....	50
Figure 1-11: Steroid hormone biosynthesis pathway. Reactions within the yellow dotted line occur in the zona glomerulosa. ....	51
Figure 1-12: The Hypothalamic-Pituitary-Adrenocortical (HPA) Axis. ....	53
Figure 1-13: Regulation of aldosterone biosynthesis under the Renin-Angiotensin- Aldosterone System (RAAS). ....	55
Figure 1-14: Genomic tandem structure of <i>CYP11B2</i> and <i>CYP11B1</i> and the Ideogram of human chromosome 8. ....	58
Figure 1-15 : miRNA stem-loop structure. ....	73
Figure 1-16: miRNA biogenesis from genomic DNA illustration. ....	74
Figure 1-17: Dicer structure. Adapted from (Sawh and Duchaine 2012). ....	77
Figure 1-18: Cell death through apoptosis or necrosis processes. ....	82
Figure 3-1: miRNA-mRNA site base-pairing. Each nucleotide (N) is numbered as 1 to 8 from the 5' end of the miRNA.....	113
Figure 3-2: Scatter plot showing levels of individual miRNAs in stimulated normal adrenal (NA) vs aldosterone-producing adenoma (APA), as analysed by microarray. $R^2=0.8706$ . ....	115
Figure 3-3: Venn diagram showing the number of expressed miRNAs present ( $>500$ AU) in NA and/or APA. ....	116
Figure 3-4: Venn diagram of differentially-expressed miRNAs i.e. those detected in only one tissue type (AU $>500$ in NA or APA) or present in both at significantly different levels (AU $>500$ in APA and NA; $p<0.05$ ). ....	116
Figure 3-5: Microarray data showing the 23 miRNAs consistently expressed at high levels in NA samples relative to APA. ....	117
Figure 3-6: Microarray data showing the 24 miRNAs consistently expressed at high levels in APA samples relative to NA. ....	118
Figure 3-7: miRNA Clusters (NA $>$ APA) detected from microarray analysis. Cluster miR-125a (A), cluster miR-15a (B) and cluster miR-195 (C)). ....	122
Figure 3-8: miRNA Clusters (NA $>$ APA) detected from microarray analysis (Cluster miR-24-1 (A), Cluster miR-24-2 (B), Cluster miR-29b-1 (C) and miR-29b-2 (D)).	123
Figure 3-9: miRNA Clusters (NA $>$ APA) detected from microarray analysis (Cluster miR-30b (A), Cluster miR-30c (B), Cluster miR-376c (C) and miR-379 (D)). ....	124
Figure 3-10: miRNA Clusters (NA $>$ APA) detected from microarray analysis (Cluster miR-424). ....	125
Figure 3-11: miRNA Clusters (APA $>$ NA) detected from microarray analysis (Cluster let-7a-1 (A), Cluster let-7a-2 (B), Cluster let-7a-3 (C) and Cluster let-7c (D))..	126
Figure 3-12: miRNA Clusters (APA $>$ NA) detected from microarray analysis (Cluster miR-103ab-1 (A), Cluster miR-103ab-2 (B), Cluster miR-122 and (C) Cluster miR- 134 (D)). ....	127

Figure 3-13: miRNA Clusters (APA>NA) detected from microarray analysis (Cluster miR-34c (A), Cluster miR-451 (B) and Cluster miR-432 (C)).	128
Figure 3-14: miRNA Clusters (APA>NA) detected from microarray analysis (Cluster miR-509-1 (A), Cluster miR-509-2 (B), Cluster miR-92a-1 (C) and Cluster miR-92a-2 (D)).	129
Figure 3-15: Cluster let-7a-1 consists of 6 miRNAs; 2 of the miRNAs are above 500 AU and differentially expressed.	130
Figure 3-16: Cluster let-7a-3 consists of 6 miRNAs; 2 of the miRNAs are above 500 AU and differentially expressed.	130
Figure 3-17: Cluster miR-134 consists of 16 miRNAs. Only 2 miRNAs (miR-134 and miR-382) showed similar pattern of expression and they are above 500 AU in APA.	130
Figure 3-18: Cluster miR-29b-1 consists of 4 miRNAs; 2 of the miRNAs are above 500 AU.	131
Figure 3-19: Cluster miR-29c/29b-2 consists of 4 miRNAs; 2 of the miRNAs are above 500 AU and differentially expressed.	131
Figure 3-20: Summary of differentially-expressed miRNA analysis in NA vs APA, conducted using Ingenuity Pathway Analysis (IPA).	134
Figure 3-21: Microarray expression of miRNAs targeting <i>HMGCR</i> .	141
Figure 3-22: Seven differentially-expressed miRNAs are predicted to target <i>HMGCR</i> .	142
Figure 3-23: miRNAs targeting <i>HMGCR</i> in LXR/ RXR Pathway.	143
Figure 3-24: miRNAs targeting <i>HMGCR</i> in AMPK (Adenosine monophosphate-activated protein kinase) Signalling.	144
Figure 3-25: miR-125a-5p is targeting <i>HMGCR</i> in Mevalonate Pathway and targeting <i>CYP11B2</i> in the Mineralocorticoid Biosynthesis Pathway.	145
Figure 4-1: Morphology of H295R Strain 1, 2, 3 and HAC 15 under compound microscope.	153
Figure 4-2: <i>CYP11B2</i> gene expression of Strain 1 (A), Strain 2 (B), Strain 3 (C) and HAC 15 (D) after Angio II Stimulation (n=6 in each group).	154
Figure 4-3: <i>CYP11B2</i> gene expression of H295R Strain 1 according to passage number, 10 to 20 (n=2 in each group).	155
Figure 4-4: <i>CYP11B2</i> gene expression of H295R Strain 1 after dbcAMP (A) and KCl (B) stimulation (n=6 in each group).	156
Figure 4-5: H295R cell proliferation in response to Angio II stimulation (100nM) in MTS (A) and in BrdU (B).	158
Figure 5-1: A: Microarray expression of miR-125a-5p (n= 3) in NA vs APA tissue. B: Similar reduction in miR-125a-5p observed in H295R cells stimulated with dbcAMP (n=6).	164
Figure 5-2: miR-125a-5p expression in H295R cells following transfection with (A) pre-miR-125a-5p or (B) anti-miR-125a-5p transfection (n=6 in each group).	165
Figure 5-3: Effects on <i>CYP11B2</i> mRNA levels in H295R Strain 1 cells following transfection with pre-miR-125a (A) or anti-miR-125a (B) (n= 3 in each group).	166
Figure 5-4: <i>HMGCR</i> mRNA levels in H295R Strain 1 cells following (A) pre-miR-125a transfection or (B) anti-miR-125a transfection (n=3 in each group).	168
Figure 5-5: miR-335-5p levels in H295R cells following (A) pre-miR-335 transfection or (B) anti-miR-335 transfection (n= 3 in each group).	169
Figure 5-6: <i>CYP11B2</i> mRNA levels in H295R Strain 1 cells following transfection with (A) pre-miR-335 or (B) anti-miR-335 (n= 3 in each group).	170
Figure 5-7: <i>HMGCR</i> levels in H295R Strain 1 cells following transfection with (A) pre-miR-335 or (B) anti-miR-335 transfection (n= 3 in each group).	171

Figure 6-1: Scatter plots showing relative miRNA levels in basal (non-treated cells) vs Angio II-, dbcAMP- and KCl-treated cells, as analysed by microarray..	179
Figure 6-2: Venn Diagram of the number of expressed miRNAs that were detected >500 AU in basal and/or Angio II-stimulated cells (H295R).....	180
Figure 6-3: Venn Diagram of the number expressed miRNAs that were detected >500 AU in basal and/or dbcAMP-stimulated cells (H295R). ....	180
Figure 6-4: Venn Diagram of the number expressed miRNAs that were detected >500 AU in basal and/or KCl-stimulated cells (H295R).....	180
Figure 6-5: Microarray data showing differentially-expressed miRNAs in basal vs Angio II-treated cells (all miRNAs shown have AU>500). ....	182
Figure 6-6: Microarray data showing differentially expressed miRNAs in Basal vs dbcAMP-treated cells (all miRNAs shown have AU>500). ....	183
Figure 6-7: Microarray data showing differentially expressed miRNAs in Basal vs KCl-treated cells (all miRNAs shown have AU>500). ....	184
Figure 6-8: Consistent pattern of miRNA expression in Angio II-stimulated cells relative to basal. ....	186
Figure 6-9: Consistent pattern of miRNA expression in dbcAMP-stimulated cells relative to basal. ....	186
Figure 6-10: Consistent pattern of miRNA expression in KCl-stimulated cells relative to basal. ....	187
Figure 6-11: miRNA Clusters detected from microarray analysis (Cluster miR-106a/ miR-20b). ....	188
Figure 6-12: miRNA Clusters detected from microarray analysis (Cluster miR-30b, Cluster miR-17/ miR-19a). ....	189
Figure 6-13: Summary of differentially expressed miRNA analysis using Ingenuity Pathway Analysis (IPA) for basal vs Angio II-treated cells. ....	191
Figure 6-14: Summary of differentially expressed miRNA analysis using Ingenuity Pathway Analysis (IPA) for basal vs dbcAMP-treated cells.....	192
Figure 6-15: Summary of differentially expressed miRNA analysis using Ingenuity Pathway Analysis (IPA) for basal vs KCl-treated cells. ....	193
Figure 6-16: IPA miRNA target genes for the basal vs Angio II-treated group. ..	197
Figure 6-17: IPA miRNA target genes for the basal vs dbcAMP-treated group...	198
Figure 6-18: IPA miRNA target gene for the basal vs KCl-treated group. ....	199
Figure 6-19: (Left) Microarray expression of mir-17-5p and miR-19a-3p across basal (blue), Angio II (red), dbcAMP (purple) and KCl treatments (green). All exhibit a consistent pattern throughout stimulation. * p<0.05 relative to basal. (Right) the primary miRNA structure of miR-17-5p and miR-19a-3p: yellow box indicates the seed sequence for both miRNA (AAAGUGC for miR-17-5p and GUGCAA for miR-19a-3p). ....	202
Figure 6-20: miR-17-5p, miR-19a-3p and their experimentally-validated targets, derived from miRNA Target Filter Analysis (IPA). ....	203
Figure 6-21:(Left) Microarray expression of mir-17-5p and miR-19a-3p across basal (blue), Angio II (red), dbcAMP (purple) and KCl treatments (green). All exhibit consistent expression throughout stimulation. (Right) the primary miRNA structure of miR-17-5p and miR-19a-3p: the yellow box indicates the seed sequence for both miRNA (AAAGUGC for miR-106a-5p and mir-20b-5p, both share similar seed sequence with miR-17-5p). * p<0.05 relative to basal.....	205
Figure 6-22: miR-106-5p and miR-20b-5p and their experimentally-validated targets, derived from miRNA Target Filter Analysis (IPA). ....	206
Figure 6-23: Aldosterone Signalling in the Epithelial Cellular Pathway. ....	215
Figure 6-24: The LXR/RXR Activation pathway.....	216
Figure 6-25: The WNT/ $\beta$ -catenin Signalling Pathway. ....	217

Figure 6-26: The Apoptosis Signalling pathway. ....	218
Figure 6-27: The VEGF Signalling Pathway.....	219
Figure 6-28: The TGF- $\beta$ Signalling Pathway. ....	220
Figure 6-29: Levels of miR-17-5p as in basal vs. Angio II-stimulated cells, as detected by (A) microarray (n= 3) and (B) realtime qRT-PCR (n= 5). ....	221
Figure 6-30: Microarray expression of miR-17-5p (A) (n= 3) in Basal vs dbcAMP and the validation in qRT PCR (B) (n= 5) in Basal vs dbcAMP stimulated cells. .	222
Figure 6-31: Microarray expression of miR-17-5p (A) (n= 3) and validation by qRT PCR (B) (n= 5) of Basal vs KCl-stimulated cells. ....	223
Figure 6-32: Microarray expression of miR-20b-5p (A) (n= 3) in Basal vs Angio II-treated cells and its validation by qRT PCR (B) (n= 6). ....	224
Figure 6-33: Levels of miR-20b-5p in Basal vs dbcAMP-stimulated H295R cells (Strain 1), as measured by (A) microarray (n= 3) and (B) realtime qRT-PCR (n= 5). ....	225
Figure 6-34: Levels of miR-20b-5p following KCl stimulation of H295R cells (Strain 1) as measured by (A) microarray (n= 3) and (B) qRT-PCR (n= 6). ....	226
Figure 6-35: Levels of miR-766-3p in basal vs Angio II-stimulated H295R cells (Strain 1) measured by (A) microarray (n= 3) and (B) realtime qRT-PCR (n= 5). .	227
Figure 6-36: Levels of miR-766-3p in Basal vs dbcAMP-stimulated H295R cells (Strain 1), as analysed by (A) microarray (n= 3) and (B) realtime qRT-PCR (n= 6). ....	228
Figure 6-37: Levels of miR-766-3p in Basal vs KCl-stimulated H295R cells (Strain 1), as analysed by (A) microarray (n= 3) and (B) realtime RT-PCR (n= 6). ....	229
Figure 6-38: <i>LDLR</i> gene expression of H295R Strain 1 in pre-miR-17 transfection (n= 3). ....	231
Figure 7-1: Consistent miRNA expression in adrenal tissues; NA vs APA (A) and in H295R cell line; basal vs Angio II (B), basal vs dbcAMP (C) and basal vs KCl (D). ....	242

## Publications

### *Abstracts (Posters & Oral Presentation)*

**Nur Izah Ab Razak**, Louise Diver, Samantha Alvarez-Madrado, Stacy Robertson, Martin McBride, Scott MacKenzie, Eleanor Davies.

Role of microRNAs in the Aetiology of Aldosterone-Producing Adenoma. DREAM (Diabetic, Renal, Endocrine & Metabolic Syndrome) Theme meeting, Institute of Cardiovascular & Medical Sciences, University of Glasgow, 17<sup>th</sup> September 2013. Poster Communication.

**Nur Izah Ab Razak**, Louise Diver, Samantha Alvarez-Madrado, Stacy Robertson, Martin McBride, Paul M. Stewart, John M Connell, Scott MacKenzie, Eleanor Davies.

Bioinformatic Analysis of Altered microRNA Production in Normal Adrenal Tissue and Aldosterone-Producing Adenoma. Endocrine Abstracts (2014) Vol. 34. Society for Endocrinology BES 2014. Poster Prize Nominee.

**Nur Izah Ab Razak**, Louise Diver, Samantha Alvarez-Madrado, Stacy Robertson, Martin McBride, Paul M. Stewart, John M Connell, Scott MacKenzie, Eleanor Davies.

Analysis of Differentially-Expressed microRNAs and their Potential Targets in Normal Adrenal Tissue and Aldosterone-Producing Adenoma. European Co-Operation in Science and Technology (COST) network on Aldosterone and Mineralocorticoid Receptor (ADMIRE): 1st European Meeting. 16<sup>th</sup> October 2014. Poster Communication.

**Nur Izah Ab Razak**, Scott MacKenzie, Louise Diver, Martin McBride, Eleanor Davies.

microRNA profiling of H295R cells following stimulation of aldosterone production: a bioinformatic study.

Endocrine Abstracts (2015) Vol. 37.

European Society of Endocrinology. 17th European Congress of Endocrinology. Oral communication.

**Nur Izah Ab Razak**, Scott MacKenzie, Louise Diver, Martin McBride, Eleanor Davies.

Bioinformatic analysis of microRNAs associated with aldosterone secretion. Endocrine Abstracts (2015) Vol. 38.

Society for Endocrinology BES 2015. Poster Communication.

## Acknowledgements

In the name of ALLAH, the Most Beneficent, the Most Compassionate, the Most Merciful. All praises be to ALLAH the Lord of universe and all mankind, I ask ALLAH to bless and bestow peace on Prophet Muhammad (Peace be upon Him), Prophet Jesus (Peace be upon Him), the companions and the messengers, and all who traverse their path.

Firstly, I would like to express my special thanks and gratitude to both of my supervisors, Prof. Eleanor Davies and Dr Scott MacKenzie for their expertise, guidance, and strong consistent support, meticulous ideas and suggestions throughout my PhD journey. I am very fortunate and grateful to have them as my supervisors, for their tremendous patience, solid commitment and I feel honoured to be supervised and mentored by them. I would like to thank Prof. Robert Fraser for the encouragement, knowledge and valuable advice throughout my writing phase. I would also like to express my gratitude to Dr Martin McBride for playing a key role in the IPA training and support. I would like to thank the statistician Dr John McClure, with data analysis in this thesis.

My sincere appreciation goes to University Putra Malaysia (UPM) and Ministry of Education (MOE) Malaysia for the awarded scholarship. To both the previous and current heads of the Human Anatomy Department, Dr Mohamed Aris and Prof. Fauziah, and to the former and current Deans of the Faculty of Medicine & Health Sciences of University Putra Malaysia, Prof. Norlijah and Prof Dato' Abdul Jalil, thank you for the strong support to my career path.

I would also like to thank the members of the group and colleagues in ICAMS: Dr Louise Diver, Dr Samantha Alvarez-Madrazo, Dr Umar, Elaine Friel, Lin Deng, Clare, Duniya and Dr Stacy Robertson, for their endless support, advice, skill and knowledge; without them, this thesis would not be possible. Thanks to officemates Dr Jahad, Dr Chris, Chris, Dr Abdul Aziz, Estrella, Josie, Valters and others, for sharing ups and down throughout this PhD journey. Thanks to the students Joe, Steven, Sarah, Topi, Jennifer and Brogan for allowing me to assist you in your projects and improving my teaching abilities and skills.

To all my friends especially the Doctors & Publication group, the Quranic recitation group in West End/ Southside and the Malaysia-Glasgow Community Society, thanks for the support. Also, to everybody who contributes to this thesis, thank you very much.

I would like to express my exceptional gratitude to my mother (Pn Hjh Zainab), father (Tn Hj Ab Razak) and my mother in law (Datin Hjh Fatonah) for their continuous prayer, infinite love and never ending support throughout my life. To my siblings, Along Nurhayati & Bang Long Kyairul, Adik Muhammad & Fatimah and Adik Fawzul, thanks for the interminable love, encouragement and help. To my nephew and niece, Adam and Aisyah, I love you so much.

Finally, to my significant other, Muhammad Fawwaz, no word to describe how blessed and grateful I am, to have the most wonderful, super supportive and amazing husband, who woke up at 3 in the morning, just to make a cup of coffee for me (and the list goes on). Thank you with all the love, kindness and respect you give to our family. To my children, Abdul Bari and Abdul 'Alim, my love to you both is immeasurable and boundless, you are my strength and the greatest motivation to complete this academic journey. I dedicate this thesis to my children, may this become an inspiration for you in the future.

## **Author's Declaration**

I declare that the work presented in this thesis is, to the best of my knowledge and belief, original and my own work, unless otherwise stated in the text. This work has not been submitted previously for a higher degree. It was carried out under the supervision of Professor Eleanor Davies and Dr Scott MacKenzie in the Institute of Cardiovascular and Medical Sciences, University of Glasgow.

Nur Izah Ab Razak

April 2016

## Definitions/Abbreviations

11 $\beta$ -HSD2	11 $\beta$ -hydroxysteroid dehydrogenase type 2
17 $\beta$ HSD1/3	17 $\beta$ -hydroxysteroid dehydrogenase type 1/3
17-OH-P	17-hydroxyprogesterone
17-OH-PREG	17-hydroxypregnenlone
18-OH-B	18-hydroxycorticosterone
21C	21 carbons
3 $\beta$ -HSD	3 $\beta$ -hydroxysteroid dehydrogenase
3 $\beta$ -HSD2	3 $\beta$ -hydroxysteroid dehydrogenase type 2
3'UTR	3 prime untranslated region
5'UTR	5 prime untranslated region
A	Adenosine
AB	Amyloid B
<i>ABCA1</i>	ATP-Binding Cassette, Sub-Family A (ABC1), Member 1 gene
ACA	Adrenocortical adenoma
ACAT	Acyl-CoA: cholesterol acyltransferase
ACC	Adrenocortical carcinoma
ACE	Angiotensin Converting Enzyme
ACTH	Adrenocorticotrophic Hormone
AD	Alzheimer disease
Adx	Adrenodoxin
A'dione	Androstenedione
Adr	Adrenodoxin
AETIO	Aetiocholanolone
AF-1	Activation function-1
AGO1-4	Argonaute Protein 1-4
AGT	Angiotensinogen gene
AKT	V-Akt Murine Thymoma Viral Oncogene
Aldo	Aldosterone
ANDRO	Androsterone
Angio II	Angiotensin II
APA	Aldosterone-producing adenoma
<i>APAF1</i>	Apoptotic peptidase-activating factor 1 gene
ARE	AU-rich elements
AT1	Angiotensin type 1 receptor
AT2	Angiotensin type 2 receptor
ATP1A1	ATPase, Na <sup>+</sup> /K <sup>+</sup> Transporting, Alpha 1 Polypeptide
ATP2B1	Plasma membrane calcium-transporting ATPase 1 gene
ATP2B3	Plasma membrane calcium-transporting ATPase 3 gene
AU	Arbitrary units
AVP	Arginine vasopressin
AVS	Adrenal venous sampling
BAH	Bilateral adrenal hyperplasia
<i>BCL2</i>	B-Cell CLL/Lymphoma 2 gene
<i>BCL2L12</i>	BCL2-Like 12 (Proline Rich) gene
BMI	Body mass index
BMP	Bone morphogenetic protein
BP	Blood pressure
bp	Base pairs
<i>BRCA1</i>	Breast Cancer 1, Early Onset gene
BrdU	Bromodeoxyuridine
BRIGHT	British Genetics of Hypertension
C	Cytosine

<b>C17</b>	Carbon 17
<b>C19</b>	Carbon 19
<b>C20</b>	Carbon 20
<b>C21</b>	Carbon 21
<b>CAH</b>	Congenital adrenal hyperplasia
<b>cAMK</b>	Ca <sup>2+</sup> / calmodulin-dependent protein kinase
<b>cAMP</b>	Cyclic adenosine monophosphate
<b>CASP2/7</b>	Caspase 2/7, Apoptosis-Related Cysteine Peptidase
<b>CCF</b>	Cosmic Calf Serum
<b>CCND1</b>	Cyclin D1 gene
<b>CDK4/ 6</b>	Cyclin-Dependent Kinase 4/ 6 gene
<b>cDNA</b>	Complementary DNA
<b>CDS</b>	Protein coding sequence
<b>CE</b>	Cholesteryl ester
<b>CHD</b>	Coronary heart disease
<b>CK1</b>	Casein Kinase 1
<b>CpG</b>	Cytosine guanine nucleotides site
<b>CRE</b>	cAMP-response element
<b>CREB</b>	cAMP-response element binding protein
<b>CRH</b>	Corticotrophin-releasing hormone
<b>CT</b>	Computerised tomography
<b>Ct</b>	Cycle threshold
<b>CTNNB1</b>	Catenin (Cadherin-Associated Protein), Beta 1 gene
<b>CVD</b>	Cardiovascular disease
<b>CYB5A</b>	Cytochrome b5 gene
<b>CYP11A1</b>	Cytochrome P450, Family 11, Subfamily A, Polypeptide 1 gene
<b>CYP11B1</b>	11 $\beta$ -hydroxylase gene
<b>CYP11B2</b>	Aldosterone synthase gene
<b>CYP17A1</b>	17 $\alpha$ -hydroxylase/17,20 lyase gene
<b>CYP19A1</b>	Aromatase gene
<b>CYP21A1</b>	21-hydroxylase gene
<b>CYP450</b>	Cytochrome P450 enzymes
<b>DAG</b>	Diacylglycerol
<b>DASH</b>	Dietary approaches to stop hypertension
<b>dbcAMP</b>	Dibutyryl cAMP
<b>DBD</b>	DNA binding domain
<b>DBP</b>	Diastolic blood pressure
<b>DCP1/ 2</b>	Decapping enzyme 1/ 2
<b>DDX6</b>	DEAD (Asp-Glu-Ala-Asp) Box Helicase 6
<b>DGCR8</b>	DiGeorge Syndrome Critical Region in Gene 8
<b>DHA</b>	Dehydroepiandrosterone
<b>DHEA</b>	Dehydroepiandrosterone
<b>DHEAS</b>	Dehydroepiandrosterone sulphate
<b>DMSO</b>	Dimethyl sulphoxide
<b>DNA</b>	Deoxyribonucleic acid
<b>dNTPs</b>	Deoxynucleotide triphosphates
<b>DOC</b>	11-deoxycorticosterone
<b>DPBS</b>	Dulbecco's Phosphate-Buffered Saline
<b>dsDNA</b>	Double-stranded deoxyribonucleic acid
<b>DUF</b>	Domain of unknown function
<b>EDC4</b>	Enhancer of mRNA decapping 4
<b>EDTA</b>	Ethylenediamine tetra-acetic acid
<b>EGFR</b>	Epithelial growth factor receptor
<b>eIF</b>	Eukaryotic initiation factor

<b>ELAVL1</b>	ELAV-like RNA binding protein 1 gene
<b>ENac</b>	Enhance epithelial sodium channel
<b>ERK1/2</b>	Extracellular signal regulated kinase 1/ 2
<b>EH</b>	Essential hypertension
<b>Exp5</b>	Exportin 5
<b>F2</b>	Fusion protein
<b>FAD</b>	Flavin adenine dinucleotide
<b>FDR</b>	False discovery rate
<b>FDX1</b>	Adrenodoxin
<b>FDXR</b>	Adrenodoxin reductase
<b>FFPE</b>	Formalin-fixed paraffin-embedded
<b>FH</b>	Familial hypercholesterolemia
<b>FHht</b>	Familial hyperkalaemic hyprtension
<b>FHA</b>	Familial hypoalphalipoproteinemia
<b>FMN</b>	Flavin monoluceotide
<b>G</b>	Guanine
<b>g</b>	G-force (relative centrifugal force)
<b>G1</b>	Gap 1 phase in cell cycle
<b>GAPDH</b>	Glyceraldehyde-3-Phosphate Dehydrogenase gene
<b>GC</b>	Glucocorticoid
<b>GJA1/ CX43</b>	Gap Junction Protein, Alpha 1
<b>GRA</b>	Glucocorticoid Remediabale Aldosteronism
<b>GR</b>	Glucocorticoid receptor
<b>GRE</b>	Glucocorticoid response elements
<b>GSC</b>	Goosecoid homeobox gene
<b>GW182</b>	Glycine-tryptophan protein of 182 kD
<b>GWAS</b>	Genome-wide association study
<b>HCC</b>	Hepatocellular carcinoma cell
<b>HCV</b>	Hepatitis C virus
<b>HDL</b>	High density lipoprotein
<b>HIF1A</b>	Hypoxia inducible factor 1, alpha subunit gene
<b>HMGCoA</b>	3-hydroxy-3-methylglutaryl-CoA
<b>HMGCR</b>	3-hydroxy-3-methylglutaryl-CoA reductase gene
<b>HSL</b>	Hormone-sensitive lipase
<b>HSP</b>	Heat-shock protein
<b>HRE</b>	Hormone responsive element
<b>HSDIIB2</b>	11 $\beta$ -hydroxysteroid dehydrogenase
<b>ICAM1</b>	Intracellular adhesion molecule 1
<b>ICMT</b>	Isoprenylcysteine carboxyl methyltransferase gene
<b>IGF-1/ 2</b>	Insulin-Like Growth Factor 1/ 2
<b>IGF1R</b>	Insulin-like growth factor 1 receptor
<b>IMM</b>	Inner mitochondrial membrane
<b>IL3/ 6</b>	Interleukin 3/ 6
<b>ITS</b>	Insulin-transferrin-selenium
<b>IUPAC</b>	International Union of Pure and Applied Chemistry
<b>IPA</b>	Ingenuity Pathway Analysis
<b>IP3</b>	Inositol trisphosphate
<b>JNC 6/ 7/ 8</b>	Sixth/ Seventh/ Eighth Joint National Committee Report
<b>K<sup>+</sup></b>	Potassium ions
<b>kb</b>	Kilobases
<b>KCNJ5</b>	Potassium Channel, Inwardly Rectifying Subfamily J, Member 5 gene
<b>kD</b>	KiloDaltons
<b>KLHL3</b>	Kelch-Like Family Member 3

<b>KRAS</b>	Kirsten rat sarcoma viral oncogene homolog gene
<b>LBD</b>	Ligand binding domain
<b>LC:MS/MS</b>	Liquid chromatography tandem mass spectrometry
<b>LD</b>	Linkage disequilibrium
<b>LDL</b>	Low-density lipoprotein
<b>LDLR</b>	Low-density lipoprotein receptor gene
<b>LNA</b>	Locked nucleic acid
<b>LOD</b>	Logarithm of the odds
<b>LXR</b>	Liver X receptor
<b>MAP3K</b>	Mitogen-Activated Protein Kinase Kinase Kinase
<b>MARK2/PAR-1</b>	Microtubule affinity-regulating kinase 2
<b>Mb</b>	Megabases
<b>mCCD</b>	Mouse cortical collecting duct
<b>MCL1</b>	Myeloid Cell Leukaemia 1 gene
<b>MCP1</b>	Monocyte chemoattractant protein 1
<b>MDR/ TAP</b>	Transporter, ATP-Binding Cassette, Sub-Family B
<b>miRISC</b>	miRNA-induced silencing complex
<b>miRNA</b>	Micro ribonucleic acid (microRNA)
<b>ml</b>	Mililitre
<b>mM</b>	Milimolar
<b>MP</b>	Membrane potential
<b>MR</b>	Mineralocorticoid receptor
<b>mRNA</b>	Messenger ribonucleic acid
<b>MRX34</b>	miR-34a mimic
<b>MTDH</b>	Metadherin
<b>mTOR</b>	Mechanistic Target of Rapamycin (Serine/Threonine Kinase)
<b>MVE</b>	Multivesicular endosomes
<b>MYLIP</b>	Myosin regulatory light chain interacting protein (IDOL)
<b>Na<sup>+</sup></b>	Sodium ions
<b>NAD</b>	Nicotinamide adenine dinucleotide
<b>NADPH</b>	Nicotinamide adenine dinucleotide phosphate
<b>NBRE</b>	NGFI-B response element
<b>ncRNA</b>	Non-coding RNA
<b>NE</b>	Nuclear envelope
<b>NF-1</b>	Nuclear-factor 1
<b>NGF</b>	Nerve growth factor
<b>NGFI-B</b>	Neuronal growth factor-induced clone B
<b>NLS</b>	Nuclear localisation signal
<b>nM</b>	NanoMolar
<b>nm</b>	Nanometer
<b>NOR-1</b>	Neuron-derived orphan receptor 1
<b>NPC</b>	Nuclear pore complex
<b>NR3C2</b>	Nuclear receptor subfamily 3 gene (MR gene)
<b>NR3C1</b>	Nuclear receptor subfamily 1 gene (GR gene)
<b>NR4A2/ 3</b>	Nuclear Receptor Subfamily 4, Group A, Member 2/ 3
<b>NURR-1</b>	Nur-related factor 1
<b>OncomiR</b>	Oncogenic miRNA
<b>OMM</b>	Outer mitochondrial membrane
<b>PA</b>	Primary aldosteronism
<b>PABP</b>	Poly A binding protein
<b>PAI1</b>	Plasminogen activator inhibitor type 1
<b>PBS</b>	Phosphate buffered saline
<b>PCR</b>	Polymerase chain reaction
<b>pEZX</b>	Reporter construct
<b>pGL3</b>	Reporter construct

PH	Primary hypertension
PI3K	Phosphoinositide 3-Kinase
PIP2	Phosphatidylinositol 4,5-bisphosphate
PKA	Protein kinase A
PKC	Protein kinase C
PLC	Phospholipase C
<i>PMEPA1/ TMEPAI</i>	Prostate transmembrane protein, androgen induced 1 gene
Pol II	RNA polymerase II
POR	P450 oxidoreductase gene
PPARD	Peroxisome proliferator-activated receptor delta
PREG	Pregnenolone
Pre-miRNA	Precursor miRNA
Pri-miRNA	Primary miRNA
<i>PTK2B</i>	Protein tyrosine kinase 2 beta gene
qRT PCR	Quantitative reverse transcription polymerase chain reaction
QTL	Quantitative Trait Locus
RAAS	Renin-angiotensin-aldosterone system
RAF1	Raf-1 proto-oncogene, serine/threonine kinase
Ran-GTP	Ras-related nuclear protein-guanosine-5'-triphosphate
RAS	Renin-angiotensin system
RISC	RNA-induced silencing complex
RLC	RNA-induced silencing complex (RISC) loading complex
RNA	Ribonucleic acid
RNAi	RNA interference
<i>RNF111</i>	Ring finger protein 111 gene
ROS	Reactive oxygen species
rpm	Revolutions per minute
RQ	Relative quantification
RRM	RNA recognition motif
rRNA	Ribosomal RNA
RT	Reverse transcription
RU-486	Glucocorticoid antagonist
<i>RUNX3</i>	Runx-related transcription factor 3 gene
RXR	Retinoid X Receptor
S	Synthesis phase of cell cycle
S1P/ S2P	SREBP-specific proteases
SBP	Systolic blood pressure
SCC	Cholesterol side-chain cleavage enzyme (Desmolase, CYP11A1)
SEM	Standard error of the mean
<i>SERPINE1/ PAI1</i>	Serpin peptidase inhibitor, clade E (nexin, plasminogen activator inhibitor type 1), member 1 gene
SF-1	Steroidogenic factor 1
<i>SGK1</i>	Serum/glucocorticoid regulated kinase 1 gene
SH	Secondary hypertension
siRNA	Short interfering ribonucleic acid
<i>SKI</i>	SKI Proto-Oncogene gene
<i>SLC9A1</i>	Solute Carrier Family 9, Subfamily A (NHE1, Cation Proton Antiporter 1), Member 1 gene
SNP	Single nucleotide polymorphism
snRNA	Small nuclear RNA
<i>SMAD4</i>	SMAD family member 4 gene
<i>SMURF1</i>	SMAD specific E3 ubiquitin protein ligase 1 gene
srRNA	Small regulatory RNA
SRB1	Scavenger receptor B1

<b>SRE</b>	Sterol regulatory response element
<b>SREBP-1</b>	Sterol regulatory element binding protein 1
<b>StAR</b>	Steroidogenic acute regulatory protein
<b>STAT</b>	Signal transduction and activator of transcription protein
<b>T</b>	Thymine
<b>TASK-1</b>	Potassium channel subfamily K member 3 (KCNK3)
<b>TBE</b>	Tris/Borate/EDTA
<b>TBP</b>	TATA-binding protein
<b>TCF4</b>	Transcription Factor 4 gene
<b>TCF</b>	T cell factor protein
<b>TE</b>	Tris/EDTA
<b>TF</b>	Transcription factor
<b>TGIF1</b>	TGFB-induced factor homeobox 1 gene
<b>TGF-<math>\beta</math></b>	Transforming growth factor-beta
<b>THA</b>	Tetrahydro-11-dehydrocorticosterone
<b>THAldo</b>	Tetrahydroaldosterone
<b>THB</b>	Tetrahydrocorticosterone
<b>THDOC</b>	Tetrahydrodeoxycorticosterone
<b>THE</b>	Tetrahydrocortisone
<b>THF</b>	Tetrahydrocortisol
<b>THS</b>	Tetrahydrodeoxycortisol
<b>T<sub>m</sub></b>	Melting temperature
<b>TNF</b>	Tumour necrosis factor gene
<b>tPA</b>	Tissue plasminogen activator
<b>TRBP</b>	Tar RNA binding protein
<b>tRNA</b>	Transfer RNA
<b>U</b>	Uracil
<b>UPL</b>	Universal ProbeLibrary
<b>UV</b>	Ultraviolet
<b>VCL</b>	Vinculin
<b>VEGF</b>	Vascular endothelial growth factor
<b>VLDLR</b>	Very low density lipoprotein receptor
<b>WHO</b>	World Health Organization
<b>WGS</b>	Whole genome sequencing
<b>WNT1/ 3/ 4</b>	Wingless-Type MMTV Integration Site Family, Member 1/ 3/ 4 gene
<b>WRE</b>	WNT response element
<b>XRN-1/2</b>	5'-3' exoribonuclease 1/2
<b>ZF</b>	Zona fasciculata
<b>ZFYVE9</b>	Zinc finger, FYVE domain containing 9 gene
<b>ZG</b>	Zona glomerulosa
<b>ZR</b>	Zona reticularis

# **1 Introduction**

## 1.1 Hypertension

The blood circulates through the vascular system under an oscillating pressure generated principally by the beating action of the heart and the tone of the resistance artery smooth muscle walls. At diastole, blood pressure is at its lowest (diastolic blood pressure: DBP) and at systole, it is at its highest (systolic blood pressure: SBP). Both DBP and SBP vary between individuals and both tend to increase with age. The higher the blood pressure, the greater the risk of cardiovascular, cerebrovascular and renal damage. Blood pressure high enough to present such a risk is called hypertension. The World Health Organisation reports that hypertension is accountable for up to 60% of cerebrovascular disease and up to 50% of ischaemic heart disease (IHD) and is the number one risk factor for mortality worldwide (WHO 2002). In the United States, the lifetime risk of hypertension is estimated to be 90% in people aged 55-56 years (Chobanian AV 2003).

It is important to emphasise that, within the general population, DBP and SBP are normally distributed. The distinction between normal blood pressure and hypertension is therefore arbitrary. The hypertension classification from the 2014 Evidence-Based Guidelines (Chobanian AV 2003) for the Eighth Joint National Committee Report (JNC 8) (James, Oparil et al. 2014) is shown in Table 1-1.

**Table 1-1: Classification of hypertension based on the JNC 8. JNC 8 is based on previous classification under JNC6 and JNC7.**

JNC 6	SBP/DBP	JNC 7
Optimal	< 120/80	Normal
Normal	120-129/80-84	Pre-hypertension
Borderline	130-139/85-89	
Hypertension	≥ 140/90	Hypertension
Stage 1	140-159/90-99	Stage 1
Stage 2	160-179/100-109	Stage 2
Stage 3	180/110	

While hypertension, the so-called silent killer, is thus readily diagnosed and treated and there now exists a battery of relatively side effect-free treatments

that delay and reduce its destructive effects, only in a very small minority of cases can it be cured due to the identification of a single cause. In the remaining majority, no unequivocal fundamental cause can be found and these are grouped into the category of essential or primary hypertension. However, it is certain that there is a spectrum of contributing causes: partly aspects of lifestyle and partly inherited factors, which interact with each other.

A number of lifestyle factors contribute to increased blood pressure and amplify its effect. One study assessed the impact of diet and macronutrient intake on SBP and DBP (Eckel, Jakicic et al. 2014). The dietary patterns were characterized by a combination of daily food intake with, in particular, high sodium and potassium content (Eckel, Jakicic et al. 2014). Numerous experimental and epidemiological data confirm the advantages of salt restriction on blood pressure (Batuman 2013). The Dietary Approaches to Stop Hypertension (DASH) trial found that decreasing salt intake from 8 g per day to 6 g (intermediate reduction) and 4 g (low reduction) reduced SBP by an average of 11.5 mmHg in hypertensive and 7.1 mmHg in normotensive people (Sacks, Svetkey et al. 2001). A meta-analysis reported that sodium intake of  $\leq 2$ g/day versus  $\geq 2$ g/day significantly reduced SBP by 3.4 mmHg and DBP by 1.5 mm Hg in adults and suggested that most people are likely to benefit from reducing their sodium intake (Aburto, Ziolkovska et al. 2013).

There is good evidence linking physical activity and hypertension (Kokkinos, Manolis et al. 2009, Cornelissen and Smart 2013), cardiovascular disease (CVD) (Myers 2003), type II diabetes mellitus (Kokkinos, Myers et al. 2009) and blood lipids (Krotkiewski, Mandroukas et al. 1979). Overweight women who performed one-hour exercise sessions 3 times per week for 6 months decreased BP (Krotkiewski, Mandroukas et al. 1979). Fitness status and exercise aptitude inversely correlate with mortality risk in healthy people (Kokkinos, Myers et al. 2008) and in subjects with pre-hypertension (Kokkinos, Myers et al. 2009) and hypertension (Kokkinos, Manolis et al. 2009). A moderate increase in exercise capacity may prevent the progression of pre-hypertension to hypertension (Faselis, Doulas et al. 2012).

Obesity associates with elevated blood pressure (Sánchez-Castillo, Velásquez-Monroy et al. 2005, Jensen, Ryan et al. 2014). A 5% weight loss causes reduction

of 3 mmHg in SBP and 2 mmHg in DBP (Jensen, Ryan et al. 2014). Aucott et al reported that a 10 kg weight loss decreases DBP by 4.6 mmHg and SBP by 6 mmHg. However, huge weight loss as a result of surgical intervention makes little difference to blood pressure (Aucott, Poobalan et al. 2005).

A significant proportion of increased blood pressure in essential hypertension is heritable. Data from family and twin studies indicate a heritable component of between 30% and 50% (Miall and Oldham 1963). The search for responsible genes has been intense and a variety of biological systems have been implicated, including those involved in corticosteroid biosynthesis. These will be reviewed in Section 1.4. Several methods, including candidate gene analysis, linkage analysis and genome-wide association study (GWAS) have been employed in the search. These are discussed further in Sections 1.6.2 to 1.6.4.

The adrenal cortex has been convincingly identified as a contributor to the genetic component of essential hypertension. The following sections explain the structure, biosynthesis, control of secretion and mechanism of action of its products with particular reference to aldosterone. The importance of cholesterol metabolism in biosynthesis is emphasised. The implication of corticosteroids in the aetiology of hypertension and heart disease is then reviewed. This includes their role in essential hypertension but also information on the growth and effects of the various types of adrenocortical neoplasms. A major experimental goal is assessment of the importance of miRNA species in the normal function of the gland and in the growth and function of tumours. Finally, it is asked, 'Do miRNAs offer an additional means of therapy for adrenal disorders?'

## **1.2 The adrenal cortex**

### **1.2.1 Structure of the adrenal gland**

The adrenal glands are paired glands located at the apex of each kidney as shown in Figure 1-1a. Each gland is comprised of an inner medulla - the source of catecholamine hormones - and a cortex, which synthesises and secretes the corticosteroids. Each gland is surrounded by a fibrous capsule, is supplied with blood by three arteries; superior suprarenal artery (branching from the inferior

phrenic artery), middle suprarenal artery (branching from the abdominal aorta) and inferior suprarenal artery (branching from the renal artery) and is drained by the suprarenal vein; the right suprarenal vein drains into the inferior vena cava and the left suprarenal vein drains into the left renal vein or the left inferior phrenic vein. The cortex consists of three layers of variable width (Figure 1-1b); they produce different hormones and their activities are controlled independently (see sections 1.4.2). The outermost layer is the zona glomerulosa and its principal product is aldosterone. In man, this zone may not always form a continuous layer; glomerulosa cells are small. Beneath this is the widest zone, the zona fasciculata, the principal product of which is cortisol. Fasciculata cells are typically large and contain lipid vacuoles rich in cholesterol. Innermost, adjacent to the medulla, is the zona reticularis which secretes largely adrenal androgens. Importantly, the adrenocortical blood flow is centripetal so that the zona glomerulosa has no direct humoral contact with the inner zones.

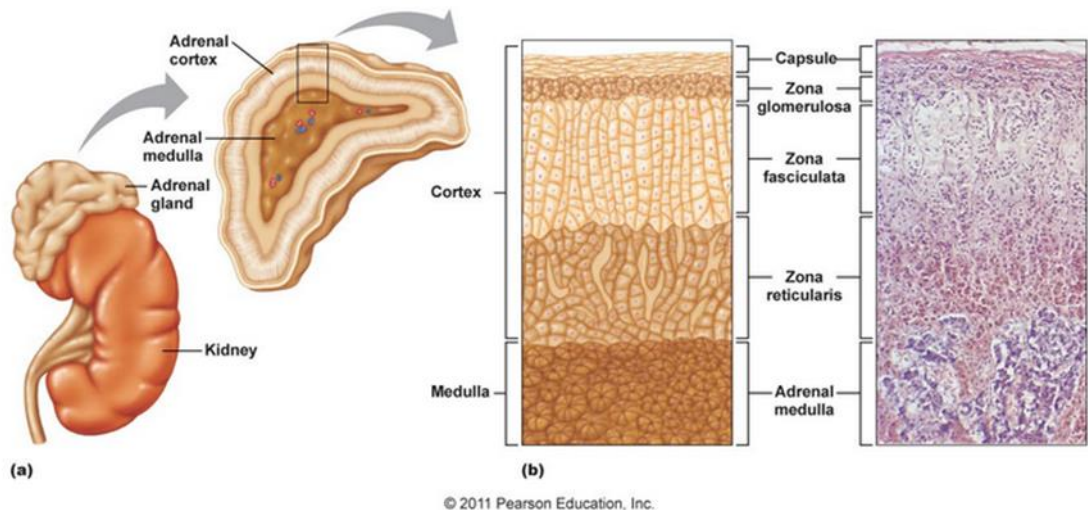


**Figure 1-1: The anatomy of the adrenal gland.**

(a) The macroscopic anatomy of the adrenal gland. (b) cross sectional diagram and microscopic section of the adrenal cortex. Adapted from (Droual 2015).

### 1.2.2 The corticosteroids

The corticosteroids are 21C compounds, consisting of a cyclopenteno-perhydrothreanthrene base, which is approximately planar, with a  $\beta$ -orientated, 2-carbon side chain, the first carbon of which bears a ketone group,

and two angular methyl groups at C18 and C19. The numbering of the rings and the carbon atoms is shown in Figure 1-2. From this basic planar structure, substituents such as hydroxyl groups of specific location and orientation determine the biological properties of the individual compounds. For example, aldosterone in Figure 1-3 is able to perform its function by virtue of its hemiacetal substituent, formed from its 11 $\beta$ -hydroxyl group and its unique 18-aldehyde group. Cortisol, in contrast, is hydroxylated at carbons 11, 17 and 21 (Figure 1-3). Corticosteroid systematic names are listed in Table 1-1.

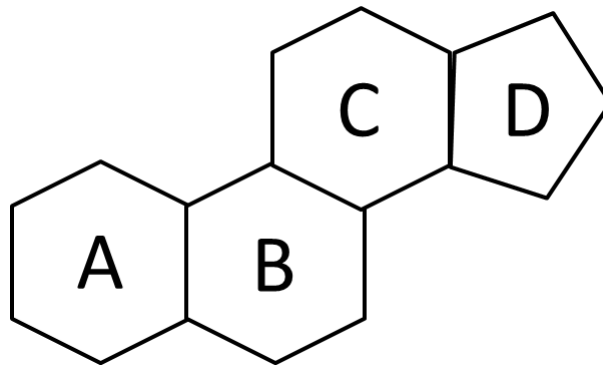


**Figure 1-2: The basic carbon structure present in all steroid hormones.**

The carbon rings are identified by the letters A to D, universally recognised by the International Union of Pure and Applied Chemistry (IUPAC).

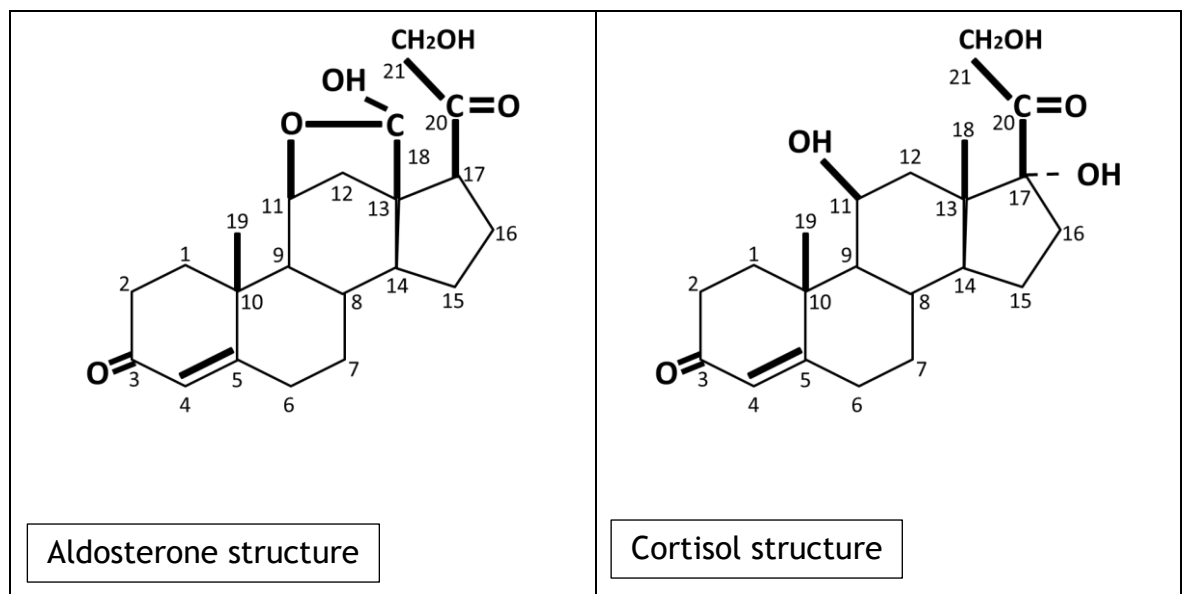


**Figure 1-3: The chemical structures of aldosterone and cortisol.**

Structures of aldosterone (left) and cortisol (right) based on the basic 4 rings of carbon; the numbering of the carbon atoms is determined by the International Union of Pure and Applied Chemistry (IUPAC).

**Table 1-1: Adrenal steroid products, their systematic names and their abbreviations.**

<b>Steroid Product</b>	<b>Systematic name</b>	<b>Abbreviation</b>
<b>11-Deoxy-Corticosterone</b>	21-dihydroxypregn-4-ene-3,20-dione	DOC
<b>11-Deoxy-Cortisol</b>	17 $\alpha$ ,21-dihydroxypregn-4-ene-3,20-dione	S
<b>17-Hydroxy-Pregnenolone</b>	3 $\beta$ ,17 $\alpha$ -dihydroxypregn-5-ene-20-one	17-OH-PREG
<b>17-Hydroxy-Progesterone</b>	17 $\alpha$ -hydroxypregn-4-ene-3,20-dione	17-OH-P
<b>18-Hydroxycorticosterone</b>	11 $\beta$ ,18,21-trihydroxypregn-4-ene-3,20-dione	18-OH-B
<b>Aldosterone</b>	11 $\beta$ -21-dihydroxypregn-4-ene-3,20-dione-18-al	Aldo
<b>Androstenedione</b>	androst-4-ene-3,17-dione	A'dione
<b>Corticosterone</b>	11 $\beta$ ,21-dihydroxypregn-4-ene-3,20-dione	B
<b>Cortisol</b>	11 $\beta$ ,17 $\alpha$ ,21-trihydroxypregn-4-ene-3,20-dione	F
<b>Dehydroepiandrosterone</b>	3 $\beta$ -hydroxyandrost-5-ene-17-one	DHEA
<b>Pregnenolone</b>	3 $\beta$ -hydroxypregn-5-ene-20-one	PREG
<b>Progesterone</b>	pregn-4-ene-3,20-dione	P

The substrate for steroidogenesis is cholesterol. The structure of this important sterol is shown in Figure 1-4. Its central role in steroid metabolism is discussed further in section 1.3.

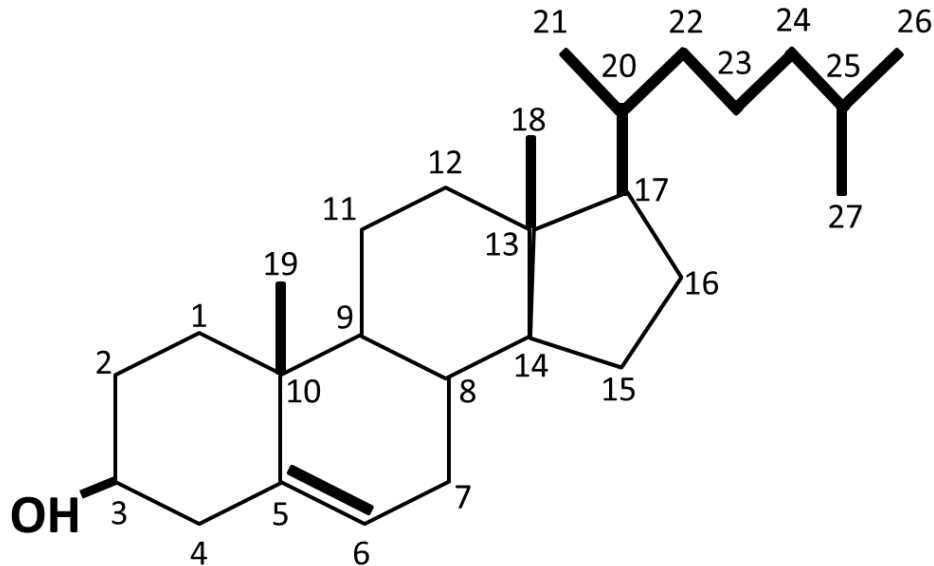


**Figure 1-4: Chemical structure of cholesterol.**

Cholesterol structure based on the basic 4 rings of carbon; the numbering of the carbon atoms is determined by the International Union of Pure and Applied Chemistry (IUPAC).

## 1.2.3 Corticosteroid effects and mechanism of action

### 1.2.3.1 The steroid receptors: structure function and distribution

#### 1.2.3.1.1 Cortisol action through the glucocorticoid receptor

Cortisol is mainly synthesized in the zona fasciculata, with a small amount from the zona reticularis. Its secretion is regulated by adrenocorticotrophic hormone (ACTH) from the anterior pituitary which, in turn, is controlled by corticotropin-releasing hormone (CRH) and arginine vasopressin (AVP) from the hypothalamus. Cortisol exerts negative feedback inhibition on the anterior pituitary and the hypothalamus. The main function of cortisol is to control blood glucose level. Cortisol stimulates

conversion of non-glucose molecules into glucose (gluconeogenesis), glycogenolysis, catabolism of protein in muscle and lipolysis in adipocytes. Cortisol is also involved in the inflammatory response, where it inhibits the synthesis and action of histamine, prostaglandins and leukotrienes. Cortisol also decreases the effectiveness of T and B lymphocytes.

Cortisol acts by binding to glucocorticoid receptor (GR), a member of the nuclear receptor superfamily (Griekspoor, Zwart et al. 2007). There are 2 known GR isoforms, GR $\alpha$  and GR $\beta$ , encoded by a single gene - NR3C1 located on chromosome 5 (5q31) - by means of alternative splicing (Smoak and Cidlowski 2007). GR $\alpha$  binds cortisol, while GR $\beta$  - which differs from GR $\alpha$  at its C-terminus - does not bind to cortisol but does bind the glucocorticoid antagonist, RU-486 (Lewis-Tuffin, Jewell et al. 2007). GR can be found in almost cells in the body.

GR $\alpha$  consists of 4 main domains: the N-terminal domain, DNA binding domain (DBD), ligand binding domain (LBD) and C-terminal domain. The N-terminal domain itself contains the transcription-enhancing activation-function-1 region (AF-1), which upregulates gene expression, as well as a site for SUMOylation (modification regulated by ubiquitin-related proteins at the post-translation level), ubiquitination (modification regulated by ubiquitin) and important basal transcription machinery (BTM). The DBD is highly conserved and comprises two  $\alpha$ -helices that coordinate two zinc fingers essential for dimerization of the hormone-receptor complex and its binding to glucocorticoid response elements (GRE), nuclear translocation and transactivation. The LBD function is to conserve competency of GR for hormone binding (Meijsing, Elbi et al. 2007). The C-terminal domain carries binding sites for heat-shock proteins (hsp) and the nuclear localisation signal (NLS) (Smoak and Cidlowski 2007, McMaster and Ray 2008).

Cortisol is lipophilic and can therefore diffuse through the plasma membrane passively to binds to GR $\alpha$  in the cytoplasm. Prior to binding, the GR is enveloped in a complex of chaperones, including heat shock proteins (hsp90, hsp70, hsp56, hsp40) (Dittmar,

Banach et al. 1998) and immunophilins (i.e FKBP59, cyclophilin 40) (Renoir, Mercier-Bodard et al. 1995), which protect it from degradation and maintain binding affinity. A cortisol molecule binds to the GR complex causing dissociation of GR $\alpha$  from the rest of the complex (hsps and immunophilins) and migration to the nucleus. The ligand-receptor complex then binds to GRE as homo- or hetero-dimers, either increasing transcription of certain genes through stabilisation of the pre-initiation complex, or inhibiting transcription of others (Zennaro 1998). See Figure 1-5.

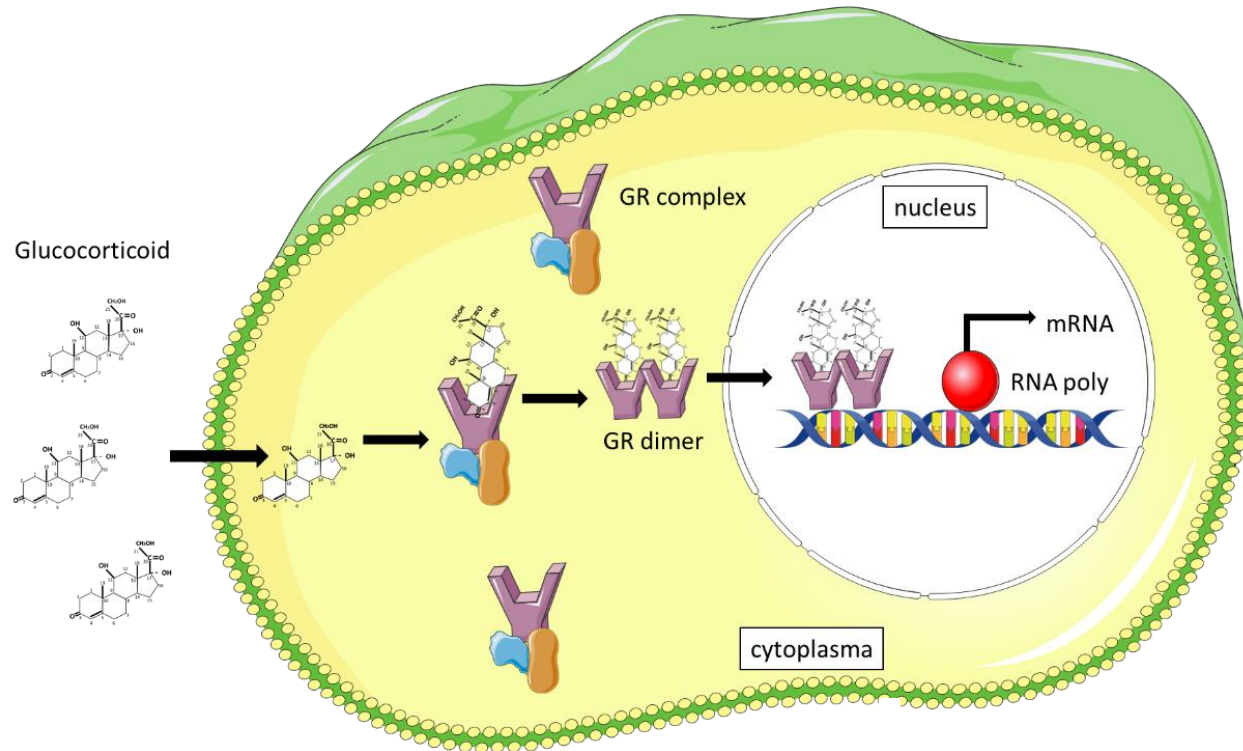


**Figure 1-5: Intracellular action of glucocorticoid from cytoplasm to nucleus.**

Glucocorticoid (GC) enters the cell membrane by diffusion. Glucocorticoid receptor (GR) usually form complexes with multiple proteins in the cytoplasm and remain inactivated. Once GC bind to GR complexes, GR dissociates from the attached protein and forms a dimer with another GR that bind to GC. GC-GR dimers translocate into the nucleus. Then, target gene transcription is initiated. Binding of activated GR homodimer to GREs (glucocorticoid response elements) promoter region activates gene transcription that encode anti-inflammatory mediators (i.e lipocortin-1, interleukin-10 and inhibitor of nuclear factor KB). RNA poly (RNA polymerase). Modified from (Holgate and Polosa 2008).

For example, the GRE located in the lipocortin gene activates transcription of this anti-inflammatory gene. Protein-protein interactions also occur; the ligand-receptor complex protein interacts with signal transduction and activator of transcription proteins (STATs). The ligand-receptor complex can also interact simultaneously with DNA and protein. For example, interaction of GR $\alpha$  complex with GREs and STATs in the Toll-like receptor 2 (TLR-2) gene (Smoak and Cidlowski 2007) is important in pathogen recognition and the activation of innate immunity (Takeda and Akira 2005).

#### 1.2.3.1.2 Aldosterone action through the mineralocorticoid receptor (MR)

Aldosterone acts mainly on epithelial cells of the renal collecting duct where transport of Na<sup>+</sup>, K<sup>+</sup> and water occur (Muto 1995). The epithelial cell reabsorbs Na<sup>+</sup> and water via a specific epithelial sodium channel, ENaC, located at the apical membrane. At the basolateral membrane, transport is driven by the Na<sup>+</sup>/K<sup>+</sup>-ATPase pump, which exchanges sodium ions for potassium and hydrogen ions. Aldosterone acts to increase the opening time of existing ion channels or to increase the total number of channels at the membrane (Connell and Davies 2005). By stimulating the opening of sodium and potassium channels in the luminal membrane and increasing the activity of the Na<sup>+</sup>/K<sup>+</sup>-ATPase pump at the basolateral membrane (Kobori, Nangaku et al. 2007), aldosterone will increase sodium chloride reabsorption and potassium secretion in the collecting duct of the nephron (Kobori, Nangaku et al. 2007).

Aldosterone acts through the mineralocorticoid receptor (MR) or corticosteroid Type I binding site (Baxter, Schambelan et al. 1976). MR is expressed in a variety of epithelial cells - including renal, lung and colon tissue (Funder 2005, Viengchareun, Le Menuet et al. 2007).

The genes encoding MR (NC3C2) and GR (NC3C1) lie on human chromosomes 4 and 5, respectively, but are closely related. They share 90% amino acid homology (Laudet, Hänni et al. 1992) and are 94% identical in their DNA-binding domain (Connell and Davies 2005). The MR has equal affinity for cortisol and aldosterone, and plasma

concentration of cortisol is a hundred-fold higher than that of aldosterone (Funder 2005). This would lead to almost total exclusion of aldosterone from MR binding due to cortisol. However, the 11 $\beta$ -hydroxysteroid dehydrogenase type 2 enzyme (11 $\beta$ -HSD2), which co-localises with MR in certain key target tissues, converts cortisol to the non-MR-binding cortisone in humans (and also the major rodent glucocorticoid corticosterone to 11-dehydrocorticosterone in rats and mice) (Funder, Pearce et al. 1988). Furthermore, 11 $\beta$ -HSD2 converts NAD to NADH, which inactivates glucocorticoid-MR complexes (Funder 2004). The ability of cortisol to bind MR is also reduced because most of it is bound to globulin in the plasma (Shigehiro and Tohru 1982). MRs are also present in non-epithelial tissues such as in cardiovascular and central nervous system where it promotes fibrosis, cardiac hypertrophy, impaired vascular function, regulates blood pressure and influences salt appetite (Connell and Davies 2005).

Like the GR, the MR is cytoplasmic in the absence of ligand (Binart, Lombes et al. 1991). Aldosterone is, again, a lipid-soluble hormone that can easily diffuse into the cytoplasm through the cellular membrane. Once aldosterone enters cells to bind and activate MR in the cytosol, the aldosterone-MR complex translocates to the nuclear compartment to bind the specific hormone responsive element (HRE) (So, Chaivorapol et al. 2007). This step is followed by recruitment of chromatin remodelling complexes to activate the transcriptional machinery and modulate the expression of aldosterone target genes (Viengchareun, Le Menuet et al. 2007). See Figure 1-6.

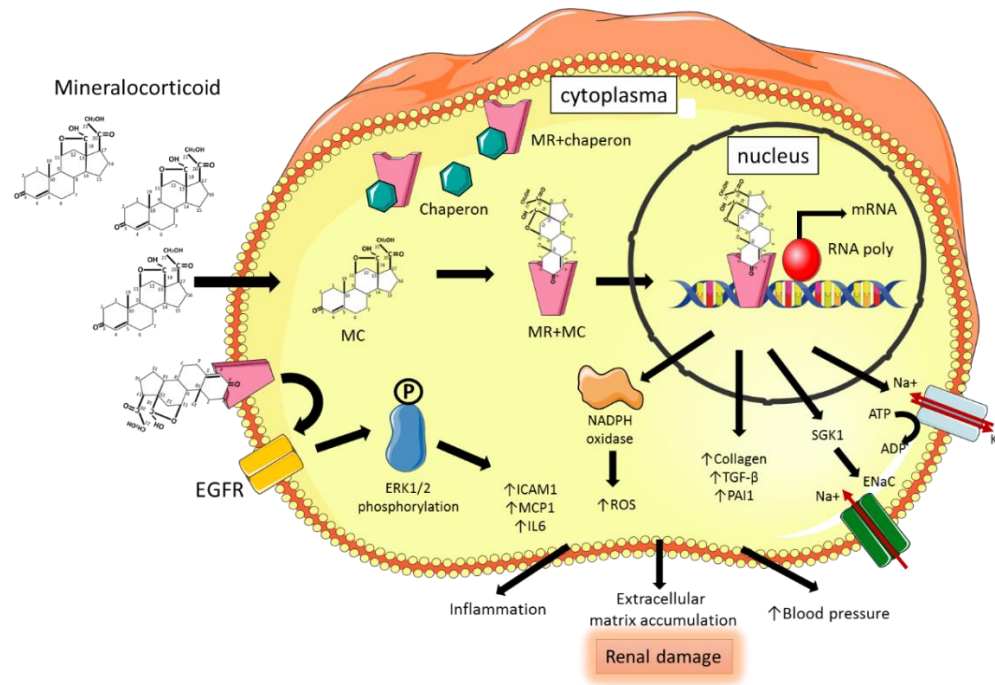


**Figure 1-6: Intracellular action of mineralocorticoid (aldosterone) from membrane to cytoplasm into nucleus.**

MR is stimulated by MC (mineralocorticoid; aldosterone) and this will lead to chaperone dissociation. The MR:MC complex is translocated into the nucleus and activates the hormone response element in the promoter region of target genes. The  $\text{Na}^+$  absorption action of aldosterone depends on SGK1, which de-represses the activity of ENaC. Aldosterone also stimulates the expression of TGF- $\beta$  and PAI1, ROS. Through the non-genomic pathway, aldosterone activates the EGFR and phosphorylates ERK1/2 to upregulate the pro-inflammatory transcription factors i.e. ICAM1, MCP1 and IL6. All of these will lead to renal fibrosis and scarring. Mineralocorticoid (MC), mineralocorticoid receptor (MR), epithelial  $\text{Na}^+$  channel (ENaC), transforming growth factor-beta (TGF-beta), plasminogen activator inhibitor, type 1 (PAI1), reactive oxygen species (ROS), epithelial growth-factor receptor (EGFR), extracellular-signal-regulated kinase 1 (ERK1)/ERK2, intracellular adhesion molecule 1 (ICAM1), interleukin 6 (IL6), monocyte chemoattractant protein 1 (MCP1). Modified from (Perico, Benigni et al. 2008).

### 1.3 Cholesterol: origin and transport

All steroid hormones are synthesized from cholesterol, most of which is imported from circulating lipoproteins (Carr and Simpson 1981) as low-density lipoprotein (LDL). Each LDL complex contains approximately 1500 cholesteryl ester (CE) particles coated with phospholipid, unesterified cholesterol and B-100 apoprotein (MS Brown 1986). Adrenal cells can also synthesise cholesterol *de novo* from acetyl CoA through the mevalonate pathway (Borkowski, Levin et al. 1967, Azhar and Reaven 2002) See Figure 1-7. Cholesterol is stored as cholesteryl ester in cytoplasmic lipid droplets (Gwynne and Strauss 1982).

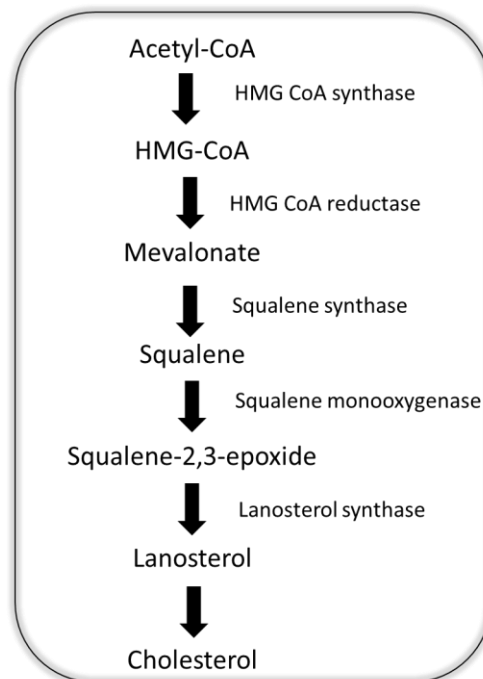


**Figure 1-7: Cholesterol synthesis pathway.**

*HMGCR* (3-hydroxy-3-methylglutaryl-CoA reductase) is the rate-limiting enzyme for cholesterol production, also known as statin target for treatment of hypercholesterolemia.

Human steroidogenic cells employ receptor-mediated-endocytosis via the low density lipoprotein receptor (LDLR), which translocates LDL from the circulation into the cell. LDLR is a glycoprotein receptor located at the cell membrane, encoded by the LDLR gene on chromosome 19p13.1-13.3 (Francke, Brown et al. 1984). After formation of the LDL-LDLR complex, it passes into the cell, fusing with lysosomes into which free cholesterol is released. This can be transported to mitochondria for steroidogenesis or re-esterified and stored in lipid droplets (Azhar and Reaven 2002). LDLR dissociates and is recycled to the cell surface to repeat endocytosis.

The level of cholesterol in the cell is controlled by sterol response element binding proteins (SREBPs) (Kim, Miyazaki et al. 2002). In cholesterol-deficient cells, the SREBP-specific proteases (S1P and S2P) cleave SREBPs to release the activated N-terminal from the membrane. This enables the binding protein to enter the nucleus and bind to sterol regulatory response elements (SREs) and activate the genes involved in cholesterol, fatty acid and triglyceride synthesis (Kim, Miyazaki et al. 2002).

A recent study showed that acyl-CoA:cholesterol acyltransferase (ACAT) esterifies free cholesterol for storage in lipid droplets and that this process is modulated by hormone-sensitive lipase (HSL) (Miller and Auchus 2011). HSL is stimulated by ACTH to increase the availability of free cholesterol. ACTH also can inhibit ACAT action, increasing intracellular cholesterol homeostasis by pumping intracellular cholesterol out to the circulation, thus reducing the level of cholesterol in the cell (Oram and Lawn 2001).

A major part of steroidogenesis is intra-mitochondrial. Cholesterol is translocated from the outer mitochondrial membrane (free cholesterol availability for steroidogenesis (Miller and Auchus 2011). The ATP-binding cassette transporter subfamily A member 1 (ABCA1), a membrane protein, contributes to intracellular transport of cholesterol from the outer mitochondrial membrane (OMM) to the inner mitochondrial membrane (IMM) by steroidogenic acute regulatory protein (StAR). At

the IMM, cholesterol side-chain cleavage enzyme, (P450<sub>scc</sub>, also known as CYP11A) converts insoluble cholesterol to soluble pregnenolone by removing all but C20 and C21 of the side chain. See Figure 1-8 (Miller 1988).

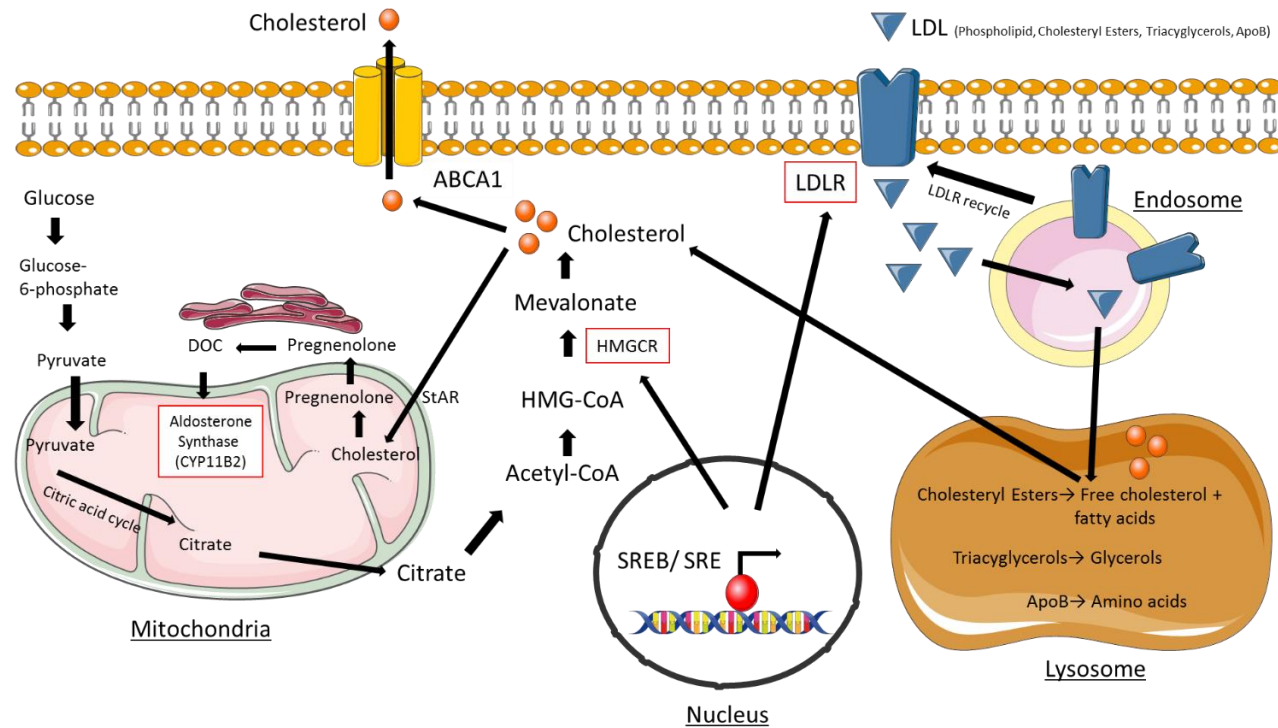


**Figure 1-8: Pathway of cholesterol biosynthesis and its relation with LDLR, HMGCR and CYP11B2.**

LDL binds to LDLR for LDL:LDL complex internalization. In the endosome, LDLR will be recycled back to the membrane while LDL will be processed in the lysosome to produce free cholesterol. Cholesterol movement into the mitochondrion is strictly controlled by StAR. In the mitochondrion, cholesterol will be synthesized to aldosterone via multiple enzymatic processes. The intracellular cholesterol is exported via ABCA1, an ATP-binding transporter. RABCA1: ATP-binding cassette A1 transporters; DOC: Deoxycorticosterone; HMGCR: 3-Hydroxy-3-Methylglutaryl-CoA Reductase; LDL: low density lipoprotein; LDLR: low density lipoprotein receptor; StAR: steroidogenic acute regulatory protein; SRE: Sterol Response Elements; SREB: sterol-response element-binding protein. Modified from (Qiagen, Singh, Yadav et al. 2015).

### 1.3.1 StAR

StAR protein possesses a hydrophobic cholesterol-binding pocket that enables transfer of cholesterol from OMM to IMM (Mathieu, Fleury et al. 2002). It is a 30 kDa mitochondrial peptide synthesized from a 37 kDa precursor (Miller 2007) and is expressed in all steroidogenic tissues. It belongs to the StAR-related lipid transfer (START) family of proteins (Soccio and Breslow 2003). There are multiple START domains mediating lipid transfer intracellularly. StarD4 and D5 are thought to be responsible for cholesterol movement from cytoplasmic lipid droplets to OMM (Riegelhaupt, Waase et al. 2010). StarD4 and D5 have StAR-like activity in COS-1 cell transfected with P450<sub>scc</sub> enzymes (Soccio, Adams et al. 2005). It is estimated that approximately 400 cholesterol molecules per minute are translocated into mitochondria by each newly-synthesized molecule of StAR (Ikonen 2008).

*StAR* gene transcription is modulated by many transcription factors, including steroidogenic factor-1 (SF-1), cAMP response element mediator, dosage-sensitive sex reversal-adrenal hyperplasia congenital critical region on the X-chromosome (DAX-1), GATA-4, CCAAT-enhancer-binding protein-β (C/EBPβ) and activator protein-1 (AP-1) (Reinhart, Williams et al. 1999). SF-1 null mice do not express *StAR* mRNA, demonstrating that *StAR* is dependent on SF-1 for its transcription (Caron, Ikeda et al. 1997). SF-1 activates the *StAR* promoter region at six binding sites (Reinhart, Williams et al. 1999). Its transcription is also activated by cAMP signalling through the cAMP-response element (CRE)-binding protein (CREB) and CRE (Manna and Stocco 2007). In lipoid congenital adrenal hyperplasia (CAH), steroidogenesis activity is severely impaired and cholesterol accumulates within the cytoplasm due to inactivating mutations of *StAR*. In rodents, where steroidogenic cells derive cholesterol from HDL through the scavenger receptor B1 (SRB1) (Johnson, Svensson et al. 1998), absence of adrenal StAR leads to increased *SRB1* expression (Cao, Zhao et al. 1999). However, steroidogenesis is not fully StAR-dependent; COS-1 cells (non-steroidogenic) transfected with F2 (a fusion protein with H2N-P450<sub>scc</sub>-Ferredoxin Reductase-

Ferredoxin-COOH) are steroidogenic despite the absence of StAR (Black, Harikrishna et al. 1994).

### 1.3.2 SF-1

The orphan nuclear receptor Steroidogenic factor-1 (SF-1) is known to have a vital role in steroidogenic tissue development and differentiation. It is encoded by the *NR5A1* gene (nuclear receptor subfamily 5, group A, member 1). Mutation of *NR5A1* can lead to infertility and absence of puberty. SF-1 is involved in the expression of all steroidogenic enzymes in adrenocortical and gonads. SF-1 activates the promoter region of steroidogenic enzymes including CYP11B1, P450cc, StAR and CYP21. Responsiveness to cAMP can be altered due to overlapping of a cAMP-sensitive promoter region with SF-1 (Val, Lefrançois-Martinez et al. 2003). In *in vivo* studies, disruption of the SF-1 gene leads to failure of adrenal and gonad development (Luo, Ikeda et al. 1994). The activation function-2 (AF-2) domain located in the ligand-binding domain (LBD) of SF-1 has a significant effect on SF-1 function and is important to transactivation of target genes. It is reported that even a single point mutation in the AF-2 domain of SF-1 significantly affects SF-1 transactivation, transforming it into a negative mutant with regards to PKA-C-dependent activation (Jacob and Lund 1998).

### 1.3.3 HMGCR

3-hydroxy-3-methylglutaryl coenzyme A reductase (HMGCR) represents the rate-limiting step for cholesterol biosynthesis. It catalyses the conversion of 3-hydroxy-3-methylglutaryl coenzyme A (HMGCoA) to mevalonic acid ((Bochar DA 1999) and Figure 1-8).

HMGCR is a target for statins, drugs used to treat high cholesterol levels. Statin as a cholesterol-lowering agent has been widely used as effective therapy for hypercholesterolaemia for more than 30 years (Goldstein and Brown 1990). Initially, the Framingham study found that there was strong correlation between high plasma

cholesterol and coronary heart disease (CHD) mortality and later specified this was due to LDL (Tobert 2003). However, this remains controversial, with strong evidence to show that inhibiting HMGCR lowers the progression of atherosclerotic development (Blankenhorn, Azen et al. 1993, Jukema, Bruschke et al. 1995, Salonen, Nyssönen et al. 1995). Over the 5 years of the 4s trial (Scandinavian Simvastatin Survival Study), 4000 patients received either simvastatin or placebo, the former significantly reducing mortality due to a decreased number of coronary deaths. This support and confirms that lowering cholesterol effectively reduces CHD morbidity and mortality (Pedersen, Berg et al. 1996).

HMGCR is also expressed in glial cells of the brain, controlling de novo synthesis of cholesterol assisted by ABCA1 importation of extracellular cholesterol. Overexpression of HMGCR along with underexpression of ABCA1 leads to accumulation of cholesterol intracellularly, resulting in increased amyloid beta (A $\beta$ ) synthesis and greater risk of Alzheimer's disease (AD) (Rodríguez-Rodríguez, Mateo et al. 2009).

Apart from cholesterol synthesis, HMGCR also contributes to stimulated migration of primordial germ cells to mesoderm from the embryonic endoderm. HMGCR mutants fail to show this migration, affecting the development of gonadal mesoderm and terminating embryogenesis (Van Doren, Broihier et al. 1998).

### **1.3.4 LDLR**

LDLR is a glycoprotein receptor at the cell membrane (Figure 1-8) that binds and internalizes ligands (i.e cholesterol-containing lipoprotein LDL), enzyme complexes (i.e protease or protease inhibitor), vitamins and much else from the extracellular area (Willnow, Nykjaer et al. 1999, Gent and Braakman 2004). In humans, LDLR is encoded by the *LDLR* gene located on chromosome 19p13.1-13.3 (Francke, Brown et al. 1984).

The mammalian LDLR family can be divided into several groups including the most important, the very-low density lipoprotein receptor (VLDLR) and apolipoprotein E

receptor 2 (Gent and Braakman 2004). Some of the family members play essential role neuronal migration, embryonic development and synaptic transmission (May, Bock et al. 2003, Schneider and Nimpf 2003).

Once the internalization of LDL occurs, it reduces expression of *HMGCR* to decrease cholesterol production and stimulate the Acyl-CoA cholesteryl acyl transferase (ACAT) to form CE from cholesterol, thus reducing cholesterol toxicity intracellularly (Shimomura, Bashmakov et al. 1997, Tamura and Shimomura 2005).

*LDLR*-impaired mice given high cholesterol diet present with hyperlipidaemia, and increased reactive oxygen species (ROS) cause vascular structure alterations (Kypreos and Zannis 2006, Lauzier, Delemasure et al. 2011). Another study delivered restored *LDLR* gene expression through intravenous injection of adenovirus in *LDLR*-null mice, thereby reducing LDL and VLDL in the circulation (Ishibashi, Brown et al. 1993).

*LDLR* defects are the most common cause of familial hypercholesterolemia (FH) and increase the risk of coronary artery disease due to severe elevation of serum LDL (Go and Mani 2012). In FH, 1 in 500 cases are due to heterozygote mutations and 1 in a million to homozygote mutation (Helen H. Hobbs 1992). In homozygotic FH, serum LDL levels are up to 800 mg/dL (normal is <100 mg/dL) with significant severe accumulation of atherosclerotic plaques at the cardiac arteries and valve. In heterozygotic cases, patients typically present with double the normal plasma LDL concentration and a 2-fold risk of coronary artery disease relative to the general population (Go and Mani 2012).

### **1.3.5 ABCA1**

ATP-binding cassette transporter subfamily A member 1 (ABCA1) is a membrane protein essential to intracellular cholesterol homeostasis (Oram and Lawn 2001). The main function of ABCA1 is to pump out intracellular cholesterol to the circulation thus reducing the level of cholesterol in the cell (Figure 1-8). Defects of ABCA1 (i.e in familial hypoalphalipoproteinemia, or FHA, or in Tangier Disease) result in severely

defective cholesterol efflux and accumulation of intracellular cholesterol ester (Bodzioch, Orso et al. 1999). During reverse cholesterol transport, ABCA1 mediates the cholesterol and phospholipid transfer onto Apo-A1, an anti-atherosclerotic property of HDL. *ABCA1* transcription is known to be stimulated by cAMP and LXR-RXR pathways in macrophages (Abe-Dohmae, Suzuki et al. 2000, Schwartz, Lawn et al. 2000), so it is suggested that the alteration of *ABCA1* expression may decrease the transition to foam cell and reduce progression of atherosclerotic plaques.

In severe accumulation of cholesterol in the cell, one study proposed that it will lead to  $\beta$ -cell apoptosis and impaired insulin secretion (Unger 1995). This was further supported by a study with *ABCA1*-null mice, which have impaired glucose tolerance despite normal insulin sensitivity, suggesting that  $\beta$ -cell function is impaired (Brunham, Kruit et al. 2007). Mice lacking LXR- $\beta$ , a transcription factor that activates *ABCA1*, have accumulation of lipid in the islets of  $\beta$ -cells, impaired glucose tolerance and reduced  $\beta$ -cell function (Gerin, Dolinsky et al. 2005).

Lipid-rich diets stimulate mesangial cell proliferation and increase glomerulosclerosis due to deposition of lipid and accumulation of foam cells in the mesangial areas (Song, Li et al. 2000). *ABCA1*-deficient mice develop kidney glomerulonephritis, severe placental malformation and HDL deficiency (Christiansen-Weber, Voland et al. 2000).

## **1.4 Biosynthesis of corticosteroids**

### **1.4.1 Enzymes**

#### **1.4.1.1 The hydroxysteroid dehydrogenases**

Hydroxysteroid dehydrogenases catalyse the oxidation of steroid hydroxyl substituents to ketone (oxo) groups. Their actions are locus- and orientation-specific. Enzymes include:

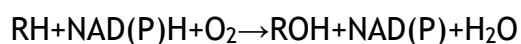
1. 3 $\beta$ -Hydroxysteroid dehydrogenase: converts pregnenolone to progesterone, 17 $\alpha$ -hydroxypregnenolone to 17 $\alpha$ -hydroxyprogesterone and dehydroepiandrosterone to androsterone
2. 11 $\beta$ -Hydroxysteroid dehydrogenase: converts cortisol to cortisone
3. 17-Hydroxysteroid dehydrogenase: converts androstenedione to testosterone
4. 20 $\alpha$ -Hydroxysteroid dehydrogenase: converts progesterone to 20- $\alpha$ -dihydroprogesterone

#### 1.4.1.2 The mixed function oxidases

Mixed-function oxidases create hydroxyl groups ('hydroxylation') using a molecule of oxygen, the second atom of which is reduced to water. They are haem-containing enzymes specific for locus and orientation. Cytochrome P450 (CYP450) enzymes participate in steroidogenesis and the synthesis of bile acids, prostaglandins and fatty acids as well as the metabolism of drugs and natural products. They contain haem and are capable of catalysing numerous reactions including hydroxylation, peroxidation, sulfoxidation, N-oxidation, epoxidation, deamination and desulfuration (Lisurek and Bernhardt 2004, Hille, Hu et al. 2009). There are six cytochrome P450 enzymes involved in steroidogenesis:

1. cholesterol side-chain cleavage enzyme, SCC, desmolase (CYP11A1)
2. 11 $\beta$ -hydroxylase (CYP11B1)
3. aldosterone synthase (CYP11B2)
4. 17 $\alpha$ -hydroxylase/17,20-lyase (CYP17A)
5. aromatase (CYP19)
6. 21-hydroxylase (CYP21).

Cytochrome P450s act as monooxygenases, using reduced nicotinamide adenine dinucleotide phosphate (NADPH) as an electron donor for molecular oxygen reduction:



Ferredoxin proteins mediate electron transfer. Adrenodoxin (also called ferredoxin 1 or FDX-1) is the human adrenal ferredoxin that helps transfer electrons from NADPH to CYP450 enzymes, mediating ferredoxin function, as shown in Figure 1-9 (Imamichi, Mizutani et al. 2014).

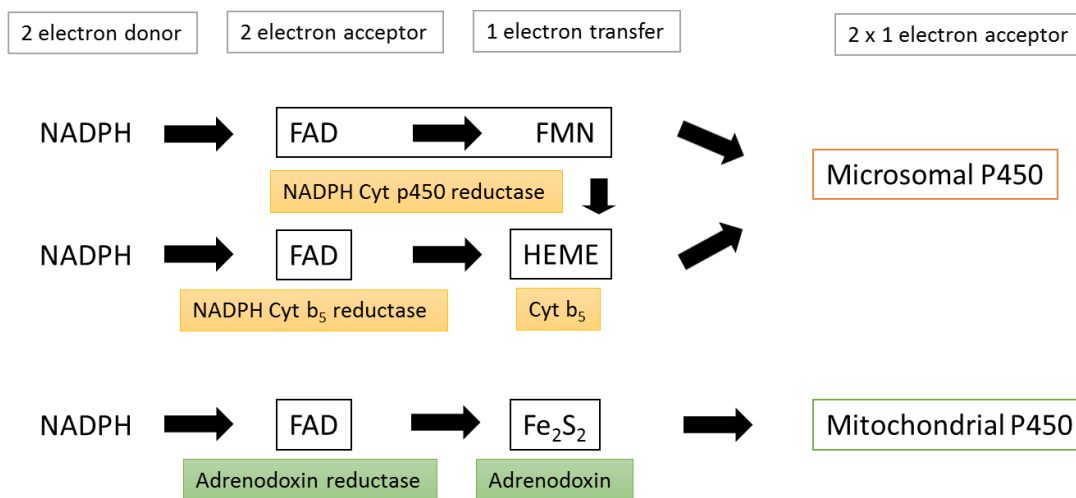


**Figure 1-9: Mitochondrial and microsomal P450 redox partners.**

FAD (flavin adenine dinucleotide), FMN (flavin mononucleotide), NADPH (nicotin-amide adenine dinucleotide phosphate). Modified from (Cederbaum 2015).

The steroidogenic pathways within the adrenal cortex are illustrated in Figure 1-10 and Figure 1-11. In the zona glomerulosa, there is a single linear pathway to aldosterone, whereby cholesterol undergoes side-chain cleavage to pregnenolone by CYP11A1, and is then oxidised to progesterone by 3HSD2. A series of hydroxylation reactions then convert progesterone to aldosterone. The unique final reaction, catalysed by CYP11B2 (aldosterone synthase), involves three consecutive modifications, each utilising one NADPH molecule, one oxygen molecule and a mitochondrial electron transfer (Payne and Hales 2004):

- 1) 11 $\beta$ -hydroxylation of DOC to produce corticosterone
- 2) 18-hydroxylation to 18-hydroxy corticosterone
- 3) 18-methyloxidation to formaldoosterone

Corticosterone is also synthesised in the zona fasciculata but, in the absence of aldosterone synthase, is not processed further. However, the human zona fasciculata, unlike the zona glomerulosa, does express 17 $\alpha$ -hydroxylase (*CYP17A1*). This microsomal enzyme acts on either pregnenolone or progesterone; their 17 $\alpha$ -derivatives are then subject to further conversions to form cortisol. 11 $\beta$ -Hydroxylase (*CYP11B1*), which catalyses the final step from 11-deoxycortisol to cortisol, has considerable homology with aldosterone synthase. These two enzymes are discussed in more detail in Section 1.4.2.3.

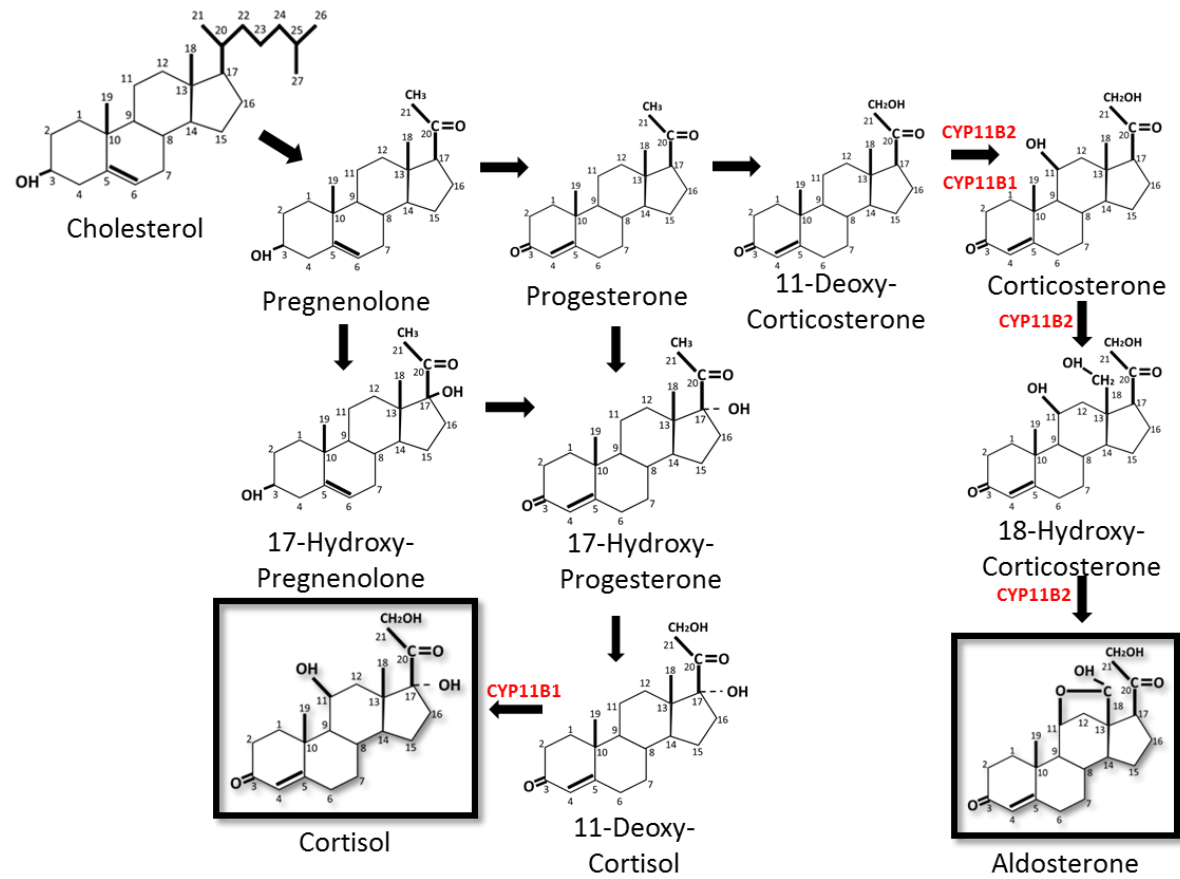
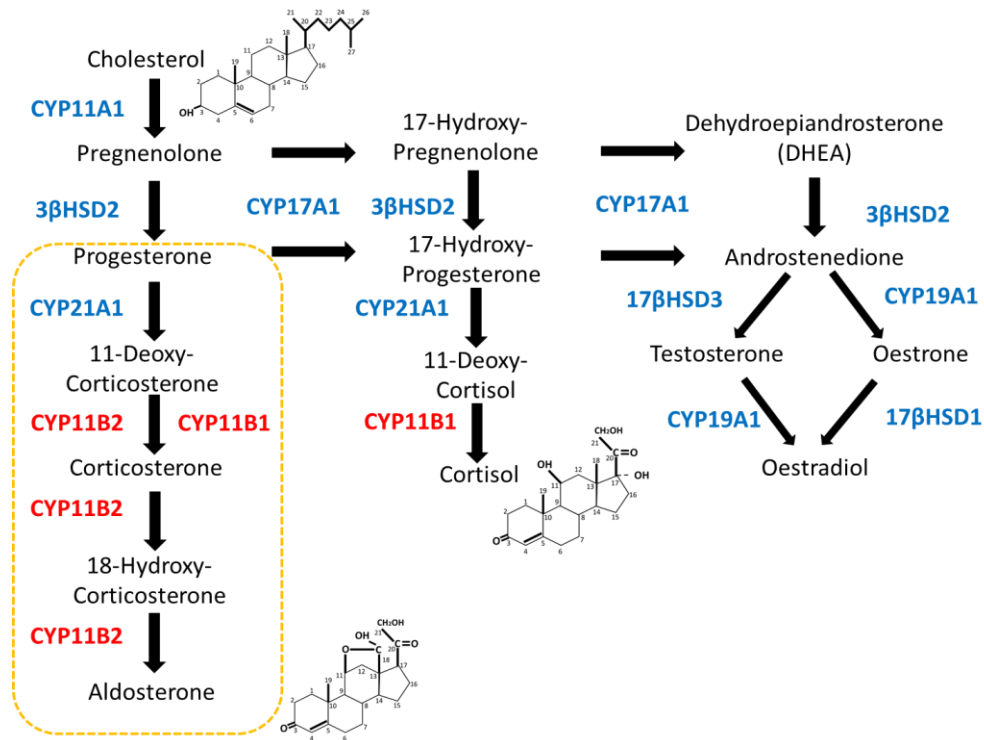


Figure 1-10: Chemical structure of steroid hormones in aldosterone and cortisol biosynthesis. Red indicates CYP11B2- and CYP11B1-mediated conversions.



**Figure 1-11: Steroid hormone biosynthesis pathway. Reactions within the yellow dotted line occur in the zona glomerulosa.**

The conversion of cholesterol to pregnenolone is catalysed by P450<sub>scc</sub> (CYP11A1). Pregnenolone is converted to progesterone by 3βHSD. Progesterone undergoes 21-hydroxylation by CYP21A1 to produce DOC (11-Deoxycorticosterone). The conversion of DOC to aldosterone involves 3 reactions: 11β-hydroxylation of DOC to produce corticosterone, 18-hydroxylation to yield 18-hydroxycorticosterone and 18-methyloxidation to form aldosterone.

## 1.4.2 Control of corticosteroid biosynthesis and secretion

### 1.4.2.1 Cortisol

#### 1.4.2.1.1 Hypothalamo-pituitary-adrenocortical (HPA) Axis

The production of cortisol is primarily regulated by ACTH via the hypothalamo-pituitary-adrenocortical (HPA) axis (Figure 1-7). Stimulation of the HPA axis occurs through stressors such as anxiety, pain, fear, arousal, aversive reaction and many others (Jeansok J. Kim 2001, Heinrichs and Koob 2004). This activates release of corticotropin-releasing hormone (CRH) and arginine vasopressin (AVP) from the hypothalamus into the hypothalamo-pituitary portal system. CRH increases cAMP and  $Ca^{2+}$  levels in corticotropic cells. Both cAMP and  $Ca^{2+}$  are known to increase pro-opiomelanocortin (POMC) mRNA levels. Aside from these second messengers, POMC gene transcription is also regulated by a variety of hormones and neuropeptides. POMC is a precursor polypeptide (241 amino acid residues) that is cleaved to form multiple peptide hormones including ACTH, melanotropins and opioid peptides of the  $\beta$ -endorphin family (Boutillier, Monnier et al. 1995). These initiate ACTH release by the corticotropic cells (Vedder 2007). ACTH activates transmembrane heterotrimeric G protein ACTH receptors (MCR2) to generate cAMP as a second messenger (Côté, Payet et al. 1999). cAMP then activates cAMP-dependent protein kinase A (PKA), which phosphorylates target proteins. Increased cortisol exerts negative feedback inhibition on CRH and ACTH at the transcriptional and secretion levels (Kellendonk, Tronche et al. 2002). Other stimulants of the HPA include interleukin-3 (IL-3) and interleukin-6 (IL-6) (Weber, Michl et al. 1997).

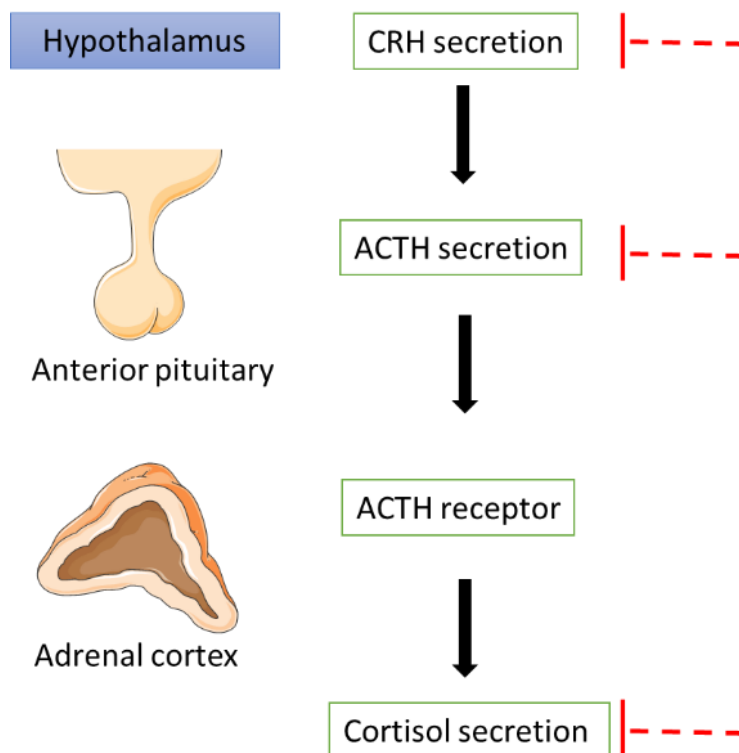


**Figure 1-12: The Hypothalamic-Pituitary-Adrenocortical (HPA) Axis.**

CRH in the hypothalamus stimulates ACTH at the anterior pituitary. By activating ACTH receptors in the adrenal gland, this will lead to cortisol secretion in the adrenal zona fasciculata. High levels of cortisol will inhibit the production of ACTH and CRH via a negative feedback-loop. Corticotropin-releasing hormone (CRH); ACTH: Adrenocorticotrophic hormone.

### 1.4.2.2 Aldosterone

#### 1.4.2.2.1 The Renin-angiotensin-aldosterone system (RAAS)

The RAAS is summarised in Figure 1-13. Its active product is angiotensin II (Angio II), a pressor octapeptide which is released in response to sodium deprivation or falls in intravascular volume. It stimulates the zona glomerulosa to produce aldosterone, principally through the Angiotensin Type 1 receptor (AT1), which will lead to aldosterone secretion (Guo, Sun et al. 2001). Binding of Angio II to the AT1 receptor activates the phosphoinositide-specific phospholipase C (PLC) to hydrolyse phosphatidylinositol 4,5-biphosphate (PIP2) and generate two second messengers, DAG and inositol 1,4,5-triphosphate (IP3). Diacylglycerol (DAG) has been shown to stimulate PKC (Bollag, Barrett et al. 1990) and selective PKC inhibitors reduce Angio

II-induced aldosterone synthesis (Kapas, Purbrick et al. 1995). IP3 stimulates aldosterone production by activating the calcium/calmodulin-dependent protein kinases (CaMK) and increasing calcium concentration in the cytoplasm (Hattangady, Olala et al. 2012); again , their inhibition decreases Angio II-induced aldosterone synthesis (Ganguly, Chiou et al. 1990).

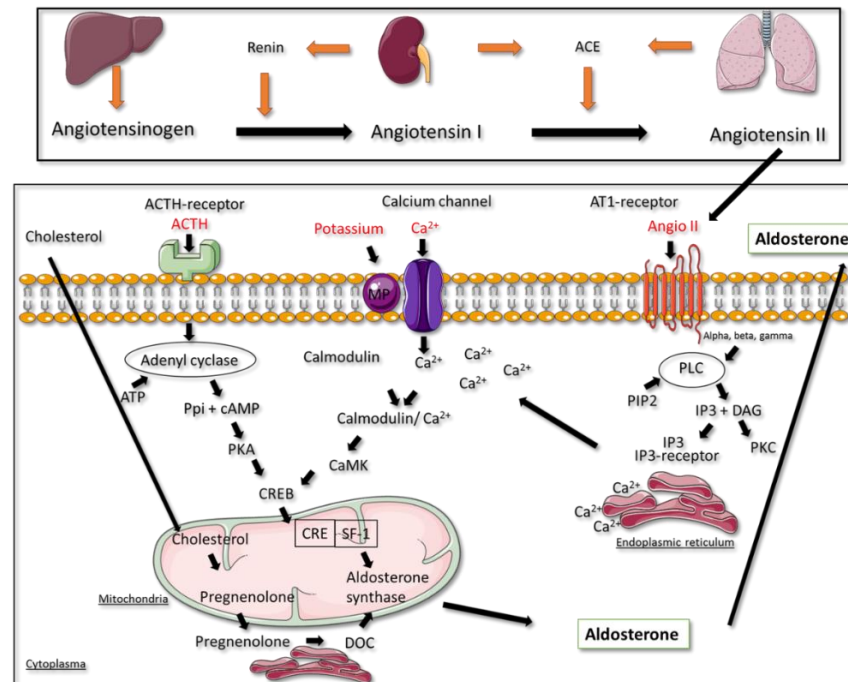


**Figure 1-13: Regulation of aldosterone biosynthesis under the Renin-Angiotensin-Aldosterone System (RAAS).**

Low intravascular blood volume (and therefore pressure) activates renin activity (secreted from renal juxtaglomerular kidney cells) and conversion of angiotensinogen to Angio I. ACE secretion from lungs and renal cells convert the Angio I to Angio II. Angio II binds to AT1-receptor and activates PLC. PLC then hydrolyses PIP2 and generates IP3 and DAG. Subsequently DAG activates PKC for vasoconstriction at the afferent arteriole of kidney and reduces aldosterone synthesis. IP3 activates the calmodulin/ $\text{Ca}^{2+}$ -dependent protein kinase (CaMK), increases intracellular calcium and activates CREB. Another cascade involved in increasing aldosterone secretion involves potassium. Increased extracellular potassium leads to cell membrane depolarisation and opening of the voltage-dependent  $\text{Ca}^{2+}$  channel, activating cAMP and CREB. ACTH also stimulates aldosterone by binding of the ACTH receptor. This leads to dephosphorylation of ATP by adenyl cyclase to generate cAMP. cAMP then activates the PKA and leads to CREB phosphorylation; through several enzymatic processes it will increase aldosterone production. ACTH: Adrenocorticotrop hormone, AT1-receptor: Angiotensin type 1 receptor, CaMK: Calmodulin kinase, IP3: Inositol triphosphate; MP: Membrane potential; PKC: Protein kinase C; PKA: Protein kinase A; PLC: Phospholipase C; PIP: Phosphatidyl inositol diphosphate, SF-1: Steroidogenic factor 1. Modified from (Delcayre and Silvestre 1999)

#### 1.4.2.2.2 Potassium ions (K<sup>+</sup>)

Zona glomerulosa cells are highly sensitive to changes in potassium level. An increase in serum potassium of 0.1mEq/l increases serum aldosterone by 25% (Himathongkam, Dluhy et al. 1975). Increased extracellular K<sup>+</sup> concentration depolarises the cell membrane, opening voltage-dependent L- and T-type Ca<sup>2+</sup> channels. The consequent influx of Ca<sup>2+</sup> again activates CaMK, which phosphorylate transcription factors required for *CYP11B2* expression (Connell and Davies 2005). Further Ca<sup>2+</sup> is released from intracellular stores (Spät and Hunyady 2004).

#### 1.4.2.2.3 Adrenocorticotrophic hormone (ACTH)

In humans and experimental animals, acute infusion of ACTH stimulates aldosterone production through the cAMP pathway (Connell and Davies 2005). However, chronic stimulation of ACTH suppresses plasma aldosterone (Hattangady, Olala et al. 2012). Chronically, ACTH may convert the phenotype of glomerulosa cells into cortisol-producing fasciculata cells or divert precursors from the mineralocorticoid to the glucocorticoid pathway (Hornsby, O'Hare et al. 1974).

#### 1.4.2.2.4 Endothelin, serotonin and adipose tissue

Endothelin is a potent vasoconstrictor and may stimulate zona glomerulosa cells to secrete aldosterone (Pecci, Cozza et al. 1994, Zhang, Azhar et al. 2012). Although the number of endothelin receptors is equal to those of AT1, endothelin is a weak aldosterone secretagogue compared to Angio II, K<sup>+</sup> and ACTH (Williams 2005). Serotonin is also a weak stimulator of aldosterone synthesis; the serotonin precursor, 5-hydroxytryptophan increases plasma aldosterone while serotonin antagonist reduces it (Shenker, Gross et al. 1985).

Adipose cells secrete several products of linoleic acid oxidation and other secretagogues that stimulate aldosterone production (Goodfriend, Ball et al. 2002, Ehrhart-Bornstein, Lamounier-Zepter et al. 2003). Plasma aldosterone levels and body

mass index correlate positively and there is an increased prevalence of hyperaldosteronism in obese patients (Calhoun and Sharma 2010). Recently, a study utilising human adrenal and H295R cells reported that obesity (endogenous leptin) and infusion (exogenous leptin) increased *CYP11B2* expression and aldosterone in dose-dependent manner (Huby, Antonova et al. 2015).

#### **1.4.2.3 CYP11B1 and CYP11B2**

Aldosterone synthase (also known as CYP11B2 or P450c11b2) has a molecular mass of 48.5 kDa and is expressed in the zona glomerulosa, where it is located on the inner mitochondrial membrane (Curnow, Tusie-Luna et al. 1991). CYP11B2 gene transcription can be stimulated by Angio II, cAMP and K<sup>+</sup> (Clyne, Zhang et al. 1997). In gene transfection studies, CYP11B2 promoter activity is directly activated by Nur-related factor 1 (NURR-1 or NR4A2) and neuron-derived orphan receptor 1 (NOR-1 or NR4A3) (Nogueira, Xing et al. 2009); both can be upregulated in the zona glomerulosa by Angio II (Bassett, Suzuki et al. 2004).

The 11 $\beta$ -hydroxylase enzyme (P450c11b1) is encoded by the CYP11B1 gene, which is highly homologous with CYP11B2; they exhibit 95% similarity in the coding sequence and 90% similarity in intronic regions (Payne and Hales 2004). CYP11B1 and CYP11B2 are located in tandem, 40 kb apart, on chromosome 8q21; each consists of 9 exons. See Figure 1-14. The greatest difference between the genes lies in their 5' untranslated regions, accounting for the differences in their expression (Mornet, Dupont et al. 1989), while minor differences in their coding regions result in their differing enzymatic functions.

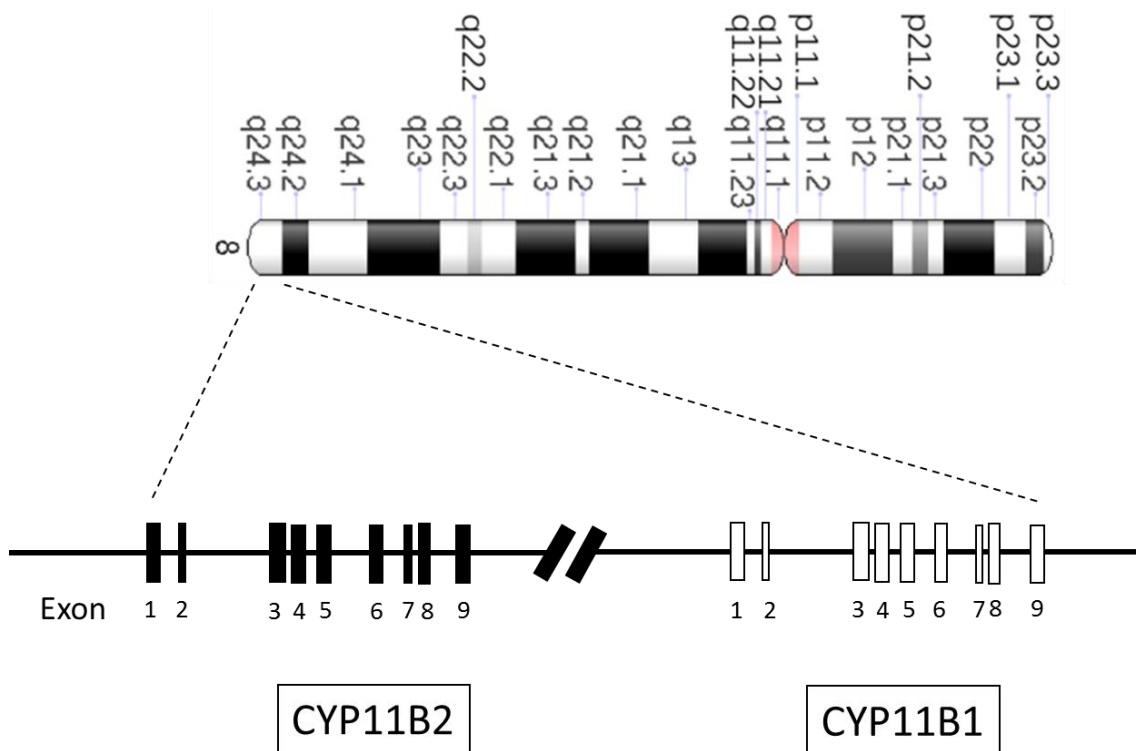


**Figure 1-14: Genomic tandem structure of *CYP11B2* and *CYP11B1* and the Ideogram of human chromosome 8.**

*CYP11B2* and *CYP11B1* located at 8q24.3. Red indicates the centromere. Modified from (Portrat, Mulatero et al. 2001, NCBI 2014).

#### 1.4.2.3.1 Polymorphisms of *CYP11B2* and *CYP11B1*

The *CYP11B2* and *CYP11B1* genes are highly polymorphic. The most commonly-studied *CYP11B2* polymorphism is a C/T variant located at position -344, relative to the coding region (rs1799998). This polymorphism has been significantly associated with altered blood pressure and aldosterone levels (White and Slutsker 1995). Davies et al (1999) reported that the T-allele at -344 occurs more frequently in hypertensive patients and associates with significantly higher levels of aldosterone metabolite (tetrahydroaldosterone) in the urine compared to -344C groups (Davies, Holloway et al. 1999). This site corresponds to a steroidogenic factor-1 (SF-1) binding site, although *in vitro* analysis showed the polymorphism had no significant effect on SF-1 binding (Bassett, Zhang et al. 2002). More recently, analysis suggests that rs1799998 is

not itself a functional polymorphism (Niu, Guo et al. 2010), it may be in linkage disequilibrium with one.

#### 1.4.2.3.2 Transcription Factors and miRNA influencing *CYP11B2* and *CYP11B1* expression

Transcription factors (TFs) bind specific sites in the promoter/ 5'UTR region of a gene to inhibit or stimulate gene expression. TFs, such as neuronal growth factor-induced clone B (NGFI-B), regulate aldosterone synthase, 11 $\beta$ -hydroxylase, 3 $\beta$ -hydroxysteroid dehydrogenase, 17 $\alpha$ -hydroxylase, and 21-hydroxylase in the adrenal gland (Nogueira and Rainey 2010, Romero, Gomez-Sanchez et al. 2010). The members of the NGFI-B nuclear orphan receptor superfamily include NR4A1 (Nur77, NGFI-B), NR4A2 (Nurr1) and NR4A3 (Nor1), and are abundantly expressed in the adrenal cortex (Romero, Gomez-Sanchez et al. 2010). NGFI-B is upregulated in the presence of Angio II in the H295R adrenocortical cell line (Romero, Gomez-Sanchez et al. 2010) and a NGFI-B response element (NBRE) has been identified within the *CYP11B2* promoter that regulates transcription (Nogueira and Rainey 2010). Other important transcription factors for *CYP11B2* and *CYP11B1* are cAMP-responsive element binding proteins (CREBs), which are shown to be subject to Angio II-regulated phosphorylation in several tissues. NURR1 can act synergistically with members of the CREB family to increase *CYP11B2* expression (Nogueira and Rainey 2010).

Transcription of *CYP11B1* is also modulated by SF-1 (Wang, Bassett et al. 2000). In a luciferase reporter construct study, co-transfection of vectors encoding SF-1 up-regulated expression of *CYP11B1* but not *CYP11B2*; also, mutation of SF-1 inhibited *CYP11B1* transcription (Bassett, Zhang et al. 2002). According to Bassett et al, the exception of *CYP11B2* from being downregulated by SF-1 is probably due to the concentration of SF-1 plasmid used in the study. Other study showed that SF-1 has a repressor domain, therefore this enable the SF-1 to downregulate *CYP11B2* and not vice versa (Ou, Mouillet et al. 2001).

In addition to the transcription factors modulating *CYP11B2* and *CYP11B1*, another factor of importance has emerged: microRNA (miRNA). This will be further discussed in Section 1.7.1.

## **1.5 The adrenal cortex and disease**

Disruption of corticosteroidogenesis has profoundly negative health implications. Adrenal failure (Addison's disease) disrupts both electrolyte and energy metabolism and, without treatment, is fatal. The effects of excess cortisol or aldosterone have already been described and are similarly debilitating. These extreme conditions are rare, comprising principally adrenocortical neoplasia and monogenic disorders of specific enzymes' gene expression. These are briefly summarised below. Recent studies, however, suggest that small deviations from normal gene expression, when sustained over a lifetime as the result of, for example, polymorphic variation or changes in regulatory factors, may be important and common determinants of health.

### **1.5.1 Adrenal tumours**

#### **1.5.1.1 Aldosterone-producing adenoma (APA)**

Primary aldosteronism (PA) is the most common cause of secondary hypertension (Scholl and Lifton 2013) and is characterized by high blood pressure, increased aldosterone secretion, hypokalaemia and low renin level. It may be associated with increased risk of renal (Rossi, Bernini et al. 2006) and cardiac disease (Anand, Mooss et al. 2006). In 30-40% of patients, PA is due to a unilateral aldosterone-producing adenoma (APA) (Ye, Mariniello et al. 2007, Sahay and Sahay 2012) and more than 60% of PA is due to bilateral adrenal hyperplasia (BAH) (Freel and Connell 2005). Adrenal carcinoma is much less frequent. According to the Endocrine Society's diagnostic guidelines (2008), the initial step differentiating APA from BAH is a computerised tomography (CT) scan, which will also exclude adrenal carcinoma where the lesion is usually more than 4 cm. APAs are usually less than 3 cm. BAH shows abnormality of

both adrenal glands. Confirmation is by adrenal venous sampling (Sahay and Sahay 2012). Differences between APA and BH are summarized in the Table 1-2.

**Table 1-2: Major differences between Aldosterone Producing Adenoma (APA) and Bilateral Adrenal Hyperplasia (BAH). ACTH: Adrenocorticotrophic Hormone; AVS: Adrenal Venous Sampling; PA: Primary Aldosteronism; ZF: Zona Fasciculata; ZG: Zona Reticularis. Modified from (Freel and Connell 2005).**

<b>Feature</b>	<b>Aldosterone-Producing Adenoma</b>	<b>Bilateral adrenal hyperplasia</b>
<b>Approximate proportion of all PA</b>	1/3	2/3
<b>Imaging common finding</b>	Unilateral solitary	Normal or bulky adrenal
<b>Common pathologic findings</b>	Predominantly ZF cells	Multiple nodules in the ZF or diffuse hyperplasia of ZG
<b>Postural response</b>	Variable (many adenomas are ACTH responsive)	Maintained
<b>Finding on AVS</b>	Increased aldosterone to cortisol ratio in affected adrenal side	No difference in aldosterone to cortisol ratio between adrenal veins
<b>Treatment</b>	Laparoscopic surgery	Medication (Aldosterone antagonists)

### 1.5.1.2 Gene mutations in APA

#### 1.5.1.2.1 KCNJ5

In APA, about 30-60% of cases have somatic mutation of the G-protein-activated inward rectifying potassium channel Kir3.4, which is encoded by the *KCNJ5* gene (Gomez-Sanchez and Oki 2013). The Kir3.4 channel is a tetrameric complex with an extracellular pore-forming region that binds with other K<sup>+</sup> channels (e.g. Kir3.1) to form heterotetrameric or homotetrameric complexes (Ishihara, Yamamoto et al. 2009, Zennaro and Jeunemaitre 2011). Mutation of K<sup>+</sup> channels can alter the selectivity filters to K<sup>+</sup>, making them non-selective channels (Heginbotham, Lu et al. 1994, Dibb, Rose et al. 2003).

In the resting state, zona glomerulosa cells have negative resting potentials and steroidogenesis remains inactive (Guagliardo, Yao et al. 2012); K<sup>+</sup> channels, including Kir3.4, TASK-1 to TASK-5 and Twik-Related Potassium Channel 1, are all intact and intracellular K<sup>+</sup> is released to extracellular compartments. Angio II decreases K<sup>+</sup> transport through the channel and also decreases the expression of Kir3.4 channel. This causes membrane depolarization and voltage-dependent Ca<sup>2+</sup> channels to open, increasing Ca<sup>2+</sup> influx and stimulating the calcium-calmodulin pathway. These events increase the expression of *CYP11B2* and therefore aldosterone production. In the case of a somatic mutation of *KCNJ5*, there is a loss of selectivity of the Kir3.4 channel, allowing the influx of Na<sup>+</sup> that leads to membrane depolarization, calcium influx and subsequent increase in *CYP11B2* gene expression (Choi, Scholl et al. 2011).

#### 1.5.1.2.2 ATP1A1 and ATP2B3

In a study of 112 APA patients, 6.3% had a somatic mutation of ATP1A1 together with increased *CYP11B2* gene expression (Williams, Monticone et al. 2014). In an earlier study of a European cohort, the prevalence of the somatic mutation of ATP1A1 was 5.2% of 308 APA patients (F. Beuschlein 2013). ATP1A1 exchanges three Na<sup>+</sup> in the cytoplasm for two K<sup>+</sup> from the extracellular compartment, each time an ATP is hydrolysed (Kaplan 2002). The *ATP1A1* gene encodes the Na<sup>+</sup>/K<sup>+</sup>-ATPase 1 that

responsible for maintaining the electrochemical gradient of Na<sup>+</sup> and K<sup>+</sup> across the plasma membrane. Blockade of the Na<sup>+</sup>/K<sup>+</sup>-ATPase pump by ouabain increases aldosterone synthesis in a dose-dependent manner (Yingst, Davis et al. 1999). The *ATP1A1* knockout mouse has been shown to have higher plasma aldosterone compared to its wild-type counterpart (Moseley, Huddleson et al. 2005).

*ATP2B3* encodes the plasma membrane Ca<sup>2+</sup> ATPase 3 (known as PMCA3), important for exporting Ca<sup>2+</sup> from the cytoplasm to extracellular compartments (Di Leva, Domi et al. 2008). The mutation of this gene is predicted to increase intracellular Ca<sup>2+</sup> concentration and increase aldosterone synthesis (F. Beuschlein 2013). This is supported by the finding that almost 1% of APA have an *ATP2B3* mutation and high levels of *CYP11B2* gene expression (Williams, Monticone et al. 2014).

#### 1.5.1.2.3 WNT β-catenin Pathway in APA

Alteration of WNT/β-catenin signalling was detected in 70% of APA (Berthon, Drelon et al. 2014). The Wnt/β-catenin is important in embryonic development and cell renewal (Berthon, Sahut-Barnola et al. 2010) and has been associated with the development of numerous cancers (Anastas and Moon 2013).

Initially, WNT (previously called Int-1) was shown to induce breast tumours in the mouse (Nusse and Varmus 1982). WNT1 stands for Wingless-type MMTV integration site family, member 1. In the absence of WNT ligands, β-catenin (encoded by *CTNNB1* gene) is phosphorylated by a complex consisting of casein kinase I (CKI), GSK3B, AXIN and APC at N-terminal serine/ threonine residues. The phosphorylated β-catenin is ubiquitinated and degraded by proteasomes. However, in the presence of WNT ligands, it binds to Frizzled/LRP receptor which inhibits the complex destruction and therefore stabilizes β-catenin. β-Catenin is translocated to the nucleus and co-operates with transcription factors of the LEF/TCF family (Berthon, Sahut-Barnola et al. 2010). The lymphoid enhancer factor (LEF)/T cell factor protein (TCF) recruits β-catenin along with its co-activators to the WNT response element (WREs) to stimulate the transcription of target genes (Arce, Yokoyama et al. 2006). β-Catenin mutation

has been observed in ACA and ACC tissue (Tissier, Cavard et al. 2005). Furthermore, mutation at the third exon of *CTNNB1* causes abnormal accumulation of  $\beta$ -catenin leading to various pathological adrenal conditions such as the primary pigmented nodular adrenocortical disease and sporadic secreting adrenocortical adenomas (Tadjine, Lampron et al. 2008). There is abundant evidence that alteration of WNT/ $\beta$ -catenin can modulate adrenocortical tumours: the  $\beta$ -catenin blocker PKF115-584 inhibits adrenocortical carcinoma cell proliferation (Doghman, Cazareth et al. 2008). Therefore, WNT/ $\beta$ -catenin pathway might be a potential therapeutic target.

#### 1.5.1.2.4 Steroidogenic Enzymes Mutation Causing Congenital Adrenal Hyperplasia (CAH).

In rare cases, mutation of gene can cause severe abnormalities and lead to hypertension. There are common clinical signs that relate to genetic abnormalities as shown Table 1-3.

**Table 1-3: Steroidogenic Enzymes that contribute to CAH.**

Enzyme	Aldosterone synthase	3- $\beta$ hydroxysteroid dehydrogenase	11- $\beta$ hydroxylase	17- $\alpha$ hydroxylase	21-hydroxylase
Encoding gene	<i>CYP11B2</i>	HSD3B2	<i>CYP11B1</i>	CYP17	CYP21A
Incidence	Rare	Rare	1 in 10000	Rare	1 in 14000
Ambiguous genitalia	Nil	Males Mild in females	Females	Males Failure of pubertal development in females	Females
Glucocorticoids	Normal	Low	Low	Low	Low
Mineralocorticoids	Low	Low	High	High	Low
Androgens	Normal	Low in males High in females	High	low	High
Blood pressure	Low	Low	High	High	Low
Sodium level	Low	Low	High	High	Low
Potassium level	High	High	Low	Low	High

## **1.6 Hypertension studies**

### **1.6.1 Monogenic disorders**

Numerous monogenic disorders leading to hypertension have been identified. The majority affect electrolyte transport at the distal tubule, directly or indirectly, by altering mineralocorticoid secretion. Monogenic disorders share several common final mechanisms: they escalate sodium and chloride reabsorption at the distal nephron, cause plasma volume expansion and decrease plasma renin activity (Garovic, Hilliard et al. 2006, Simonetti, Mohaupt et al. 2012). Although such disorders are rare, they illustrate the clear genetic influence on BP and haemodynamic, and are of great research interest. Monogenic hypertension can present with severe hypertension, early onset (although not always) and often with a positive family history. Low-renin activity and metabolic acidosis with hyperkalaemia or metabolic alkalosis with hypokalaemia are characteristic but plasma aldosterone concentration may be low as that of the minor mineralocorticoid, DOC, is often markedly increased (Simonetti, Mohaupt et al. 2012). Examples of monogenic disorders are shown in Table 1-4.

Smaller but still significant variations in the activity of these systems may exist to a wide extent in the general population. These have been sought using various different techniques.

**Table 1-4: Summary of Monogenic Loci Associated with BP (Modified from Padmanabhan, Caulfield et al. 2015).**

Locus	Gene	Monogenic Syndrome	Inheritance	Blood pressure
1p36.13	CLCNKB	Bartter syndrome, type 3	Autosomal recessive	Low
1p31.1	ATP1A1	Sporadic aldosterone producing adenoma		High
2q36.2	CUL3	Pseudohypoaldosteronism, type IIE	Autosomal dominant	High
3p25.3	VHL	von Hippel-Lindau syndrome	Autosomal dominant	High
3p21.3	CACNA1D	Sporadic aldosterone producing adenoma		High
4q31.2	NR3C2	Hypertension exacerbation in pregnancy, Pseudohypoaldosteronism type I	Autosomal dominant	Low
8q24.3	<i>CYP11B1</i> , <i>CYP11B2</i>	Familial hyperaldosteronism type 1 glucocorticoid remediable aldosteronism,	Autosomal dominant	High
		Corticosterone methyloxidase II deficiency	Autosomal recessive	High
		Steroid 11 $\beta$ -hydroxylase deficiency	Autosomal recessive	High
10q11.2	RET	Multiple endocrine neoplasia, type IIA	Autosomal dominant	High
10q24.3	CYP17A1	17-alpha-hydroxylase deficiency	Autosomal recessive	High
11q24.3	KCNJ5	Familial Hyperaldosteronism type III	Autosomal dominant	High
12p12.3	WNK1	Pseudohypoaldosteronism type IIC Gordon syndrome	Autosomal dominant	High
16p12.2	SCNN1B, SCNN1G	Liddle Syndrome	Autosomal dominant	High
16q13	SLC12A3	Gitelman syndrome	Autosomal recessive	Low
16q22.1	HSD11B2	Apparent Mineralocorticoid Excess		High
Xq28	ATP2B3	Sporadic aldosteroneproducing adenoma		High

### 1.6.2 Candidate gene analysis

Candidate gene analysis predicts from clinical and physiological research over many years those genes affecting blood pressure and tests their importance in study populations. This is illustrated by studies of *CYP11B1* and *CYP11B2* and other genes that affect their expression. Angiotensinogen, which is encoded by the *AGT* gene, a constituent of the renin-angiotensin-aldosterone system, cleaves product of angiotensin I, angiotensin II and angiotensin III which are regulators of BP via water and sodium homeostasis (Padmanabhan, Caulfield et al. 2015). Many SNPs have been identified in the coding and non-coding regions of the *AGT* gene. Although *AGT* SNPs have been reported to associate with hypertension, results have been inconsistent. The SNPs -217AA and -6GG associated with increased risk of hypertension, and a weak linkage was also found for the G-217A and A-6G polymorphisms (Wu, Chiang et al. 2004).

Choi et al identified a *KCNJ5* gene mutation in APA and in hereditary hypertension (Choi, Scholl et al. 2011). To date, 5 different types of *KCNJ5* mutation have been identified and most of them cause depletion in membrane selectivity, causing sodium leakage that leads to membrane depolarization and opening of voltage-gated  $\text{Ca}^{2+}$  channels, as described above (Williams, Monticone et al. 2014).

### 1.6.3 Linkage analysis

The aim of linkage analysis is to identify genomic loci that influence specific characteristics, known as quantitative trait loci (QTL). The best example of linkage studies in hypertension is probably the British Genetic of Hypertension (BRIGHT) study (Caulfield, Munroe et al. 2003). The increased use of genome-wide association studies (GWAS) (see below) has reduced linkage analysis use, but the recent availability of whole-genome sequencing (WGS) may cause it to increase again (Ott, Wang et al. 2015). Linkage is assessed by a specific score called logarithm of the odds (LOD), the

standard score for linkage mapping of major genes, based on disease related phenotypes; positive LOD scores indicate the presence of linkage (Morton 1996).

Identification of specific regions of the chromosome linked to a monogenic trait in hypertension can be performed using linkage analysis by genotyping (Padmanabhan, Caulfield et al. 2015). Louis-Dit-Picard et al combined linkage analysis with whole exome sequencing to identify *KLHL3* gene mutations in familial hyperkalemic hypertension (FHHT) (Louis-Dit-Picard, Barc et al. 2012). A list of linkage studies is provided in Table 1-5.

**Table 1-5: Selected linkage studies in hypertension**

Study	Chromosomal Region	Participant
(Pan, Chen et al. 2000)	17q	59 Han Chinese families in Taiwan
(Rao, Province et al. 2003)	2p	HyperGEN network; 650 African American sibling pairs 915 white sibling pairs
(Province, Kardia et al. 2003)	2p	GenNet, GENOA, HyperGEN, SAPPHIRE network; 6245 participant
(Shmulewitz, Heath et al. 2006)	20p12	2188 participant from Pacific Island of Kosraen, Federated States of Micronesia
(Caulfield, Munroe et al. 2003)	6q	British Genetics of Hypertension (BRIGHT) study; 2010 sibling pairs from 1599 severely hypertensive family
(Koivukoski, Fisher et al. 2004)	2p12-q22.1 3p14.1-q12.3	Metaanalysis in Caucasians

### 1.6.4 Genome-wide association studies

The genome-wide association study (GWAS) identifies genomic variation associated with a specific trait - in particular disease - across the human genome. The method is currently being used to look for association between BP and SNPs distributed throughout the entire genome by linear regression for continuous phenotypes or by logistic regression for dichotomous phenotypes (Ehret and Caulfield 2013). High-throughput genotyping using microarray chips enables the researcher to detect up to a million SNPs in thousands of subjects. GWAS is connected to linkage disequilibrium (LD) for functional variants (Padmanabhan, Newton-Cheh et al. 2012). For example, a study by Padmanabhan et al. showed that rs13333226 associates with hypertension and chronic kidney disease (Padmanabhan, Melander et al. 2010).

Several GWAS have recognised the *CYP17A1* locus as associated with hypertension (Levy, Ehret et al. 2009, Newton-Cheh, Johnson et al. 2009). 17 $\alpha$ -Hydroxylase deficiency is an autosomal recessive defect of the *CYP17A1* gene causing depletion of glucocorticoid and sex steroids with simultaneous mineralocorticoid (DOC) excess (Goldsmith, Solomon et al. 1967, MM Grumbach 2003). Patients present with hypertension and hypokalaemia (Yanase, Simpson et al. 1991, Miller and Auchus 2011). Recently, the focus GWAS has brought to bear on the *CYP17A1* locus has resulted in the identification of common SNPs with functional effects that may explain its association with blood pressure (Diver, MacKenzie et al. 2016).

## **1.7 The nature, synthesis and regulatory role of microRNA.**

### **1.7.1 microRNA**

MicroRNA (miRNA) are small single-stranded non-coding RNAs (ncRNA), 18-22 nucleotides (nt) long, which regulate target messenger RNA (mRNA) levels post-transcriptionally through cleavage or translational repression (Bartel 2004). miRNA bind to a specific 3'untranslated region (3'UTR) located on the target mRNA or, less commonly, to a protein-coding (CDS) or 5'UTR sequence. They are estimated to regulate the transcription of approximately 30% of the human protein-coding genome. The first miRNA to be recognized was the nematode *Caenorhabditis elegans* small non-coding RNA (ncRNA), lin-4, in 1993. This was shown to be an important agent in its development. Many more have since been discovered in many species and they were officially named miRNAs in 2001 by Ruvkun (Ruvkun 2001, Jeffrey 2008). By 2014, 2469 novel human miRNAs had been identified and 1098 of these had been validated experimentally (Friedlander, Lizano et al. 2014). The discovery of miRNA regulation of mRNA transcription has been a huge breakthrough. Over the last 20 years, the number of miRNA studies has grown exponentially, studying mechanisms, function and relevance to disease. The following sections outline the structure, synthesis and action of miRNAs, mainly in the human and with particular reference to adrenocortical function.

### **1.7.2 miRNA structure.**

The biogenesis of miRNAs differs from that of other RNAs since they derive from transcripts that fold back on themselves to form a distinctive hairpin structure due to sequence complementary (Bartel 2004). See Figure 1-15.

### **1.7.3 miRNA biogenesis.**

miRNA biogenesis is summarised in Figure 1-16 and in the following sections.

### 1.7.3.1 In the nucleus.

miRNAs are encoded by DNA which may be situated in introns or exons, or else be scattered among intergenic sequences (Jeffrey 2008). miRNAs are transcribed from the genome by RNA polymerase II or RNA polymerase III to form a primary-miRNA (pri-miRNA) transcript (Lee, Kim et al. 2004, Borchert, Lanier et al. 2006). Pri-miRNA is several kilobases long and contains at least one hairpin-like structure, or often several stem-loop structures (a polycystronic pri-miR). Polycystronic pri-miRNAs are called clusters; they will be discussed later. A pri-miRNA contains one stem structure consisting of a polyadenylated tail (poly(A)) at the 3' end and a 7-methyl-guanylate cap at the 5' end (Cai, Hagedorn et al. 2004).

Regulation of pri-miRNA transcription involves adenosine deaminase action on RNA (ADAR). This deaminase catalyses conversion of adenosine nucleotides to inosine in an editing process known as A-to-I (Luciano, Mirsky et al. 2004). The editing process can affect miRNA processing by preventing dsRNA from being recognized and cleaved by Dicer (Scadden 2005), which would impair miRNA maturation (Kawahara, Megraw et al. 2008). pri-miRNA processing in mammalian cells requires heme. Unprocessed pri-miRNAs are quickly degraded via an as-yet unknown pathway so that they do not accumulate in the nucleus (Weitz, Gong et al. 2014).



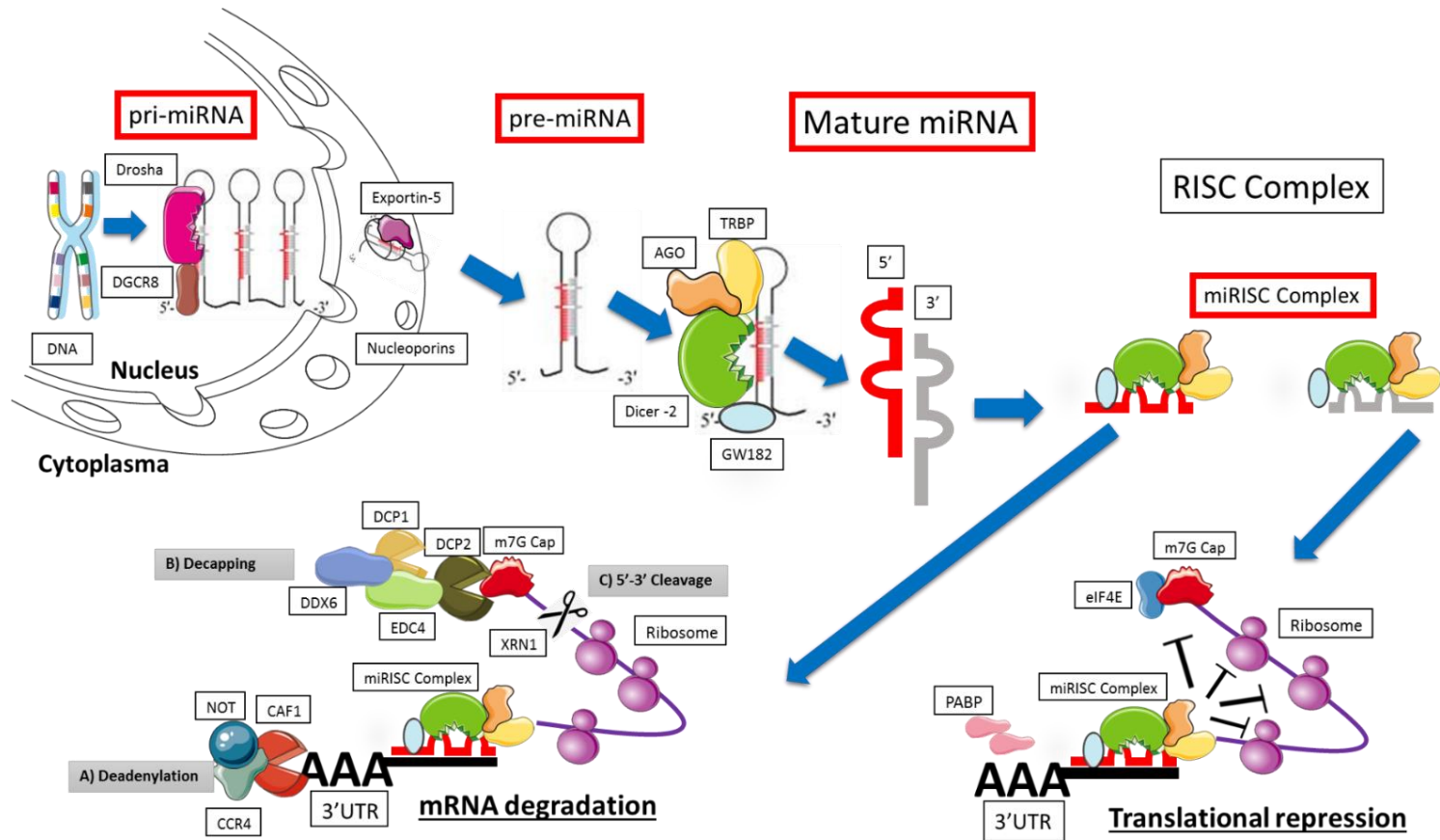


**Figure 1-16: miRNA biogenesis from genomic DNA illustration.**

The biogenesis starts with pri-miRNA transcription from genomic DNA. The stem-loop sequence of the pri-miRNA is cleaved by Drosha with DGCR8 to form pre-miRNA. The pre-miRNA is then exported to the cytoplasm by Exportin-5 through nucleoporin. It is further processed to a mature miRNA sequence by Dicer-2 with AGO2 and TRBP assistance. The mature miRNA is incorporated by the RISC complex and binds mRNA targets to cause translational repression or mRNA degradation. Modified from (Sethi, Kulkarni et al. 2013).

The stem-loop sequence of pri-miRNA is cleaved at the stem junction with the hairpin structure by RNase III Drosha to form precursor-miRNA (pre-miRNA). Drosha requires the DiGeorge syndrome critical region in gene 8 (DGCR8) which is a double-stranded RNA-binding protein in Homo sapiens. (This function is served by Pasha in *Drosophila melanogaster* and *C. elegans* (Denli, Tops et al. 2004, Han, Lee et al. 2004, Lee, Kim et al. 2004).) Drosha and DGCR8, which are highly conserved in animals, form the large microprocessor complex. The C-terminal domain of DGCR8 interacts with the middle domain of Drosha to stabilize the complex (Yeom, Lee et al. 2006). There are 3 alternative models describing how Drosha identifies a pri-miRNA:

- (a) Drosha identifies its cleavage site on the 5' end of pri-miRNA due to significant enrichment of 2-4 nt symmetrical internal loops near the cleavage site (Warf, Johnson et al. 2011).
- (b) Drosha recognizes the cleavage site by its position: ~11 bps from the stem-loop junction of the miRNA. DGCR8 may act as a molecular anchor that measures the distance (Han, Lee et al. 2006).
- (c) Drosha crops by reference to the start of the terminal loop of the pri-miRNA. Even a slight variation in the structure of the terminal loop will impair miRNA processing in the nucleus (Zhang and Zeng 2010).

Apart from Drosha/DGCR8, there are other proteins included in the microprocessor complex such as SMAD proteins (Blahna and Hata 2012), the DEAD-box helicases p68 (known as DD5X) and p72 (DDX17) (Fukuda, Yamagata et al. 2007), heterogeneous nuclear ribonucleoproteins and the Ewing's sarcoma family of proteins which contains a RNA recognition motif (RRM) and a zinc-finger domain (Gregory, Yan et al. 2004). This microprocessor complex then cleaves the pri-miRNA to a shorter 60-70nt hairpin known as precursor-miRNA (pre-miRNA), a double-stranded RNA hairpin molecule, consisting of a 2-nucleotide 3' overhang with an hydroxyl group and a 5' phosphate group with a region of imperfect base-pairing (Cullen 2004). The pre-miRNA is exported to the cytoplasm for further processing.

### 1.7.3.2 Nucleus-cytoplasm transportation

The nuclear envelope (NE) separates the nucleus from the cytoplasm. Pre-miRNAs are exported from the nucleus into the cytoplasm through the central channel of nuclear pore complexes (NPCs), termed nucleoporins, in the nuclear envelope. Pre-miR transport depends on Exportin 5 (Exp5) or importin  $\beta$ , a specific receptor that recognizes NPCs and interacts with the small Ran GTPase, a co-factor that controls the direction of miRNA transport. Exp5 belongs to the karyopherin family whose members play a significant general role in the nuclear export of noncoding RNAs including tRNAs, snRNAs and rRNAs (Lei and Silver 2002). Exportin-5 recognizes RNAs containing a minihelix structure, a cis-acting export element that consists of a double-stranded stem which has more than 14 nucleotides and bears a base-paired 5' end and an approximate 3-8 nucleotide protruding 3' end (Gwizdek, Ossareh-Nazari et al. 2004). The exportin-5-Ran GTPase complex exports the pre-miRNA to cytoplasm through the nucleoporins.

### 1.7.3.3 Cytoplasmic processing

Once in the cytoplasm, pre-miRNA is further processed by RNase III Dicer to mature miRNA, approximately 22 nucleotides long. Dicer is a highly conserved RNase which acts on specific double-stranded RNA (dsRNA) to generate small regulatory RNAs (srRNAs), which include miRNAs. Dicer has 2 main domains, C-terminal and N-terminal, which each have specific properties and functions (Figure 1-17). The C-terminal domain comprises a large helicase domain which can differentiate between a perfect duplex and a hairpin structure in RNA (Doyle, Badertscher et al. 2013), and acts as an autoinhibitor, needed for production of small RNAs. This is followed by a small domain of unknown function (DUF283). Plant studies suggest that DUF may mediate protein-protein interaction with Dicer cofactors and may be involved in dsRBD folding and the PAZ domain, a conserved nucleic acid binding structure that plays a vital role in the docking of the 2nt 3' overhang dsRNA into the Dicer. (Sawh and Duchaine 2012). The N-terminal consists of RNase IIIa and IIIb together with the double-

stranded RNA binding domain (dsRBD) which differentiates between pre-miRNA and dsRNA substrate (Wostenberg, Lary et al. 2012); this may stabilize the interaction between Dicer and its substrate RNA (Zhang, Kolb et al. 2004). Deletion of human dsRBD significantly reduces Dicer's ability to cleave RNAs (Ma, MacRae et al. 2008). The distance between the PAZ and RNase III domains is a 'molecular ruler' which Dicer uses to generate RNAs of an exact length (Figure 1-17) (Sawh and Duchaine 2012).

miRNA interacts with TRBP and Argonaute 2 (AGO2), one of the components of the RNA-inducing silencing complex (RISC) to cleave pre-miRNA and form mature miRNA. TAR RNA-binding protein (TRBP) consists of three-double stranded RNAs, and is an important component of the Dicer-containing complex. TRBP associates with Dicer and AGO2 to form a complex catalysing the cleavage process of pre-miRNA. A study has shown that TRBP knockdown lead to destabilization of Dicer and represses miRNA synthesis (Chendrimada, Gregory et al. 2005).

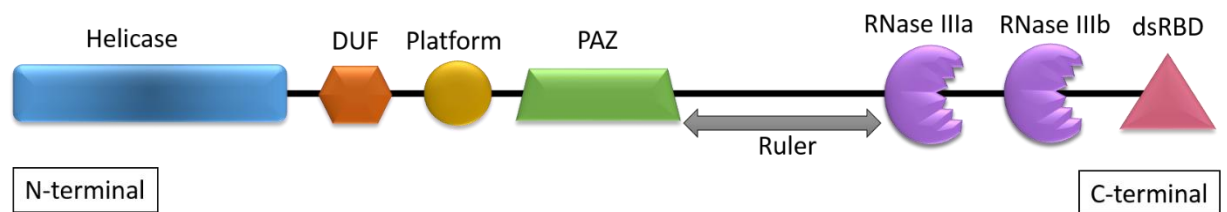


**Figure 1-17: Dicer structure. Adapted from (Sawh and Duchaine 2012).**

#### 1.7.3.4 Argonaute Loading

The process of Argonaute loading of small RNAs differs between species (Hutvagner and Simard 2008). The main function of Argonaute is miRNA maturation. It is a highly conserved protein complex consisting in mammals of four components: AGO1, -2, -3 and -4. However, only AGO2 has a cleavage function and is relevant to siRNA regulation (Liu 2004). It consists of four domains: the N-terminal, PAZ, Mid and PIWI. The PAZ domain binds to the 3' end of miRNAs and can distinguish small regulatory RNAs such as miRNA from degraded RNAs by their characteristic 3'-overhang (Hutvagner and Simard 2008). The PIWI domain acts as a binding pocket for the 5' end of miRNA (Pillai, Bhattacharyya et al. 2007). Argonaute forms a complex with the RISC-loading complex (RLC) through an interaction between Dicer-2 and AGO2. It cleaves the

passenger strand of the small-interference RNA (siRNA) (Hutvagner and Simard 2008) leaving the guide strand to form the active complex referred to as the miRNA-containing ribonucleoprotein particle (miRNP) (Ender and Meister 2010). The selection of RNA strand depends on the thermodynamic stability of the 5' end of the small RNA. This is known as the 'asymmetry rule'. The less stable 5'-end will be incorporated into the miRNP and the opposite strand, referred to as miRNA\* (miRNA star) or the passenger strand, is degraded (Hutvagner and Simard 2008, Ender and Meister 2010). There are many databases available which predict the probability and strength of miRNA:mRNA interaction on the basis of thermodynamic properties, including Ingenuity Pathway Analysis.

### **1.7.3.5 miRNA Target Repression or Destruction**

Mature miRNAs can either induce the degradation of specific mRNAs or repress their translation (Wang, Liang et al. 2008). They achieve this as part of an RNA-induced silencing complex (RISC), which binds partially to a complementary site located within the 3'UTR of its mRNA target. Although most of metazoan miRNA targets the 3'UTRs of mRNA (Bartel 2009), targeting can also occur at the 5'UTR and open reading frames (ORFs) (Kloosterman, Wienholds et al. 2004). The most important factor determining mRNA destabilization or repression is the strength of complementarity between the miRNA and the mRNA target. Perfect complementarity leads to endonucleolytic cleavage, mediated by AGO2, whereas a mismatched bond in the central region of the miRNA leads to translational repression (Ender and Meister 2010).

#### **1.7.3.5.1 Translational Repression**

miRNA can repress translation at the initiation step or at the post-initiation phase (Petersen, Bordeleau et al. 2006). Several mechanisms have been suggested to explain how miRNA regulates mRNA translation, including the dissociation of eIF4 from the 5'terminal m7G cap of mRNA, blocking of the 60S ribosome subunit, interference of the eIF4 complex's function and repression of the elongation step (Petersen, Bordeleau et al. 2006, Filipowicz, Bhattacharyya et al. 2008, Carthew and Sontheimer 2009). Another study reported that AGO proteins compete with eIF4E to binding the 5'cap and repress translation (Kiriakidou, Tan et al. 2007).

#### 1.7.3.5.2 mRNA Degradation

Disruption of the binding of GW182 to eIF4G (Eukaryotic Translation Initiation Factor 4 Gamma) and the PABP (poly-A binding protein) can inhibit translation initiation and preventing circularisation (Gu and Kay 2010). At the 3'UTR of target mRNA, miRNA recruits Argonaute to interact with GW182 which mediates deadenylation and shortens the poly(A) tail. GW182 and the AGO1 complex recruit deadenylase, which is necessary for the removal of the m7G cap to disrupt translation. This is further illustrated by a study showing GW182 depletion improves mRNA stability (Pillai, Bhattacharyya et al. 2007). Other *in vivo* and *in vitro* studies report that miRISC recruits NOT, (CAF1 Chromatin Assembly Factor 1) and CCR4 (Chemokine (C-C Motif) Receptor 4) to remove the 3' poly(A) tail from target mRNA (deadenylation) (Behm-Ansmant, Rehwinkel et al. 2006, Wu, Fan et al. 2006). This is followed by a decapping process performed by DCP1 (Decapping MRNA 1), DCP2 (Decapping MRNA 2) along with EDC4 (Enhancer of MRNA decapping 4) and DDX6 (DEAD (Asp-Glu-Ala-Asp) Box Helicase 6) (Figure 1-16). Decapped mRNAs are then removed by XRN1 (exonuclease) in the cytoplasm (Behm-Ansmant, Rehwinkel et al. 2006, Wu, Fan et al. 2006).

#### 1.7.4 miRNA Clusters

miRNA clusters are derived from capped and polyadenylated pri-miRNA precursors (Cai, Hagedorn et al. 2004). The majority of miRNAs are encoded within intergenic regions but some are encoded within mRNA introns or in ncRNA genes (Rodriguez, Griffiths-Jones et al. 2004). There is much evidence to suggest that clustered miRNAs are transcribed as polycistrons from long primary transcript miRNAs, producing one or more hairpin precursors that show great sequence similarity. (Tanzer and Stadler 2004, Altuvia, Landgraf et al. 2005). One study showed that if 3000nt is used as a distance threshold, 37% of human miRNAs are in such clusters. The percentage increases to almost 50% if the distance threshold is set at 10000 nt. The miRNA clusters have a highly conserved pattern, suggesting that the expression of the constituent miRNAs is co-regulated (Altuvia, Landgraf et al. 2005). miRNA are more clustered than other non-coding RNA like snoRNA and tRNA (Altuvia, Landgraf et al. 2005).

A microarray profiling study showed that proximal pairs of miRNAs in clusters are usually co-expressed. miRNAs encoded less than 50kb apart are usually derived from the same transcript. The correlation of expression is reduced significantly if this distance exceeds 50 kb. However, there are some miRNAs clusters spanning distances of more than 50 kb that can still be highly correlated; these include miR-7-miR-9 (>750 kb) and miR-128-miR-138 (8 Mb) (Baskerville and Bartel 2005). Another study, using the expressed sequence tag method, also showed that distant miRNAs such as miR-100, let-7 and miR-125 may reside on the same transcript (Altuvia, Landgraf et al. 2005).

miRNAs within a cluster may exert a concerted action. The polycistronic miRNA cluster, miR-17-92, has a strong correlation with a variety of tumours in humans and animals, including Burkitt's lymphoma (Woods, Thomson et al. 2007), colorectal carcinoma (Tsuchida, Ohno et al. 2011), lung carcinoma (Hayashita, Osada et al. 2005) and ovarian cancer (Fan, Liu et al. 2010) and contributes to the regulation of angiogenesis. Here, VEGF, an angiogenic chemokine, induces cluster expression and leads to a reduction in the levels of the angiogenic molecule, thrombospondin-1 levels (Suárez, Fernández-Hernando et al. 2008). In *Drosophila melanogaster*, miRNA clusters tend to target the same genes (Grün, Wang et al. 2005). Interestingly, one study reported that TFs regulating a particular miRNA gene tend also to regulate its mRNA target (Wang, Li et al. 2011). Thus, clustered miRNAs might regulate a common pathway by targeting the same individual gene or by targeting several genes in the same pathway.

### 1.7.5 miRNA in the Circulation

miRNA is transcribed and regulated within in the cell. However, it can also be detected extracellularly, particularly in the blood (Valadi 2007, Pegtel, Cosmopoulos et al. 2010, Diehl, Fricke et al. 2012, Raposo and Stoorvogel 2013, Eldh, Olofsson Bagge et al. 2014, Huang and Chen 2014, Melo, Sugimoto et al. 2014). miRNA can be transported into the circulation in a heterogeneous group of cell-released microvesicles, including exosomes, microparticles and apoptotic membranes (Figure 1-18). Exosomes are lipid bilayers that transport protein, lipids or nucleic acids, including miRNA and mRNA, from the cell cytosol into the extracellular compartment (Valadi 2007). They are small, ranging from 50-90 nm, endocytic in origin and arise from the fusion of multivesicular endosomes (MVE) with plasma membrane (Harding, Heuser et al. 1984). Almost all cell types produce exosomes through the fusion of MVE with cell membranes from a variety of sources, including B cells, T cells, mast cells, platelet, oligodendrocytes, Schwann cells, intestinal cells and tumour cells (Raposo, Nijman et al. 1996, Raposo, Tenza et al. 1997, Blanchard, Lankar et al. 2002, Valadi 2007, Raposo and Stoorvogel 2013, Sluijter and van Rooij 2015). Pre-miRNAs in a complex with Dicer, AGO2 and TRBP are present in exosomes of cancer cells and mediate silencing of mRNA in the specific target cell transcriptome (Melo, Sugimoto et al. 2014). miRNAs are protected by exosomes from degradation by RNase which is abundant in the blood (Pegtel, Cosmopoulos et al. 2010). miRNAs within exosomes are therefore stable in the circulation and might provide a convenient biomarker in clinical diagnosis.

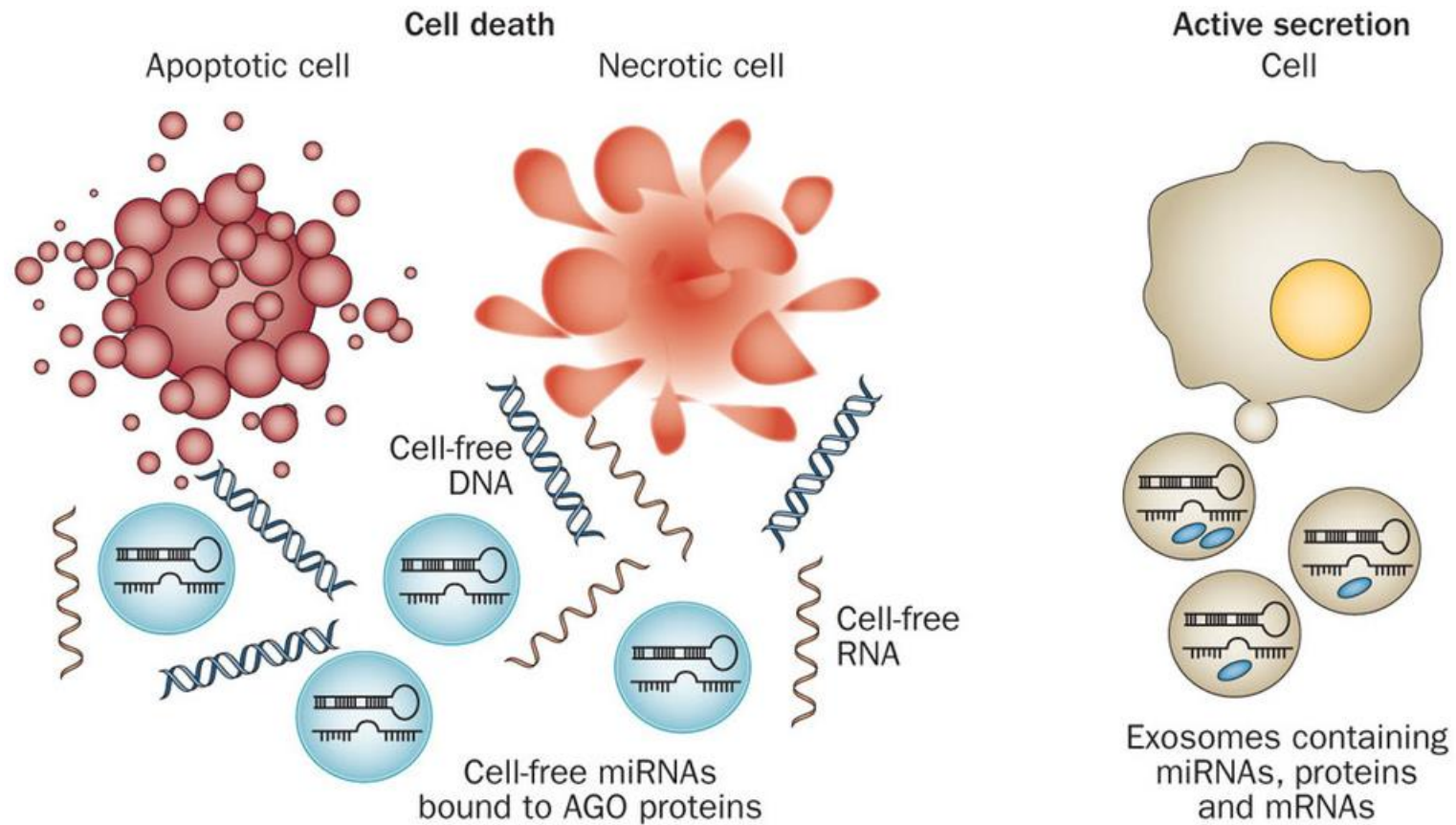


**Figure 1-18: Cell death through apoptosis or necrosis processes.**

These processes release long DNA strands, RNA transcripts and the miRNA-AGO complex within apoptotic bodies. miRNA also can be excreted from viable cells through exosomes. Adapted from (Schwarzenbach, Nishida et al. 2014).

## 1.7.6 miRNA in Adrenal Tumours

Most adrenal tumours are clinically silent and therefore diagnosis and treatment are frequently delivered at a later stage of the disease when effective treatment is likely to have a poorer outcome. At present, there is no reliable method of differentiating benign from malignant tumours except the identification of distant metastases (Gimm, DeMicco et al. 2012). The principal treatment for unilateral APA is laparoscopic adrenalectomy. Most patients are diagnosed through extensive investigation, including computed tomography (CT) imaging, adrenal venous sampling (AVS) and histological examination of excised tissue, all of which require expensive specialist medical expertise. A simple screening method facilitating early diagnosis would be valuable. miRNA might provide the basis for such a method (Igaz, Igaz et al. 2015).

### 1.7.6.1 miRNA in adrenocortical carcinoma

Differential expression of miRNAs has been reported between normal adrenal tissue and both benign and malignant adrenocortical tumours, as shown in Table 1-6 and Table 1-7 (Soon, Tacon et al. 2009, Özata, Caramuta et al. 2011, Patterson, Holloway et al. 2011, Schmitz, Helwig et al. 2011, Chabre, Libé et al. 2013, Patel, Boufraquech et al. 2013, Szabo, Luconi et al. 2014). It is reasonable to surmise that these differentially-expressed miRNAs may be involved in tumourigenesis and/or tumour function. In adrenocortical carcinoma (ACC), miR-483-3p and miR-483-5p which are overexpressed have been proposed as oncogenic miRNAs (oncomiRs) (Soon, Tacon et al. 2009, Patterson, Holloway et al. 2011, Chabre, Libé et al. 2013). Inhibition of both miRNAs *in vitro* decreased cell proliferation (Özata, Caramuta et al. 2011). The miR-483 gene is located on chromosome 11, within the second intron of the *IGF2* gene, which is highly expressed in ACC (Bertherat and Bertagna 2009). Increased expression of IGF-2 could possibly stimulate cellular proliferation rate and tumour development (Veronese, Lupini et al. 2010). This hypothesis is supported by the results of an *in vitro* study that showed IGF-2 inhibition by IGF-1 receptor blockade reduces cell proliferation (Barlaskar, Spalding et al. 2009). However, miR-483 overexpression is not exclusive to adrenocortical tumours and is also overexpressed, for example, in colon, breast and liver carcinomas and in Wilms' tumours (Veronese, Lupini et al. 2010).

In addition to miR-483 upregulation, miR-503 (Soon, Tacon et al. 2009, Özata, Caramuta et al. 2011), miR-210 (Özata, Caramuta et al. 2011, Szabo, Luconi et al. 2014, Velázquez-Fernández, Caramuta et al. 2014), miR-675 (Schmitz, Helwig et al. 2011) and miR-21 (Özata, Caramuta et al. 2011) are all overexpressed in ACC. High expression of miR-503 is significantly associated with shorter survival in ACC patients (Özata, Caramuta et al. 2011), parathyroid carcinoma (Corbetta, Vaira et al. 2010) and retinoblastoma (Zhao, Yang et al. 2009). miR-210 plays a vital role in angiogenesis (Zeng, He et al. 2014), cell proliferation (Zuo, Wen et al. 2015) and is associated with poor cancer survival (Hong, Yang et al. 2012). miR-21 is highly expressed in most human tumours, including ACC (Özata, Caramuta et al. 2011). A pharmacological miR-21 antagonist might therefore benefit sufferers from many cancers, especially those for which there is as yet no specific treatment (Sicard, Gayral et al. 2013).

In contrast, miR-195 (Soon, Tacon et al. 2009, Özata, Caramuta et al. 2011, Patterson, Holloway et al. 2011, Chabre, Libé et al. 2013, Velázquez-Fernández, Caramuta et al. 2014), miR-335 (Soon, Tacon et al. 2009, Schmitz, Helwig et al. 2011, Chabre, Libé et al. 2013) and miR-497 (Özata, Caramuta et al. 2011, Chabre, Libé et al. 2013, Velázquez-Fernández, Caramuta et al. 2014) are all downregulated in ACC compared to NA and ACA. miR-195 induces cell cycle arrest by targeting the cell cycle genes, *Cdc25l* and *Ccnd*, in skeletal muscle stem cells (Sato, Yamamoto et al. 2014) and acts as a tumour suppressor in hepatocellular carcinoma cells (HCC) by blocking the G1/S transition through several targets, including CCND1, CDK6 and E2F3, thereby suppressing the Rb-E2F signalling pathway (Xu, Zhu et al. 2009). miR-335 is downregulated in human HCC and inhibits HCC proliferation and migration through ROCK1 regulation (Liu, Li et al. 2015). miR-497 also suppresses cell proliferation by decreasing the S phase of cell cycle and inhibiting cell migration and tissue invasion in pancreatic malignancy (Xu, Wang et al. 2014).

**Table 1-6: Previous studies analysing miRNA expression in ACC and ACA.**  
(ACC: adrenocortical carcinoma, ACA: adrenocortical adenoma).

Author	miRNA expression (ACC vs ACA)	
	Up-regulated	Down-regulated
Szabo et al 2014	miR-100 miR-181b miR-184 miR-210 miR-483-5p	
Patel et al 2013	miR-34a miR-483-5p	
Chabre et al 2013	miR-139-5p miR-148b miR-376a miR-483-5p miR-503 miR-508-3p miR-509-3p miR-513a-5p miR-514 miR-93	miR-195 miR-199a-3p miR-199a-5p miR-335 miR-376a miR-497
Patel et al 2013	miR-34a miR-483-5p	
Patterson et al 2011	miR-1246 miR-1308 miR-483-5p miR-642  miR-665	let-7a let-7d let-7f let-7g miR-100 miR-125a-5p miR-125b miR-126 miR-1290 miR-193b miR-195 miR-214 miR-26a miR-26b miR-29a miR-34a miR-600 miR-768-5p
Schmitz et al 2011		miR-139-3p miR-335  miR-675

**Table 1-7: Previous studies analysing miRNA expression in ACC and ACA.****(ACC: adrenocortical carcinoma, ACC: adrenocortical adenoma).**

Author	miRNA expression (ACC vs ACA)	
	Up-regulated	Down-regulated
Deniz M özata et al 2011	let-7a let-7d let-7e let-7f let-7g let-7i miR-106b miR-10b miR-1202 miR-125a-5p miR-127-3p miR-1275 miR-136 miR-140-5p miR-15b miR-1975 miR-21 miR-210 miR-29a miR-29b miR-320b miR-320c miR-320d miR-331-3p miR-361-5p miR-376c miR-410 miR-424 miR-432 miR-483-3p miR-483-5p miR-487b miR-503 miR-506 miR-513a-5p miR-513b miR-513c miR-514 miR-720 miR-886-3p	miR-101 miR-151-3p miR-195 miR-1974 miR-1977 miR-199a-3p miR-199a-5p miR-202 miR-214 miR-29c* miR-30a miR-494 miR-497 miR-557 miR-572 miR-877* miR-99a
Soon et al 2009	miR-339-5p miR-130b miR-483-5p miR-106b miR-148b miR-93 miR-135a miR-320a miR-503 miR-450a miR-542-3p miR-143 miR-181b miR-542-5p	miR-335 miR-195 miR-557 miR-708 miR-29* miR-617 miR-647 let-7c miR-202
Tombol et al 2009	miR-184 miR-503 miR-210	miR-511 miR-214

### 1.7.6.2 miRNA in aldosterone regulation and adrenocortical adenoma (ACA)

In primary aldosteronism (PA), the adrenal gland secretes inappropriately high levels of aldosterone. Aldosterone excess increases cardiovascular morbidity and mortality independent of elevated blood pressure.

Aldosterone-regulating miRNAs have already been identified in several studies. Romero et al showed that miR-21 increases aldosterone secretion (Romero, Plonczynski et al. 2008) suggesting it may be repressing the expression of genes that themselves inhibit aldosterone biosynthesis (As miRNA is only capable of repression, miR-21 cannot directly stimulate *CYP11B2* mRNA synthesis). However, Robertson et al. demonstrated that miRNA-24 directly inhibits *CYP11B2* (and *CYP11B1*) mRNA expression, thereby significantly altering aldosterone production *in vitro* (Robertson, MacKenzie et al. 2013).

Several microarray studies, have been validated by subsequent qPCR studies, showing differences in miRNA expression between normal adrenal (NA) and adrenocortical adenoma (ACA) tissue, as shown in Table 1-8 (Soon, Tacon et al. 2009, Tömböl, Szabó et al. 2009, Özata, Caramuta et al. 2011, Patterson, Holloway et al. 2011, Robertson, MacKenzie et al. 2013, Velázquez-Fernández, Caramuta et al. 2014, He, Cao et al. 2015). In qPCR studies, mir-139-5p is more highly expressed in APA than in NA and has been proposed as a marker to differentiate APA from non-functioning adenomas (NFA) (Velázquez-Fernández, Caramuta et al. 2014). mir-210 was significantly more highly expressed in ACA than in NA in two independent studies (Özata, Caramuta et al. 2011, Velázquez-Fernández, Caramuta et al. 2014). miR-210 has been shown to be important in other carcinoma such as laryngocarcinoma (Zuo, Wen et al. 2015) and has been proposed as potential biomarker in glioma prognosis and diagnosis (Shang, Hong et al. 2014).

Significant downregulation of miR-375 and miR- 7 in ACA compared to NA has been reported in 3 validated independent studies (Soon, Tacon et al. 2009, Tömböl, Szabó et al. 2009, He, Cao et al. 2015). miR-375 targets metadherin (MTDH), also known as Astrocyte Elevated Gene-1, which is involved in the tumorigenesis of various tumours, including those of breast (Li, Zhang et al.

2008), prostate, kidney, bladder (Wang, Wei et al. 2014) and thyroid (Li, Wang et al. 2014). *MTDH* protein is upregulated in APA while endogenous downregulation of the *MTDH* gene by mir-375 suppresses Akt-Ser473 phosphorylation (He, Cao et al. 2015), a reaction which is implicated in cell growth, proliferation and survival (Bayascas and Alessi).

Aldosterone downregulates miR-335-5p, miR-290-5p and miR-1983 and also enhances epithelial sodium channel (ENaC) transport in mouse cortical collecting duct (mCCD) epithelial cells (Edinger, Coronello et al. 2014); aldosterone's effect may be partially accomplished by this mechanism.

There is now strong evidence that aldosterone production is at least partly controlled by miRNAs. The full extent of microRNA involvement merits further study.

**Table 1-8: Previous studies analysing miRNA expression in ACA vs NA.  
(ACA: adrenocortical adenoma, NA: Normal Adrenal).**

Author	miRNA expression (ACA vs NA)	
	Up-regulated	Down-regulated
He, Juan et al 2015	miR-29b miR-29c	miR-7 miR-375
Velázquez-Fernández et al 2014	miR-10b miR-139-5p miR-186 miR-195 miR-21 miR-210 miR-30e mir-34a miR-497 miR-520d-3p	
Robertson et al 2013	miR-34c-3p	miR-10b miR-24
Patterson et al 2011		miR-100
Deniz M özata et al 2011	miR-195 miR-21 miR-210 miR-497	
Soon et al 2009		miR-7
Tombol et al 2009		miR-375

## **1.7.7 miRNA in clinical trials**

### **1.7.7.1 Miravirsen (miR-122 antagonist) in hepatitis C**

miR-122 is highly expressed in hepatocellular cells and plays a critical role in hepatitis C virus (HCV) RNA stability by binding to two specific target sites at the 5' UTR of the HCV genome (Henke, Goergen et al. 2008). This generates an oligomeric miR-122-HCV complex that protects the HCV genome from degradation and increases its affinity for its target (Janssen, Reesink et al. 2013). The binding sites for miR-122 are conserved across HCV subtype and genotypes (Janssen, Reesink et al. 2013).

In 2010, Miravirsen, a specific mir-122 blocker, was introduced by Santaris Pharma for phase II clinical trials for hepatitis C treatment via a subcutaneous route. Miravirsen is a construct of locked nucleic acid (LNA) ribonucleotides that is complementary to miR-122. It is the first miRNA antagonist to be used in a clinical trial. The complementary binding of Miravirsen and miR-122 reduces HCV replication in chimpanzees (Lanford, Hildebrandt-Eriksen et al. 2010) and humans (Janssen, Reesink et al. 2013). Miravirsen targets the stem structure of miR-122 precursors and disrupts the processing of pri-122 and pre-miR-122 by inhibiting Drosha and Dicer (Gebert, Rebhan et al. 2014). In the phase 2 clinical study, commenced at several international centres, Miravirsen decreased the HCV load in the majority of patients and no adverse events were reported during the 18-week trial (Janssen, Reesink et al. 2013). However, a recent study reported that the mir-122 antagonist's ability to inhibit HCV replication is severely reduced in the presence of any HCV mutation at the 5'UTR, even alteration of a single nucleotide (Israelow, Mullokandov et al. 2014). Therefore, future Miravirsen and miR-122-based medication for HCV may need to be customized according to the HCV sequence.

### **1.7.7.2 MRX-34 (miR-34a mimic) in liver cancer and liver metastases**

miR-34a is a tumour suppressor. It is either lost or downregulated in many malignancies (Bouchie 2013). It stimulates G1 cell cycle arrest, senescence, apoptosis and acts as a tumour silencer because of the irregular CpG methylation

of its promoter (Lodygin, Tarasov et al. 2008). miR-34 regulates many cancer-related genes, including *BCL2*, *CDK4/6*, *WNT 1/3*, *NOTCH-1* and *β-catenin*, and plays an important role in the p53 tumour suppressor pathway (Beg, Borad et al. 2014).

In 2013, Mirna Therapeutics, a biotechnology company in Texas, pioneered the Phase 1 clinical study of the first miR-34a mimic (MRX34) in patients with unresectable primary liver cancer or metastases with liver involvement (Christoph 2013). MRX-34, a miR-122 mimic, is a double-stranded RNA that can be given by the intravenous route. It is delivered within the special licensed liposome, Smarticles (Bouchie 2013) to avoid degradation by RNase in bloodstream. The study followed the standard protocol for oncology study design with two phases: dose-escalation and enrichment (Christoph 2013). The aim was to restore normal endogenous mir-122 tumour suppressor function (Bouchie 2013). MRX34 prescription showed a manageable safety profile in these patients.

## 1.8 Conclusion

Corticosteroid hormones are important in blood pressure regulation and there is evidence that their biosynthesis is regulated in part by microRNA. Now, in order to clarify which miRNAs regulate this system, I will analyse the microRNA profiles of normal adrenal (NA) and aldosterone-producing adenoma (APA) tissue, and also of adrenocortical cells stimulated to produce aldosterone in order to identify key changes. By investigating such differences *in vivo* and *in vitro*, in combination with bioinformatic analysis, I intend to identify microRNAs that affect systems relevant to APA pathology, including steroidogenesis and cholesterol biosynthesis.

## 1.9 Aims

1. To analyse changes to the microRNA profile when aldosterone production is altered in APA tissue and in stimulated H295R adrenocortical cells.
2. To use bioinformatic analysis to predict those miRNAs most likely to affect and regulate the system.
3. To experimentally validate these bioinformatic findings.

## **2 Materials and Methods**

## **2.1 Cell Culture**

### **2.1.1 H295R**

H295R cells were originally derived from a 48-year-old woman who presented with malignant adrenocortical carcinoma (Gazdar, Oie et al. 1990). Three separate strains (H295R strain 1, 2 and 3) and the monoclonal HAC15 cell line were later derived from this original line and were provided to us courtesy of Professor William Rainey (Medical College of Georgia, GA, U.S.A). Each has its own distinctive culture conditions and slight variations in their characteristics (Wang and Rainey 2012).

### **2.1.2 Culturing Technique**

Cell culture was performed in monolayer under sterile conditions in tissue culture flasks, with specific medium and supplement at 37°C in a humidified chamber (5% CO<sub>2</sub>, 95% air). The cells were cultured until approximately 70-80% confluent, then the medium was removed and the cells washed with phosphate buffered saline (PBS) solution. To detach cells from the flask surface, Trypsin-EDTA 0.25% (Ambion®, Life Technologies, Paisley) was added for 5 minutes. 5 ml DMEM-F12 medium was then added to inactivate the trypsin and the cells were centrifuged at 1500g for 5 minutes. The supernatant was removed and the cell pellet was re-suspended in new complete growth medium and aliquoted into a new flask (T150). Cells were fed every 3-4 days.

Cells were maintained in Dulbecco's modified Eagle medium (DMEM) with F12 supplement (Invitrogen, Paisley, U.K). Specific medium for each strain is specified in Table 2-1:

Table 2-1: H295R Strains, HAC 15 and their medium specification.

Cell Type	Medium	Serum/ Serum Replacement Agent	Antibiotics
H295R Strain 1	DMEM-F12 containing HEPES buffer, L-Glutamine and pyridoxine HCl medium (Life Technologies, Paisley, U.K)	5% NuSerum (VWR Jencon, Leicestershire, U.K)	1% of 1 IU penicillin, 100 µg/ml Streptomycin (Invitrogen, Paisley, U.K) 0.5 ml Gentamicin (Life Technologies, Paisley, U.K)
H295R Strain 2	DMEM-F12 containing HEPES buffer, L-Glutamine and pyridoxine HCl medium (Life Technologies, Paisley, U.K)	1% insulin-transferrin -selenium (ITS) (BD Biosciences, Paisley, U.K) 2.5% Ultrosor G (Corning, France)	1% of 1 IU penicillin, 100 µg/ml Streptomycin (Invitrogen, Paisley, U.K) 0.5 ml Gentamicin (Life Technologies, Paisley, U.K)
H295R Strain 3	DMEM-F12 containing HEPES buffer, L-Glutamine and pyridoxine HCl medium (Life Technologies, Paisley, U.K)	10% Cosmic Calf Serum (Thermo Fisher Scientific, Erembodegem, Belgium)	1% of 1 IU penicillin, 100 µg/ml Streptomycin (Invitrogen, Paisley, U.K) 0.5 ml Gentamicin (Life Technologies, Paisley, U.K)
HAC 15	DMEM-F12 containing HEPES buffer, L-Glutamine and pyridoxine HCl medium (Life Technologies, Paisley, U.K)	1% insulin-transferrin -selenium (ITS) (BD Biosciences, Paisley, U.K) 2.5% Ultrosor G (Corning, France)	1% of 1 IU penicillin, 100 µg/ml Streptomycin (Invitrogen, Paisley, U.K) 0.5 ml Gentamicin (Life Technologies, Paisley, U.K)

### 2.1.3 Cryopreservation

The cells could be cryopreserved for long-term storage by pelleting, as in section 2.1.2, then resuspending the cells in complete growth medium supplemented with 10% dimethyl sulphoxide (DMSO) (Thermo Fisher Scientific, Loughborough, U.K) to prevent ice crystal formation. Cell suspensions were then aliquoted and transferred to cryovials and frozen at -80°C using isopropanol and Nalgene Cryo-Container (Thermo Fisher Scientific, Loughborough, U.K) before being placed in liquid nitrogen for long-term storage.

### 2.1.4 Cell Resuscitation

Cells from liquid nitrogen were thawed on ice and slowly brought to room temperature before transfer to a 37°C water bath. The cell suspension in the vial was aliquoted to a universal container with 10 ml fresh growth medium. This was centrifuged at 1500 g for 5 minutes and the medium containing DMSO removed. The cell pellet was then resuspended with 5 ml fresh medium and transferred to a T25 flask (Corning) and cultured as described in section 1.2.

### 2.1.5 Cell Counting

Cell suspension, as prepared in 2.1.2, was used for cell counting with a Bright Line Haemocytometer (Sigma Aldrich, Poole, U.K). The cell pellet was resuspended with 10 ml medium and 20 µl of this cell suspension placed on the haemocytometer under a coverslip, applied by capillary action across the chamber. The number of cells was assessed under a light microscope by counting and averaging the number of cells in each 1mm square. Each small square of the haemocytometer represents a total volume of 1 mm<sup>3</sup>.

$$1 \text{ mm}^3 = 0.001 \text{ cm}^3$$

$$1 \text{ mm}^3 \times 1000 = 0.001 \times 1000 \text{ cm}^3 = 1 \text{ cm}^3 = 1 \text{ ml}$$

As 1 cm<sup>3</sup> is equivalent to 1 ml, the following calculation is adapted to calculate the cells concentration per ml:

$$\text{Cell number/ ml} = \text{average cell count per square} \times 10^3 \times \text{original volume}$$

On the basis of this count, a set number of cells was used to seed new plates. For a 6-well plate,  $5 \times 10^5$  cells were added to each well, while for 24-well plates,  $8 \times 10^4$  cells were added. 96-well plates had  $2 \times 10^4$  cells pipetted into each well.

## 2.2 Stimulation of Cells

### 2.2.1 Angiotensin II (Angio II), 100 nM, Dibutyryl-cyclic adenosine monophosphate(dbcAMP), 1 mM and Potassium Chloride (KCl), 20 mM

As part of the studies, it was necessary to stimulate cells with various factors known to influence steroidogenesis. To prepare cells for stimulation, they were seeded to plate wells, as above, and incubated at  $37^\circ\text{C}$  (5%  $\text{CO}_2$ ) for 24 hours. Later, medium was removed and replaced with complete growth medium also containing the relevant factor and incubated at  $37^\circ\text{C}$  for a further 0, 6, 12 or 24 hours, as required. The factors used were:

- Angiotensin II (Angio II) (Tocris Bioscience, Bristol, U.K): 100 nM
- Dibutyryl-cyclic adenosine monophosphate (dbcAMP) (Sigma-Aldrich, Dorset, England): 1 mM
- Potassium chloride (KCl) (BDH AnalaR®, Poole, England): 20 mM

## 2.3 Pre-miR<sup>TM</sup> and Anti-miR<sup>TM</sup> Transfection of Cells

### 2.3.1 Lipofectamine Transfection

Transfection of attached H295R cells with specific pre-miR<sup>TM</sup> and anti-miR<sup>TM</sup> (Ambion ® Life Technologies, Paisley, U.K) was performed using Lipofectamine reagent. Cells were trypsinised and diluted to  $16.67 \times 10^4$  cells/ml in a 6-well plate in normal medium and incubated at  $37^\circ\text{C}$  incubation for 24 hours. Later, transfection reagent master mix was prepared by mixing 8  $\mu\text{l}$  of Lipofectamine 2000 transfection agent (Ambion ® Life Technologies, Paisley, U.K) with 192  $\mu\text{l}$  of OptiMEM® (Ambion ® Life Technologies, Paisley, U.K) for 10 minutes. Separately, the pre-miR<sup>TM</sup> or anti-miR<sup>TM</sup> were prepared by adding 24  $\mu\text{l}$  of each of the miRNA to 176  $\mu\text{l}$  OptiMEM® medium. 200  $\mu\text{l}$  of the miRNA/ OptiMEM® was then added to 200  $\mu\text{l}$  of the Lipofectamine 2000/OptiMEM® and incubated for another 20 minutes. 400  $\mu\text{l}$  of this mixture was added to each well plate,

followed by 2600 µl of fresh cell medium. This was rocked gently to mix reagent then incubated at 37°C for 3 hours. The transfected cells were washed with 1 ml DPBS and prepared for cell lysis and RNA extraction.

### **2.3.2 siPORT™ NeoFX Transfection**

Transfection of H295R cells in suspension was conducted using siPORT™ NeoFX (Applied Bioscience, Warrington, U.K). The cells were trypsinised as in section 2.1.2 and counted as in section 2.1.5. Using 6-well plates, the cells were diluted to a concentration of  $2 \times 10^5$ / ml using fresh medium and the suspension was incubated at 37°C until required. The master mix of transfection reagent was prepared by adding 9 µl siPORT™ NeoFX to 291 µl OptiMEM®. Separately, 24 µl of specific pre-miR™ or anti-miR™ was added to 276 µl OptiMEM® for 10 minutes. 300 µl of miRNA/ OptiMEM® was then added to 300 µl of the Lipofectamine 2000/OptiMEM and incubated for another 20 minutes. 600 µl of this mixture was added to each well plate, followed by 2400 µl cell fresh medium. This was rocked gently to mix reagent then incubated at 37°C for 24 hours. The transfected cells were washed with 1 ml DPBS prior to cell lysis and RNA extraction.

## **2.4 Proliferation Assay**

### **2.4.1 CellTiter 96® Aqueous Non-Radioactive Proliferation Assay Using MTS Promega Assay**

The CellTiter 96® AQueous Non-Radioactive Cell Proliferation Assay (Promega, Madison, U.S.A) is used to assess cell proliferation, using a colorimetric method to determine the number of proliferating viable cells. The assay is composed of a solution of a novel tetrazolium compound [3-(4,5-dimethylthiazol-2-yl)-5-(3-carboxymethoxyphenyl)-2-(4-sulfophenyl)-2H-tetrazolium, inner salt; MTS(a)] and an electron-coupling reagent (phenazine methosulfate; PMS). In tissue culture medium, the MTS is bioreduced by cells into formazan rendering it soluble. Using 96-well plates, the absorbance of the formazan can be measured directly at 490 nm.

Following cell stimulation (Section 1.6), medium was removed completely and 100 µl of fresh culture media was added to each well of the 96-well plate

followed by 20  $\mu$ l of MTS assay. The plate was incubated at 37°C for 1 to 4 hours, with the colorimetric reaction progress being measured after 1, 2, 3 and 4 hours of incubation on the plate reader.

#### **2.4.2 Bromodeoxyuridine Cell Proliferation Assay (BrdU)**

Bromodeoxyuridine (BrdU) is used to detect and assess cell population that are actively synthesizing new DNA. BrdU is a thymidine analogue that is incorporated into newly synthesized DNA in the Synthesis (S) phase of the cell cycle.

Subsequently, an anti-BrdU antibody binds incorporated BrdU and is conjugated with Goat Anti Mouse IgG HRP antibody, which catalyses the conversion of chromogenic substrate tetramethylbenzidine (TMB) from a colourless to blue or yellow solution.

After 2-24 hours of BrdU incubation, fixative/denature solution was added to cells. Cells were seeded in 24-well plates at  $8 \times 10^4$  cells per well. 400  $\mu$ l of culture medium, with cells, was added to each well and incubated for 24 hours. Cells were then washed with DPBS and serum-starved medium was added. Cells were incubated for a further 48 hours before addition of 10 nM Angio II or 100 nM Angio II with 1 mM of BrdU for 48 hours.

BrdU Label dilution was prepared by adding the label to culture medium in 1:2000 ratio. 80  $\mu$ l of BrdU Label dilution was then pipetted into each well and incubated for 24 hours. The BrdU Label was then removed and 800  $\mu$ l Fixative/ Denaturing Solution added to each well and left for 30 minutes at room temperature. All liquid was removed from the well and 100 x Anti-BrdU Antibody 1:100 in Antibody Dilution Buffer solution was prepared. 400  $\mu$ l of the Anti-BrdU Antibody was added to each well and incubated at room temperature for one hour. 1x Wash Buffer was prepared by adding 25 ml of 20X concentration solution to 475 ml deionized water and each well washed three times. Conjugate was prepared by diluting reconstituted (in 1x PBS) Peroxidase Goat Anti-Mouse IgG HRP Conjugate in Conjugate Diluent, which was passed through a 0.2-micron filter. 400  $\mu$ l of conjugate solution was pipetted into each well and incubated for 30 minutes at room temperature. Wells were washed with 1x Wash buffer, then the entire plate was flooded with dH<sub>2</sub>O, which was removed by inversion. In the dark, 400  $\mu$ l of Substrate Solution was added to each well and left at room

temperature for 15 minutes. 400 µl of Stop Solution was then added to each well (without removing the Substrate Solution) and its absorbance measured within 30 minutes using the Spectrophotometric Plate Reader at 450 nm.

## **2.5 Lysing Cells with Qiazol**

Qiazol Lysis Agent is a monophasic solution of phenol and guanidine thiocyanate that disrupts cells through lysis of fatty tissues and releases RNA; lysis reagent also inhibits RNases. Prior to lysis, cell medium was removed from wells and cells washed with DPBS before adding 700 µl of Qiazol Lysis Reagent.

## **2.6 RNA Extraction and DNase Treatment Using miRNeasy Mini Kit (QIAGEN, Crawley, UK)**

The miRNeasy Mini Kit (QIAGEN, Crawley, UK) was used to isolate total RNA, including the microRNA fraction, from cells. The standard kit protocol was followed, including the optional DNase treatment, as follows. After cell lysis with Qiazol Lysis Agent, the cell culture plate was placed at -80°C overnight to complete homogenization (cell lysate can be stored at -80°C for several months). Subsequently, the homogenate was thawed at room temperature for 5 minutes to promote dissociation of nucleoprotein complexes then transferred to 1.5 ml RNase-free tubes. 140 µl chloroform was added to the homogenate, which was shaken vigorously for 15 seconds, then left at room temperature for 2 minutes. Centrifugation for 15 minutes at 12000 x g at 4°C separated the samples into 3 phases. The upper colourless aqueous phase contains RNA; the interphase contains DNA and the lower, red organic phase contains proteins and lipid. The upper phase was pipetted into a new 1.5 ml RNase-free tube. 525 µl of 100% ethanol was added and mixed thoroughly. 700 µl of the sample was then loaded on to an RNeasy mini spin column and centrifuged for 15 second at 8000 x g at room temperature; the flow-through was discarded and the step repeated for the remainder of the sample.

DNase treatment was then performed. 350 µl of RWT Buffer was pipetted on to the RNeasy Mini spin column and centrifuged for 15 seconds at 8000 x g; the flow-through was discarded. 10 µl DNase I stock solution was mixed with 70 µl Buffer RDD and gently mixed by inversion. 80 µl of this DNase I incubation mix

was pipetted directly on to the RNeasy Mini spin column membrane and left at room temperature for 15 minutes. 350 µl Buffer RWT was pipetted on to the RNeasy Mini spin column and centrifuged for 15 seconds at 8000 x g.

After on-column DNase digestion, 500 µl RPE Buffer was added to the RNeasy Mini spin column and centrifuged at 8000 x g for 15 seconds; flow-through was discarded. This step was repeated with a longer centrifugation for 2 minutes to dry the spin column and ensure no carry over of ethanol. The RNeasy Mini spin column was placed in a new 2 ml collection tube and centrifuged at full speed for 1 minute then transferred again to a new 1.5 ml RNase-free tube. Finally, 30-50 µl RNase-free water was added directly to the RNeasy Mini spin column membrane and centrifuged for 1 minute at 8000 x g to elute the RNA.

## 2.7 Nucleic Acid Quantification

To determine the quantity and purity of nucleic acid, a Nanodrop ND-100 spectrophotometer with ND-1000 v3.10 software (Labtech International LTD, Lewes, East Sussex, UK) was used. Initially the Nanodrop setting was set up to measure RNA. 2 µl of RNase free water was loaded to the Nanodrop base pedestal and the arm was lowered. It was blanked prior to sample measurement using RNase-free water. The nucleic acid concentration is calculated as following using the Beer-Lambert Law of absorption:

$$\text{RNA concentration } (\mu\text{g/ ml}) = (A_{260} \text{ reading} - A_{320} \text{ reading}) \times 40$$

The ratio of absorption at 260 nm and 280 nm ( $A_{260/280}$ ) is an indicator of RNA purity; ratios of 1.8 to 2 indicates high RNA purity.

## 2.8 Agarose Gel Electrophoresis

Agarose gels (1%) were prepared to analyse PCR product. 1 g Ultrapure agarose (Invitrogen, Paisley, U.K) was added to 100 ml of 1 x TBE buffer. The mixture was heated to dissolve the powder in a microwave oven at full power for 1-2 minutes then allowed to cool slightly before addition of 1 µl of ethidium bromide solution (10 mg/ml; Sigma-Aldrich, Poole, U.K) in a fume hood. This was then poured into a tray with a 20-well comb (Teflon comb) and left to set. The

resulting gel was immersed in 1 X TBE buffer in an electrophoresis tank and the comb removed. 5 µl dye (0.02 % bromophenol blue, 0.02 % xylene cyanol and 2.5 % glycerol) was added to 5 µl sample before loading the sample into a well. 5 µl of 1 kb DNA size ladder (Promega, Madison, WI, USA) was added to assess the resolution of molecular size. Gels were run for 50 minutes at 90 volts. The DNA fragments were visualised under UV light on a transilluminator machine (Bio-Rad Laboratories, Hemel Hempstead, U.K) and analysed by Multi-Analyst software v 1.1 (Bio-Rad) at 302 nm.

## **2.9 Reverse Transcription**

Reverse Transcription (RT) of single-stranded RNA to complementary DNA (cDNA) was achieved using the miScript II Reverse Transcription Kit (QIAGEN, Crawley, U.K). The supplied 10x miScript Nucleics Mix contain dNTPs, rATP, oligo-dT primers and internal synthetic RNA control (miRNA reverse transcription control (miRTC)). The 5x miScript HiFlex Buffer promotes conversion of miRNA or mRNA into cDNA for realtime PCR quantification (Sections 2.10 and 2.11).

For each sample 150-200 ng of DNase-treated RNA was mixed with 2 µl of Reverse Transcriptase Mix, 4 µl of 5x miScript HiFlex Buffer and 2 µl of 10x miScript Nucleics. The total volume of 20 µl was made up with RNase-free water in a 96-well PCR plate. A negative reverse transcriptase (-RT) control was included for each sample as control to assess the specificity of qRT-PCR reaction to detect genomic DNA. The plate was sealed with clear polyolefin StarSeal (PCR seal) and centrifuged prior to reaction run.

The reaction was run on Multi Block System Satellite 0.2 Thermo Cooler (Thermo Fisher Scientific, U.K), see Table Table 2-2.

**Table 2-2: Reaction cycle of miScript Reverse-transcription.**

Step	Time (minutes)	Temperature
Reverse Transcription	120	37°C
Inactivation of RT mix	5	95°C
	Hold	10°C

After the samples were run, 80 µl of RNase-free water was added to each and they were stored at -20°C until required.

## 2.10 Quantitative Real-Time Polymerase Chain Reaction (Universal Probe Library)

Detection of messenger RNA (mRNA) was performed by quantitative realtime PCR (realtime qPCR) in a 384-well PCR plate (Thermo Fisher Scientific, U.K) using TaqMan® Gene Expression Master Mix containing AmpliTaq Gold® DNA Polymerase, Uracil-DNA Glycosylase (UDG), UP (Ultra Pure), deoxyribonucleotide triphosphates (dNTPs) with deoxyuridine triphosphate (dUTP), ROX Passive Reference dye and buffer. The Universal Probe Library (UPL) probe system (Roche Applied Science, Indianapolis, USA) was used, consisting of 165 pre-validated probes. These Locked Nucleic Acid (LNA) PCR probes are labelled with fluorescein (FAM) at the 5' end and a dark quencher dye at the 3' end and offer greater specificity than SYBR-green-based assays. Each assay consists of a UPL probe combined with a specially-designed primer pair (Eurofins MWG Operon, Ebersberg, Germany), as shown in Table 2-7.

The realtime PCR reaction mix is prepared as shown in Table Table 2-3.

**Table 2-3: Taqman reaction components.**

Reagent	Volume/ Reaction
TaqMan® Gene Expression Master Mix	5.0µl
UPL Probe	0.1µl
Primer (Forward)	0.4µl
Primer (Reverse)	0.4µl
Nuclease-Free Water	2.1µl
cDNA (template RNA)	2.0µl

8 µl of Taqman master mix was added to 2 µl cDNA in the well of a 384-well plate. 3 technical replicates were set up for each RT positive (RT+) cDNA samples and 3 technical replicates for the RT negative sample. cDNA was prepared as described in Section 1.9. Negative water blank for control reactions were also included. The plate was sealed, centrifuged (1000g, 1 minute at room temperature) and run on QuantStudio™ 7 Flex Real-Time PCR Systems (Applied Biosystem by Life Technologies, Carlsbad, CA, USA) using SDS software QuantStudio™ 7 Flex Real-Time PCR System Software (Applied Biosystem by Life Technologies, Carlsbad, CA, USA). The cycling protocol is shown in Table 2-4.

**Table 2-4: Reaction cycle of Taqman qRT PCR.**

Step	Time	Temperature	Cycles
Enzyme activation	10 minutes	95°C	1
Denaturation	15 seconds	95°C	40
Annealing and extension	1 minute	60°C	40

## 2.11 SYBR Green Quantitative Real-Time Polymerase Chain Reaction

The detection of mature miRNA was analysed using miScript SYBR Green PCR Kit (QIAGEN, Crawley, U.K.) and 10X miScript Primer Assays (see Table 2-8). Supplied lyophilised primer Assay was mixed with 550 µl of TE buffer (pH 8) and stored at -20°C. Reactions were prepared as shown in Table 2-5.

**Table 2-5: SYBR Green reaction components.**

Reagent	Volume/Reaction
QuantiTect SYBR Green PCR Master Mix (2X)	10 $\mu$ l
10X miScript Universal Primer	2.0 $\mu$ l
10X miScript Primer Assay	2.0 $\mu$ l
Nuclease-Free Water	4.0 $\mu$ l
cDNA (template RNA)	2.0 $\mu$ l

8 $\mu$ l of SYBR Green master mix was added to 2  $\mu$ l of cDNA in each well. 3 technical replicates were set up for RT positive (RT+) cDNA samples and 3 technical replicates for the RT negative sample. cDNA was prepared as described in Section 1.9. The mixture was centrifuged for 1000 g, 1 minute at room temperature. It was run on QuantStudio™ 7 Flex Real-Time PCR Systems (Applied Biosystem by Life Technologies, Carlsbad, CA, USA) using SDS software QuantStudio™ 7 Flex Real-Time PCR System Software (Applied Biosystem by Life Technologies, Carlsbad, CA, USA) with cycle as mentioned below:

**Table 2-6: Reaction cycle of SYBR Green qRT PCR.**

Step	Time	Temperature (°c)	Cycles
Enzyme activation	15 minutes	95	1
Denaturation	15 seconds	94	
Annealing	30 seconds	55	40
Extension	30 seconds	70	
	15 seconds	95	
Melt curve	15 seconds	60	1
	15 seconds	95	

## 2.12 Analysis of qPCR Results

Amplification of PCR product increases fluorescence from PCR probe or SYBR Green dye, as measured by the QuantStudio™ 7 Flex Real-Time PCR cycler. The  $C_t$  (cycle threshold) is the PCR cycle number at which a predetermined level of fluorescence is achieved. The  $C_t$  is inversely proportional to the starting amount of target template and this is used for qPCR analysis. For these studies, the  $\Delta\Delta C_t$

system of quantitative analysis was used. This employs a 'housekeeping' gene as a constant benchmark, measured alongside the gene/miRNA of interest.

Therefore,

$$\Delta C_t = C_t \text{ sample} - C_t \text{ housekeeper}$$

GAPDH (for Taqman) and RNU-48 (for SBR Green) were used as 'housekeeping genes', acting as normalising controls for RNA concentration and correcting for minor discrepancies during pipetting. Both housekeepers were validated for consistent expression and reproducibility.

The  $\Delta\Delta C_t$  can then be calculated from these as follows:

$$\Delta\Delta C_t = \Delta C_t \text{ sample} - \Delta C_t \text{ reference}$$

And the fold change (RQ) in mRNA or miRNA calculated as:

$$\text{Fold change} = 2^{-(\Delta\Delta C_t)}$$

## 2.13 Microarray Analysis

For miRNA profile studies of adrenal tissues (normal adrenal and APA tissues) and H295R cells (basal and stimulated H295R), the total RNA was prepared by Dr Stacy Robertson (adrenal tissues) and Dr Louise Diver (H295R cells). The group size for the adrenal tissue study was dictated by the availability of suitable clinical samples. We initially received 4 control samples (normal adrenal) and were able to subsequently match these with 4 aldosterone-producing adenoma samples. The four non-diseased control samples were more difficult to obtain and determined our sample size.

The RNAs were sent for microarray analysis by LC Sciences (Houston, Texas, U.S.A.) using miRNA  $\mu$ Paraflo® technology microarray (version 10.1). Briefly, RNA was labelled with fluorescent dye and hybridised overnight on a specific microfluidic chip containing probes for 723 human miRNAs and control RNA. The chip was scanned using a GenePiz 4000B laser scanner and analysed using Array-Pro image software. The raw data were subtracted to background and

underwent data adjustment including data filtering,  $\log_2$  transformation, gene centering and normalisation. The manufacturers recommend a signal cut-off of 500 AU as the optimal threshold below which any miRNA should be regarded as absent; we employed this threshold for our studies. The need for such a threshold arises from the non-specific, background fluorescence, which is an unavoidable feature of this method, and requires the imposition of an arbitrary cut-off point for all measurements.

## **2.14 miRBase Database Release 19: August 2012**

The miRBase Database is the primary online repository for all known miRNAs and provides comprehensive miRNA nomenclature, sequence data, annotation and predicted gene target information. The most recent version is Release 21: June 2014 that contains 28645 entries of hairpin precursor miRNAs, 35828 mature miRNAs from 223 species (miRBase 2014), including 2588 mature human miRNAs (Kozomara A 2014). miRBase is accessible online at <http://www.mirbase.org/>.

miRBase started from an initial 218 entries of miRNA and has been developed to almost 30000 entries 12 years later. The miRNA names use the prefix “miR” followed by unique and specific identifying number that are assigned sequentially regardless organism. The similar identifying numbers are given to identical or almost identical miRNA sequence. Almost all miRNAs precursor produced mature miRNA from either the 5’ end or 3’ hair-pin strand, the annotation of mature miRNA will be added ‘5p’ or ‘3p’, based on the origin they are cleaved from (Ambros, Bartel et al. 2003).

## **2.15 Ingenuity Pathway Analysis (IPA)**

Ingenuity Pathway Analysis (IPA) software provides predicted target genes for miRNAs using miRNA Target Filter database. The database is derived from peer-reviewed scientific literature (Ingenuity Expert Finding, Ingenuity ExpertAssist Finding), miRecords, Tarbase and TargetScan Human. The miRNA target filter can be filtered through several mechanism including disease type, organ type, pathway affected and confidence level as described in the following:

The filter system is based on 3 confidence levels;

- 1) Experimentally observed miRNA-mRNA interaction (result based on validated experiment).
- 2) Highly predicted miRNA-mRNA interaction.
- 3) Moderately predicted miRNA-mRNA interaction.

## 2.16 Statistical Analysis

The reason we did the microarray is to screen for changes in miRNAs expression. All the unadjusted p-value data from LC Sciences were analysed using False Discovery Rate (FDR) Calculator to adjust the p-value. Ideally, the miRNAs with significant adjusted p-value would be taken forward for further analysis. However, if the FDR value is not significant, there are 2 options. Firstly, terminate any further investigation or secondly choose the most significant hits from the microarray analysis. In my thesis, the analysis of FDR values was done by Dr John McClure. Based on FDR calculation, the p-values provided by LC Sciences were not significant. As advised by Dr John McClure, I have chosen to analyse the most significant miRNAs based on the p-value and the miRNAs that have relevant biological input (with  $p < 0.05$ ). In addition, I have done further experiment to validate these screening results by qRT PCR.

Unless specified otherwise, the data shown are presented as mean  $\pm$  standard error of the mean (SEM), with qRT PCR data expressed as RQ  $\pm$  SEM or  $1/dCt \pm$  SEM. For in vitro experiments, at least 3 biological samples were performed with a minimum of 3 technical replicate were performed, unless stated otherwise.

We are not just using a simple T-test here because we have adjusted the p-value for multiple testing using FDR. None of the results were significant, so we proceeded to analyse the most significant hits of the microarray results using unadjusted p-value. Differences with a p value  $< 0.05$  were regarded as statistically significant. Statistical calculations were performed using GraphPad Prism Version 5 (GraphPad Software, Inc, San Diego, CA).

## **2.17 Ethical Board**

The four normal adrenal tissue samples were obtained from patients (adult) undergoing nephrectomy with local ethical approval from the University of Birmingham. The other four samples of APA tissues (FFPE) were acquired from the Biobank of University of Glasgow and were held in accordance of Human Tissue Act with the local ethical review board permission. The samples were then handled by Dr Stacy Robertson for RNA extraction and other related protocols. We were unable to access to the clinical data for these samples for reasons of ethics and privacy.

Table 2-7: List of TaqMan Gene Expression Assay

Gene	Primer (Forward)	Primer (Reverse)	UPL Probe #
<i>GAPDH</i>	GCTCTCTGCTCCTCCTGTTT	ACGACCAAATCCGTTGACTC	60
<i>CYP11B1</i>	ACTAGGGCCCATTTTCAGGT	GGCAGCATCACACACACC	68
<i>CYP11B2</i>	GCACCTGCACCTGGAGATG	CACACACCATGCGTGGTCC	57
<i>CYP17A1</i>	CTATGCTCATCCCCACAG	TTGTCCACAGCAAACCTACC	67
<i>HMGCR</i>	GACGCAACCTTTATATCCGTTT	TTGAAAGTGCTTTCTCTGTACCC	85
<i>HTR4</i>	AATGGATCCACACATGTAATAAGG	GGTGACACTGACTCTCCCACT	86
<i>FDX1</i>	CTTTATAGGTCAACCGGAAGG	CTGGAGTGGCGGAGAGAC	11
<i>KCNJ5</i>	GGAAGCTCCGATCTCAACAA	CCTGGTTCATGGCATTCTTA	33
<i>WNT4</i>	GCAGAGCCCTCATGAACC	CACCCGCATGTGTGTCAG	74
<i>LDLR</i>	CCACGGTGGAGATAGTGACA	CTCACGCTACTGGGCTTCTT	53

Table 2-8: List of SYBRGreen miRNA Assay used

miRNA Assay	miRNA Sequence	Assay Product Code
hsa-miR-24-3p	5'UGGCUCAGUUCAGCAGGAACAG 3'	MS00006552
hsa-miR-21-5p	5'UAGCUUAUCAGACUGAUGUUGA 3'	MS00006552
hsa-miR-125a-5p	5' UCCCUGAGACCCUUUAACCUUGUGA	MS00003423
hsa-miR-335	5' UCAAGAGCAAUAACGAAAAAUGU 3'	MS00003976
hsa-miR-106a-5p/ miR-17-5p	5' CAAAGUGCUUACAGUGCAGGUAG 3'	MS00029274
hsa-miR-154-3p	5' AAUCAUACACGGUUGACCUAUU 3'	MS00031479
hsa-miR-19a-3p	5' UGUGCAAUUCUAUGCAAACUGA 3'	MS00003192
hsa-miR-20b-5p	5' CAAAGUGCUCAUAGUGCAGGUAG 3'	MS00003206
hsa-miR-766-3p	5' ACUCCAGCCCCACAGCCUCAGC 3'	MS00005439

### **3 Microarray Analysis of microRNA in Normal Human Adrenal (NA) and Aldosterone-Producing Adenoma (APA) Tissues**

### 3.1 Introduction

Microarray analysis is one of the techniques that can be implemented to detect the expression of miRNAs. Microarray allows the analysis of thousands of genes simultaneously in one experiment: a time- and cost-efficient investigation.

Microarray can be classified (Abdullah-Sayani, Bueno-de-Mesquita et al. 2006) into the following types :

1. Expression profiling
2. Comparative genomic hybridization (CGH)
3. Single nucleotide polymorphism analysis (SNP)
4. Resequencing arrays (RA)

Expression profiling and CGH are used to compare gene expression in normal vs disease states for tumour classification and prognostic purposes. SNP analysis is used to detect specific polymorphisms or mutations, helping to determine genetic predisposition to certain diseases and the discovery of DNA-based drug candidates. RA is utilised to sequence the genome for somatic mutation identification in cancer. In addition to the numerous ‘wet’ laboratory experimental analyses available for miRNA investigation (e.g microarray, qRT PCR, deep-sequencing and others), *in silico* analysis can also be utilised to facilitate the prediction of genes targeted by miRNA relatively quickly and cost-effectively, before commencing the more expensive and time-consuming other techniques.

In this chapter, the miRNA Target Filter in IPA was employed to determine putative targets for miRNAs of interest. miRNA Target Filter combines several bioinformatic miRNA tools: TargetScan, TarBase, miRecords and Ingenuity® Knowledge Base (IPA 2016). The ‘seed’ site refers to the second to seventh nucleotides of the miRNA from the 5’ end. Bartel et al reported that seed site base-pairing is one of the robust measure for many target miRNA target database, where it increases the reliability and reducing the false positive prediction (Bartel 2009). Tarbase and miRecords identify the experimentally validated miRNA-mRNA interaction from miRBase and published articles while Ingenuity ® Knowledge Base demonstrates thousands of miRNA-related finding

from published articles which are manually curated by Ingenuity Scientific experts (IPA 2016).

The mRNA targets predicted by the TargetScan algorithm refers to the conserved 7mer and 8mer seed match site of each miRNA (IPA 2016). 7-8mer (7mer-A1, 7mer-m8 and 8mer) seed matches associate with the strongest targeting efficiency (Figure 3-1) and are used to predict metazoan conserved miRNA targets (Friedman, Farh et al. 2009). In order of increasing strength of base-pairing, a 7mer-A1 site has a seed match with an adenosine base in the mRNA sequence complementary to miRNA nucleotide 1 (Figure 3-1). Next strongest is a 7mer-m8 site, composed of a seed match supplemented by a Watson-Crick match at miRNA nucleotide 8. The most stable bonding between mRNA and miRNA results from an 8mer comprising a seed match at both miRNA nucleotide 8 and an A at nucleotide 1.

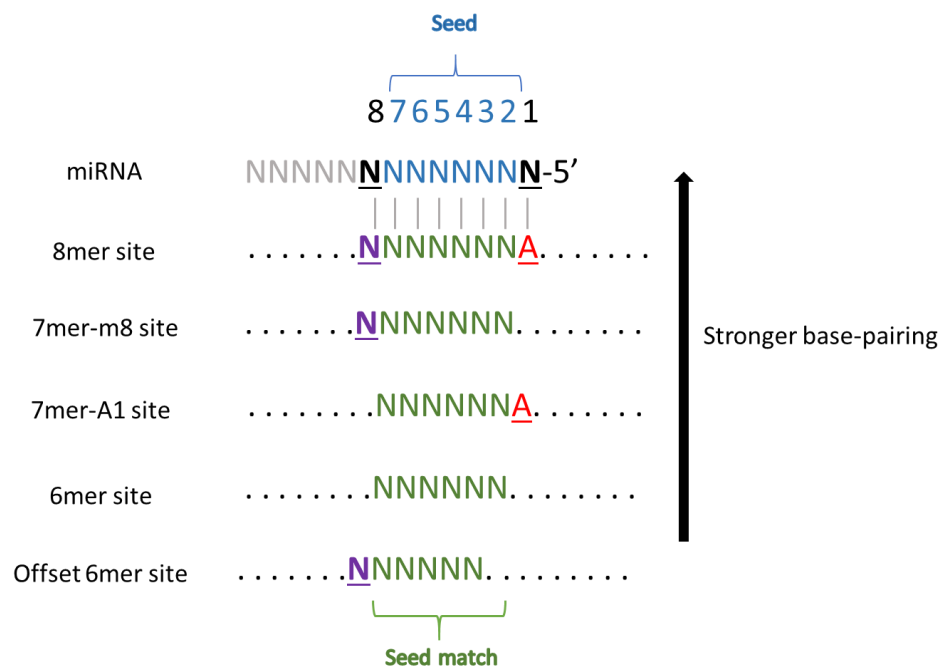


**Figure 3-1: miRNA-mRNA site base-pairing. Each nucleotide (N) is numbered as 1 to 8 from the 5' end of the miRNA.**

Blue nucleotides are the core seed site of the miRNA and black nucleotides mark the start (N1) and end (N8) of the site. Green nucleotides are the complementary sites in the mRNA sequence. Red A denotes adenosine and the purple nucleotide at position 8 increase the recognition strength of the target by miRNA. Modified from (Friedman, Farh et al. 2009).

## 3.2 Aims

- 1) To establish and identify significant differences between the miRNA profiles of normal adrenal (NA) and aldosterone-producing adenoma (APA) tissue using microarray analysis methods.
- 2) To utilise bioinformatic analysis methods (Ingenuity Pathway Analysis; miRNA target Filter) to identify experimentally validated or predicted mRNA targets of miRNAs differentially-expressed between NA and APA tissue, which are likely to be relevant to adrenal function and APA pathology.

## 3.3 Result

### 3.3.1 miRNA expression in microarray

Total RNA was extracted from 4 different samples of normal human adrenocortical (NA) tissue and 4 different samples of human aldosterone-producing adenoma (APA). The RNA quantity was determined using the Nanodrop (Section 2.7) and the quality assessed by Agilent Bioanalyser chip. RNA samples were then sent for miRNA profile analysis by microarray microfluidic chip (LC Sciences, Houston, Texas). LC Sciences also conducted their own quality control procedures on the RNA samples.

The large dataset from LC Sciences is further selected based on the manufacturer recommendation. According to the recommendations of the microarray manufacturer (LC Sciences, Houston, Texas), a 500 arbitrary unit (AU) cut-off point was applied as the detection threshold for individual miRNAs. The microarray analysis generated a list of miRNAs present in one or both tissue types (i.e. miRNAs >500 AU) and also of miRNAs differentially expressed between tissue types (i.e. miRNAs present in only one tissue type at >500 AU, or miRNAs present in both tissue types at >500AU but at significantly different levels ( $p < 0.05$ ). Figure 3-2 shows positive correlation of mean fluorescence intensity of miRNA expression between normalised NA and APA, suggesting the majority of miRNA levels remain highly consistent between the two tissues.

Of the 723 screened miRNAs, 77 were detected at levels >500 AU in NA and/or APA. Of these, 50 were expressed in both NA and APA, 12 were present in NA

only and 15 in APA only (Figure 3-3). Of the 50 miRNAs present in both tissues, 20 were differentially expressed ( $p < 0.05$ ; Figure 3-4). Of the total 47 miRNAs differentially expressed (i.e. present in only one tissue or present in both and differentially expressed ( $p < 0.05$ )), 23 were more highly expressed in NA tissues (Figure 3-5) and 24 miRNAs were more highly expressed in APA (Figure 3-6).

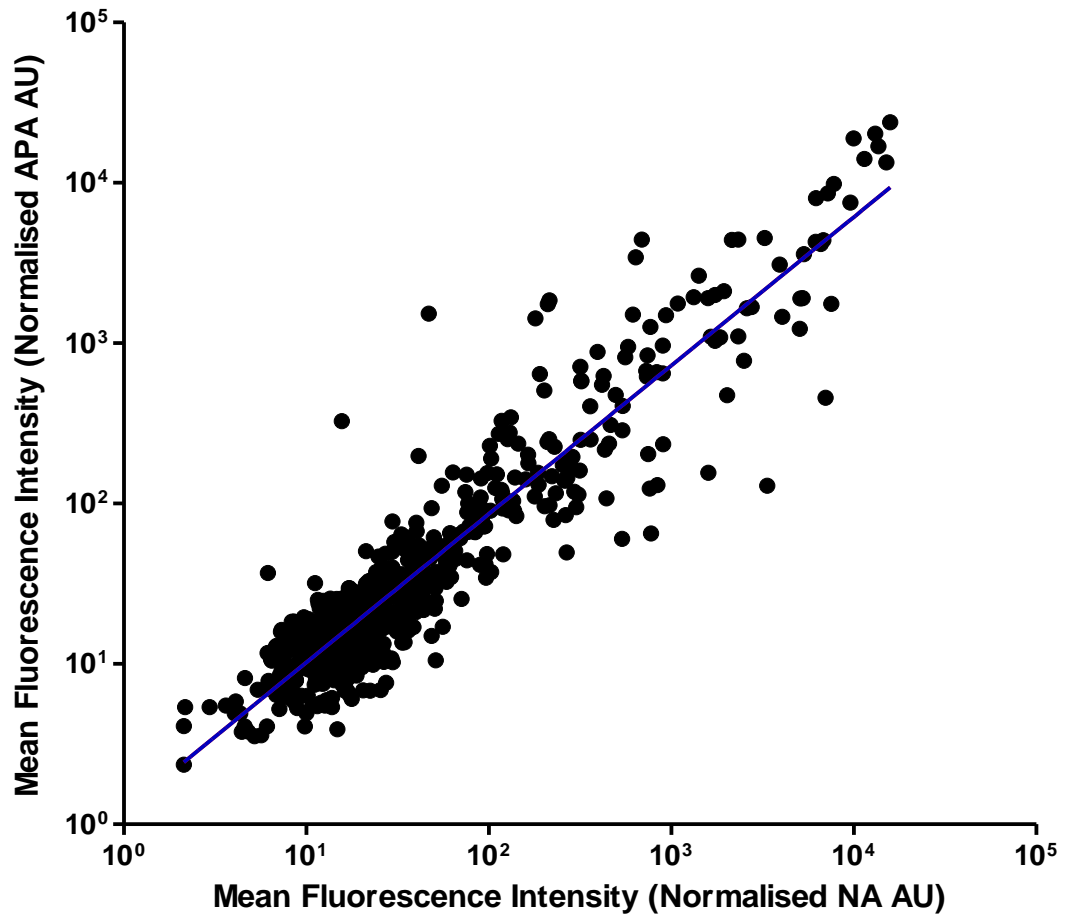


Figure 3-2: Scatter plot showing levels of individual miRNAs in stimulated normal adrenal (NA) vs aldosterone-producing adenoma (APA), as analysed by microarray.  $R^2=0.8706$ .

### 3.3.2 miRNA expression more than 500 Arbitrary Units (AU)

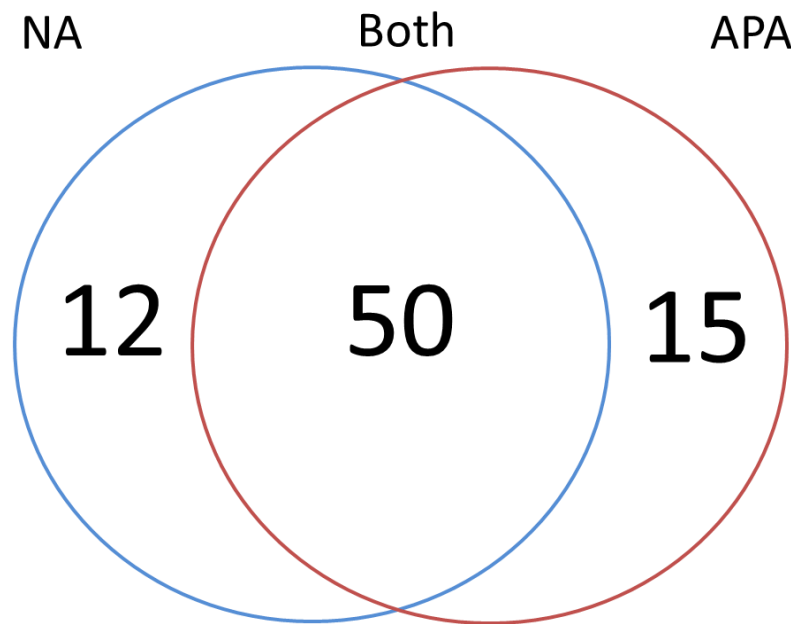


Figure 3-3: Venn diagram showing the number of expressed miRNAs present (>500 AU) in NA and/or APA.

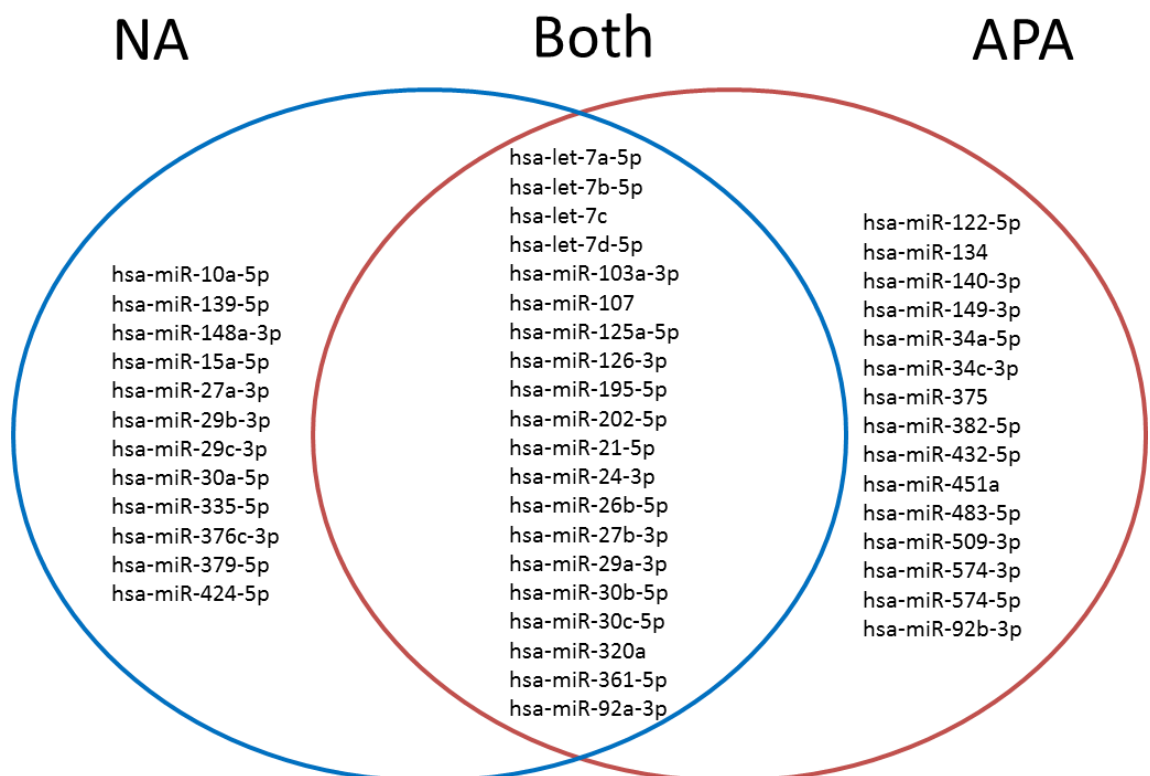


Figure 3-4: Venn diagram of differentially-expressed miRNAs i.e. those detected in only one tissue type (AU>500 in NA or APA) or present in both at significantly different levels (AU>500 in APA and NA;  $p<0.05$ ).

Note that fewer miRNAs are listed compared to Figure 3-3; this is because this figure contains only miRNAs of AU >500 and with  $p<0.05$  between both tissues.

### More highly expressed miRNAs in NA

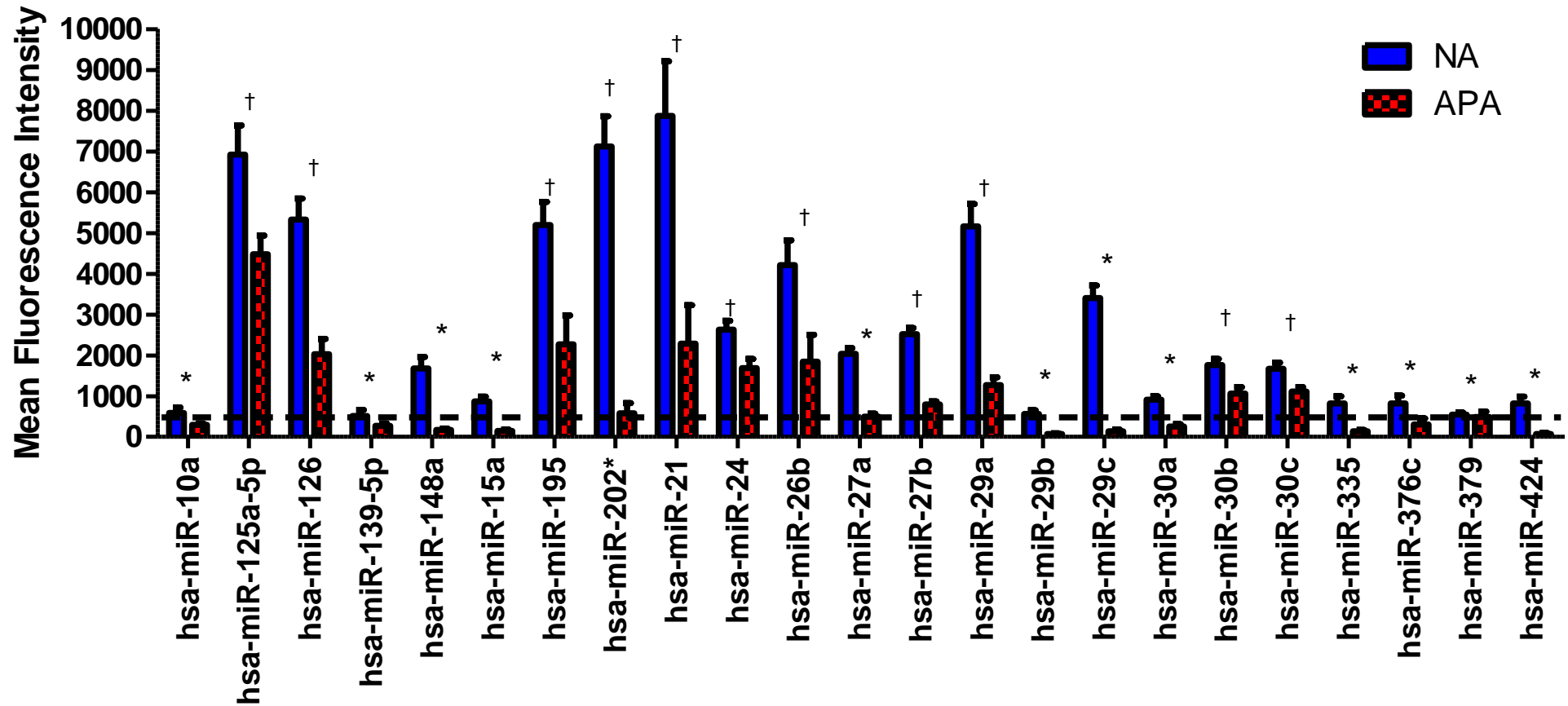


Figure 3-5: Microarray data showing the 23 miRNAs consistently expressed at high levels in NA samples relative to APA.

\*miRNAs >500AU in NA but not APA; †miRNAs present in both tissues but at significantly different levels ( $p < 0.05$ ).

### More highly expressed miRNAs in APA

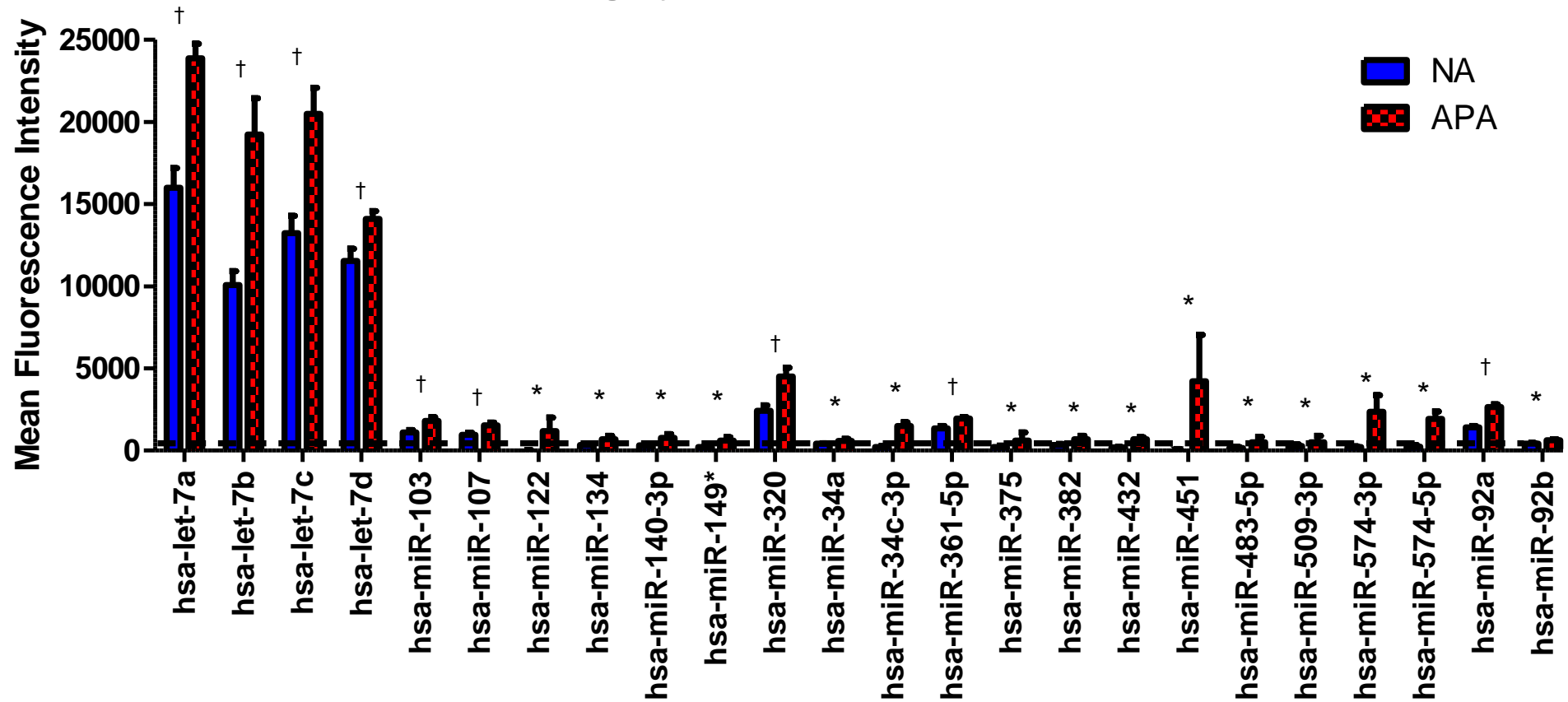


Figure 3-6: Microarray data showing the 24 miRNAs consistently expressed at high levels in APA samples relative to NA.

\*miRNAs >500AU in APA but not NA; †miRNAs present in both tissues but at significantly different levels ( $p < 0.05$ ).

### 3.3.3 miRBase analysis of the differentially-expressed miRNAs in NA and APA.

miRBase is the main online repository providing standardised nomenclature for miRNAs, sequences, annotation and mRNA target prediction. Starting from an initial 218 miRNA entries in 2002, it has developed to include almost 30,000 entries as of 2014. The latest version is miRBase Release 21: June 2014. It contains 28,645 entries of hairpin precursor miRNAs, including 35,828 mature miRNAs from 223 species (miRBase 2014). The miRNA naming convention uses the prefix 'miR' followed by a unique and specific identifying number (e.g. miR-768) that is assigned sequentially regardless of organism. Similar identifying numbers are given to identical or almost identical miRNA sequences (e.g. miR-125a and miR-125b). Almost all miRNA precursors produce mature miRNA from either the 5' end or the 3' hair-pin strand; mature miRNA are annotated as '5p' or '3p' on the basis of this (e.g. miR-768-5p) (Ambros, Bartel et al. 2003). Each species has a specific prefix designation (for example, in humans 'hsa' is added prior to the miRNA name i.e hsa-miR-17).

The microarray data were analysed using the current miRBase release (Release 21: June 2014). Of the differentially-expressed miRNAs, two (miR-768-3p and miR-768-5p) were excluded from further analysis as these had been reclassified by miRBase as 'dead miRNA' entries due to their overlap with the annotated snoRNA, HBII-239 (miRBase 2014), meaning they are unlikely to be real functional miRNAs.

According to microarray, the most abundantly expressed miRNAs are the let-7 miRNAs: let-7a-5p (average fluorescence intensity 23866,  $p=0.0019$ ), let-7b-5p (average fluorescence intensity 19235,  $p=0.0082$ ), let-7c (average fluorescence intensity 20486,  $p=0.0089$ ) and let-7d-5p (average fluorescence intensity 14091,  $p=0.029$ ). These miRNAs are uniformly up-regulated in APA tissue (Figure 3-6). The most significant difference in miRNA expression between tissues is that of miR-29c-3p ( $p=0.000043$ ), which is upregulated in NA relative to APA (Figure 3-5).

### 3.3.4 miRNA Clusters Expression in NA and APA Tissues

As classified by miRBase Release 21, a group of miRNAs located on the same chromosome and within 10 kb of one another are termed a miRNA cluster (Zhang, Azhar et al. 2012, miRBase 2014). There is evidence that the miRNAs derived from clusters tend to have similar function and associate with similar disease states (Lu, Zhang et al. 2008). In my study, members of 27 different miRNAs clusters were identified in NA or APA tissue (Figure 3-7 to Figure 3-14).

Expression levels of different members of the same miRNA cluster often follow similar patterns. For example, Cluster let-7a-1, located on chromosome 9 (Figure 3-11 A), contains let-7a-5p and let-7d-5p, which were both significantly upregulated in APA samples, as shown in Figure 3-11 and Figure 3-15. A further member of this cluster, let-7f-5p, shows a similar pattern of expression (upregulated in APA), but it is not differentially significant. Even though let-7d-3p was judged significantly different between the two phenotypes (high in APA), the expression level in both tissues was <500 AU, so it is technically not expressed in either tissue (Figure 3-11). Similarly, no expression of the remaining cluster members, let-7a-3p and let-7f-1-3p, was detected from the microarray. In Cluster let-7a-3 (Figure 3-16), two miRNAs show consistent expression: let-7a-5p and let-7b-5p.

Furthermore, two miRNAs from Cluster miR-134 (miR-134 and miR-382) are consistently upregulated in APA (Figure 3-17). These miRNAs are located at chromosome 14.

Two members of Cluster miR-29b-1 (miR-29a-3p, miR-29b-3p; both  $p < 0.05$ , >500 AU) (Figure 3-18) are highly expressed in NA. The other 2 miRNAs in the cluster (miR-29a-5p and miR-29b-1-5p) show a consistent pattern of expression (the mean fluorescence intensity of the miRNAs are higher in NA), but the p-value is >0.05 (Figure 3-8). Cluster miR-29a/ 29b-1 is located on chromosome 7.

Cluster miR-29b-2 (consists of miR-29b-3p, miR-29c-3p both  $p < 0.05$ , >500 AU) (Figure 3-19) is down-regulated in APA tissues. Mature miR-29b-3p originates from 2 distinct miRNA precursors: stem-loop mir-29b-2 which is located at

chromosome 1 and stem-loop mir-29b-1 which is located at chromosome 7. The sequence of mature miR-29b-3p remains the same (UAGCACCAUUUGAAAUCAGUGUU) despite differences in miRNA precursor loops (miRBase 2014).

Another cluster that shows a similar expression pattern is Cluster miR-15a (Figure 3-7), where miR-15a-5p and miR-16-5p show a similar trend towards upregulation in NA tissues, although this is not significant.

Cluster miR-24-1 and Cluster miR-24-2 each feature members that are overexpressed in NA and in APA (Figure 3-8). The mature form of miR-24-3p is synthesized from two different primary miRNAs; miR-24-1 in chromosome 9 and miR-24-2 from chromosome 19.

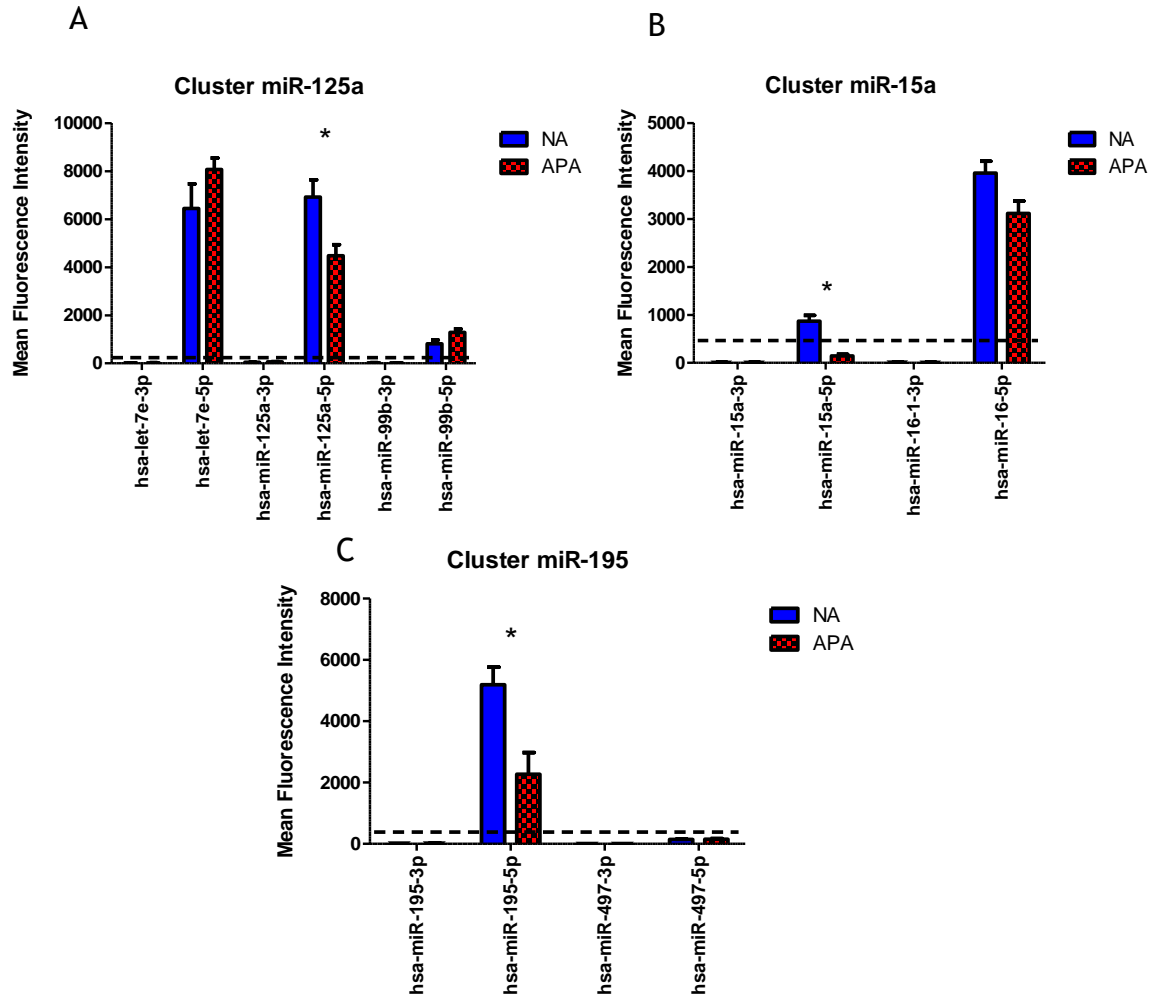


**Figure 3-7: miRNA Clusters (NA>APA) detected from microarray analysis. Cluster miR-125a (A), cluster miR-15a (B) and cluster miR-195 (C).**

Blue bars indicate miRNAs that are expressed in NA and red bars indicate APA (\* $p < 0.05$ ).

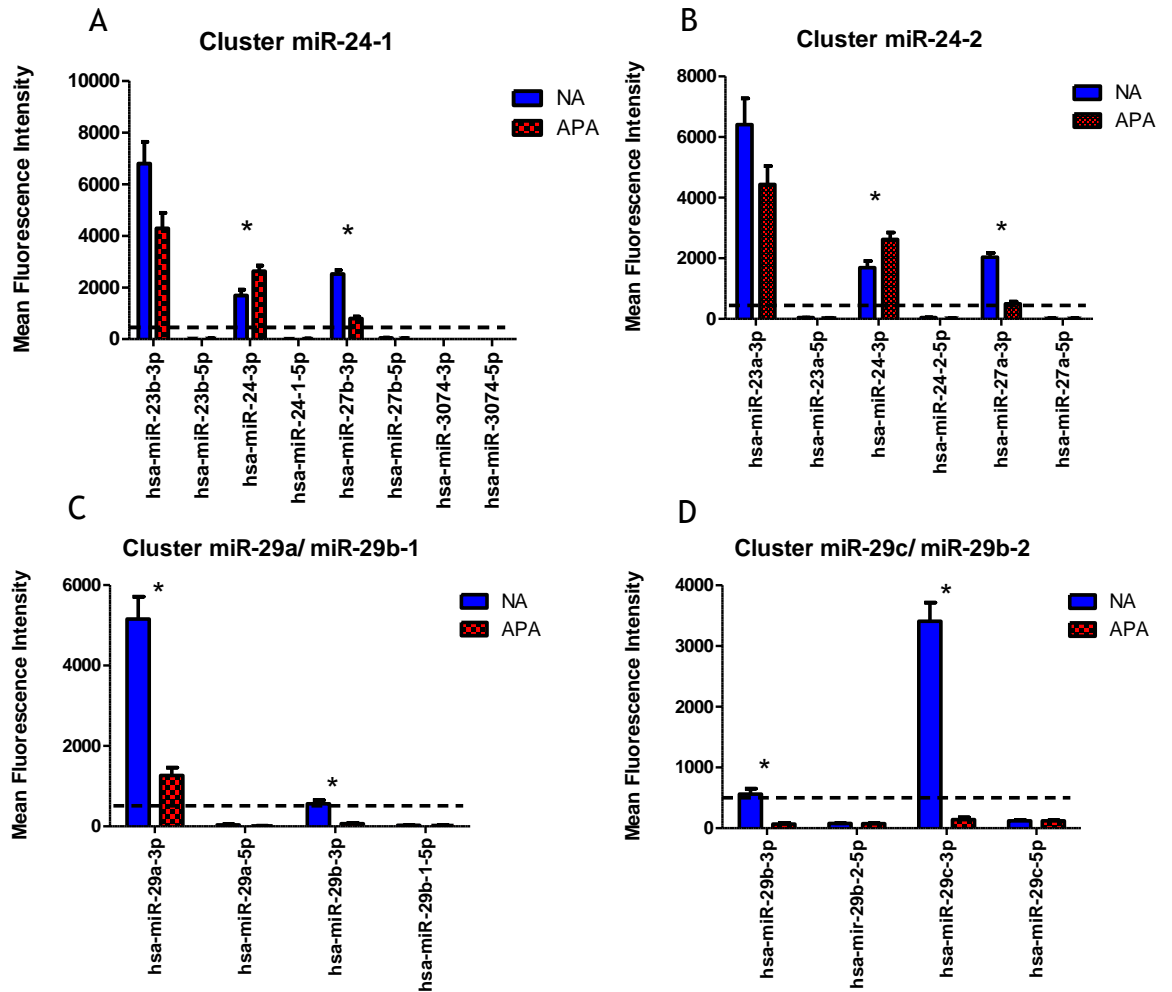


**Figure 3-8: miRNA Clusters (NA>APA) detected from microarray analysis (Cluster miR-24-1 (A), Cluster miR-24-2 (B), Cluster miR-29b-1 (C) and miR-29b-2 (D)).** Blue bar indicates miRNAs that are expressed in NA and red bars indicate APA (\* $p < 0.05$ ).

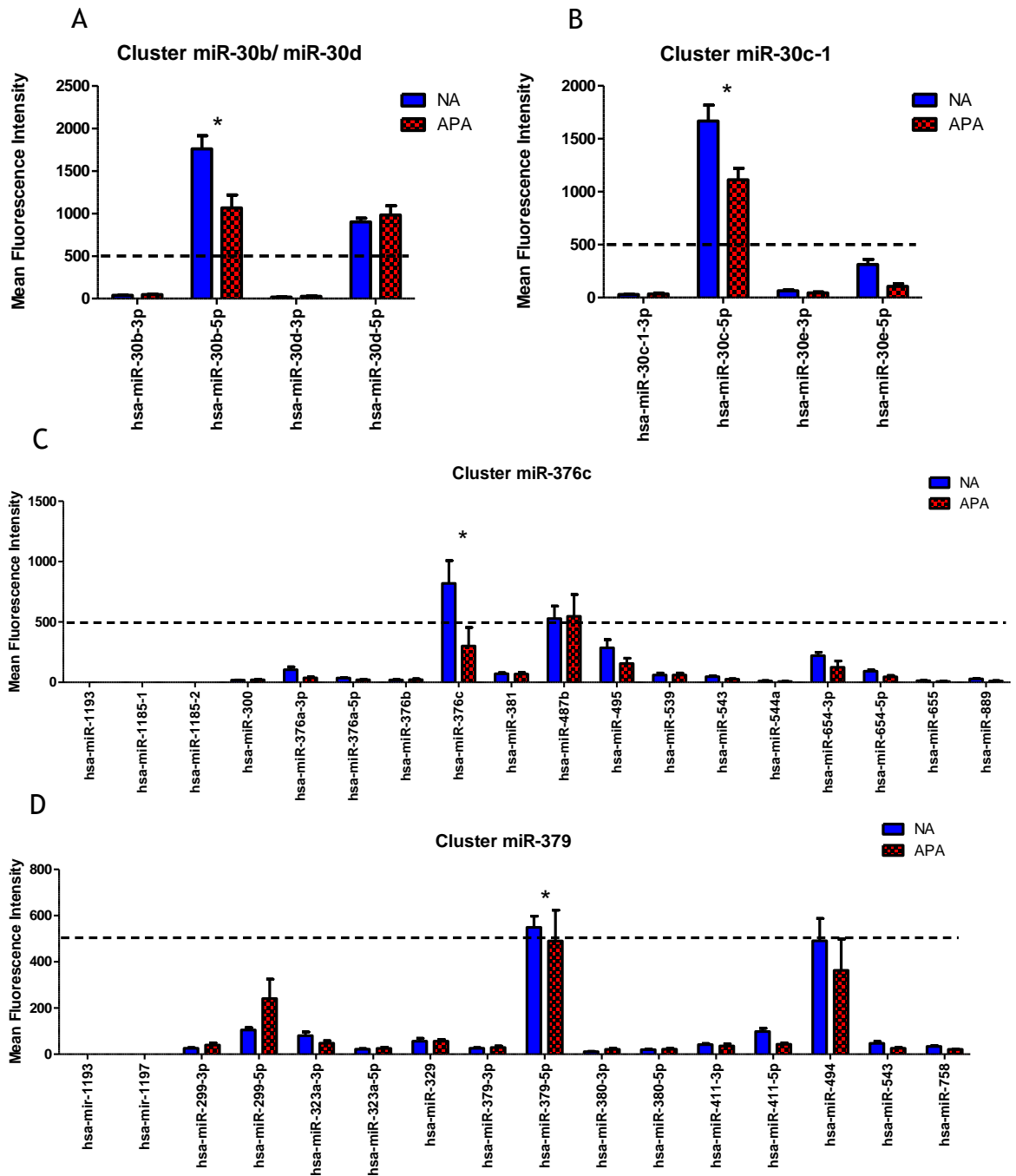


**Figure 3-9: miRNA Clusters (NA>APA) detected from microarray analysis (Cluster miR-30b (A), Cluster miR-30c (B), Cluster miR-376c (C) and miR-379 (D)).**

Blue bars indicate miRNAs that are expressed in NA and red bars indicate APA (\* $p < 0.05$ ).

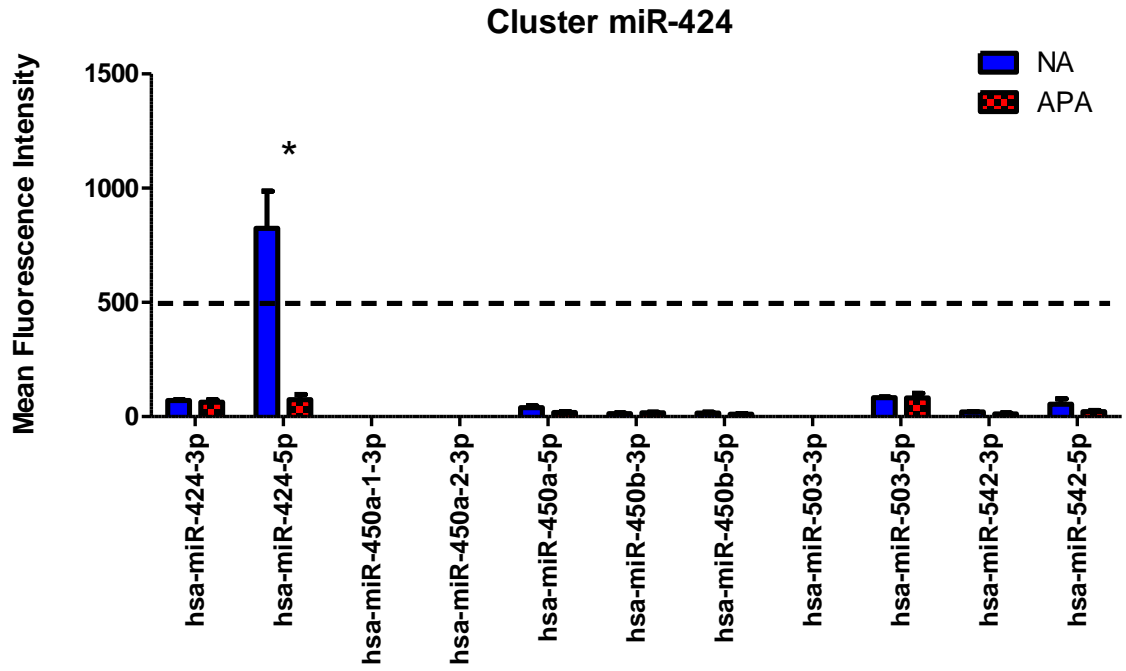


**Figure 3-10: miRNA Clusters (NA>APA) detected from microarray analysis (Cluster miR-424).**

Blue bars indicate miRNAs that are expressed in NA and red bar indicates APA (\* $p < 0.05$ ).

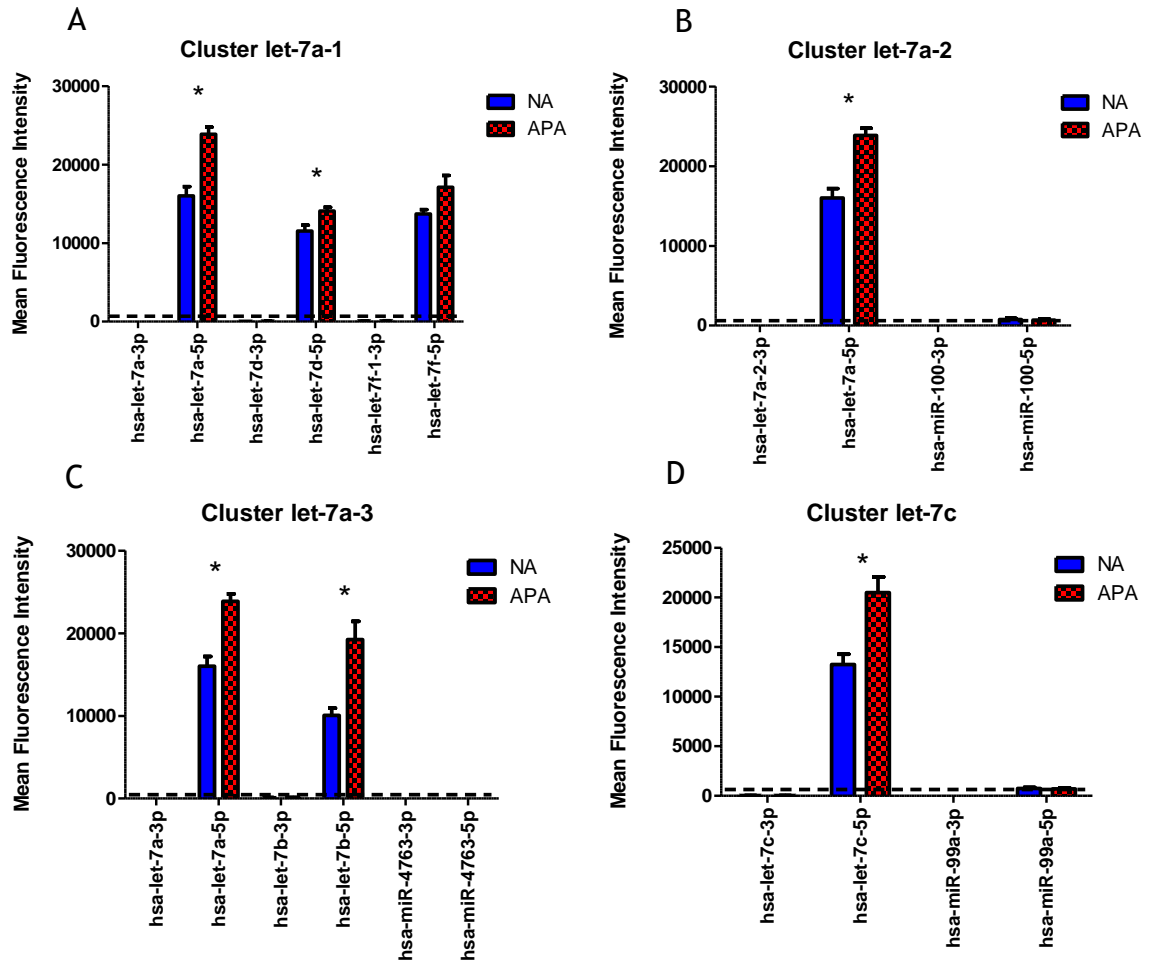


**Figure 3-11: miRNA Clusters (APA>NA) detected from microarray analysis (Cluster let-7a-1 (A), Cluster let-7a-2 (B), Cluster let-7a-3 (C) and Cluster let-7c (D)).**

Blue bars indicate miRNAs that are expressed in NA and red bars indicate APA (\* $p < 0.05$ ).

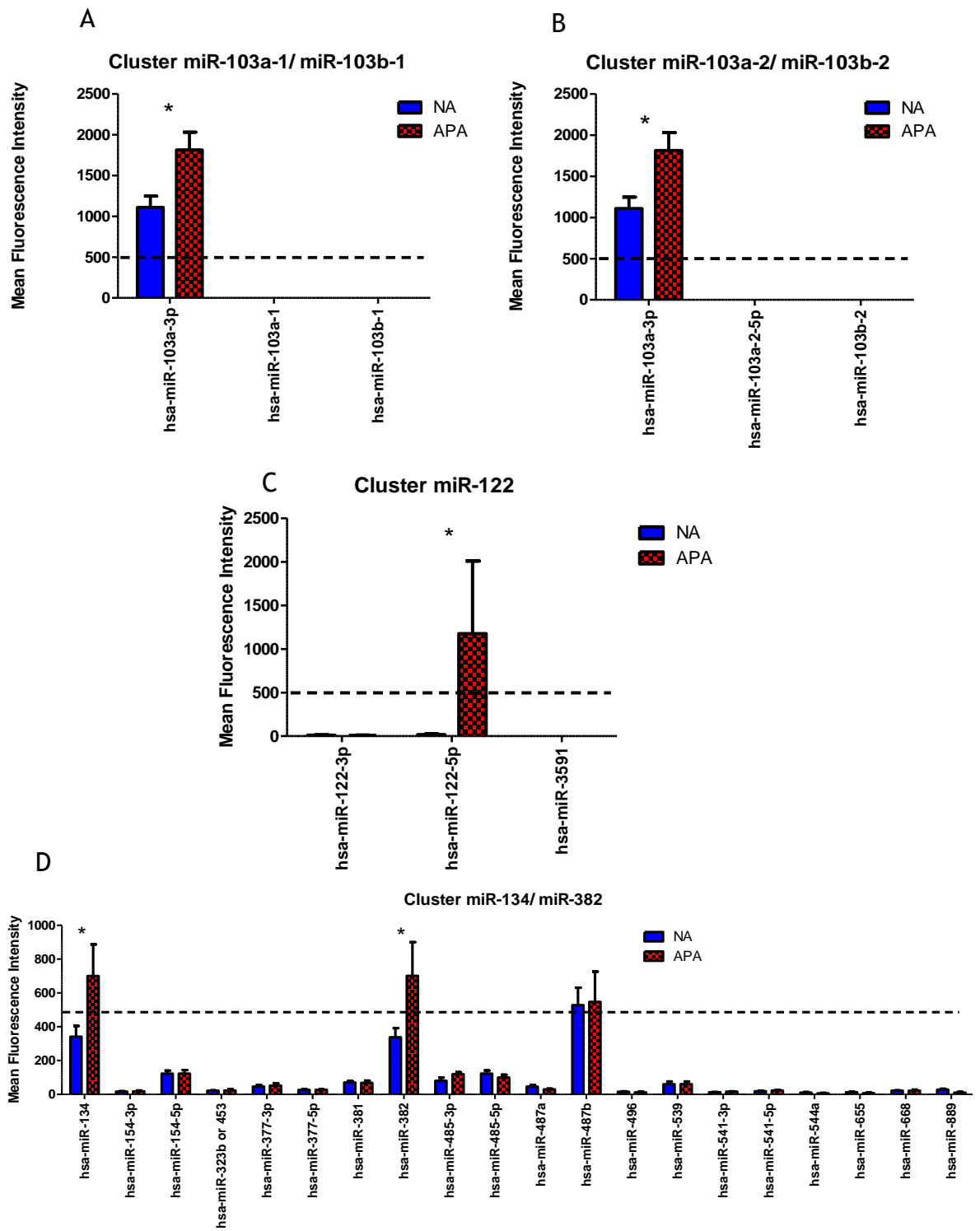


**Figure 3-12: miRNA Clusters (APA>NA) detected from microarray analysis (Cluster miR-103ab-1 (A), Cluster miR-103ab-2 (B), Cluster miR-122 and (C) Cluster miR-134 (D)).**

Blue bars indicate miRNAs that are expressed in NA and red bars indicate APA (\* $p < 0.05$ ).

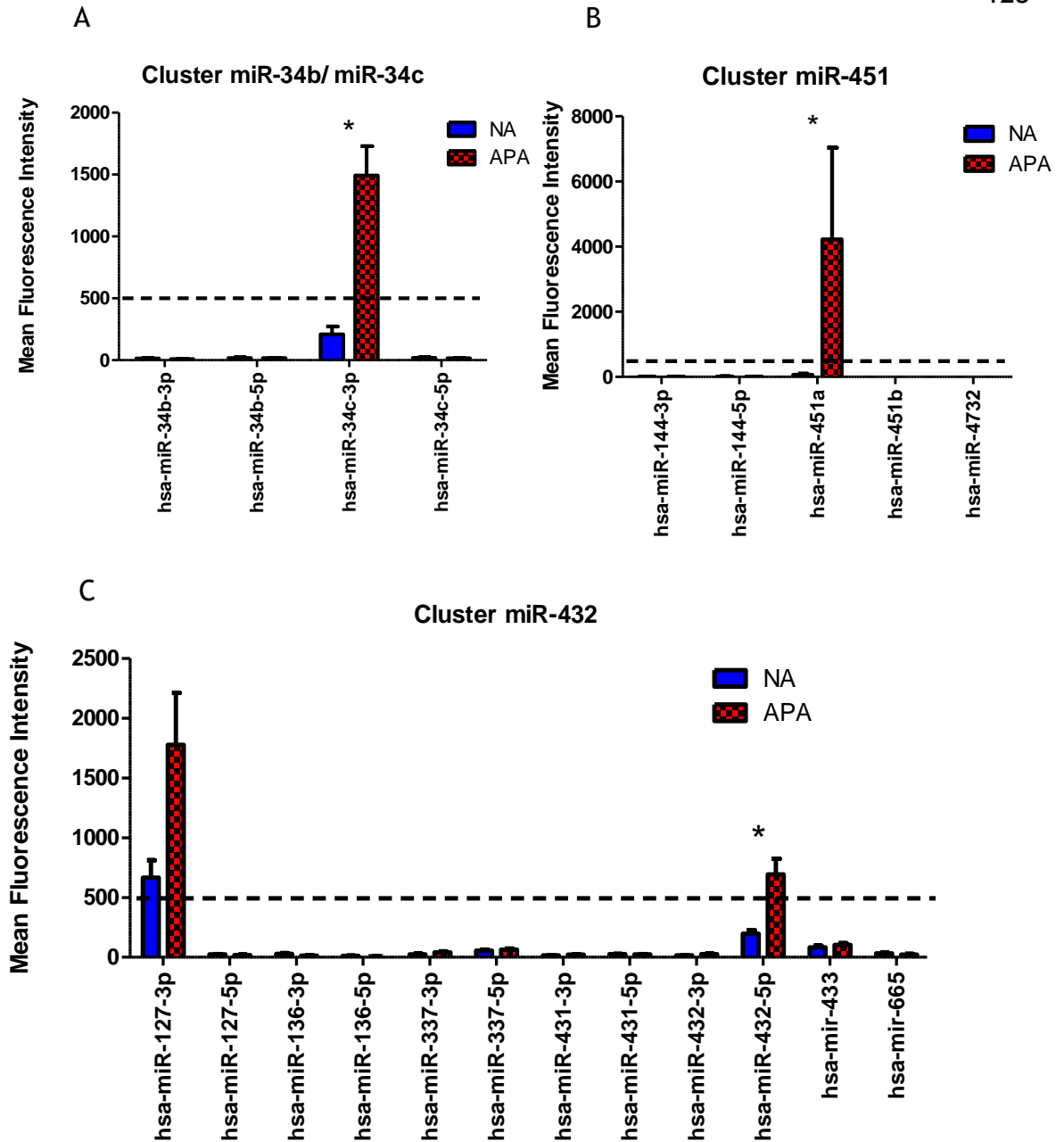


**Figure 3-13: miRNA Clusters (APA>NA) detected from microarray analysis (Cluster miR-34c (A), Cluster miR-451 (B) and Cluster miR-432 (C)).**

Blue bars indicate miRNAs that are expressed in NA and red bars indicate APA (\* $p < 0.05$ ).

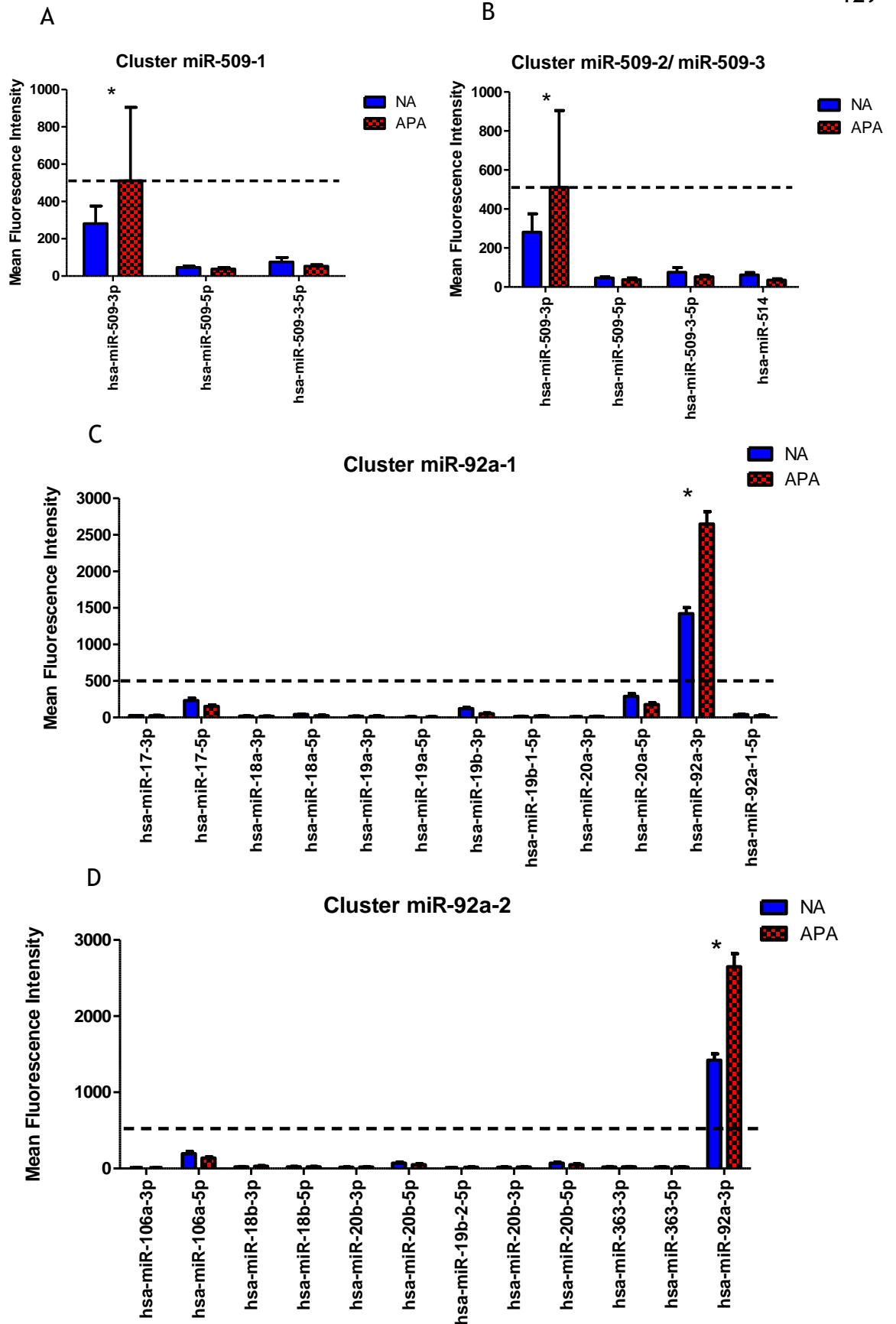


**Figure 3-14: miRNA Clusters (APA>NA) detected from microarray analysis (Cluster miR-509-1 (A), Cluster miR-509-2 (B), Cluster miR-92a-1 (C) and Cluster miR-92a-2 (D)).** Blue bars indicate miRNAs that are expressed in NA and red bars indicate APA (\* $p < 0.05$ ).

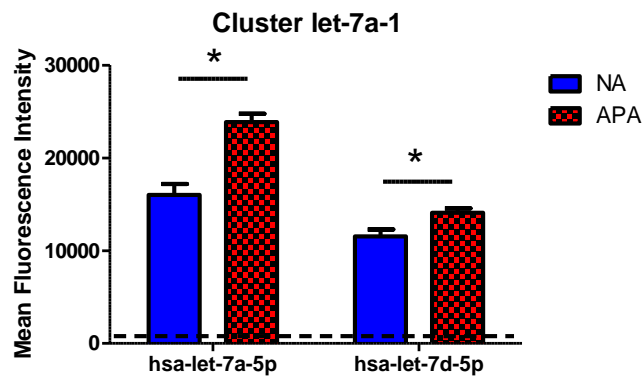


**Figure 3-15: Cluster let-7a-1 consists of 6 miRNAs; 2 of the miRNAs are above 500 AU and differentially expressed.**

The blue bars represent normal adrenal (NA) and the red bars represent adrenal producing adenoma (APA). The dotted line indicates the 500 AU cut-off point, \*p-value <0.05.

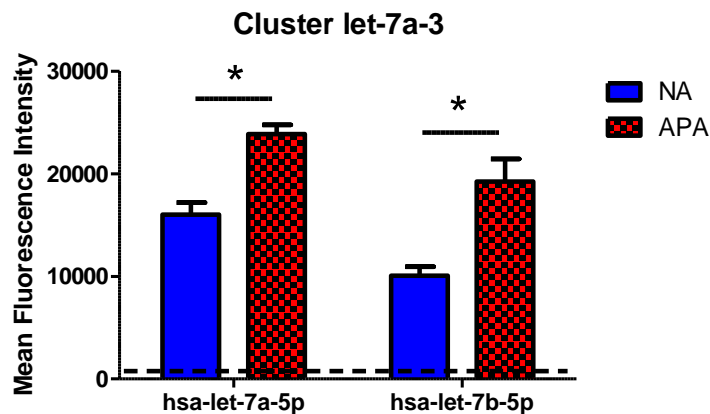


**Figure 3-16: Cluster let-7a-3 consists of 6 miRNAs; 2 of the miRNAs are above 500 AU and differentially expressed.**

The blue bars represent normal adrenal (NA) and the red bars represent adrenal producing adenoma (APA). The dotted line indicates the 500 AU cut-off point, \*p-value <0.05.

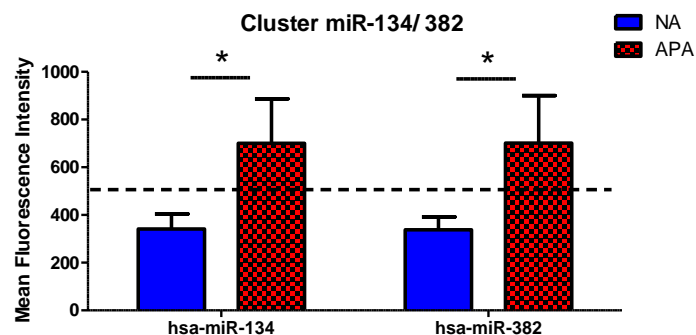


**Figure 3-17: Cluster miR-134 consists of 16 miRNAs. Only 2 miRNAs (miR-134 and miR-382) showed similar pattern of expression and they are above 500 AU in APA.**

The others are mostly not expressed in microarray (<500 AU). The blue bars represent normal adrenal (NA) and the red bars represent adrenal producing adenoma (APA). The dotted line indicates the 500 AU cut-off point, \*p-value <0.05.

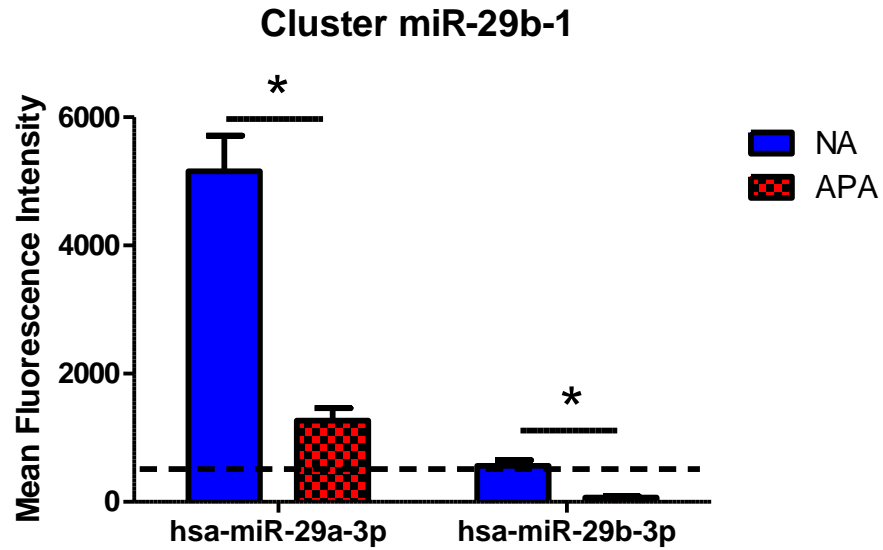


**Figure 3-18: Cluster miR-29b-1 consists of 4 miRNAs; 2 of the miRNAs are above 500 AU.** 2 of the miRNAs are above 500 AU and differentially expressed. The blue bars represent normal adrenal (NA) and the red bars represent adrenal producing adenoma (APA). The dotted line indicates the 500 AU cut-off point. \*p-value <0.05.

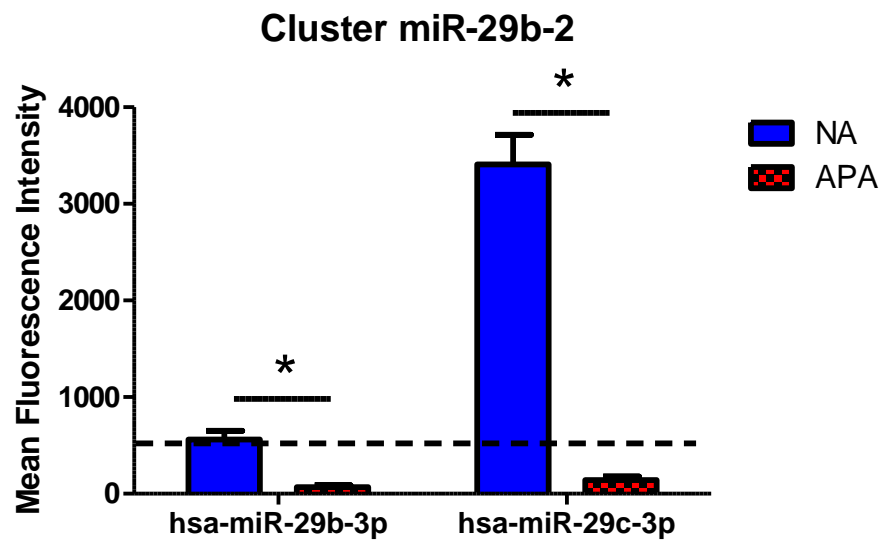


**Figure 3-19: Cluster miR-29c/29b-2 consists of 4 miRNAs; 2 of the miRNAs are above 500 AU and differentially expressed.** The blue bars represent normal adrenal (NA) and the red bars represent adrenal producing adenoma (APA). The dotted line indicates the 500 AU cut-off point, \*p-value <0.05.

### 3.3.5 Ingenuity® Systems Pathway Analysis (microRNA target Filter)

Having analysed the presence and differential expression levels of miRNAs between tissue types, further analysis of possible biological function was conducted using Ingenuity® Systems Pathway Analysis software (IPA; Ingenuity Systems, Redwood City, CA USA; <http://www.ingenuity.com>). This enables plausible messenger RNA targets of the differentially-expressed miRNAs to be determined in order to assess their possible molecular and cellular functions.

47 Differentially-expressed miRNAs ( $p < 0.05$ ,  $> 500$  AU), as identified from the microarray data, were uploaded to the IPA system. Subsequently, using miRNA Target Filters, 34 miRNAs were automatically selected (Figure 3-20) while 13 miRNAs are not included in the IPA analysis. The 13 miRNAs were excluded either due to no interaction being detected between the miRNA and mRNA or because the miRNAs were not listed in the database. These 34 miRNAs included those that share the same seed sequences (as shown in Table 3-1 and Table 3-2), which are termed 'synonymous miRNA'. These filtered miRNAs were then analysed using various software resources such as Ingenuity Expert Finding, Ingenuity Expert Assist Finding, miRecords, Tarbase and TargetScan Human. When predicting possible targets for miRNAs, different levels of rigour can be applied to the results. For example, it can be requested that only experimentally validated miRNA-mRNA interactions demonstrated in a previously published study be included in the results. Alternatively, highly and/or moderately predicted mRNA targets can also be included; although less rigorous, these predictions produce a greater number of 'hits' than the obviously more limited list of validated interactions.

Data may also be filtered by specific disease type (e.g. endocrine, cardiovascular and cancer), by specific pathway (e.g. hormone/ sterol biosynthesis, apoptosis, cell growth, proliferation and development) and by organ system (e.g. adrenal gland). When all these filters are applied, the number of mRNA targets predicted for the 34 miRNAs under investigation reduce dramatically from 11,933 to 116 (Figure 3-20).

The next sections will focus on particular genes (i.e CYP11B2, HMGCR and others) and the pathways relevant to APA pathogenesis that are identified by IPA as being apparently targeted by multiple miRNAs.

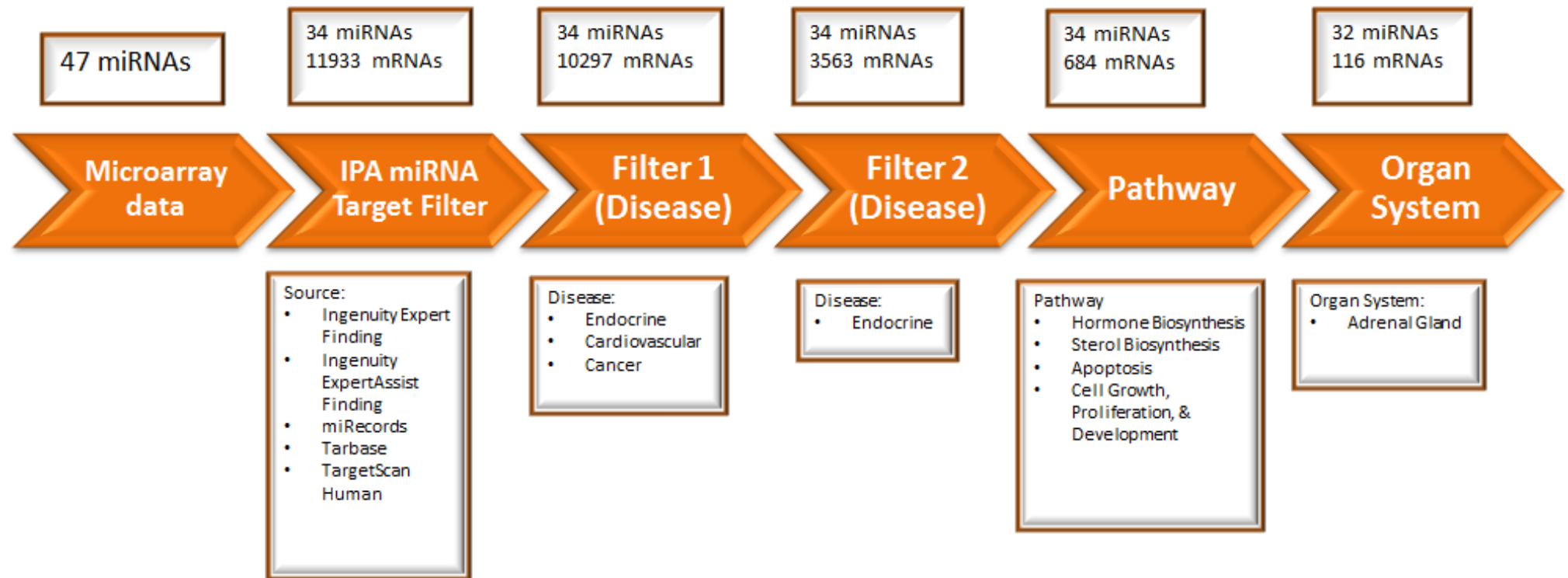


**Figure 3-20: Summary of differentially-expressed miRNA analysis in NA vs APA, conducted using Ingenuity Pathway Analysis (IPA).**

Using the IPA miRNA Target Filter, the number of miRNAs under investigation was reduced from 47 to 34. Applications of further filters then reduced the predicted number of target mRNAs for these 34 miRNAs from 11,933 to 116.

**Table 3-1: Synonymous miRNAs expressed in NA (>500 AU) i.e. miRNAs having similar seed sequence and therefore sharing similar mRNA targets (IPA).**

miRNA (miRBase Acession)	Synonym miRNAs/ Overlapped miRNAs (miRBase Acession)	Seed Sequence	Number of targeted mRNA from different genes
hsa-miR-10a-5p		ACCCUGU	780
hsa-miR-125a-5p	hsa-miR-125b-5p	CCCUGAG	1531
hsa-miR-126a-3p		CGUACCG	111
hsa-miR-139-5p		CUACAGU	690
hsa-miR-148a-3p		CAGUGCA	1197
hsa-miR-15a-5p	hsa-miR-16-5p	AGCAGCA	2020
	hsa-miR-195		
	hsa-miR-424		
hsa-miR-21-5p		AGCUUUAU	615
hsa-miR-24-3p		GGCUCAG	1394
hsa-miR-26b-5p	hsa-miR-26a-5p	UCAAGUA	1095
hsa-miR-27a-3p	hsa-miR-27b-3p	UCACAGU	1654
hsa-miR-29b-3p	hsa-miR-29a-3p	AGCACCA	1492
	hsa-miR-29c-3p		
hsa-miR-30c-5p	hsa-miR-30a-5p	GUAAACA	1592
	hsa-miR-30b-5p		
hsa-miR-335-5p		CAAGAGC	637
hsa-miR-376c-3p		ACAUAGA	667
hsa-miR-379-5p		GGUAGAC	448

**Table 3-2: Synonymous miRNAs expressed in APA (>500 AU) i.e. miRNAs having similar seed sequence and therefore sharing similar mRNA targets (IPA).**

miRNA (miRBase Acession)	Synonym miRNAs/ Overlapped miRNAs (miRBase Acession)	Seed Sequence	Number of targeted mRNA from different genes
hsa-let-7a-5p	hsa-let-7b/c/d-5p	GAGGUAG	1396
hsa-miR-103-3p	hsa-miR-107	GCAGCAU	1255
hsa-miR-140-3p		ACCACAG	792
hsa-miR-149-3p		GGGAGGG	2606
hsa-miR-320a	hsa-miR-320b	AAAGCUG	1073
hsa-miR-34a-5p		GGCAGUG	1477
hsa-miR-34c-3p		AUCACUA	302
hsa-miR-361-5p		UAUCAGA	561
hsa-miR-375-3p		UUGUUCG	263
hsa-miR-382-5p		AAGUUGU	447
hsa-miR-432		CUUGGAG	491
hsa-miR-451a		AACCGUU	190
hsa-miR-483-5p		AGACGGG	461
hsa-miR-509-3p		GAUUGGU	346
hsa-miR-574-3p		ACGCUCA	199
hsa-miR-574-5p		GAGUGUG	564
hsa-miR-92a-3p	hsa-miR-92b-3p	AUUGCAC	1139

### 3.3.5.1 Experimentally Validated Targets of clustered differentially-expressed miRNAs.

IPA analysis identified 3 miRNAs clusters containing differentially-expressed constituents to be of particular interest.

The first is cluster let-7a-1 which contains, among others, the differentially expressed miRNAs let-7a-5p and let-7d-5p (Figure 3-11). Both of these miRNAs are significantly downregulated in NA compared to APA. let-7f-5p also shows a similar downregulation pattern in NA, but it is not significant. IPA analysis lists 132 experimentally-validated mRNA targets for members of this cluster, 131 of them human. Interestingly, these validated targets include DICER1, which expresses the key component of miRNA processing. Overexpression of let-7 significantly reduces expression of DICER1 at the mRNA and protein levels; furthermore, downregulation of DICER1 itself reduces let-7 expression (Tokumaru, Suzuki et al. 2008). let-7a and let-7c have also been shown experimentally to target HMGA2 (High-mobility group A2), an early embryonic gene that is up-regulated in many advanced cancers and whose expression correlates with poor prognosis (Shell, Park et al. 2007, Peng, Laser et al. 2008).

The other two clusters, cluster miR-29b-1 (Figure 3-18) and cluster miR-29b-2 (Figure 3-19), both contain miRNAs that are upregulated in NA relative to APA and have similar seed sequences (i.e. are synonymous), as shown in Table 3-1. These clusters share 57 experimentally-validated targets according to the IPA database. Among the targeted genes are COL1A1, COL1A2, COL3A1 and COL5A3, which are involved in atherosclerosis signalling. These are discussed later in this chapter.

**Table 3-3: Cluster let-7a and let-7b miRNAs share the same experimentally-validated mRNA targets as a result of their synonymous seed sites.**  
Source: IPA database.

Validated targets for cluster let-7a and let-7b					
1GF2BP2	CDK6	FANCD2	LIN28A	PRRC2A	SMC1A
AARSD1	CDKAL1	FNDC3A	MARS2	PTGS2	SMOX
ACP1	CHMP2A	GAK	MED28	PXDN	SNAP23
ADGRG1	COIL	GEMIN7	MLLT1	RABGAP1L	SPCS3
AGO4	COL1A2	GRPEL2	MRM1	Ras	SPRYD4
AKAP8	COMMD9	GTPBP3	MRPS24	RBM19	SYPL1
ANAPC1	CSDE1	GYS1	MRPS33	RDH10	TAF9B
ATAD3B	CSNK1D	HMGA1	MTPN	RHO6	TAGLN
ATP6V1F	DAD1	HMGA2	MTRR	RHOB	TGFBR1
ATP6VOA1	DHX57	HMOX1	MYC	RPP38	THBS1
AURKB	DICER1	HYOUT	NEDD4	RRP8	TLR4
BCL2L1	DOCK5	IFIT5	NF2	RTCA	TMEM2
BCL7A	DRD3	IFRD1	NRAS	SCYL1	TPM2
BMP2K	DSP	IGF2BP1	NXN	SEPT3	TRIM71
BSG	DUSP12	IGF2BP3	PGRMC1	SIGMAR1	TRMT1
CALCOCO2	DUSP23	IPO4	POLD2	SLC1A4	TTC9C
CAPG	EIF3J	ITGB3	POLR2C	SLC25A1	TUSC2
CARHSP1	EIF4G2	KCNJ16	POM121C	SLC25A13	UGT8
CASP3	F2	KLK10	PPP1R7	SLC25A24	UHRF1
CCND1	FADS2	KRAS	PRDM1	SLC25A32	VIM
CDC25A	FAM105A	KRT19	PRIM1	SLC38A1	VPS39
CDIPT	FAM96A				

**Table 3-4: Clusters miR-29b-1 and miR-29b-2 miRNAs share the same experimentally-validated mRNA targets as a result of their synonymous seed sites.**  
Source: IPA database.

Validated target for cluster miR-29b-1 and miR-29b-2			
ACVR2A	DCP2	MAPRE2	TCL1A
ARPC3	DNMT3A	MCL1	TDG
BACE1	DNMT3B	MLF1	TET1
CAV2	DUSP2	MYBL2	TGFB3
CD276	FAM3C	NASP	Tpm1
CDC42	FBN1	NAV3	TRIM9
CDK6	FRAT2	PIK3R1	TUBB2A
CNOT8	GAS7	PPIC	YY1
COL15A1	GMFB	PPM1D	ZFP36L1
COL1A1	GPR37	PTEN	
COL1A2	HDAC4	PURA	
COL3A1	HMG3	RERE	
COL4A1	INSIG1	SHROOM2	
COL4A2	KCTD3	SP1	
COL5A2	KLF4	SPARC	
COL5A3	LAMC1	SRSF10	
	LOXL2		

### 3.3.5.2 *HMGCR*, a potential miRNA target

One of the most striking results of IPA analysis concerns the *HMGCR* gene. *HMGCR* targeting by miRNA was chosen to be one of the main focuses of investigation in this thesis. This is due to its function as a limiting enzyme for cholesterol synthesis, and the fact that cholesterol is the main substrate for steroidogenesis. 3-Hydroxy-3-methylglutaryl-coenzyme A (HMG-CoA) reductase (*HMGCR*) is a rate-limiting enzyme for cholesterol biosynthesis. It is involved in various canonical pathways including Retinoid-X-Receptor/ Liver-X-Receptor (LXR/ RXR) signalling (Figure 3-23), Adenosine Monophosphate-Activated Protein Kinase (AMPK) signalling (Figure 3-24) and the Mevalonate Pathway (Figure 3-25). Targeting of *HMGCR* in the mevalonate cascade may have therapeutic applications by inhibiting cholesterol biosynthesis. As cholesterol is the main substrate for steroidogenesis, there are obvious implications for APA function.

Seven of the differentially-expressed miRNAs are predicted to target *HMGCR*: miR-125a-5p, miR-27a-3p, miR-27b-3p, miR-29a-3p, miR-29c-3p and miR-335-5p (Figure 3-22). Each is downregulated in APA (Figure 3-21).

miR-27a-3p (chromosome 19) and miR-27b-3p (chromosome 9) share the seed sequence UCACAGU, while miR-29a-3p (chromosome 7), miR-29b-3p (chromosome 7 & 1) and miR-29c-3p (chromosome 1) share the seed sequence AGCACCA (Table 3-1).

Two differentially-expressed clusters are involved in targeting *HMGCR*: Cluster miR-29a-3p/ miR-29b-3p and Cluster miR-29b-3p/ miR-29c-3p.

miR-125a-5p is potentially the most interesting of these miRNAs. miR-125a-5p (previously miR-125a in earlier miRBase versions) is transcribed from chromosome 19 as part of a cluster with let-7e, miR-125a, and miR-99b (Figure 3-7). TargetScan Human predicts mature miR-125a-5p (seed CCCUGAG) targets human *HMGCR* mRNA (aggregate PCT=0.289, total context + score= 0.211) and also *CYP11B2* mRNA (aggregate PCT=0.06, total context + score= 0.377), suggesting it may be able to simultaneously target the mevalonate pathway and the mineralocorticoid pathway, as shown in Figure 3-25.

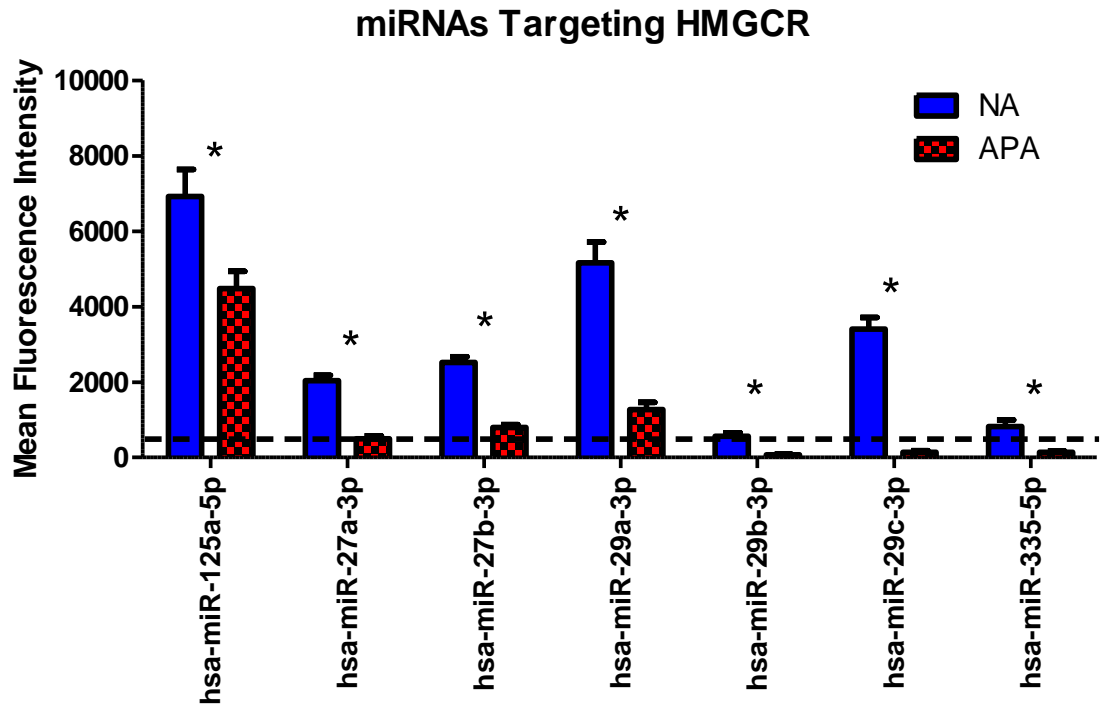


**Figure 3-21: Microarray expression of miRNAs targeting *HMGCR*.**  
All of the miRNAs were downregulated in APA compared to NA tissues (\* $p < 0.05$ ).

## HMGCR &amp; 4 miRNAs

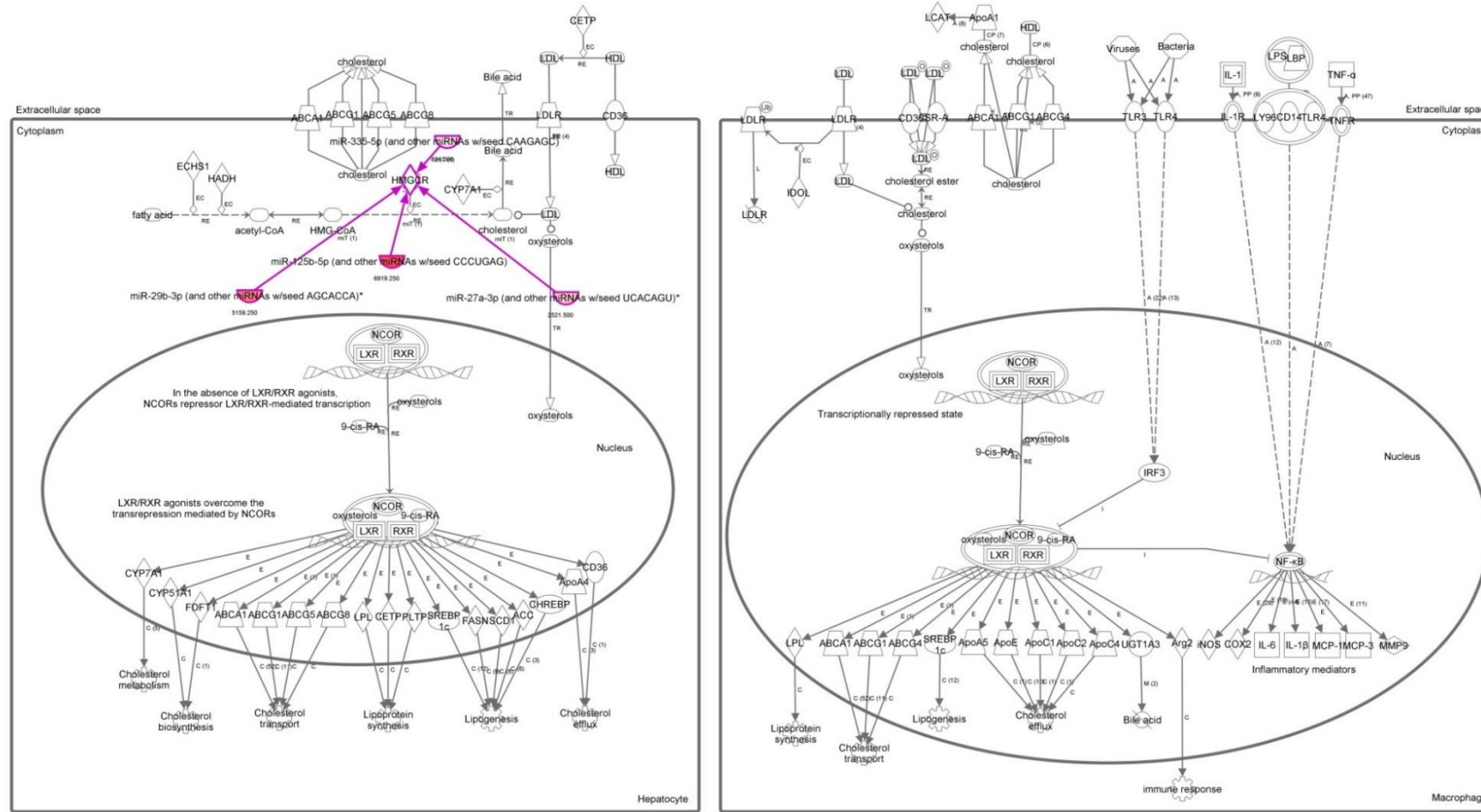


© 2000-2015 QIAGEN. All rights reserved.

**Figure 3-22: Seven differentially-expressed miRNAs are predicted to target *HMGCR*.**

Note that only 4 direct interactions are shown in this diagram, as IPA groups the three synonymous miRNAs together.

LXR/RXR Activation 4 miRNAs NA High



© 2000-2015 QIAGEN. All rights reserved.

**Figure 3-23: miRNAs targeting *HMGCR* in LXR/ RXR Pathway.**  
 All of the miRNAs are highly upregulated in NA tissue (p<0.05, >500 AU).



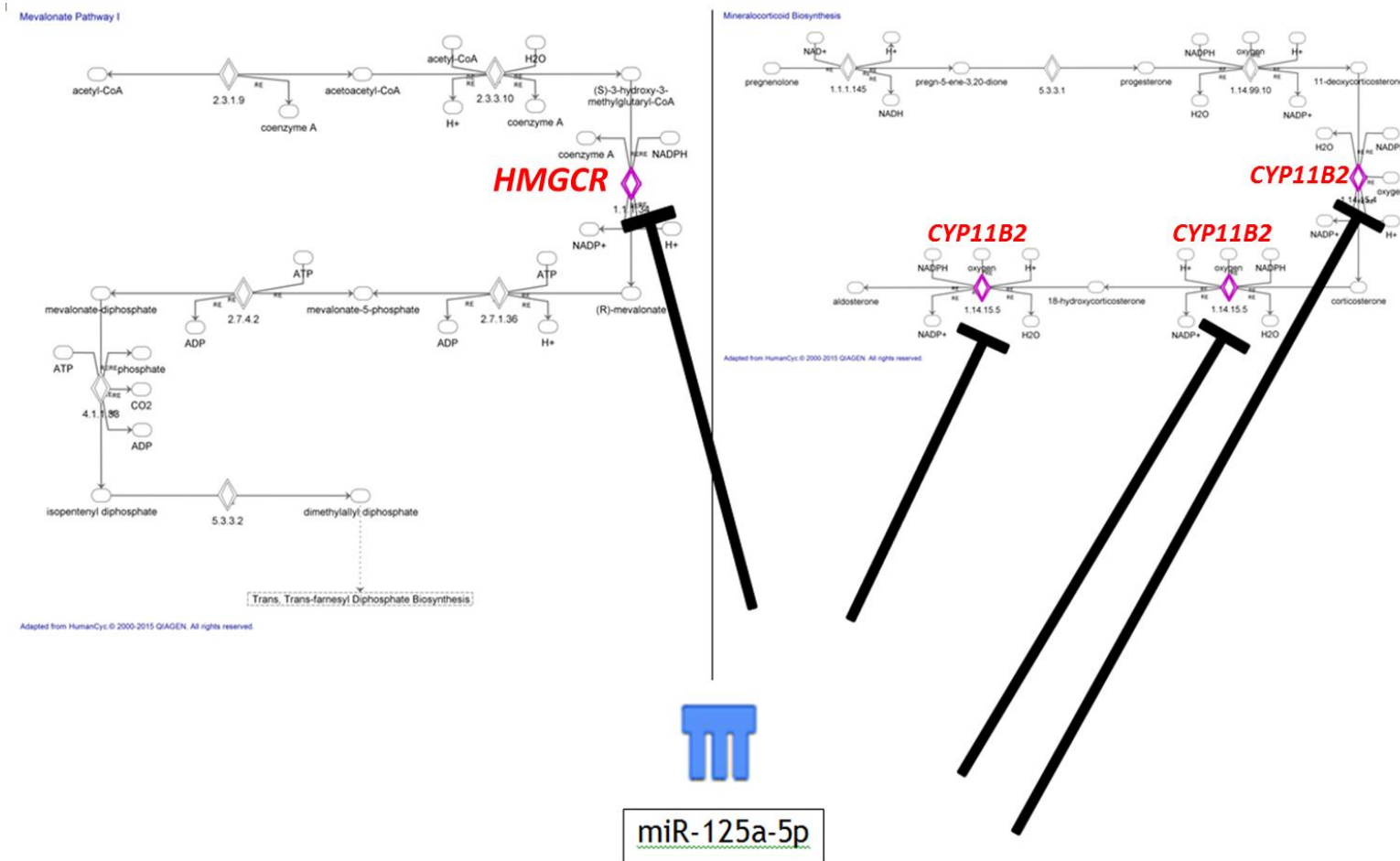


Figure 3-25: miR-125a-5p is targeting *HMGCR* in Mevalonate Pathway and targeting *CYP11B2* in the Mineralocorticoid Biosynthesis Pathway.

### 3.4 Discussion

The microarray analysis presented here shows 23 miRNAs to be expressed at significantly higher levels in NA relative to APA, including miR-125a-5p, miR-27a/b-3p, miR-29a/b/c-3p and miR-30a/b/c-5p (Figure 3-5). Conversely, 24 miRNAs were significantly upregulated in APA relative to NA (Figure 3-6). The summary of miRNA expression in APA vs NA is as shown in Chapter 1 (Table 1-8). For miRNA expression in ACC vs ACA see Table 1-6 and Table 1-7. Some of these results are not in agreement with the Velázquez-Fernández study where, for example, mir-29c-3p was found to be downregulated in NA and miR-320a was downregulated in APA (Velázquez-Fernández, Caramuta et al. 2014). On the other hand, there are areas of agreement between the two studies, including the finding that miR-92a and mir-361-5p are more highly expressed in APA relative to NA (Velázquez-Fernández, Caramuta et al. 2014). The differences of these results may be due to non-homogenous cell populations in the APA and NA samples. Furthermore, the samples used in Velázquez-Fernández et al. 2014 were obtained from snap-frozen tissues and were analysed by a different microarray platform i.e. Agilent Technologies' human microarray (Velázquez-Fernández, Caramuta et al. 2014).

Although the 47 differentially-expressed miRNAs identified here represent just a small fraction of the 723 miRNAs detectable by microarray, the number and variety of possible mRNA targets for these 47 is so potentially large that careful use of bioinformatic tools is required in order to focus on the pathways most likely to be relevant in the development and pathogenesis of APA. Filtering of data by IPA led to the highlighting of miR-125a, miR-335, cluster miR-29b and cluster let-7a.

miR-29c is clustered in miR-29b group. The downregulation pattern of miR-29c in APA is in accordance with the low expression of miR-29c in nasopharyngeal carcinomas (NPC). The low level of miR-29c is correlated with high levels of COL1A1, COL1A2 and COL3A1. miR-29c inhibits the luciferase activity at the 3'UTR of the mentioned genes (Sengupta, den Boon et al. 2008). However in another study, miR-29 was found to be upregulated in aortic dilation (Boon, Seeger et al. 2011) and aortic aneurysms (Maegdefessel, Azuma et al. 2012). It is correlated with significant downregulation of many extracellular matrix

components (Boon, Seeger et al. 2011, Maegdefessel, Azuma et al. 2012). One study suggests that anti miR-29 could improve vascular integrity during aneurysm (Boon, Seeger et al. 2011) and markedly increase elastin expression in Williams-Beuren syndrome (characterized with aortic stenosis) (Zhang, Huang et al. 2012). miR-29a, miR-29b and miR-29c inhibit the expression of COL1A1, COL1A2, COL3A1, COL4A1 and numerous extracellular matrix protein. These genes and proteins can lead to cardiac, liver, renal and pulmonary fibrosis. It is suggested that anti miR-29 could be used as a therapeutic method for aneurysm, vulnerable plaque and pro-elastin/pro-collagen therapies (Van Rooij and Olson 2012). This study is supported by another experiment where miR-29b was shown to suppress alpha 1 collagen (COL1A1) mRNA and protein level through 3'UTR binding in human stellate culture cells. COL1A1 is involved in liver fibrogenesis. This study proposed miR-29b as a therapeutic tool for antifibrotic therapy (Ogawa, Iizuka et al. 2010). In diabetic-induced rat, miR-29a, miR-29b and miR-29c are upregulated in microarray of the Goto-Kakizaki (GK) rat compared to healthy controls. Validation with Northern blotting shows upregulation of the 3 paralogs miRNA in muscle, fat and liver of diabetic rat, all of which are the target tissues of insulin action. Increased miR-29a/b/c might cause insulin resistance by repressing insulin-stimulated glucose uptake (He, Zhu et al. 2007).

Members of the let-7 family (let-7a-5p, let-7b-5p, let-7c and let-7d-5p) were consistently upregulated in APA tissues (Figure 3-6). In one study, let-7a and let-7d were downregulated in ACC compared to ACA (Patterson, Holloway et al. 2011). However, Özata et al reported a different finding, where let-7a and let-7d were both increased significantly in ACC compared with ACA (Özata, Caramuta et al. 2011). In other tumours, members of let-7 family were significantly suppressed in primary malignant melanoma compared to the control (benign melanocytic nevi). let-7b overexpression in melanoma samples via in vitro analysis downregulated the expression of cyclins D1, D3, A and cyclin-dependent kinase 4 (CDK4) at 3'UTR region. let-7b inhibited cell-cycle progress and stopped the growth of melanoma cells (Schultz, Lorenz et al. 2008). let-7e directly suppresses Cyclin D1, resulting in the inhibition of G(1) cell cycle progress in a breast carcinoma cell line (Mitra, Das et al. 2011). let-7d is upregulated in transition of breast ductal carcinoma in situ (DCIS) to invasive ductal carcinoma (IDC) (Volinia, Galasso et al. 2012). In the chemical-induced

hepatocarcinogenesis rat model, several circulating miRNAs are highly elevated; e.g. let-7a, let-7f. Both of these miRNAs are even detected at the early stages of hepatocarcinogenesis, indicating that they might be useful as predictive tools to monitor development of carcinogenesis (Sukata, Sumida et al. 2011).

miR-125a-5p shares the same seed sequence with miR-125b-5p shown in Table 3-1. It is downregulated in APA compared to NA (Figure 3-5). Patterson et al, showed a downregulation pattern of expression of miR-125a-5p and mir-125b in ACC compared to ACA (Patterson, Holloway et al. 2011). Özata et al found the opposite, where the miR-125a-5p was upregulated in ACC compared to ACA (Özata, Caramuta et al. 2011). In the urinary system, the expression of miR-125b was significantly decreased in bladder cancer tissue and bladder cancer cell lines. This in vitro experiment showed that miR-125b inhibits the formation of cancer colonies and suppresses bladder tumour in mice. Among miR-125b targets are E2F3 and Cyclin A2, both essential for cell cycle transition (G1/ S phase). miR-125b inhibits the expression of E2F3 and Cyclin A2. This experiment suggested that miR-125b may be involved in cell cycle regulation via the E2F3-Cyclin A2 signalling pathway and that downregulation of miR-125b may be a contributing factor to tumorigenesis (Huang, Luo et al. 2011). Furthermore, miR-125a-5p inhibits migration and invasion of lung carcinoma. Epidermal growth factor receptor (EGFR) activation significantly repressed miR-125a-5p. EGFR regulates progression of epithelial malignancy. These data suggest that miR-125a-5p might be a metastasis suppressor (Wang, Mao et al. 2009). In another study, miR-125b was significantly suppressed in malignant melanoma cell lines and downregulates c-Jun protein. C-Jun is the main regulator for melanoma progression (Kappelmann, Kuphal et al. 2013). miR-125b is located close to the deletion genomic region (epicentre of 11q23) in chronic lymphocytic leukaemias (CLLs). The aggressive and slow type of human CLL showed low expression of miR-125b. In in-vitro analysis, miR-125b increases the downregulation of T53 mRNA in MEC2 cells (cell line derived from B-chronic lymphocytic leukaemia) (Tili, Michaille et al. 2012). On the other hand, miR-125b is abundantly expressed in squamous cell carcinoma (SCC). It directly repressed the MAP kinase gene and Vps4B (vacuolar protein-sorting 4 homolog B) that prolong the activation of epidermal growth factor receptor (EGFR) signalling that subsequently leads to cell proliferation, cell migration and adhesion (Zhang, Ge

et al. 2014). miR-125a is overexpressed in the hyperglycaemic hepatocyte of the Goto-Kakizaki (GK) rat and in adipose tissue (Herrera, Lockstone et al. 2009).

*HMGCR* is a rate-limiting enzyme for cholesterol biosynthesis. *HMGCR* is also involved in the LXR/ RXR Pathway (Figure 3-23) and in AMPK (Adenosine monophosphate-activated protein kinase) signalling (Figure 3-24) through the Mevalonate Cascade (Figure 3-25). *HMGCR* expression is negatively mediated by sterols and non-sterol metabolites originating from mevalonate. The enzyme is suppressed by cholesterol derived from internalization of LDL via the LDLR. Inhibition of *HMGCR* induces the expression of LDLR in hepatocytes which leads to increased plasma LDL catabolism and subsequent decrease in plasma cholesterol level. This will eventually reduce the formation of atherosclerosis. *HMGCR* is targeted by statin, which lowers the cholesterol level. Statin is a potent cholesterol lowering drug that lowers cardiovascular mortality in hypercholesterolemia patients (Gould, Rossouw et al. 1998). The decrease in intracellular cholesterol stimulates SREBP, increasing LDLR and hence upregulating LDL uptake from plasma and reducing cholesterol in the circulation. miR-125a-5p is predicted to target *HMGCR* and *CYP11B2* mRNAs. It is suggested that miR-125a-5p might be a therapeutic tool to decrease cholesterol level and to repress the production of aldosterone in APA.

miR-335 has a total of 637 target mRNAs predicted by IPA analysis. Among these is *HMGCR*. Similar to miR-125a-5p, this miRNA is downregulated in APA tissues. In 2009, miR-335 was reported to be downregulated in ACC compared to ACA (Soon, Tacon et al. 2009). This study is supported by Schmitz et al. and Chabre et al., who found miR-335 to be low in ACC compared to ACA (Schmitz, Helwig et al. 2011, Chabre, Libé et al. 2013). Overexpression of miR-335 not only inhibits human mesenchymal stem cell (hMSCs) proliferation, migration and differentiation but also decreases their adipogenic and osteogenic potential (Tome, Lopez-Romero et al. 2011). Furthermore, in breast cancer, miR-335 suppresses tumour reinitiation and metastasis (Png, Yoshida et al. 2011).

### 3.5 Conclusion

In conclusion, the studies in this chapter have identified from microarray profiling that regulation of certain miRNA clusters are consistently differentially regulated in similar in APA relative to normal adrenal tissue and share similar experimentally-validated targets. Furthermore, my analysis predicts several targets of these dysregulated miRNAs to be involved in corticosteroid and cholesterol biosynthesis pathway. In order to validate the putative targets and miRNAs involved, it is necessary to conduct *in vitro* analysis; results of this will be presented in Chapter 5. However, it was first necessary to optimise the selected *in vitro* cell model, and this is described in Chapter 4.

## **4 Optimisation of H295R Cells**

## 4.1 Introduction

The NCI-H295 cell line was developed from human adrenocortical carcinoma and is capable of corticosteroid biosynthesis (Gazdar 1990). However, this original strain grew very slowly and only loosely attached to surfaces. Therefore, new subtypes were developed by flushing out floating cells and culturing the remaining attached cells. The different subtypes and their culturing conditions are as described in Chapter 2. This chapter describes a series of studies conducted to characterise and compare the different cell strains in order to choose the most suitable model for my subsequent studies.

This chapter also describes attempts to validate some of the microarray and bioinformatic result from Chapter 3 (Normal adrenal vs APA) and Chapter 6 (Basal H295R vs Stimulated Cells; Angio II (100 nM), dbcAMP (1 mM) and KCl (20 mM)).

## 4.2 Aim

The aim of my study is to combine bioinformatic and laboratory-based approaches (in vitro analysis) to investigate the role of miRNAs in the aetiology of APA and assess their role in the regulation of steroid production and cholesterol pathway. The chapter aim is therefore adrenocortical cell characterization

## 4.3 Results

### 4.3.1 Adrenocortical Cell Characterization

#### 4.3.1.1 H295R Cell Line Morphology.

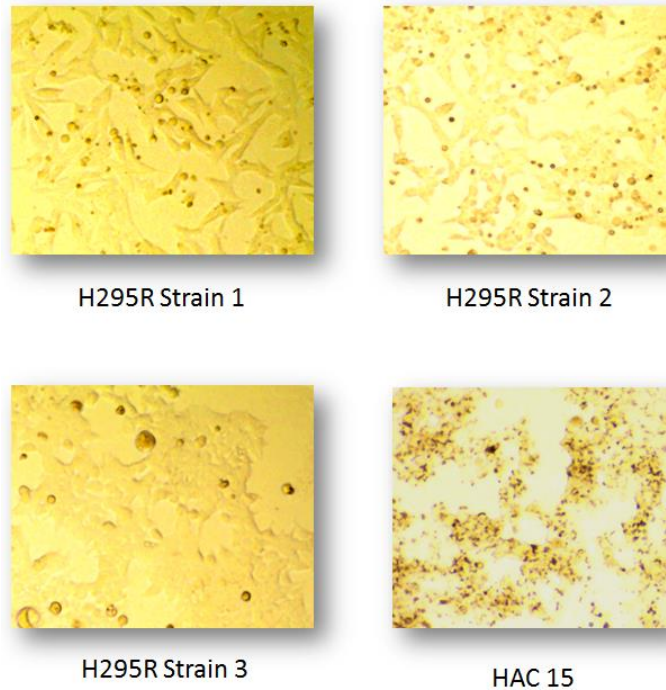


**Figure 4-1: Morphology of H295R Strain 1, 2, 3 and HAC 15 under compound microscope.**

The four strains were termed H295R-S1, H295R-S2 and H295R-S3 (Le, Liu et al. 2013), based on the differing serum supplements used for their culture, and HAC 15, which was developed from an isolated clonal population of H295R cell lines; it was thought to be a novel line but subsequent array analysis showed it to be derived from contaminating H295R cells (Jeniell Parmar 2008). These lines respond well to  $K^+$  and Angio II treatment by increasing aldosterone production but show a modest effect on cortisol output in response to ACTH (Le, Liu et al. 2013) by second messenger action, dbcAMP. This due to the extremely low expression of ACTH receptor in H295R cell lines.

### 4.3.1.2 *CYP11B2* Gene Expression in Angiotensin II-Stimulated Cells

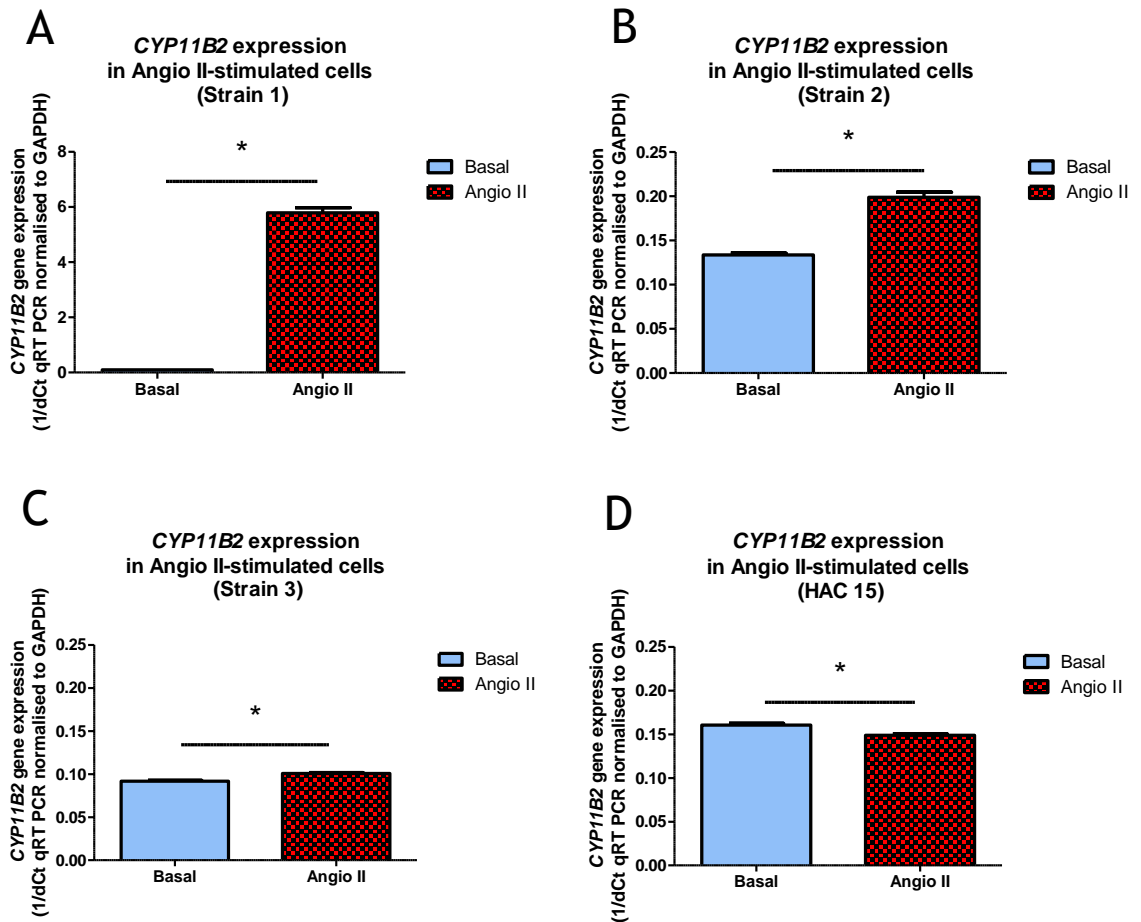


**Figure 4-2:** *CYP11B2* gene expression of Strain 1 (A), Strain 2 (B), Strain 3 (C) and HAC 15 (D) after Angio II Stimulation (n=6 in each group).

See Table 4-1 for fold change and Ct values. \* indicates p<0.05.

*CYP11B2* gene expression was assessed under basal and stimulated conditions (Angiotensin II, 100nM, 24 hours). Prior to Angio II stimulation, the H295R cells were seeded for 24 hours to allow cells to adhere to the culture wells. In order to optimise the experimental method, Angio II was used as a positive control. Angio II, via Angiotensin Type I Receptor (AT1), has been shown to stimulate cell growth, regulates gene expression of growth factors, cytokines and activates multiple intracellular signalling cascade and transcription factors (Kim and Iwao 2000). Under Angio II stimulation, as shown in Figure 4-2 and Table 4-1, Strain 1 showed the highest expression of *CYP11B2* (25-fold) followed by strain 2 (5-fold) and strain 3 (2-fold). On the other hand, HAC 15 demonstrated downregulation of *CYP11B2* gene expression, against expectations (Figure 4-2 D).

#### 4.3.1.3 Passage number effect on *CYP11B2* Gene Expression

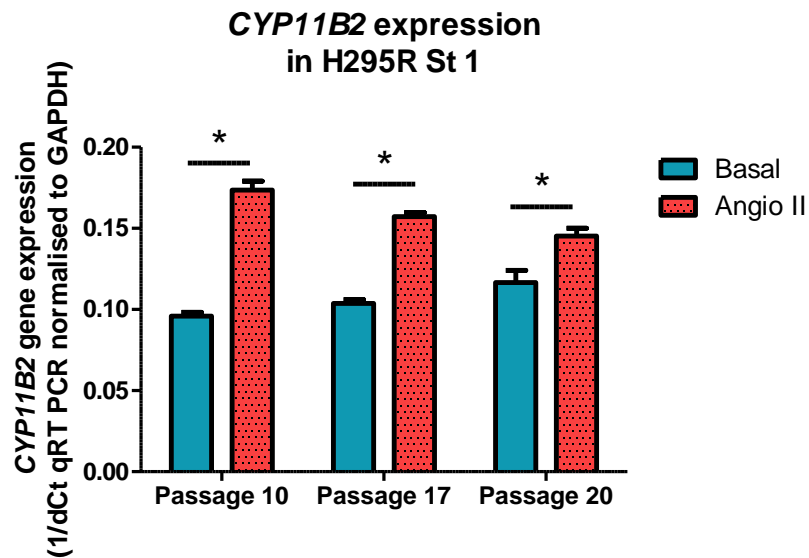


**Figure 4-3: *CYP11B2* gene expression of H295R Strain 1 according to passage number, 10 to 20 (n=2 in each group).**

Expression is normalised to GAPDH. See Table 4-3 for fold change and Ct values. \* indicates  $p < 0.05$ .

As Strain 1 consistently showed the highest and most significant rise in *CYP11B2* expression in stimulated cells, study of the effect of passage number on its responsiveness was performed. Cells were stimulated with 100 nM of Angio II for 24 hours at passages 10, 17 and 20. Figure 4-3 and Table 4-3 show that Angio II responsiveness decreased with passage number (*CYP11B2* fold-change decreased from 25 to 4 from passages 10 to 20), with the stimulation of *CYP11B2* more pronounced in younger cells.

#### 4.3.1.4 *CYP11B2* Gene Expression in dbcAMP-, and KCl-Stimulated Cells

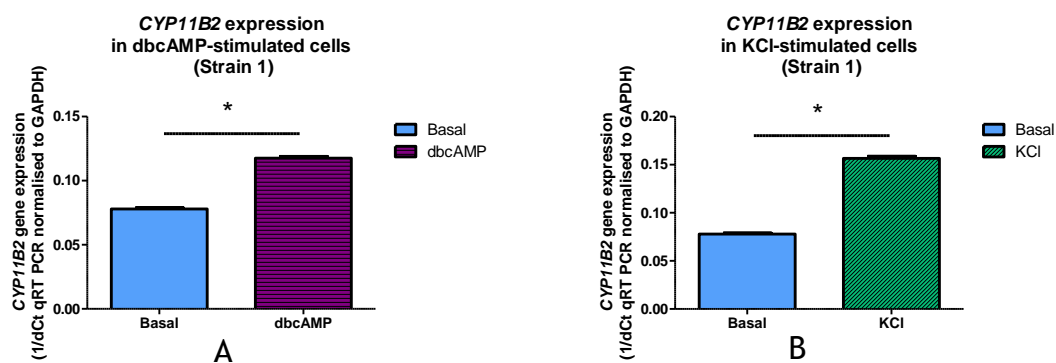


**Figure 4-4: *CYP11B2* gene expression of H295R Strain 1 after dbcAMP (A) and KCl (B) stimulation (n=6 in each group).**

See Table 4-2 for fold-change and Ct values. \* indicates p<0.05.

H295R Strain 1 was further investigated for trophic responses by stimulating the cells with dbcAMP (1 mM) and KCl (20 mM) for 24 hours. Both of these significantly increased *CYP11B2* gene expression relative to basal conditions (Figure 4-4 and Table 4-2).

**Table 4-1: CYP11B2 expression in different strains of H295R cells.**

Ct=cycle threshold; ddCt= delta delta Ct; n= biological sample number; SD= standard deviation.

Cell Strain	n	Basal Mean Ct (SD)	CYP11B2 Mean Ct (SD)	ddCt	Fold Change (Relative to basal=1)	p-value
H295R Strain 1	6	30.28 (0.52)	25.54 (0.31)	-4.66	25.22	0.00
H295R Strain 2	6	25.45 (0.38)	22.41 (0.22)	-2.44	5.44	0.00
H295R Strain 3	6	29.09 (0.40)	28.10 (0.22)	-0.97	1.95	0.00
HAC 15	6	25.73 (0.39)	25.97 (0.17)	0.49	0.71	0.00

**Table 4-2: CYP11B2 expression following stimulation (Angio II, dbcAMP and KCl) of H295R cells (Strain 1).**

Ct=cycle threshold; ddCt= delta delta Ct; n= biological sample number; SD= standard deviation.

Stimulation	n	Basal Mean Ct (SD)	CYP11B2 Mean Ct (SD)	ddCt	Fold Change (Relative to basal=1)	p-value
Angio	6	30.28 (0.52)	25.54 (0.31)	-4.66	25.22	0.00
dbcAMP	6	34.32 (0.69)	29.58 (0.28)	-4.33	20.08	0.00
KCl	6	34.32 (0.69)	27.66 (0.26)	-6.44	88.85	0.00

**Table 4-3: CYP11B2 expression by passage number in H295R cells (Strain 1).**

Ct=cycle threshold; ddCt= delta delta Ct; n= biological sample number; SD= standard deviation.

Passage (H295R Strain 1)	n	Basal Mean Ct (SD)	CYP11B2 Mean Ct (SD)	ddCt	Fold Change (Relative to basal=1)	p-value
Passage 10	6	30.28 (0.52)	25.54 (0.31)	-4.66	25.22	0.00
Passage 17	6	29.45 (0.46)	26.10 (0.17)	-3.30	9.87	0.00
Passage 20	6	26.57 (1.09)	24.76 (0.58)	-1.82	3.52	0.01

### 4.3.1.5 H295R Cell Proliferation in Response to Angiotensin II (100 nM) in MTS and BrdU

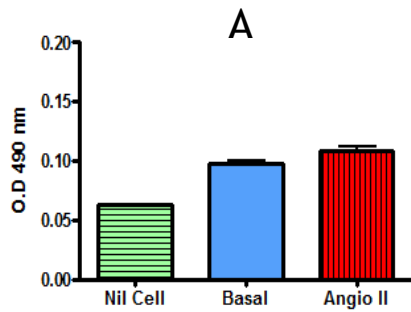


Figure 5A : H295R 24 Hours Stimulation (MTS)

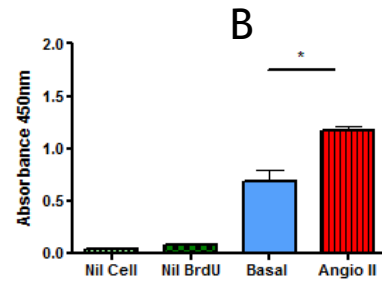


Figure 4A : H295R Cell Proliferation for 24H Angiotensin II (100nM) stimulation \*p<0.05

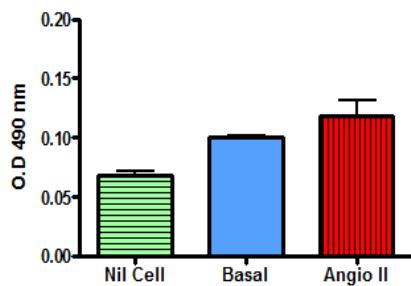


Figure 5B : H295R 48 Hours Stimulation (MTS)

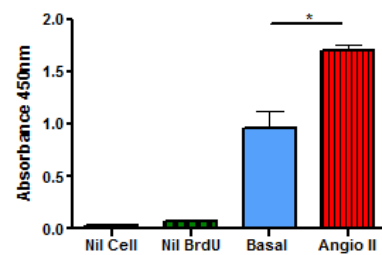


Figure 4B : H295R Cell Proliferation for 48H Angiotensin II (100nM) stimulation \*p< 0.05

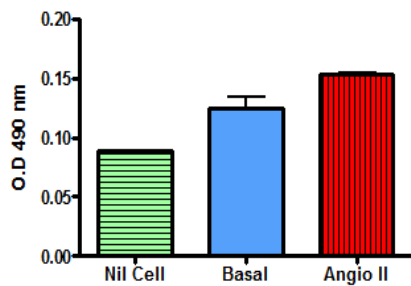


Figure 5C : H295R 72 Hours Stimulation (MTS)

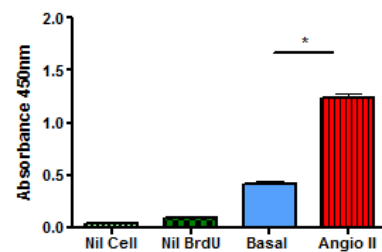


Figure 4C : H295R Cell Proliferation for 72H Angiotensin II (100nM) stimulation \*p<0.05

**Figure 4-5: H295R cell proliferation in response to Angio II stimulation (100nM) in MTS (A) and in BrdU (B).**

n=4 in each group. \* indicates p<0.05.

Next, the cells were quiescent for 48 hours to arrest cell proliferation (as described in Chapter 2, Material & Method, Section 2.4). After 2 days without any serum supplement to the cells, they were stimulated with 100 nM Angio II to assess its effect on cell proliferation. There was a trend towards increased proliferation using the MTS assay for 24, 48 and 72 hours but this did not achieve significance (Figure 4-5 A). However, the proliferation of H295R was significant using the BrdU assay (Figure 4-5 B) at time points from 24 to 72 hours post-stimulation. The optimal proliferation time point was noted as 48 hours.

## 4.4 Discussion

Gazdar et al established the human adrenocortical tumour cell line from a patient with invasive primary adrenocortical carcinoma patient (Gazdar, Oie et al. 1990). As previously noted, these NCI-H295R cells grew in floating clumps and had >96 hours doubling time. It was the first cell line established to produce steroids. However the cells were developed further for monolayer cultures (Rainey, Bird et al. 1994), to suit laboratory use and the doubling time shortened to 48 hours. This resulted in different strains, each with different serum supplementation required for cell growth (Wang, Rowland et al. 2012).

In this chapter, a series of studies was conducted to characterise and compare the different strains in order to choose the most suitable model for subsequent in vitro studies. In order to optimise the experimental method, I used Angiotensin II (Angio II) as my positive control. Angio II, via Angiotensin Type I Receptor (AT<sub>1</sub>), has been shown to stimulate cell growth, regulate gene expression of growth factors and cytokines, and activate multiple intracellular signalling cascade and transcription factors (Kim and Iwao 2000). In this study, it was clearly shown that Angio II stimulated *CYP11B2* gene expression in Strains 1, 2 and 3 (Figure 4-2), with the greatest stimulation being in Strain 1. This strain also showed upregulation of *CYP11B2* following dbcAMP and KCl stimulation (Figure 4-4). The finding is supported by several studies indicating that the cell line is an effective model for steroidogenesis (Bird, Hanley et al. 1993, Xing, Edwards et al. 2011). H295R-Strain 1 is commercially available from the American Type Culture Collection (ATCC CRL-2128), grows in Nu-Serum type I (Wang and Rainey 2012) and is able to produce steroid under basal and stimulated conditions.

The key factor in cell culture experiment is the quality of the cells. The cells determine the reliability and reproducibility result; if impaired, these will introduce great variability into the experiment. The H295R cell line showed reduced *CYP11B2* responsiveness with increasing passage number (Figure 4-3). This is consistent with a de-differentiation of the cells from their steroidogenic phenotype as passage number increases. this is a well-recognised phenomenon; a previous study, using RAW 264.7 (ATCC® TIB-71™) cells, showed significant reduction in the quality of protein expression with high passage (Linda Jacobsen

2007). O'Driscoll et al compared low passage (18) and high passage (40) of MIN-6 cells and found that there were significant differences of mRNA expression that involved in proliferation, adhesion and secretion (O'Driscoll L et al. Phenotypic and global gene expression changes in low and high passage MIN6 cells (O'Driscoll, Gammell et al. 2006).

Study of selected miRNA effects on gene expression requires optimised transfection of the newly-characterised H295R cells. Transfection is defined as the process of deliberately introducing nucleic acid (e.g. RNA, miRNA) into cells. There are several methods of RNA delivery including microRNA injection, electroporation and lipid-mediated transfection, using agents such as Lipofectamine™ 2000. Lipofectamine™ 2000 had been chosen as the transfection agent for this model because it is effective for transfecting adhered cell, even though it is reported to cause cytotoxicity in some cell lines (Zhong, Wei et al. 2008). However, many in vitro experiments report successful transfection of H295R cells with Lipofectamine™ 2000 (Bouizar, Ragazzon et al. 2010, He, Cao et al. 2015, Udhane, Pandey et al. 2015). Lipofectamine™ 2000 is a cationic liposome that forms a complex with nucleic acids, Lipofectamine interacting with their negatively-charged sugar-phosphate backbones. The cationic state of the complex will overcome the electrostatic repulsion of the cell membrane and permit entry to the cell. This allows miRNA, for example, access to the cell's intracellular processing mechanisms. Some studies support the ability of Lipofectamine™ 2000 complex to penetrate the intact nuclear envelope (Dalby, Cates et al. 2004).

In conclusion, my optimisation studies established H295R strain 1 at lower passage numbers as the best cell line to be used for validation of microarray data. This validation will be the focus of the next chapter.

## **5 Validation of NA vs APA Microarray Study**

## 5.1 Introduction

Microarray study has permitted the analysis of thousands of gene expression profiles for various diseases. In Chapter 3, we were able to determine miRNA profiles in NA vs APA tissue by microarray. Microarray has limited depth of analysis due to the relatively low amount of RNA used in this particular method. Normally only a small (microgram) amount of RNA is utilised for standard hybridisation and detection of gene expression in microarray analysis. Therefore, further analysis using higher concentration of RNA is needed for validation purposes. The optimal validation method is qRT-PCR. In this chapter, 2 key miRNAs were selected for further analysis: miR-125a-5p and miR-335-5p. Both of these were predicted to block *HMGCR*, a very important gene for cholesterol production. Interestingly, both of these miRNAs were shown to have similar effects to *CYP11B2*, despite only miR-125a-5p being a putative target for the aldosterone synthase gene, according to IPA.

## 5.2 Aim

To validate microarray results and IPA prediction by qRT-PCR.

## 5.3 Result: Validation of the microarray and bioinformatic study of Normal Adrenal vs APA

### 5.3.1 miR-125a-5p

#### 5.3.1.1 miR-125a-5p in Microarray and qRT PCR

In microarray analysis of NA vs APA microRNA expression, miR-125a-5p was found to be downregulated in APA tissues (Figure 5-1 A). In order to examine whether this change in miR-125a-5p expression might be related to the dysregulated aldosterone biosynthesis of APA, aldosterone production was stimulated *in vitro* using the H295R adrenocortical cells model, incubated with dbcAMP to mimic the ACTH stimulation of aldosterone secretion by adrenocortical tissue *in vivo* (Saruta, Okuno et al. 1979). miR-125a-5p levels were then quantified in these cells by realtime SYBR Green qRT-PCR (see Chapter 2, Section 2.11). In a similar manner to the tissue, miR-125a-5p-5p was downregulated in the dbcAMP-stimulated cells relative to the basal state (Figure 5-1 B; Table 5-1). This

suggests that changes in the expression of miR-125a-5p are a statistically significant phenomenon related to changes in aldosterone regulation.

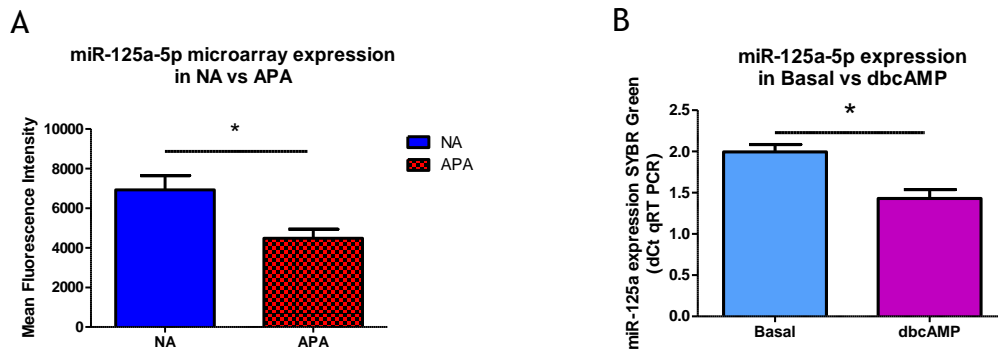


**Figure 5-1: A: Microarray expression of miR-125a-5p (n= 3) in NA vs APA tissue. B: Similar reduction in miR-125a-5p observed in H295R cells stimulated with dbcAMP (n=6).**  
\* indicates  $p < 0.05$ .

**Table 5-1: miR-125a-5p expression in Basal vs dbcAMP-stimulated cells (Strain 1).**

Ct= cycle threshold; ddCt= delta delta Ct; n= biological sample number; SD= standard deviation.

miRNA	n	Basal Mean Ct (SD)	dbcAMP Mean Ct (SD)	ddCt	Fold Change (Relative to basal= 1)	p-value
miR-125a-5p	6	19.87 (0.19)	20.35 (0.10)	0.57	0.68	<0.01

### 5.3.1.2 miR-125a-5p Expression in Transfected Cells

To further investigate the role of miR-125a-5p, H295R Strain 1 was transfected with pre-miR-125a or anti-miR-125a-5p. The transfection efficiency was assessed by SYBR Green qRT-PCR (see Chapter 2, Section 2.11). miR-125a-5p was found to be highly expressed following pre-miR-125a-5p transfection (311-fold increase; Table 5-2; Figure 5-2 A) and significantly downregulated following anti-miR-125a-5p transfection (Figure 5-2 B).

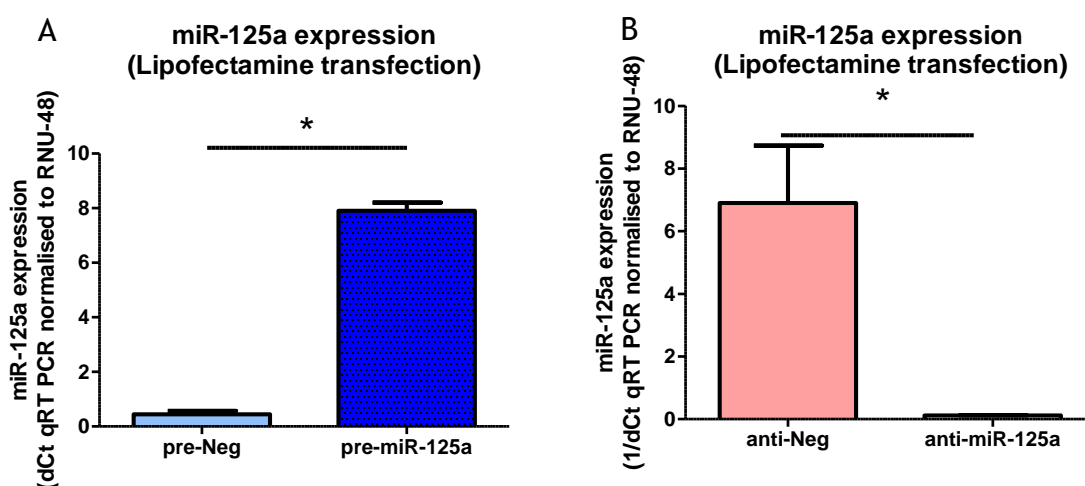


**Figure 5-2:** miR-125a-5p expression in H295R cells following transfection with (A) pre-miR-125a-5p or (B) anti-miR-125a-5p transfection (n=6 in each group).

\* indicates  $p < 0.05$ .

**Table 5-2: miR-125a-5p expression following precursor-miRNA transfection.**

Ct= cycle threshold; ddCt= delta delta Ct; n= biological sample number; SD= standard deviation.

miRNA	n	Pre-Neg Mean Ct (SD)	Pre-miRNA Mean Ct (SD)	ddCt	Fold Change (Relative to basal= 1)	p- value
miR-125a-5p	6	15.94 (0.18)	8.47 (0.62)	-8.28	311.42	<0.01

**Table 5-3: miR-125a-5p expression following anti-miRNA transfection.**

Ct= cycle threshold; ddCt= delta delta Ct; n= biological sample number; SD= standard deviation.

miRNA	n	Anti-Neg Mean Ct (SD)	Anti-miRNA Mean Ct (SD)	ddCt	Fold Change (Relative to basal= 1)	p- value
miR-125a-5p	6	15.91 (0.29)	24.28 (0.58)	8.08	0.00	<0.01

The effects of these transfections on the cells' expression of steroidogenesis-related genes and targets predicted by IPA were then investigated.

### 5.3.1.3 *CYP11B2* Gene Expression in Pre-miR-125a and Anti-miR-125a Transfection

In IPA analysis, miR-125a-5p was predicted to bind *CYP11B2* mRNA. This effect was tested in vitro by transfecting H295R cells with pre-miR-125a to significantly increase miR-125a-5p levels (see above). This resulted in a significant reduction in *CYP11B2* mRNA (Figure 5-3 A and Table 5-4). Conversely, transfection with anti-miR-125a to reduce the miR levels significantly increased *CYP11B2* mRNA levels (Figure 5-3 B and Table 5-5). These results are consistent with the IPA prediction of a direct action by miR-125a-5p on *CYP11B2* mRNA.

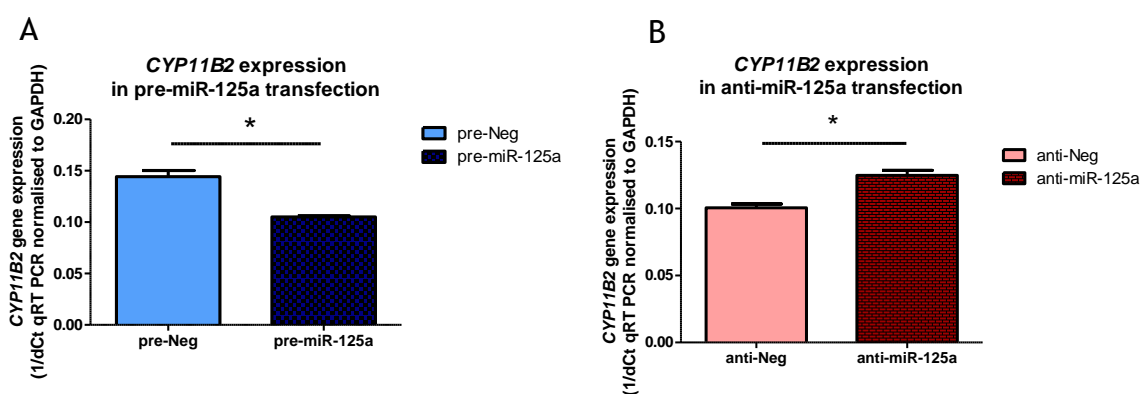


**Figure 5-3: Effects on *CYP11B2* mRNA levels in H295R Strain 1 cells following transfection with pre-miR-125a (A) or anti-miR-125a (B) (n= 3 in each group).**

\* indicates  $p < 0.05$ .

**Table 5-4: *CYP11B2* gene expression in H295R cells (Strain 1) transfected with precursor-negative miRNA (Pre-Neg) or precursor-miRNA-125a (Pre-miRNA-125a).**

Ct= cycle threshold; ddCt= delta delta Ct; n= biological sample number; SD= standard deviation.

Gene	n	Pre-Neg Mean Ct (SD)	Pre-miRNA-125a Mean Ct (SD)	ddCt	Fold Change (Relative to basal= 1)	p-value
<i>CYP11B2</i>	3	26.58 (0.65)	30.10 (0.34)	2.56	0.17	0.00

**Table 5-5: *CYP11B2* gene expression in H295R cells (Strain 1) transfected with *CYP11B2* anti-negative miRNA (Anti-Neg) or anti-miRNA-125a.**

Ct= cycle threshold; ddCt= delta delta Ct; n= biological sample number; SD= standard deviation.

Gene	n	Anti-Neg Mean Ct (SD)	Anti-miRNA-125a Mean Ct (SD)	ddCt	Fold Change (Relative to basal= 1)	p-value
<i>CYP11B2</i>	3	29.53 (0.19)	28.22 (0.40)	-1.93	3.81	0.01

### 5.3.1.4 *HMGCR* Gene Expression in Pre-miR-125a and Anti-miR-125a Transfection

The IPA prediction of a direct regulatory effect of miR-125a-5p on *HMGCR* was also tested in this system. Despite showing trends toward decreased *HMGCR* mRNA following pre-miR-125a transfection (Figure 5-4 A) and an increase after anti-miR-125a transfection (Figure 5-4 B), these effects did not achieve significance.

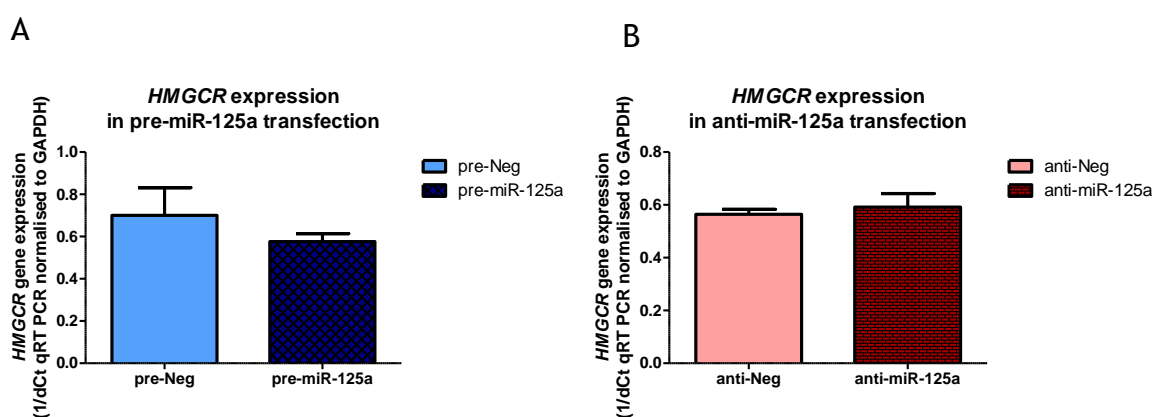


Figure 5-4: *HMGCR* mRNA levels in H295R Strain 1 cells following (A) pre-miR-125a transfection or (B) anti-miR-125a transfection (n=3 in each group).

Table 5-6: *HMGCR* expression in H295R cells (Strain 1) transfected with precursor-negative miRNA (Pre-Neg) or precursor-miRNA-125a (Pre-miRNA-125a).

Ct= cycle threshold; ddCt= delta delta Ct; n= biological sample number; SD= standard deviation.

Gene	n	Pre-Neg Mean Ct (SD)	Pre-miRNA-125a Mean Ct (SD)	ddCt	Fold Change (Relative to basal= 1)	p-value
<i>HMGCR</i>	6	21.36 (0.30)	21.96 (0.55)	0.15	0.90	0.56

Table 5-7: *HMGCR* expression in H295R cells (Strain 1) transfected with anti-negative miRNA (Anti-Neg) or anti-miRNA-125a.

Ct=cycle threshold; ddCt= delta delta Ct; n= biological sample number; SD= standard deviation.

Gene	n	Anti-Neg Mean Ct (SD)	Anti-miRNA-125a Mean Ct (SD)	ddCt	Fold Change (Relative to basal= 1)	p-value
<i>HMGCR</i>	6	21.33 (0.27)	21.74 (0.18)	-0.03	1.02	0.82

## 5.3.2 miR-335-5p

### 5.3.2.1 miR-335-5p Expression in Transfected Cells

Similar to miR-125a-5p, above, miR-335-5p was identified by microarray as being downregulated in APA relative to NA tissue, and was also predicted by IPA to target *CYP11B2* and *HMGCR* expression through direct action on their respective mRNAs. To investigate this further, H295R Strain 1 cell was this time transfected with pre-miR-335 and anti-miR-335. miR-335-5p was significantly increased 1431-fold following pre-miR transfection (Figure 5-5 and Table 5-8) in the precursor transfection but no changes were noted in transfection of anti-miR-335-5p.

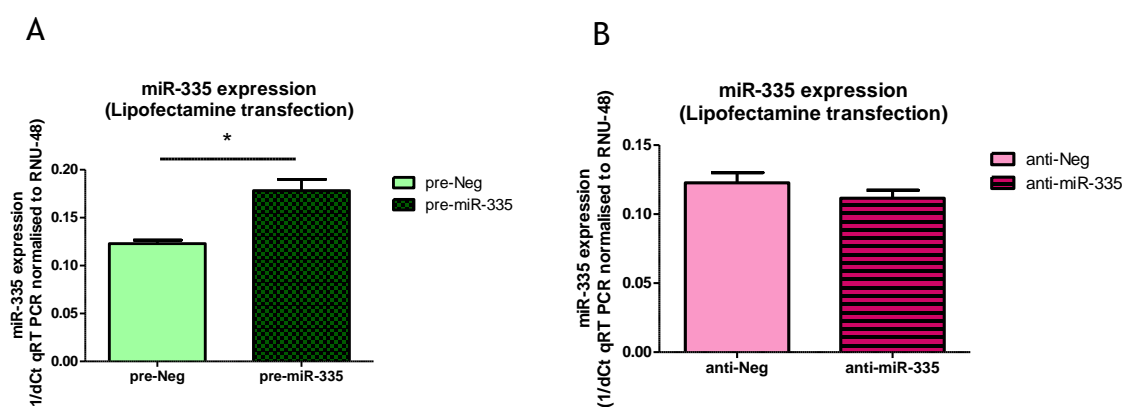


**Figure 5-5: miR-335-5p levels in H295R cells following (A) pre-miR-335 transfection or (B) anti-miR-335 transfection (n= 3 in each group).**

\* indicates  $p < 0.05$ .

**Table 5-8: miR-335-5p expression following precursor-miRNA transfection.**

Ct= cycle threshold; ddCt= delta delta Ct; n= biological sample number; SD= standard deviation.

miRNA	n	Pre-Neg Mean Ct (SD)	Pre-miRNA-335 Mean Ct (SD)	ddCt	Fold Change (Relative to basal= 1)	p- value
miR-335-5p	3	26.71 (0.37)	12.58 (0.64)	-13.81	14317.20	<0.01

**Table 5-9: miR-335-5p expression following anti-miRNA transfection.**

Ct= cycle threshold; ddCt= delta delta Ct; n= biological sample number; SD= standard deviation.

miRNA	n	Anti-Neg Mean Ct (SD)	Anti-miRNA-335 Mean Ct (SD)	ddCt	Fold Change (Relative to basal= 1)	p- value
miR-335-5p	3	26.66 (0.70)	27.51 (0.87)	0.80	0.58	0.32

### 5.3.2.2 *CYP11B2* Gene Expression in Pre-miR-335 and Anti-miR-335 Transfection

miR-335-5p action on *CYP11B2* mRNA was investigated in the transfected cells. This confirmed suppression of *CYP11B2* mRNA levels following pre-miR-335 transfection (Figure 5-6 A and Table 5-10). However, the same significant effect was also observed following anti-miR-335 transfection (Figure 5-6 B); this result contradicts the hypothesis, which predicted that anti-miR-335 should upregulate the miR-335-5p expression.

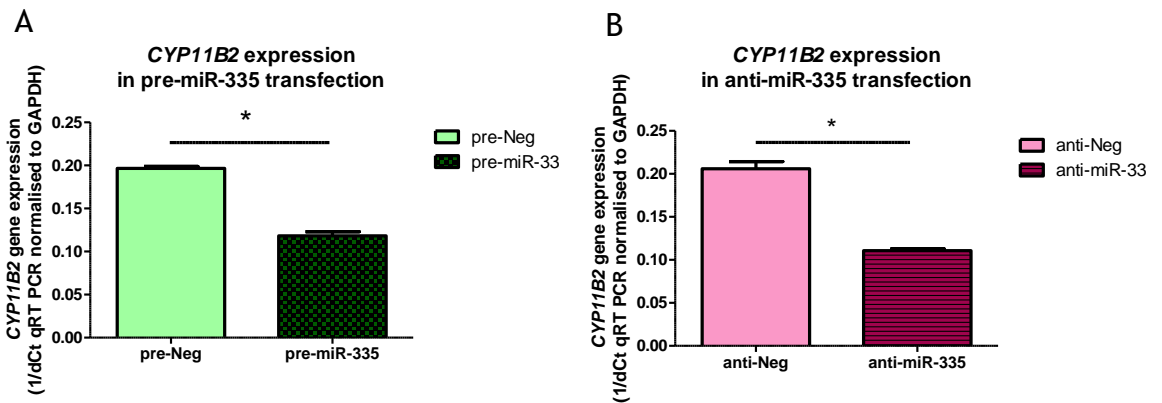


**Figure 5-6:** *CYP11B2* mRNA levels in H295R Strain 1 cells following transfection with (A) pre-miR-335 or (B) anti-miR-335 (n= 3 in each group). \* indicates p<0.05.

**Table 5-10:** *CYP11B2* mRNA levels in H295R Strain 1 cells following transfection with precursor-negative miRNA (Pre-Neg) and precursor-miRNA-335 (pre-miR-335). Ct= cycle threshold; ddCt= delta delta Ct; n= biological sample number; SD= standard deviation.

Gene	n	Pre-Neg Mean Ct (SD)	Pre-miRNA-125a Mean Ct (SD)	ddCt	Fold Change (Relative to basal= 1)	p-value
<i>CYP11B2</i>	3	24.30 (0.50)	27.46 (0.47)	3.40	0.09	<0.01

**Table 5-11:** *CYP11B2* mRNA levels in H295R Strain 1 cells following transfection with *CYP11B2* anti-negative miRNA (Anti-Neg) and anti-miRNA-335 (anti-miR-335). Ct= cycle threshold; ddCt= delta delta Ct; n= biological sample number; SD= standard deviation.

Gene	n	Anti-Neg Mean Ct (SD)	Anti-miRNA-125a Mean Ct (SD)	ddCt	Fold Change (Relative to basal= 1)	p-value
<i>CYP11B2</i>	3	24.15 (0.42)	27.83 (0.36)	4.17	0.06	<0.01

### 5.3.2.3 *HMGC*R Gene Expression in Pre-miR-335 and Anti-miR-335 Transfection

*In vitro* analysis also confirms this predicted suppression of *HMGC*R mRNA levels following pre-miR-335 transfection (Figure 5-7 A and Table 5-12). However, again anti-miR-335 transfection (Figure 5-7 B) also results in suppression of the same mRNA.

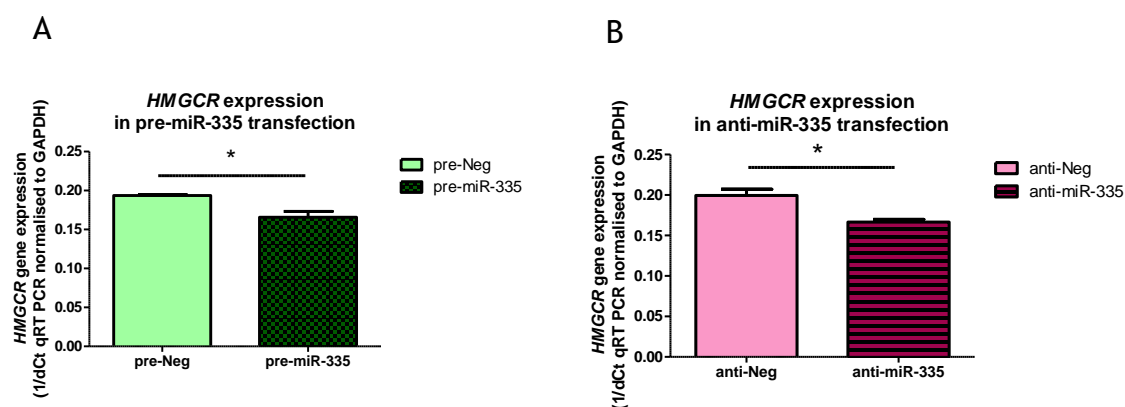


**Figure 5-7: *HMGC*R levels in H295R Strain 1 cells following transfection with (A) pre-miR-335 or (B) anti-miR-335 transfection (n= 3 in each group).**

\* indicates p<0.05.

**Table 5-12: *HMGC*R mRNA levels in H295R Strain 1 cells following transfection with precursor-negative miRNA (Pre-Neg) and precursor-miRNA-335 (Pre-miR-335).**

Ct= cycle threshold; ddCt= delta delta Ct; n= biological sample number; SD= standard deviation.

Gene	n	Pre-Neg Mean Ct (SD)	Pre-miRNA-125a Mean Ct (SD)	ddCt	Fold Change (Relative to basal= 1)	p-value
<i>HMGC</i> R	3	24.37 (0.35)	25.03 (0.46)	0.89	0.54	0.03

**Table 5-13: *HMGC*R mRNA levels in H295R Strain 1 cells following transfection with *HMGC*R anti-negative miRNA (Anti-Neg) and anti-miRNA-335 (anti-miR-335).**

Ct= cycle threshold; ddCt= delta delta Ct; n= biological sample number; SD= standard deviation.

Gene	n	Anti-Neg Mean Ct (SD)	Anti-miRNA-125a Mean Ct (SD)	ddCt	Fold Change (Relative to basal= 1)	p-value
<i>HMGC</i> R	3	24.31 (0.19)	24.79 (0.06)	0.98	0.51	0.01

## 5.4 Discussion

In this part of the study, selected miRNAs differentially expressed in NA vs APA and predicted to bind important steroidogenic mRNAs (see Chapter 3) were analysed further. miR-125a-5p levels had been reduced in APA tissue according to microarray analysis (Figure 5-1 A), and this finding was supported by its downregulation in dbcAMP-stimulated cells (Figure 5-1 B). This indirect method of comparison was necessary because there were no more APA or NA RNA samples available for direct realtime RT-PCR (qRT PCR) validation of the microarray results. Therefore, stimulated cells from the H295R Strain 1 adrenocortical cell line were used instead. This is the best available model for these studies (see Chapter 4) but the expression of ACTH receptor is very low in these cells. Because of this, dbcAMP was used to mimic the stimulatory ACTH action on aldosterone production rather than ACTH itself. Cells stimulated with dbcAMP were intended to mimic the pathological condition in APA, where high levels of ACTH are detected. This is supported by Arnaldi et al, who observed overexpression of ACTH-receptor mRNA in APA but not in adrenocarcinoma (Arnaldi, Mancini et al. 1998). The summary of differential expression of miRNA in APA vs NA is shown in Chapter 1, Table 1-8.

pre-miR-125a transfection of cells significantly reduced *CYP11B2* mRNA, while inhibition of miR-125a-5p production increased transcript levels almost fourfold. This finding is supported by a previous pEZX-reporter plasmid study, where pre-miR-125a was co-transfected into HeLa cells along with a reporter plasmid containing the *CYP11B2* 3'UTR; this significantly suppressed the reporter plasmid's luciferase activity, offering further evidence of a direct interaction between this miRNA and *CYP11B2* transcripts (Stacy Wood 2011). In another recent study, suppression of miR-125a-5p expression in colon cancer cell lines and colon cancer tissue inhibited their proliferation. This was the result of the microRNA targeting antiapoptotic genes (*BCL2*, *BCL2L12* and *MCL-1*) (Tong, Liu et al. 2015). In hepatocellular carcinoma, miR-125a-5p is also reported to suppress the P13K/ AKT/mTOR signalling pathway that is involved in the migration and invasion of liver cancer cells (Tang, Li et al. 2015).

Several miRNAs downregulated in APA, including the two studied in this chapter, are predicted by IPA to target *HMGCR*. Although there was no significant

evidence that miR-125a-5p targets *HMGCR*, pre-miR-335 did reduce levels of the mRNA *in vitro*. *HMGCR* is a rate-limiting gene in cholesterol production and so may be an important determinant of steroid biosynthesis. However, no validation studies have been done to evaluate whether reduction of *HMGCR* expression has a direct effect on adrenal steroidogenesis *in vivo*. Nevertheless, rat *in vivo* studies show that statins (especially simvastatin) result in downregulation of *CYP17A1* expression in ovarian theca-interstitial cells (Sokalska, Stanley et al. 2014).

miR-335-5p expression in cancer tissues has already received much attention. As reported by Schmitz et al, the significant upregulation of miR-335-5p observed in adrenocortical carcinoma (ACC) is proposed as a potential diagnostic tool to discriminate ACC from adrenocortical adenoma (ACA) (Schmitz, Helwig et al. 2011). This is supported by Soon et al, who reported that the expression of miR-335-5p is also suppressed in ACA relative to its ACC counterpart (Soon, Tacon et al. 2009). However, in breast carcinoma, overexpression of miR-335-5p positively correlates with expression of the tumour suppression gene *BRCA1*, inhibiting cell viability and stimulating apoptosis (Heyn, Engelmann et al. 2011). In this experiment, despite downregulation of *CYP11B2* and *HMGCR* gene expression in the pre-miR-335 transfection, both were also suppressed in anti-miR-335 transfection. This may be due to insufficient level of anti-miR-335 in the cell to negatively regulate miR-335-5p or may be due to an alternative pathway (or gene) modulating the function of anti-miR-335 and leading to decrease levels of *CYP11B2* and *HMGCR* mRNA.

However, despite the predictions of IPA, some of the targets were not validated by lab experiment. This may be due to incorrect prediction of the strength of complementary binding between miRNAs and mRNAs. IPA classifies base-pairing as highly-predicted (8mer) or moderately-predicted (7mer). Highly-predicted targets have a higher chance of forming base-pairs between miRNA and mRNA. Furthermore, the non-validated targets may be due to inefficiency of miRNA transfection, either due to poor cell line responsiveness or the efficacy of transfection protocol. In addition, to find the cell line that is a precise model for the tissue of interest is challenging. To date, the most suitable cell line used for steroid regulation is H295R cells, which is a human adrenocortical carcinoma cell line, not APA. This might lead to discrepancies in validation.

## 5.5 Conclusion

In summary, this chapter has been able to experimentally validate some of the IPA predictions, in particular effects of miR-125a-5p and miR-335-5p. Both of these miRNAs have been predicted and validated to be involved in steroidogenesis and cholesterol biogenesis. This is a novel finding in steroid and cholesterol regulation. Further experiments are needed to extend this result so that it might contribute to the improvement of diagnosis and treatment of APA and other diseases relevant to steroid biosynthesis and cholesterol handling.

## **6 Analysis of microRNA in Basal, Angiotensin II, dbcAMP- and KCl-Stimulated H295R Cells.**

## 6.1 Introduction

As in Chapter 3, microarray analysis is again utilised here for miRNA expression analysis. I subjected H295R cells to three different types of aldosterone stimulation: angiotensin II (Angio II), potassium (in the form of KCl) and dibutyryl cAMP (dbcAMP), to mimic ACTH stimulation; non-stimulated basal cells were used as controls. After 24 hours, I isolated RNA and confirmed stimulation by qRT-PCR of *CYP11B2* (aldosterone synthase) mRNA. The microRNA profile of each sample was then analysed by microarray and differentially-expressed miRNAs were identified. Finally, bioinformatic analysis was used to identify possible targets through which differentially-expressed miRNAs might affect steroid or cholesterol production. This was achieved using the Ingenuity Pathway Analysis (IPA) software.

Subsequently I validated by qRT-PCR the significant changes in expression observed in microarray by using the more reliably quantitative method of qRT-PCR. It was my intention to look at the consistently downregulated miRNAs that emerge from microarray as listed below:

1. miR-106a-5p
2. miR-154-3p
3. miR-17-5p
4. miR-196b-5p
5. miR-19a-3p
6. miR-20b-5p
7. miR-766-3p

However, expression of one of these miRNAs was found to be marginal from microarray (i.e miR-196b-5p), so was excluded from further study. I present validation of the 6 remaining miRNAs under each of the 3 stimulatory conditions (Angio II, dbcAMP and KCl). IPA also predicts that miR-17 will suppress the expression of LDLR; I investigate whether this miRNA significantly downregulates this predicted target.

## 6.2 Aim

1. To identify significant differences in microRNA profile between cells stimulated for aldosterone production and their basal counterparts.
2. To identify mRNA targets of key differentially-expressed microRNAs.
3. To experimentally validate the consistently expressed miRNA from all 3 stimulation groups - as assessed by microarray - using qRT-PCR.
4. To experimentally validate expression of the putative target of miR-17, LDLR, by qRT PCR.

## 6.3 Microarray results

Total RNA was extracted from 3 biological samples (in each group) of non-stimulated H295R cells (basal), Angiotensin II-stimulated cells (Angio II), dbcAMP-stimulated cells (dbcAMP) and KCl-stimulated cells (KCl). The RNA quantity was determined by Nanodrop (Section 2.7) and further assessed by Agilent Bioanalyser chip for quality analysis. The RNA samples were sent for miRNA profile analysis by microarray microfluidic chip (LC Sciences, Houston, Texas). Prior to that, all RNAs were subjected to quality control testing by the company.

Similar to the data presented in Chapter 3, as recommended by the microarray manufacturer, a 500 arbitrary unit (AU) cut-off point was applied to the miRNA detection threshold. The microarray analysis identified a list of expressed miRNAs (i.e. miRNAs that register > 500AU in basal or stimulated cells) and differentially-expressed miRNAs (i.e. miRNAs expressed in both basal and stimulated cells at >500 AU, but at significantly different levels ( $p < 0.05$ )). 2019 miRNAs were screened in each of the cell groups. There is a strong positive correlation between miRNA expression in the basal group and each of the 3 stimulated groups (Figure 6-1), suggesting the majority of miRNAs do not alter significantly under stimulation.

- Relative to basal, Angio II treatment resulted in differential expression of 32 miRNAs, of which 12 were present in both Angio II and basal cells but at significantly different levels ( $p < 0.05$ ), 13 were present only in the basal group and 7 only in the Angio II group (Figure 6-5).
- dbcAMP treatment altered 84 miRNAs, of which 53 were expressed in both groups at different levels ( $p < 0.05$ ), 19 in basal only and 12 in dbcAMP-treated cells only (Figure 6-3).
- KCl treatment altered 61 miRNAs, of which 45 were expressed in both groups at different levels ( $p < 0.05$ ), 5 in basal only and 11 in KCl-treated cells only (Figure 6-4).

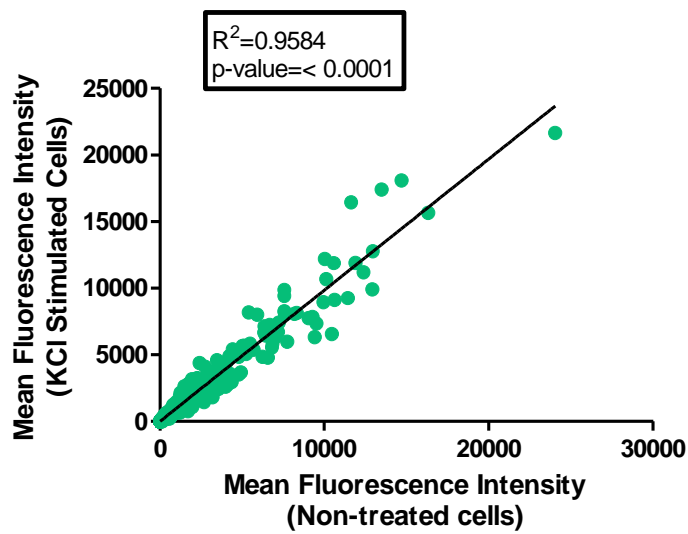
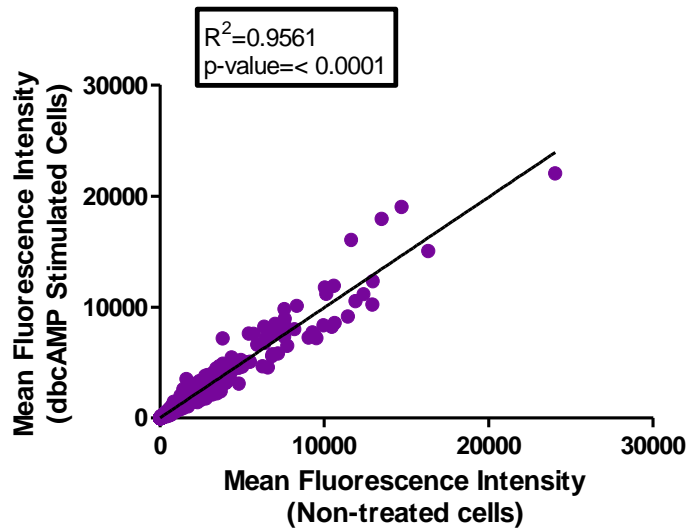
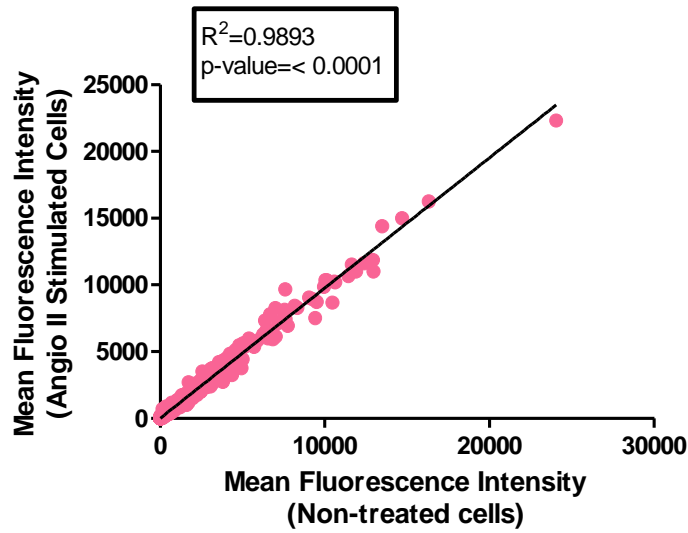
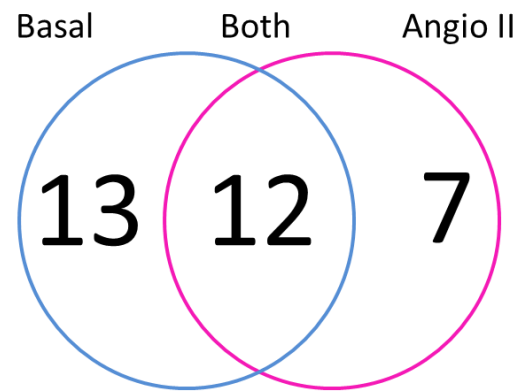
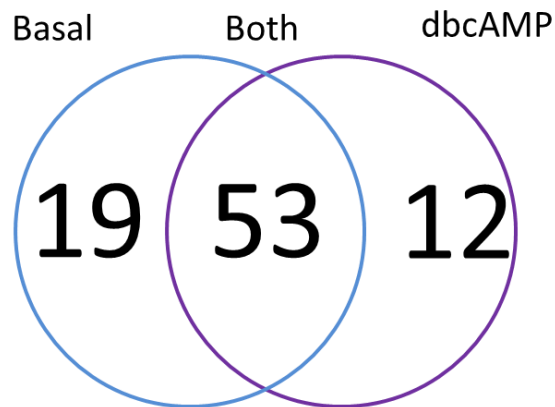


Figure 6-1: Scatter plots showing relative miRNA levels in basal (non-treated cells) vs Angio II-, dbcAMP- and KCl-treated cells, as analysed by microarray.



**Figure 6-2: Venn Diagram of the number of expressed miRNAs that were detected >500 AU in basal and/or Angio II-stimulated cells (H295R).**

miRNAs listed as 'Both' were detected in both basal and stimulated cells, but at significantly different levels ( $p < 0.05$ ).



**Figure 6-3: Venn Diagram of the number expressed miRNAs that were detected >500 AU in basal and/or dbcAMP-stimulated cells (H295R).**

miRNAs listed as 'Both' were detected in both basal and stimulated cells, but at significantly different levels ( $p < 0.05$ ).

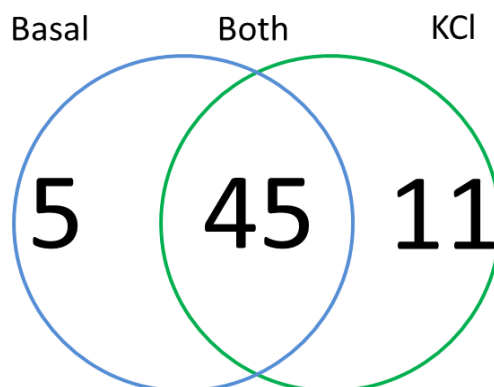


**Figure 6-4: Venn Diagram of the number expressed miRNAs that were detected >500 AU in basal and/or KCl-stimulated cells (H295R).**

miRNAs listed as 'Both' were detected in both basal and stimulated cells, but at significantly different levels ( $p < 0.05$ ).

### **6.3.1 Differentially Expressed miRNAs in Basal vs Angiotensin II, dbcAMP and KCl; miRBase Annotation**

The latest miRBase Release 21: June 2014, contains 28,645 entries of hairpin precursor miRNAs, including 35,828 mature miRNAs from 223 species (miRBase 2014). The miRNA names use the prefix “miR” followed by a unique and specific identifying number assigned sequentially regardless of organism. Similar identifying numbers are given to identical or almost identical miRNA sequences. As almost all miRNA precursors produce mature miRNA from either the 5’ or 3’ end of the hair-pin strand, ‘5p’ or ‘3p’ is added to the annotation (Ambros, Bartel et al. 2003). The microarray data were further analysed utilising the latest miRBase Release 21: June 2014.

Quantitative data relating to the differentially-expressed miRs mentioned above are provided in Figure 6-5, Figure 6-6 and Figure 6-7, below. The most abundantly-expressed miRNA is miR-23b-3p. It is highly expressed in dbcAMP-stimulated cells (average fluorescence intensity 19,005, p-value=0.0006) and is similarly up-regulated in both dbcAMP and KCl-stimulated cells (but not Angio II stimulated cells) relative to basal (Figure 6-6).

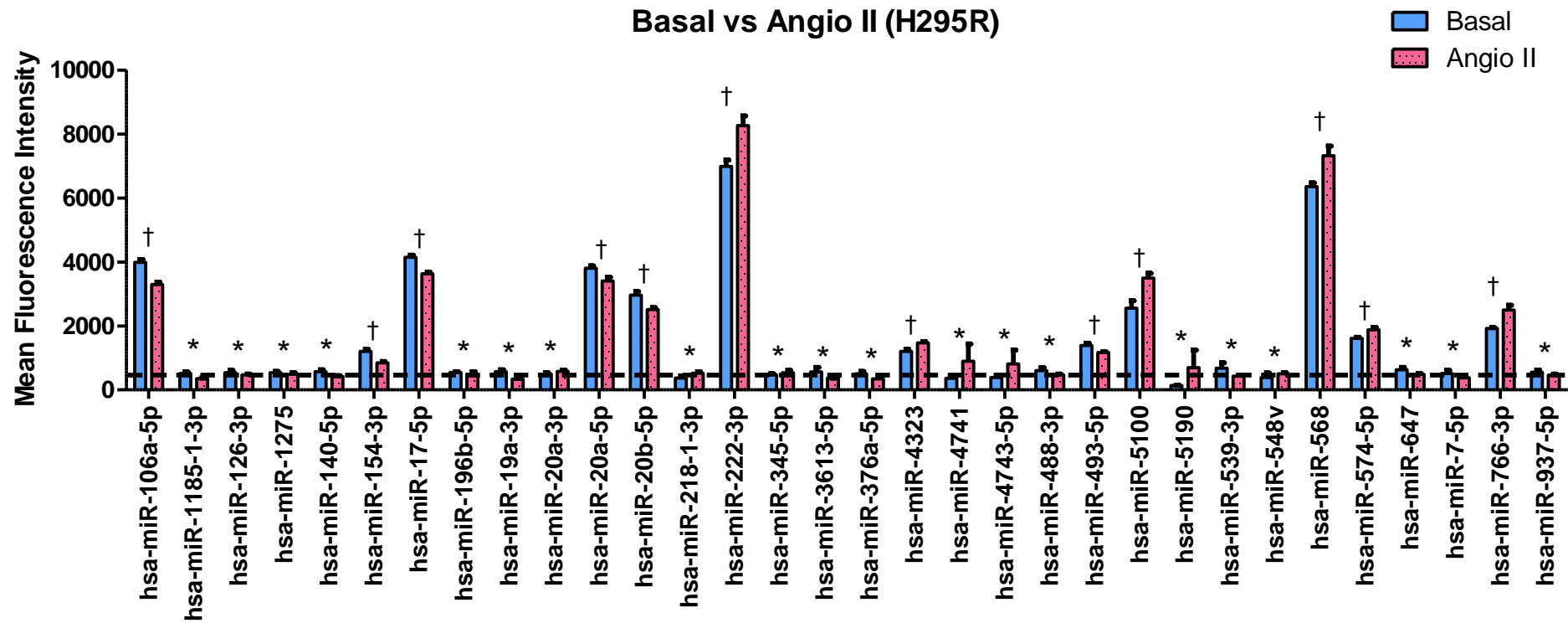


**Figure 6-5: Microarray data showing differentially-expressed miRNAs in basal vs Angio II-treated cells (all miRNAs shown have AU>500).**

\*miRNAs >500AU in APA or NA; †miRNAs present in both tissues but at significantly different levels ( $p < 0.05$ ).

## Basal vs dbcAMP (H295R)

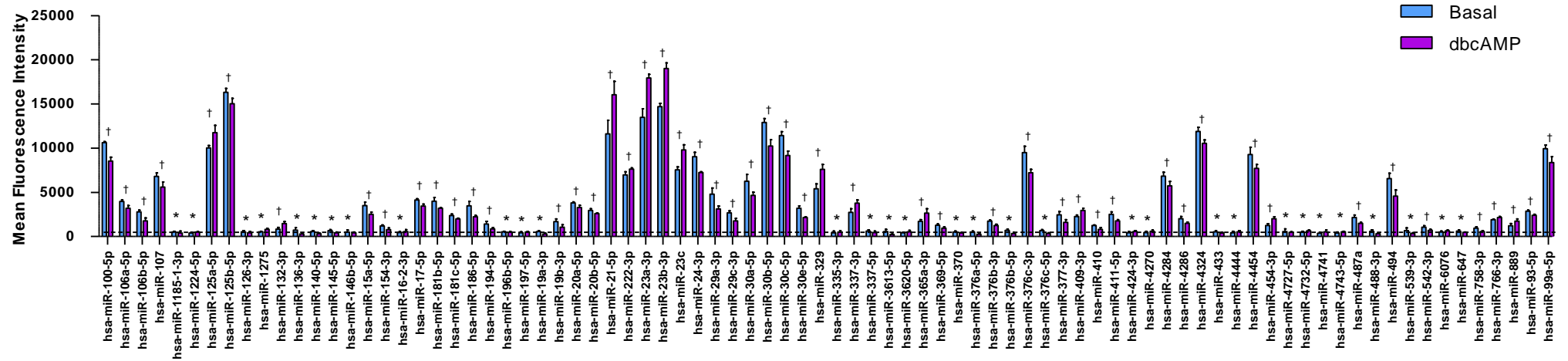


**Figure 6-6: Microarray data showing differentially expressed miRNAs in Basal vs dbcAMP-treated cells (all miRNAs shown have AU>500).**

\*miRNAs >500AU in APA or NA; †miRNAs present in both tissues but at significantly different levels ( $p < 0.05$ ).

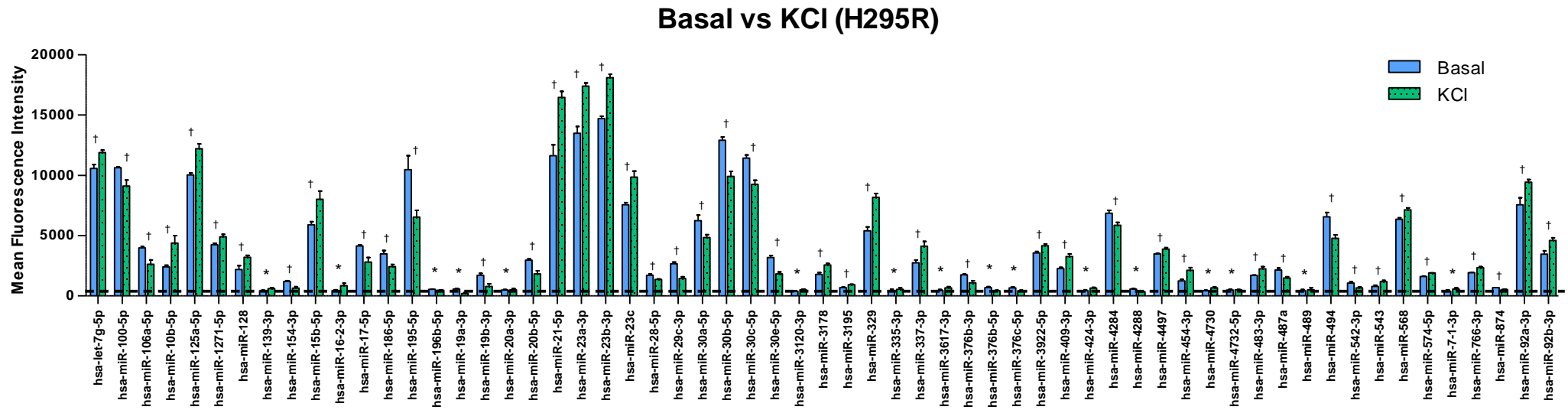


**Figure 6-7: Microarray data showing differentially expressed miRNAs in Basal vs KCI-treated cells (all miRNAs shown have AU>500).**

\*miRNAs >500AU in APA or NA; †miRNAs present in both tissues but at significantly different levels ( $p < 0.05$ )

### 6.3.2 Consistent miRNA Expression Across the 3 Stimulatory Treatments (Angio II, dbcAMP and KCl) & The Cluster Involved

Relative to basal, the 7 miRNAs consistently differentially expressed across Angio II, dbcAMP and KCl-stimulated cells are:

- 1) hsa-miR-106a-5p
- 2) hsa-miR-154-3p
- 3) hsa-miR-17-5p
- 4) hsa-miR-196b-5p
- 5) hsa-miR-19a-3p
- 6) hsa-miR-20b-5p
- 7) hsa-miR-766-3p

These are downregulated in each of the stimulated groups (Figure 6-8 to Figure 6-10). miR-154-3p is clustered with 22 other miRNAs (not listed here), none of which are consistently expressed throughout the stimulated groups. On the other hand, neither miR-196b-5p nor miR-766-3p belong to any cluster.

miR-106a-5p and miR-20b-5p are found within the same cluster, which is located on chromosome X. They have similar seed sequences for mRNA targets (AAAGUGC). Other miRNAs from the same cluster are miR-106-3p, miR-18b-3p, miR-18b-5p, miR-19b-3p, miR-19b-5p, miR-363-3p, miR-363-5p, and miR-92a-3p. Furthermore, miR-106a-5p, miR-19b-3p, miR-20b-5p have similar patterns of expression while miR-92a-3p exhibits an opposite trend, being upregulated by the 3 stimulations. However, miR-106a-3p, miR-18b-3p, miR-18b-5p, miR-363-3p and miR-363-5p are expressed below 500 AU.

miR-17-5p and miR-19a-3p are from the same cluster on chromosome 13. They are encoded by the miR-17-92 gene inside a single polycistronic transcript along with 4 other miRNAs (miR-18a, miR-20a, miR-19b-1 and miR-92a-1). They have similar pattern of expression with other miRNAs within the same cluster; miR-20a-5p and miR-19b-3p. In contrast, miR-92a-3p shows an opposite pattern where the miRNA is highly upregulated in the 3 stimulated groups. miR-17-3p, miR-18a-5p, miR-18a-3p, miR-19a-5p, miR-19b-1-5p and miR-92a-1-5p are not expressed in the samples (<500 AU).

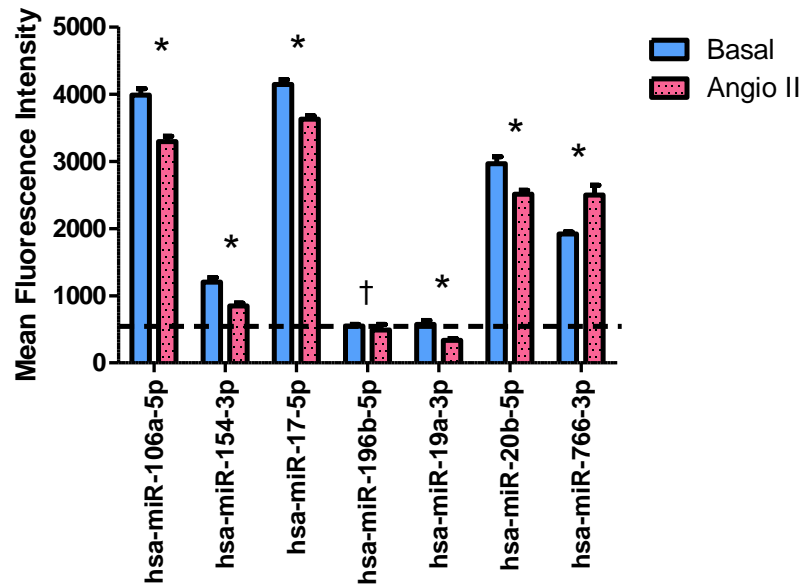


**Figure 6-8: Consistent pattern of miRNA expression in Angio II-stimulated cells relative to basal.**

The dotted line indicates the detection cut-off point of 500 AU (n=3 in each group). †miRNAs >500AU in APA or NA; \*miRNAs present in both tissues but at significantly different levels (p<0.05).

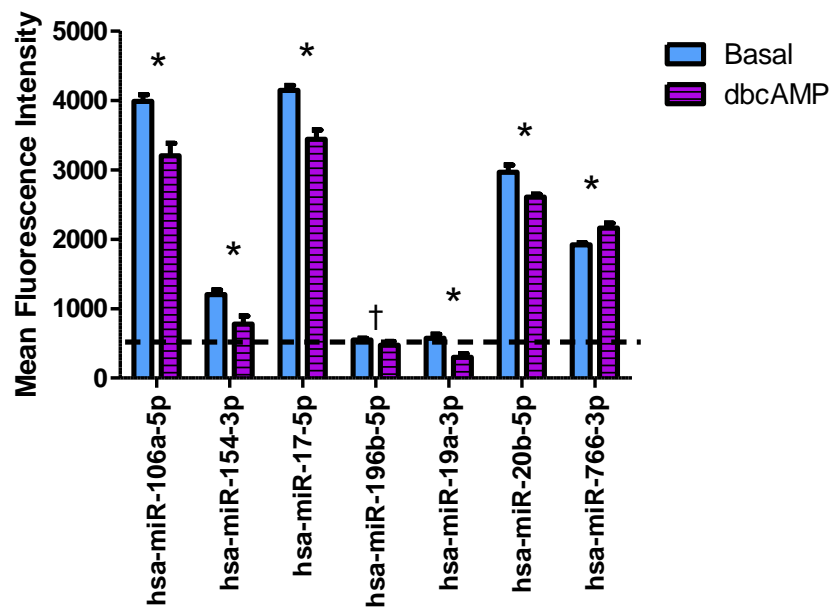


**Figure 6-9: Consistent pattern of miRNA expression in dbcAMP-stimulated cells relative to basal.**

The dotted line indicates the detection cut-off point of 500 AU (n=3 in each group). †miRNAs >500AU in APA or NA; \*miRNAs present in both tissues but at significantly different levels (p<0.05).

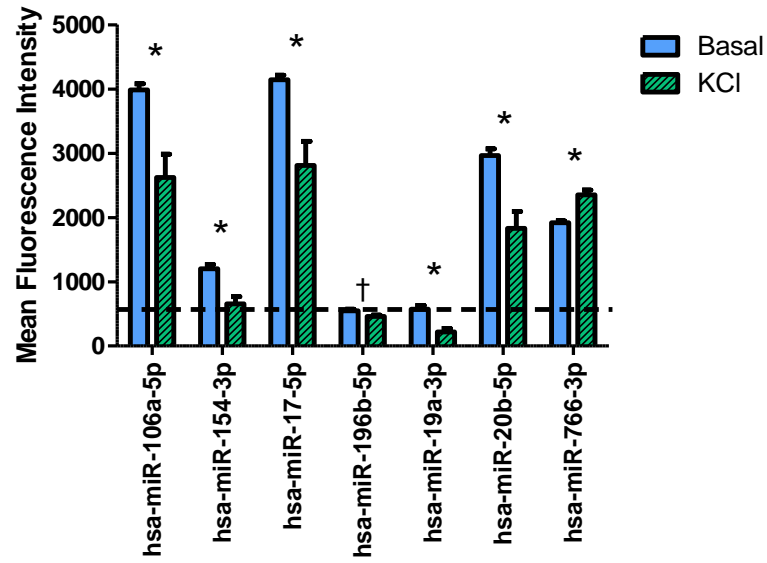


**Figure 6-10: Consistent pattern of miRNA expression in KCI-stimulated cells relative to basal.**

The dotted line indicates the detection cut-off point of 500 AU (n=3 in each group). †miRNAs >500AU in APA or NA; \*miRNAs present in both tissues but at significantly different levels ( $p < 0.05$ ).

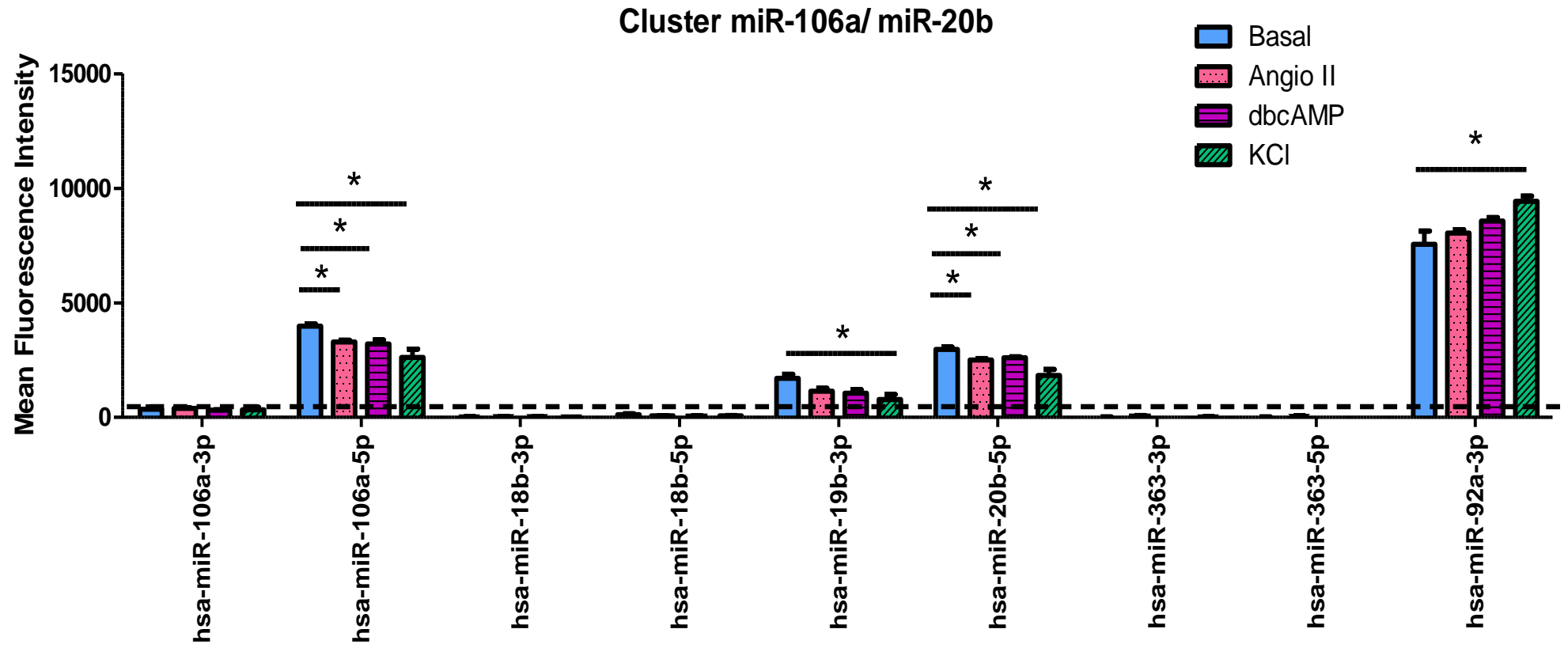


Figure 6-11: miRNA Clusters detected from microarray analysis (Cluster miR-106a/ miR-20b).

\*  $p < 0.05$  relative to basal.

## Cluster miR-17/ miR-19a

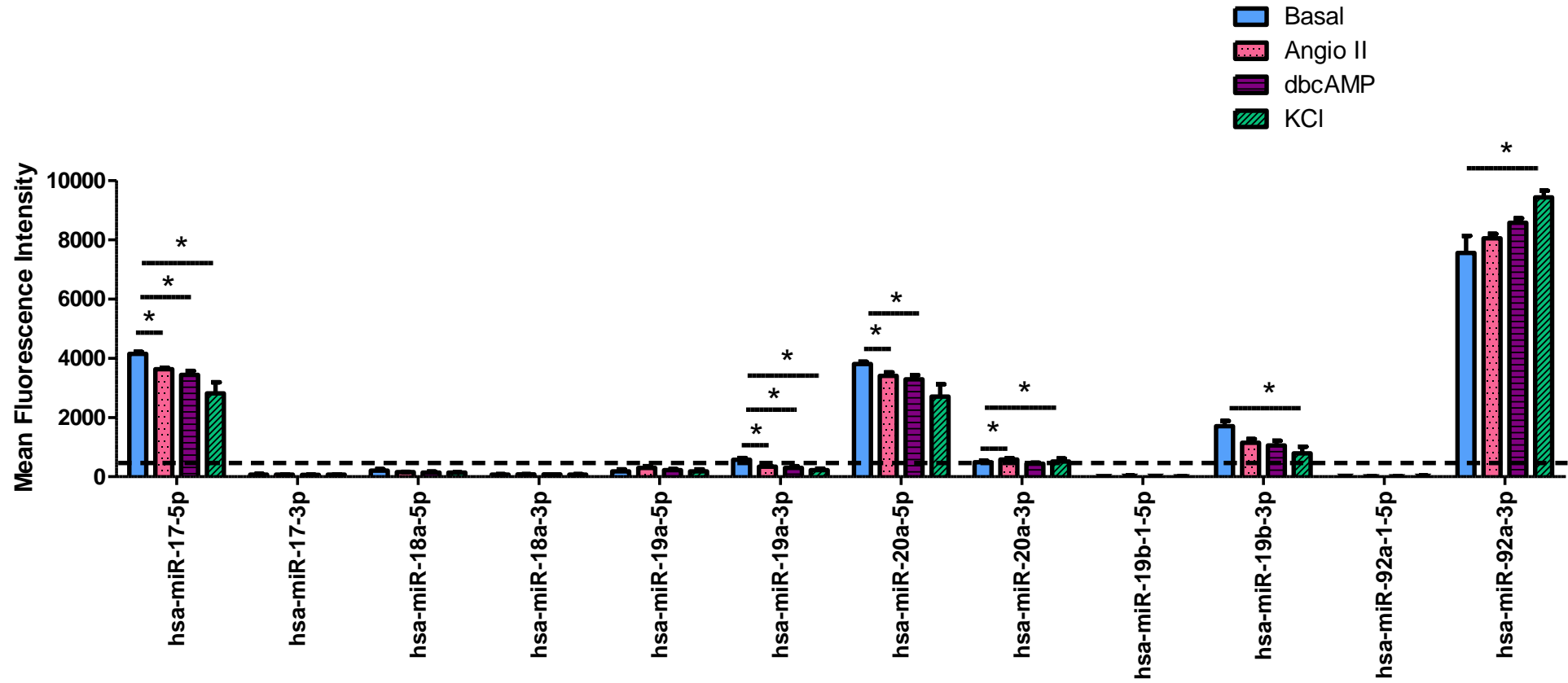


Figure 6-12: miRNA Clusters detected from microarray analysis (Cluster miR-30b, Cluster miR-17/ miR-19a).

\*  $p < 0.05$  relative to basal.

## 6.4 Ingenuity® Systems Pathway Analysis (microRNA target filter)

Ingenuity® Systems Pathway Analysis (IPA; Ingenuity Systems, Redwood City, CA USA; <http://www.ingenuity.com>) software was utilised to determine differentially-expressed miRNAs and their putative targets along with their molecular and cellular functions. The sources of the miRNA Target Filter are Ingenuity Expert Finding, Ingenuity ExpertAssist Finding, miRecords, Tarbase and TargetScan Human.

The filter system is based on 3 confidence levels;

- 1) Experimentally observed miRNA-mRNA interaction (result based on validated experiment).
- 2) Highly predicted miRNA-mRNA interaction.
- 3) Moderately predicted miRNA-mRNA interaction.

Comparing basal vs Angio II groups, 32 differentially-expressed miRNAs (>500 AU) from the microarray data were uploaded into the IPA system. Subsequently, using miRNA Target Filter, 22 miRNAs were automatically selected. These 22 miRNAs include overlapping miRNAs that share the same seed sequence. (This will be fully explained in the next section.) Initially, utilising all 3 levels of confidence, the 22 miRNAs were predicted to target 9517 mRNAs. However, applying experimentally observed confidence levels sharply reduced the number of miRNAs to 9 and mRNAs to 108 (Figure 6-13).

Similarly, comparing the basal vs dbcAMP groups, with 84 differentially-expressed miRNAs, 61 were included by the IPA miRNA Target Filter with 13683 mRNA targets predicted. When limited to experimentally observed findings, only 28 miRNAs targeting 696 mRNAs were included for further analysis (Figure 6-14).

Finally, 61 differentially-expressed miRNAs from the basal vs KCl groups were reduced to 42 miRNAs with 12391 target mRNAs in the database. Of these, 22 miRNAs and 706 mRNAs were identified as experimentally validated by the database (Figure 6-15).

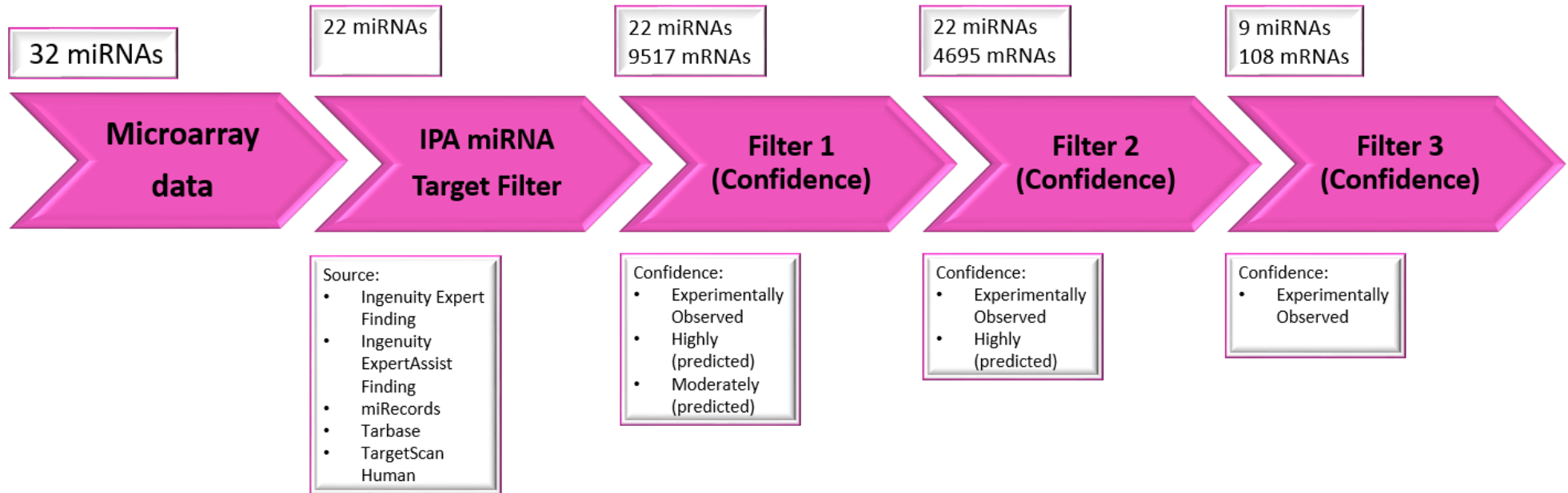


**Figure 6-13: Summary of differentially expressed miRNA analysis using Ingenuity Pathway Analysis (IPA) for basal vs Angio II-treated cells.**

Using IPA miRNA Target Filter, the number of miRNAs decreases from 32 to 9 and the number of target mRNAs from 9517 to 108. The filter is based on 3 levels of confidence (experimentally observed, highly predicted and moderately predicted), as shown above.

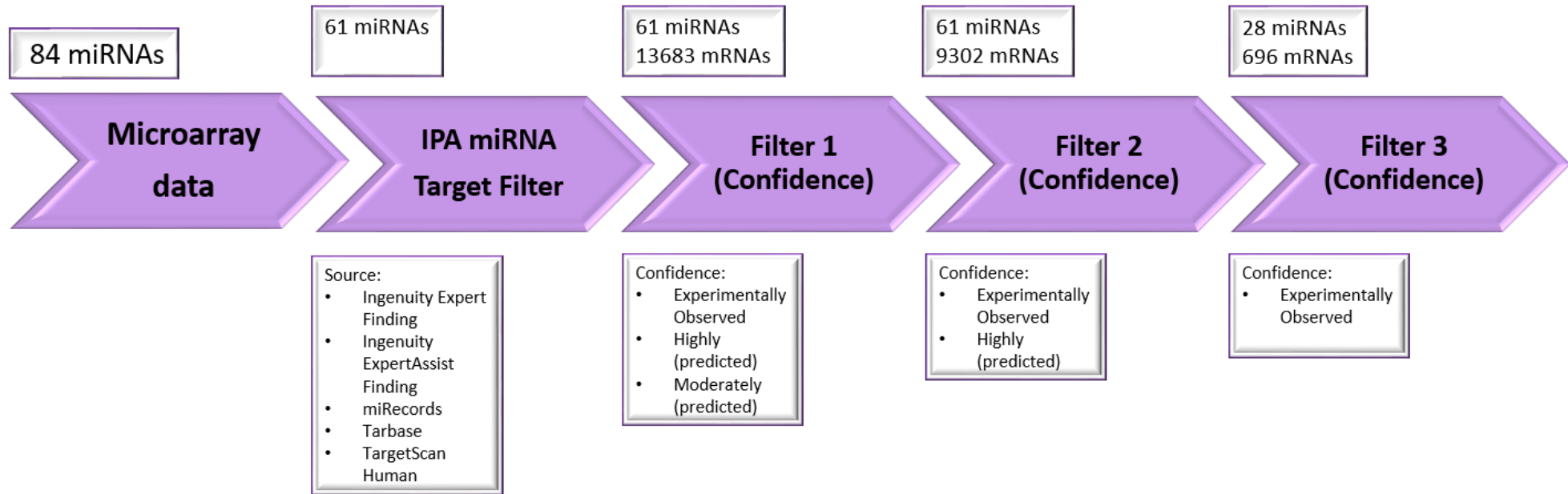


**Figure 6-14: Summary of differentially expressed miRNA analysis using Ingenuity Pathway Analysis (IPA) for basal vs dbcAMP-treated cells.**

Using IPA miRNA Target Filter, the number of miRNAs decreases from 84 to 28 and the number of target mRNAs from 13,683 to 696. The filter is based on 3 levels of confidence (experimentally observed, highly predicted and moderately predicted), as shown above.

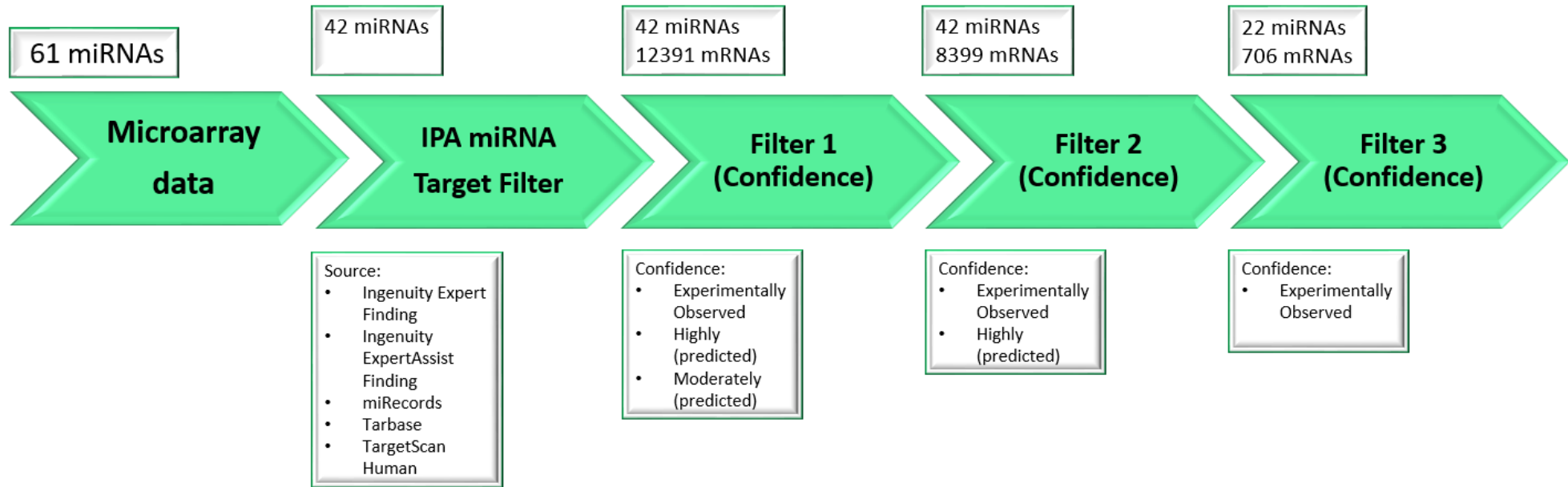


**Figure 6-15: Summary of differentially expressed miRNA analysis using Ingenuity Pathway Analysis (IPA) for basal vs KCI-treated cells.**

Using IPA miRNA Target Filter, the number of miRNAs decreases from 61 to 22 and the number of target mRNAs from 12391 to 706. The filter is based on 3 levels of confidence (experimentally observed, highly predicted and moderately predicted), as shown above.

## 6.5 Synonymous miRNAs, seed sequences and the number of targeted mRNAs (IPA Database).

The miRNA seed sequence is vital in determining its complementary binding to target mRNA. Several annotated miRNAs have identical seed sequences. These overlapping miRNAs are termed 'synonymous miRNAs'. A full list of synonymous miRNAs differentially expressed in this study is shown in the tables presented in the Appendix.

For the purposes of clarity and understanding, in this chapter synonymous miRNAs are presented separated by an oblique symbol (/) e.g. the synonymous miRNAs miR-125b-5p and miR-125a-5p will be listed as 'miR-125b-5p/miR-125a-5p'.

The miRNAs hsa-miR-17-5p, hsa-miR-106a-5p, hsa-miR-106b-5p, hsa-miR-20a-5p, hsa-miR-20b-5p and hsa-miR-93-5p share the seed sequence, AAAGUGC, and therefore have the same predicted 1418 mRNA targets. However, despite their high homology, these miRNAs are derived from different clusters and different chromosomes.

Some of these miRNAs are therefore not included in the IPA analysis using miRNA Target Filter. Examples are: hsa-miR-1185-1-3p, hsa-miR-136-3p, hsa-miR-139-3p, hsa-miR-16-2-3p, hsa-miR-20a-3p, hsa-miR-218-1-3p, hsa-miR-335-3p, hsa-miR-3617-3p, hsa-miR-376b-5p, hsa-miR-376c-5p, hsa-miR-493-5p, hsa-miR-5100, hsa-miR-5190, hsa-miR-539-3p, hsa-miR-6076, hsa-miR-7-1-3p, hsa-miR-937-5p.

## 6.6 IPA Target Filter Analysis: mRNA targets involved in steroidogenesis, cholesterol synthesis and related pathways

### 6.6.1 *CYP11B2, CYP11B1 & CYP17A1*

As shown in Figure 6-16, 4 miRNAs target the CYP11B2 gene: miR-1275, miR-4323, miR-647 and miR-766-3p (Basal vs Angio II).

In the basal vs dbcAMP group (Figure 6-17), 4 miRNAs are predicted to target CYP11B2 (miR-125a-5p, miR-1275, miR-647 and miR-766-3p). Four miRNAs - some different - are also predicted to target CYP11B2 from the basal vs KCl group (Figure 6-18); miR-125a-5p, miR-708-5p/miR-28-5p, miR-766-3p and miR-874-3p.

Only the basal vs KCl group contains differentially-expressed miRNAs predicted to target the other steroidogenic genes CYP11B1 (miR-874-3p) and CYP17A1 (miR-4730).

### 6.6.2 *HMGCR, ABCA1, LDLR & other related genes*

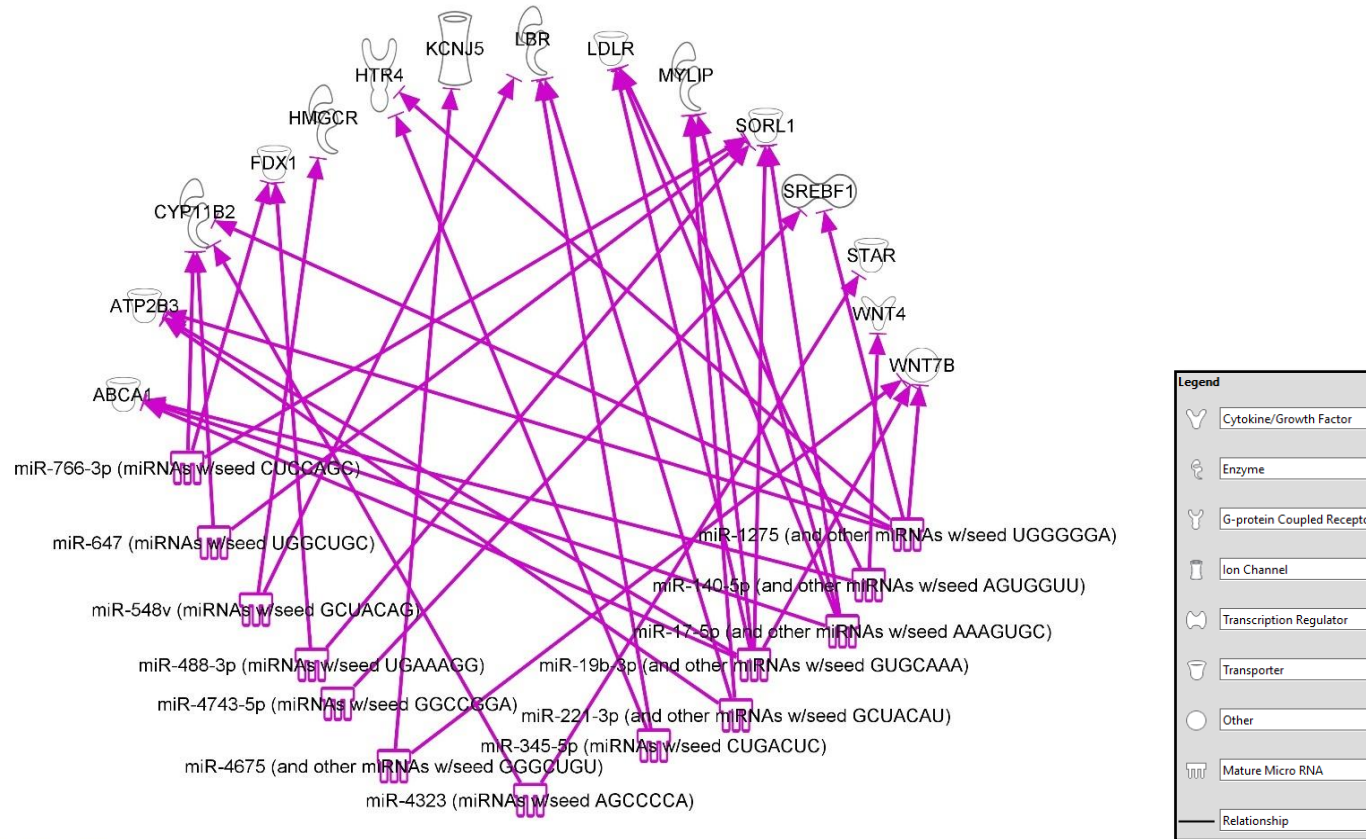
From the basal vs Angio II group (Figure 6-16), miR-548v is predicted to target HMGCR. Several other miRNAs (miR-140-5p, miR-17-5p, miR-106a-5p, miR-19a-3p, miR-20b-5p and miR-19b-3p) are predicted to target ABCA1 and LDLR.

Figure 6-17 shows miRNA-mRNA interactions in the basal vs dbcAMP groups. HMGCR is targeted by miR-125b-5p/miR-125a-5p, miR-145-5p, miR-29b-3p/miR-29a-3p/miR-29c-3p, miR-365-3p/miR-365a-3p and miR-4324. ABCA1 is targeted by hsa-miR-130a-3p/miR-454-3p, miR-140-5p, miR-145-5p, miR-17-5p/miR-106a-5p/miR-19a-3p/miR-20b-5p, miR-19b-3p and miR-23a-3p. LDLR has similar targeting miRNAs to ABCA1, plus miR-30c-5p, miR-344d-3p/miR-410, miR-4284 and miR-4286.

For the basal vs KCl groups (Figure 6-18), HMGCR is targeted by miR-125b-5p/miR-125a-5p and miR-29b-3p/miR-29a-3p/miR-29c-3p. ABCA1 is targeted by miR-128-3p, hsa-miR-130a-3p/miR-454-3p, miR-17-5p/miR-106a-5p/miR-19a-3p/miR-20b-5p, miR-19b-3p and miR-23a-3p.

Other possibly relevant mRNAs predicted to be targeted include KCNJ5, STAR, WNT4, WNT7B, ATP2B3, FDXR and several more, as shown in Figure 6-16 to Figure 6-18.

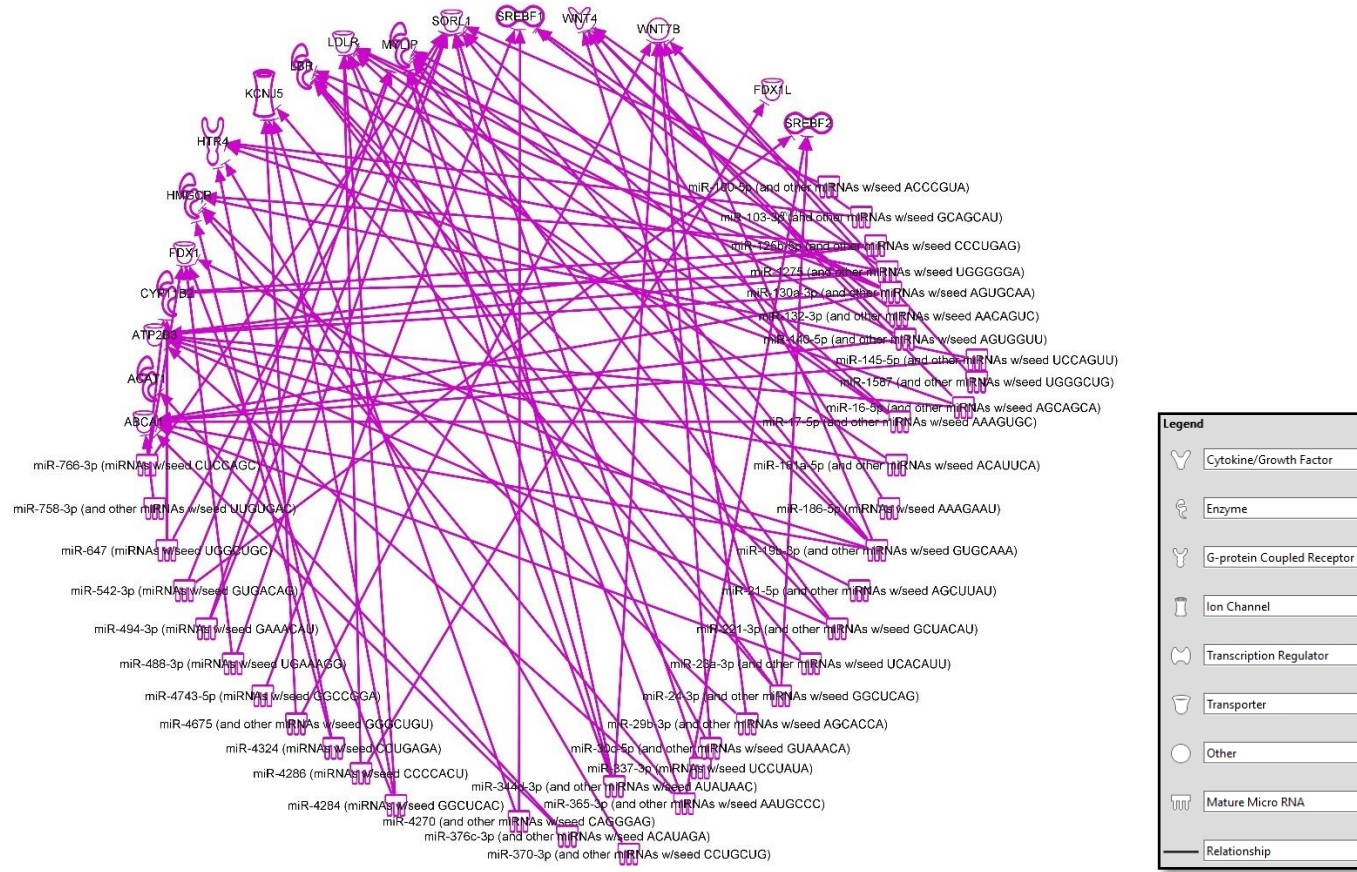
Path Designer Angio Steroid Cholesterol mRNA



© 2000-2015 QIAGEN. All rights reserved.

**Figure 6-16: IPA miRNA target genes for the basal vs Angio II-treated group.**  
 The arrow from each miRNA indicates inhibition of the target gene.

Path Designer dbcAMP mRNA Steroid Cholesterol



© 2000-2015 QIAGEN. All rights reserved.

**Figure 6-17: IPA miRNA target genes for the basal vs dbcAMP-treated group.**  
 The arrow from each miRNA indicates inhibition of the target gene.

Path Designer KCI mRNA Steroid Cholesterol mRNA

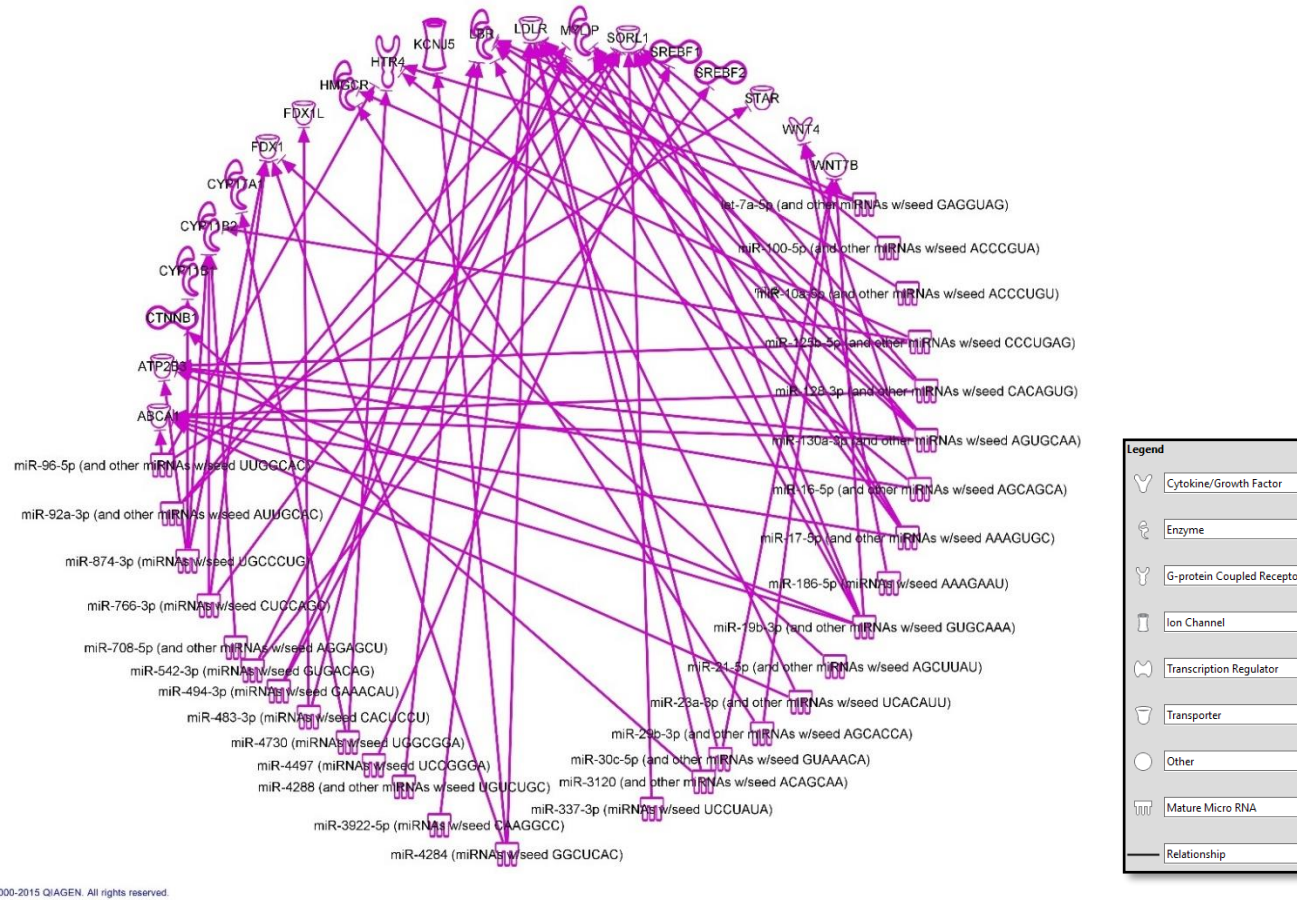


**Figure 6-18: IPA miRNA target gene for the basal vs KCI-treated group.**  
 The arrow from each miRNA indicates inhibition of the target gene.

## 6.7 IPA Target Filter Analysis: experimentally-validated mRNA targets by cluster.

### 6.7.1 Cluster miR-17-5p and miR-19a-3p (Chromosome 13).

The miRNAs miR-17-5p and miR-19b-3p originate from a primary miRNA encoded at chromosome 13q31.3. Both of these miRNAs are significantly downregulated by all of the stimulations (Angio II, dbcAMP and KCl (Figure 6-19). However, despite originating from the same cluster, the seed sequences of these 2 miRNAs are distinct: AAAGUGC for miR-17-5p and GUGCAAA for miR-19a-3p (Figure 6-19). miR-17-5p shares a similar seed sequence with hsa-miR-106a-5p, hsa-miR-106b-5p, hsa-miR-20a-5p, hsa-miR-20b-5p and hsa-miR-93-5p. miR-19a-3p shares its seed sequence with miR-19b-3p (GUGCAAA). Based on IPA analysis, there are 42 experimentally-validated targets for miR-17-5p and 11-experimentally validated targets for miR-19a-3p.

From the Ingenuity Expert Finding literature database, human miR-17-5p has been shown to target CCND1 by quantitative RT-PCR, luciferase reporter gene assay (Yu, Wang et al. 2008) and Western blotting (Deshpande, Pastore et al. 2009). PTEN is another mRNA targeted by miR-17-5p and miR-19a-3p (Lima, Busacca et al. 2011). miR-17 reduces activation-induced cell death and decreases inducible regulatory T-cell differentiation. The function of miR-17 is mediated by TGFBR2 and CREB1. The loss of miR-17-92 in CD4 T cells results in tumour evasion and this study suggests that regulation of miR-17 could enhance the effectiveness of T cell-based tumour therapy (Jiang, Li et al. 2011). miR-17-5p is shown to directly target HBP1 (HMG-box transcription factor 1) in breast cancer cells (Li, Bian et al. 2011). E2F transcription factor 1 (E2F1), E2F transcription factor 2 (E2F2) and E2F transcription factor 3 (E2F3) are the validated targets for cluster miR-17-92. These are essential for cell cycle function, inducing the expression of genes involved in progression of G1 phase to S phase (Slaby, Svoboda et al. 2009). High cluster mir-17-92 level leads to downregulation of E2F1 protein, thus inhibiting apoptosis (Woods, Thomson et al. 2007). Janus kinase 1 (JAK1), is another validated target for miR-17; it plays a crucial role in vascular homeostasis and it is required for sprouting angiogenesis (Doebele, Bonauer et al. 2010).

miR-19a-3p targets *CCDN1*, as ascertained by luciferase reporter gene assay, Western blotting and quantitative RT-PCR (Qin, Wang et al. 2010). miR-19a has oncogenic activity through repression of *PTEN*, a tumour suppressor in the *Emmu-myc* model of mouse B-cell lymphoma (Olive, Bennett et al. 2009). miR-19a is upregulated in human embryonic stem cells (hES) and inversely expressed relative to *ERBB4* (*erb-b2* receptor tyrosine kinase 4) mRNA; mutation of *ERBB4* has been associated with cancer (Tsai, Singh et al. 2010).

Other experimentally-validated targets of the clustered miRNAs miR-17-5p and miR-19-3p are shown in Figure 6-19.

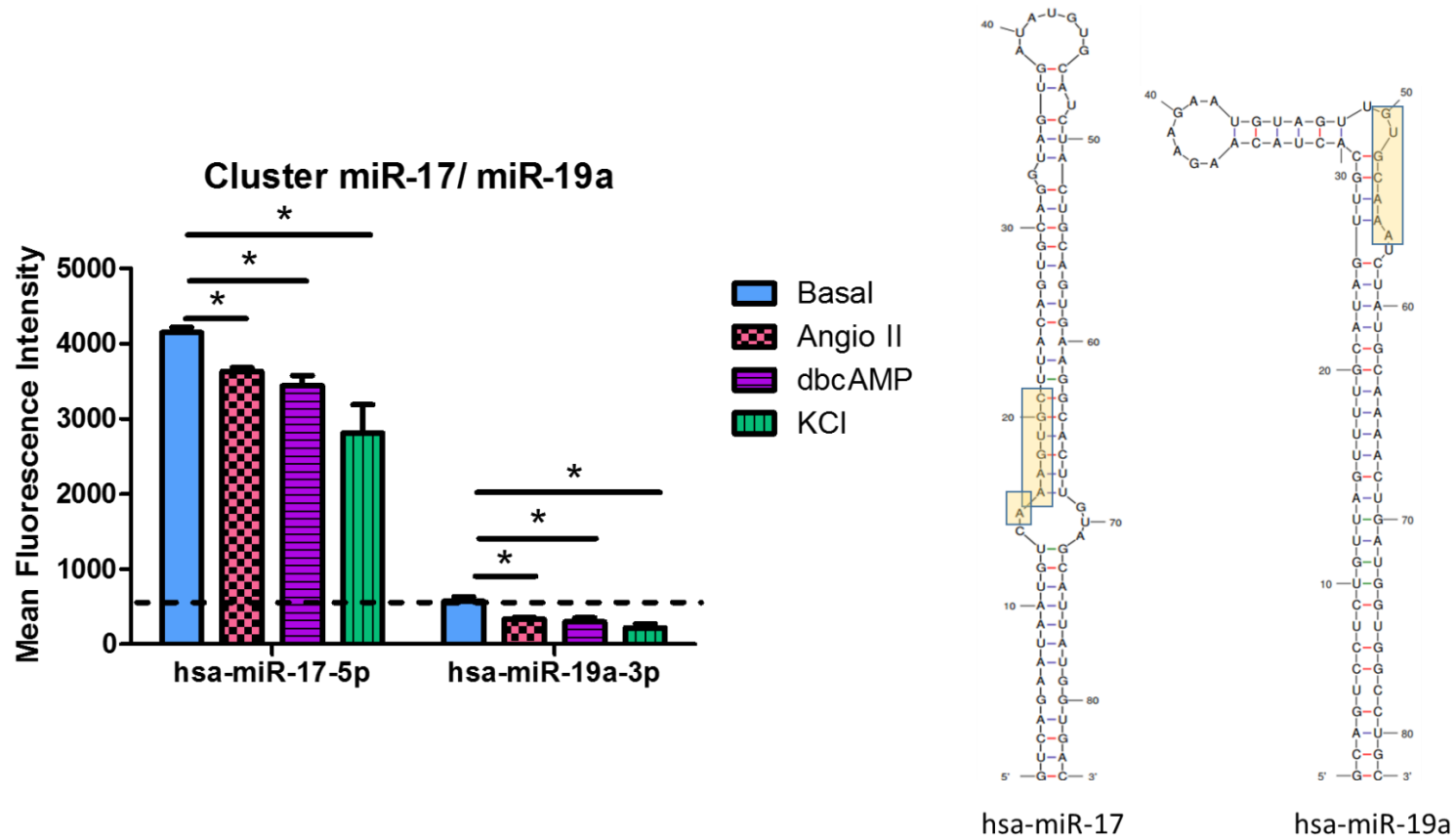
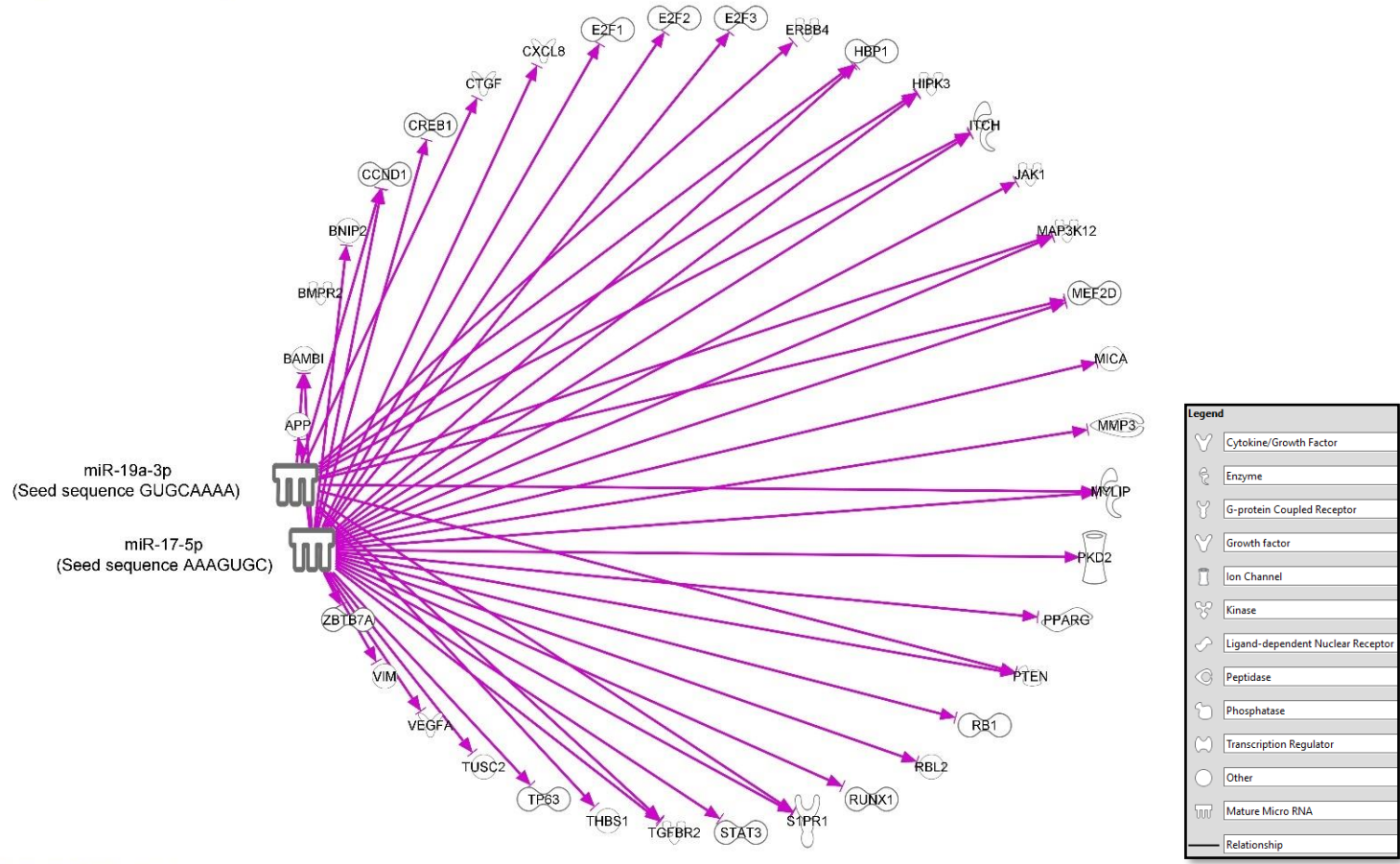


Figure 6-19: (Left) Microarray expression of mir-17-5p and miR-19a-3p across basal (blue), Angio II (red), dbcAMP (purple) and KCl treatments (green). All exhibit a consistent pattern throughout stimulation. \*  $p < 0.05$  relative to basal. (Right) the primary miRNA structure of miR-17-5p and miR-19a-3p: yellow box indicates the seed sequence for both miRNA (AAAGUGC for miR-17-5p and GUGCAA for miR-19a-3p).

Path Designer miR17 miR19a & valid target



© 2000-2015 QIAGEN. All rights reserved.

Figure 6-20: miR-17-5p, miR-19a-3p and their experimentally-validated targets, derived from miRNA Target Filter Analysis (IPA).

### **6.7.2 Cluster miR-106a-5p and miR-20b-5p (Chromosome X).**

The miRNAs miR-106a-5p and miR-20b-5p originate from a primary miRNA located on chromosome X. Both miRNAs are significantly downregulated following stimulation with Angio II, dbcAMP and KCl (Figure 23). Furthermore, they share the same seed sequence (AAAGUGC), as does miR-17-5p. Both miRNAs share their seed sequence with hsa-miR-106b-5p, hsa-miR-20a-5p, hsa-miR-20b-5p and hsa-miR-93-5p. Based on IPA analysis, there are 42 experimentally validated targets for miR-106a-5p and miR-20b-5p.

In the transgenic mouse model for Alzheimer's disease, miR-106b is shown to target TGF $\beta$ 2 receptor (Wang, Liu et al. 2010). In chronic lymphocytic leukaemia (CLL), exogenous transfection with miR-106b demonstrates that ITCH is a direct target for this miRNA (Sampath, Calin et al. 2009). E2F1, E2F2 and E2F3 are modulated by the cluster members miR-106a-92 and miR-106b-25 (a miR-17-92 cluster paralog) (Bueno, Gómez de Cedrón et al. 2010). miR-106b is upregulated in human gastric tumours and develops a negative-feedback loop to E2F1 gene expression (Petrocca, Visone et al. 2008)

miR-20a facilitates the transition through G1 in normal diploid human cells and the inhibition of the miRNA leads to an accumulation of E2F1 transcription factor (Pickering, Stadler et al. 2008). ESR1 is targeted by miR-20b, as demonstrated by luciferase reporter gene assay (Akingbemi, Ge et al. 2003).

miR-106a-5p and miR-20b-5p also share mRNA targets with miR-17-p (Figure 6-20 and Figure 6-22).

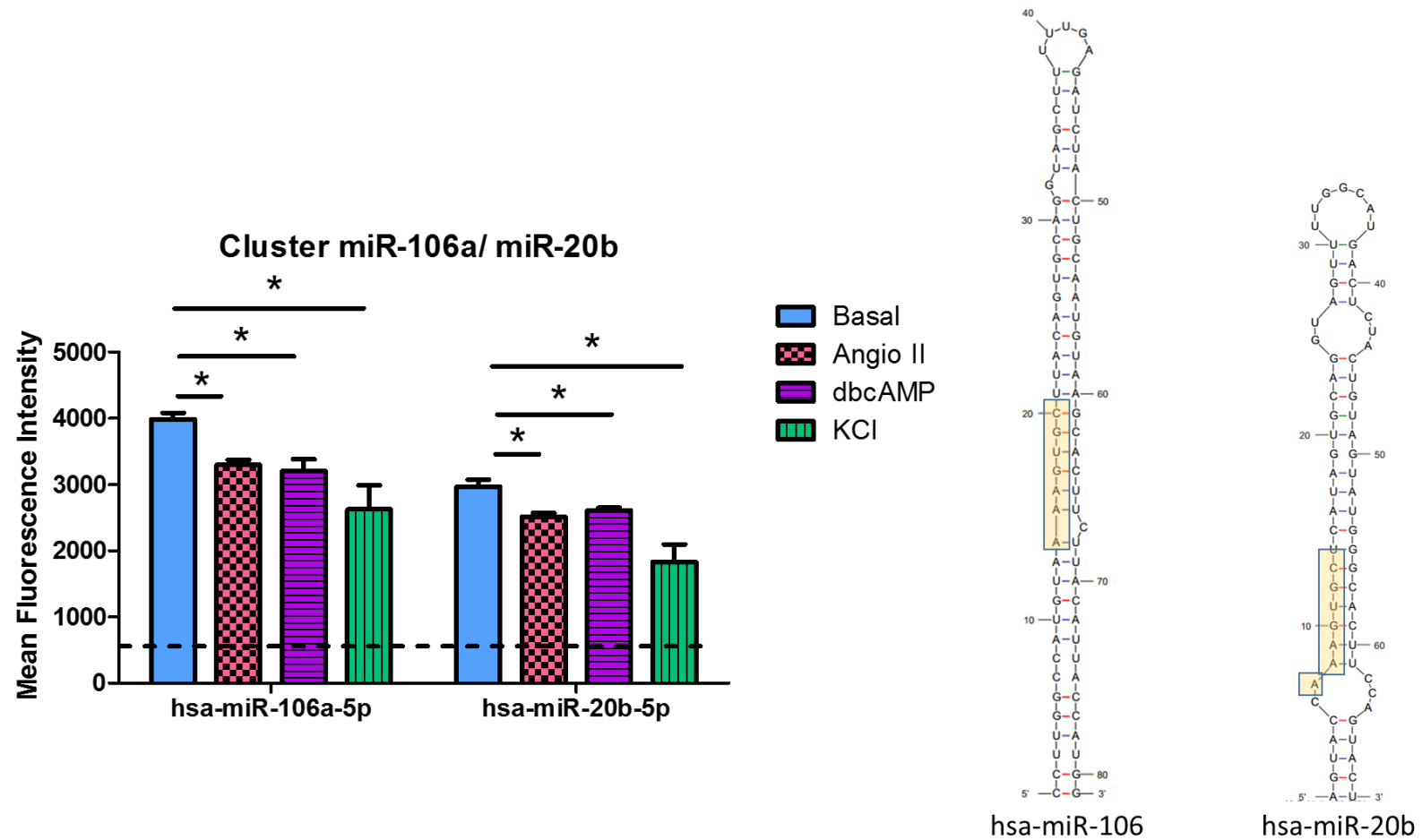
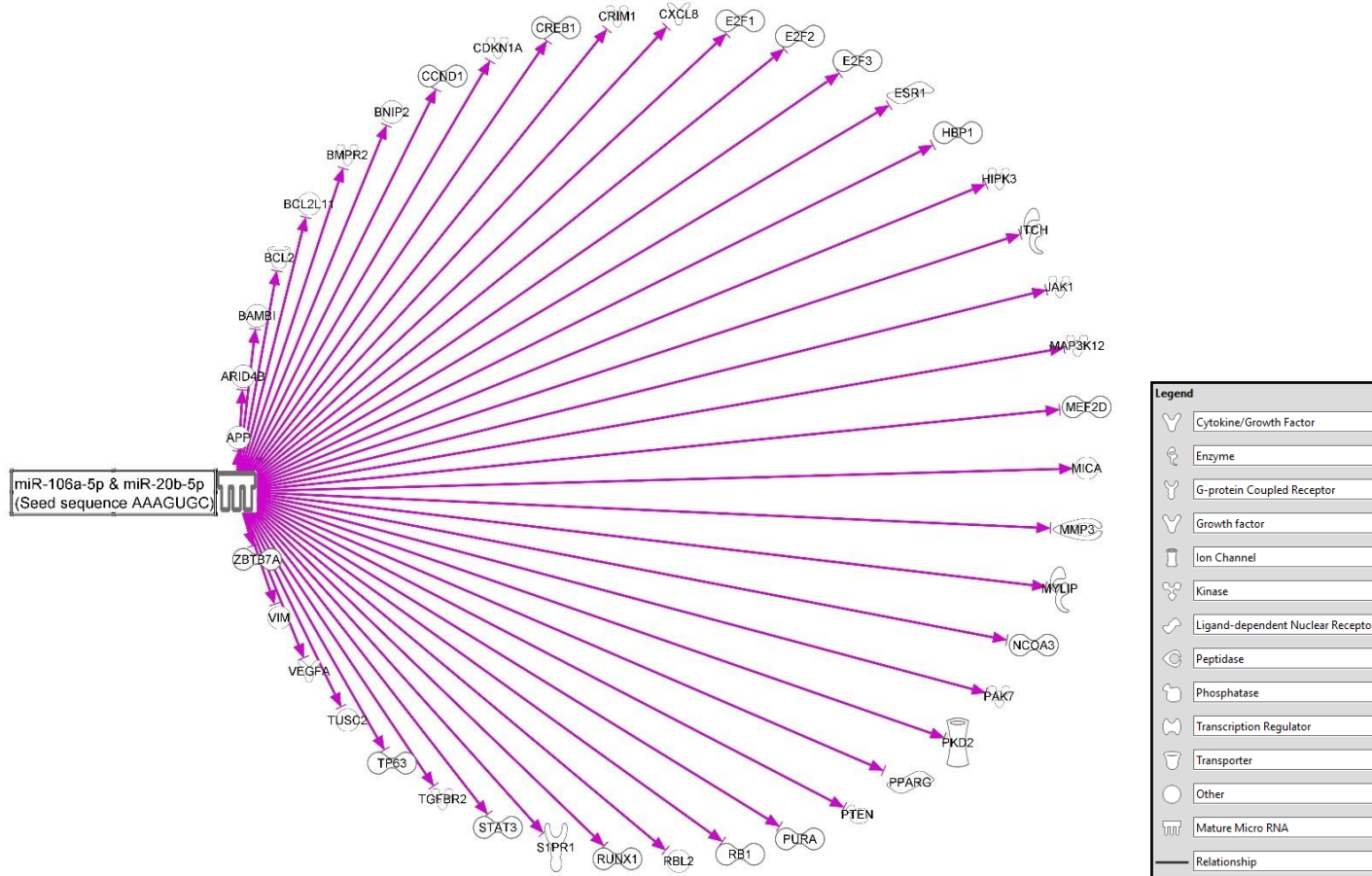


Figure 6-21:(Left) Microarray expression of mir-17-5p and miR-19a-3p across basal (blue), Angio II (red), dbcAMP (purple) and KCl treatments (green). All exhibit consistent expression throughout stimulation. (Right) the primary miRNA structure of miR-17-5p and miR-19a-3p: the yellow box indicates the seed sequence for both miRNA (AAAGUGC for miR-106a-5p and miR-20b-5p, both share similar seed sequence with miR-17-5p). \*  $p < 0.05$  relative to basal.

Path Designer miR-17 106a 20b and validated target



© 2000-2015 QIAGEN. All rights reserved.

Figure 6-22: miR-106-5p and miR-20b-5p and their experimentally-validated targets, derived from miRNA Target Filter Analysis (IPA).

### 6.7.3 IPA Canonical Signalling Involving cluster miR-17-5p/miR-19a-3p miRNAs.

The cluster miRNAs miR-17-5p/miR-19a-3p are predicted by IPA Canonical Pathways Signalling to target a few important pathways relevant to steroidogenesis, biosynthesis of cholesterol, apoptosis, angiogenesis and tumour development.

Specifically, the IPA Canonical Pathways involved are:

1. Aldosterone signalling in epithelial cells (Figure 6-23)
2. LXR/ RXR activation (Figure 6-24)
3. WNT/  $\beta$ -catenin signalling (Figure 6-25)
4. Apoptosis signalling (Figure 6-26)
5. VEGF signalling (Figure 6-27)
6. TGF- $\beta$  signalling (Figure 6-28)

#### 6.7.3.1 Genes Targeted by miR-17/19 in Aldosterone Signalling in the Epithelial Cell Pathway

miR-19b-3p/miR-19a-3p (and other mature microRNAs with seed GUGCAAA) target the Mineralocorticoid Receptor (MR). The *NR3C2* (nuclear receptor subfamily 3, group C, member 2) gene encodes the mineralocorticoid receptor (MR) which facilitates aldosterone's actions on salt and water balance. The MR protein acts as a ligand-dependent transcription factor that binds to mineralocorticoid response elements in order to stimulate target genes. Mutations of *NR3C2* cause autosomal dominant pseudohypoaldosteronism type I, a disorder presenting with urinary salt wasting, early onset hypertension, severely exacerbated in pregnancy. MR mediates the biological action of aldosterone via water-salt homeostasis, stimulates inflammation, increases cardiovascular remodelling, causes endothelial dysfunction and impairs pancreatic insulin released (Ronconi, Turchi et al. 2012).

miR-19b-3p/miR-19a-3p (and other mature microRNA with seed GUGCAAA) targets RAF1 (Raf-1 proto-oncogene, serine/threonine kinase). RAF1 is a cellular

homolog of the viral raf gene (v-raf) and encodes MAP kinase 3 (MAP3K) which plays an important role in the cell cycle, apoptosis, cell differentiation and cell migration. By targeting RAF1, these miRNAs might reduce apoptosis and increase cell proliferation in tumours. These miRNAs are also predicted to bind with KRAS (Kirsten rat sarcoma viral oncogene homolog) which encodes a protein member of the small GTPase superfamily.

miR-19b-3p/miR-19a-3p (and other mature microRNA with seed GUGCAA) also target SGK1 (serum/glucocorticoid regulated kinase 1) that encodes serine/threonine protein kinase, involved in several cellular responses. The kinase activates some sodium, potassium and chloride channels (i.e renal sodium excretion). Upregulation of this gene may contribute to hypertension and diabetic nephropathy. Furthermore, it targets SLC9A1 that encodes the Na<sup>+</sup>/H<sup>+</sup> antiporter from the solute carrier family 9 (plasma membrane transporter) expressed in kidney and intestine. The protein is essential for pH balance, cell migration and cell volume and tumour growth.

miR-17-5p (and other mature microRNA with seed AAAGUGC) is predicted to target ICMT (isoprenylcysteine carboxyl methyltransferase), that encodes enzymes that modify isoprenylated C-terminal cysteine residues (posttranscriptionally).

### 6.7.3.2 Genes Targeted by miR-17/ 19 in the LXR/RXR Activation pathway

Both miR-17 and miR-19 target LDLR, ABCA1 and IDOL. LDLR (low density lipoprotein receptor) encodes a cell surface protein receptor that is responsible for LDL endocytosis. LDL is then processed by lysosomes and degraded to produce cholesterol (under the control of HMGCR). The ABCA1 (ATP-binding cassette, sub-family A (ABC1), member 1) gene encodes a member of the ABC transporter family, that acts as a cholesterol efflux pump in the cellular lipid removal pathway. Mouse miR-19b-3p/miR-19a-3p (and other mature microRNAs with seed GUGCAA) and mouse miR-17-5p (and other mature microRNAs with seed AAAGUGC) target mouse IDOL/MYLIP (myosin regulatory light chain interacting protein) in T-cell leukaemia (high expression of cluster miR-17-92 is detected in human T-cell leukaemia) (Landais, Landry et al. 2007). IDOL acts as an E3 ubiquitin ligase to elicit ubiquitination and degradation of LDLR. One study suggests that structure-based IDOL inhibitors might have therapeutic potential to treat cardiovascular disease by increasing LDLR abundance (Sorrentino, Scheer et al. 2011). IDOL increases degradation of LDLR by C-terminal domain ubiquitination, leading to limitation of cholesterol uptake. Cells deficient of IDOL exhibit high levels of LDLR protein and high rates of LDL uptake (Scotti, Hong et al. 2011).

miR-19b-3p/miR-19a-3p (and other mature microRNA with seed GUGCAA) target the TNF (tumour necrosis factor) gene that encodes proinflammatory cytokines in the TNF superfamily. It is mainly secreted by macrophages and is involved in cell proliferation, lipid metabolism, coagulation, apoptosis and cell migration.

miR-17-5p (and other mature microRNA with seed AAAGUGC) is predicted to target the ABCG4 (ATP-binding cassette, sub-family G (WHITE)), member 4) gene, which encodes another transporter, a member of the White subfamily mostly expressed in liver. No specific function has been described.

### 6.7.3.3 Genes Targeted by miR-17/ 19 in the WNT/ $\beta$ -catenin Signalling pathway

Both miR-17 and miR-19 target Cyclin D1 (product of the CCND1 gene). Cyclin D1 is also a validated target of miR-17-5p as shown in breast cancer experiments (Yu, Wang et al. 2008). miR-17-5p also significantly suppresses cyclin D1 at its 3'UTR in mantle cell lymphoma (MCL) (Deshpande, Pastore et al. 2009). Cyclin D1 forms a complex with CDK4 and CDK6 that is required for cell cycle G1/ S transition. Mutation of the gene is frequently observed in many tumours and may therefore contribute to tumorigenesis. CCND1 also has been shown to be a validated target for miR-19a in human umbilical vein endothelial cells (Qin, Wang et al. 2010). The miR-17-5p cluster downregulates cyclin D1 translation in human breast tumour cell lines. The cluster suppressed cell proliferation and colony formation by inversely regulating CCND1 via a conserved 3'UTR miRNA-binding site, leading to inhibition of S-phase of cell cycle (Yu, Wang et al. 2008). The overexpression of cyclin D1 is significant in mantle cell lymphoma. The level of cyclin D1 can be significantly reduced by the miR-17-92 cluster that directly binds to the 3'UTR of cyclin D1 (Deshpande, Pastore et al. 2009). One study showed that transfection of miR-19a significantly downregulates the cyclin D1 gene and protein in endothelial cells. This leads to cell arrest at the G1/S transition (Qin, Wang et al. 2010).

miR-19b-3p/miR-19a-3p (and other mature microRNA with seed GUGCAA) are predicted to target GJA1/CX43. GJA1 (gap junction protein, alpha 1, 43kDa), a member of the connexin family that encodes a component of the gap junction protein that provides a route for low molecular weight material diffusion from cell to cell. It is crucial in controlling heart contraction and embryonic development. Mutation is associated with heart malformation. The miRNA also targets NLK (nemo-like kinase), involved in ATP binding, kinase activity and transcription factor binding that are involved in hepatocellular carcinoma. It also targets MARK2/PAR-1. MARK2 (MAP/microtubule affinity-regulating kinase 2) that encode the Par-1 family of serine/threonine protein kinases. It is a vital cell polarity regulator in epithelial and neuronal cells and controls microtubule stability.

miR-17-5p (and other mature microRNAs with seed AAAGUGC) is predicted to target TCF4 (transcription factor 4) and PPARD. The PPARD (peroxisome proliferator-activated receptor delta) gene encodes the peroxisome proliferator-activated receptor (PPAR). PPAR is a nuclear receptor and mediates various disorders, including cancer, atherosclerosis, diabetes and obesity. In a knockout mouse model, the protein was shown to be involved in lipid metabolism and cell proliferation. The TCF4 gene encodes a basic helix-hoop-helix transcription factor that plays an important role in the nervous system. PPAR is a nuclear hormone receptor that binds peroxisome proliferators and regulates the number and size of peroxisomes generated by cells. PPAR may be involved in diabetes, obesity, atherosclerosis and cancer.

#### **6.7.3.4 Genes Targeted by miR-17/ 19 in the Apoptosis Signalling pathway**

Both miR-17 and miR-19 target *BCL2L11/BIM*. The *BCL2L11* gene (BCL2-like 11 (apoptosis facilitator)) encodes a member of the BCL-2 family, which can act as pro- or anti-apoptotic regulators. Gene expression can be stimulated by nerve growth factor (NGF). It is involved in neuronal and lymphocyte apoptosis.

miR-19b-3p/miR-19a-3p (and other mature microRNA with seed GUGCAAA) is predicted to target *APAF1* and *RAF1*. *APAF1* (apoptotic peptidase-activating factor 1) encodes a cytoplasmic protein that initiates apoptosis. *RAF1* (Raf-1 proto-oncogene, serine/threonine kinase) is a cellular homolog of the viral raf gene (v-raf) and encodes MAP kinase 3 (MAP3K), playing an important role in the regulation of genes involved in the cell cycle, apoptosis, cell differentiation and cell migration.

miR-17-5p (and other mature microRNA with seed AAAGUGC) is predicted to target *MAP3K5/ASK1*, *BCL2*, *CASP2*, *CASP7* and *MCL1*. The *MAP3K5* (mitogen-activated protein kinase 5) protein is involved in MAPK kinase and c-Jun N-terminal kinase activation. *BCL2* encodes outer mitochondrial membrane proteins that block the death of some cells (e.g. lymphocyte apoptosis). The *CASP2* (caspase 2, apoptosis-related cysteine peptidase) gene encodes a member of the cysteine-aspartic acid protease (caspase) family, involved in stress-induced cell death pathways, the cell cycle and tumorigenesis oppression. The *CASP7* (caspase 7, apoptosis-related cysteine peptidase) gene encodes cysteine-

aspartic acid protease (caspase) family. This family plays an important function in the completion-phase of cell apoptosis. The *MCL1* (myeloid cell leukaemia 1) gene encodes anti-apoptotic protein (member of BCL-2 family).

#### **6.7.3.5 Genes Targeted by miR-17/ 19 in the VEGF Signalling pathway**

miR-19b-3p/miR-19a-3p (and other mature microRNA with seed GUGCAA) is predicted to target ELAVL1/HUR, PTK2B/PYK2 and RAF1. ELAVL1 (ELAV-like RNA binding protein 1) encodes a member of the ELAVL family of RNA-binding proteins. The proteins contain multiple RNA recognition motifs and specifically bind to AU-rich elements (AREs) found in the 3'UTRs of miRNA. The gene is highly expressed in cancers. PTK2B (protein tyrosine kinase 2 beta) encodes tyrosine kinase in the cytoplasm that increases calcium influx and activates the MAPK signalling pathway. RAF1 (Raf-1 proto-oncogene, serine/threonine kinase) is a cellular homolog of viral raf gene (v-raf) and encodes MAP kinase 3 (MAP3K). It plays an important role in regulation of genes involved in the cell cycle, apoptosis, cell differentiation and cell migration.

miR-17-5p (and other mature microRNA with seed AAAGUGC) is predicted to target BCL2, HIF1A and VCL. BCL2 encodes outer mitochondrial membrane proteins that block the death of some cells (e.g. lymphocyte apoptosis). The VCL (vinculin) gene encodes a cytoskeletal protein involved in cell-cell and cell-matrix junctions. Impairment of VCL is the cause of dilated cardiomyopathy type 1W. This disease is characterized by a dilated ventricle and systolic malfunction and lead to arrhythmias and congestive heart failure. The HIF1A (hypoxia inducible factor 1, alpha subunit (basic helix-loop-helix transcription factor)) gene encodes the transcription factor, hypoxia-inducible factor-1 (HIF-1),  $\alpha$ -subunit, which will bind with the  $\beta$ -subunit to form a heterodimer. HIF1A is involved in angiogenesis, increasing oxygen delivery and helping metabolic adaptation to hypoxia.

#### **6.7.3.6 Genes Targeted by miR-17/ 19 in the TGF- $\beta$ Signalling pathway**

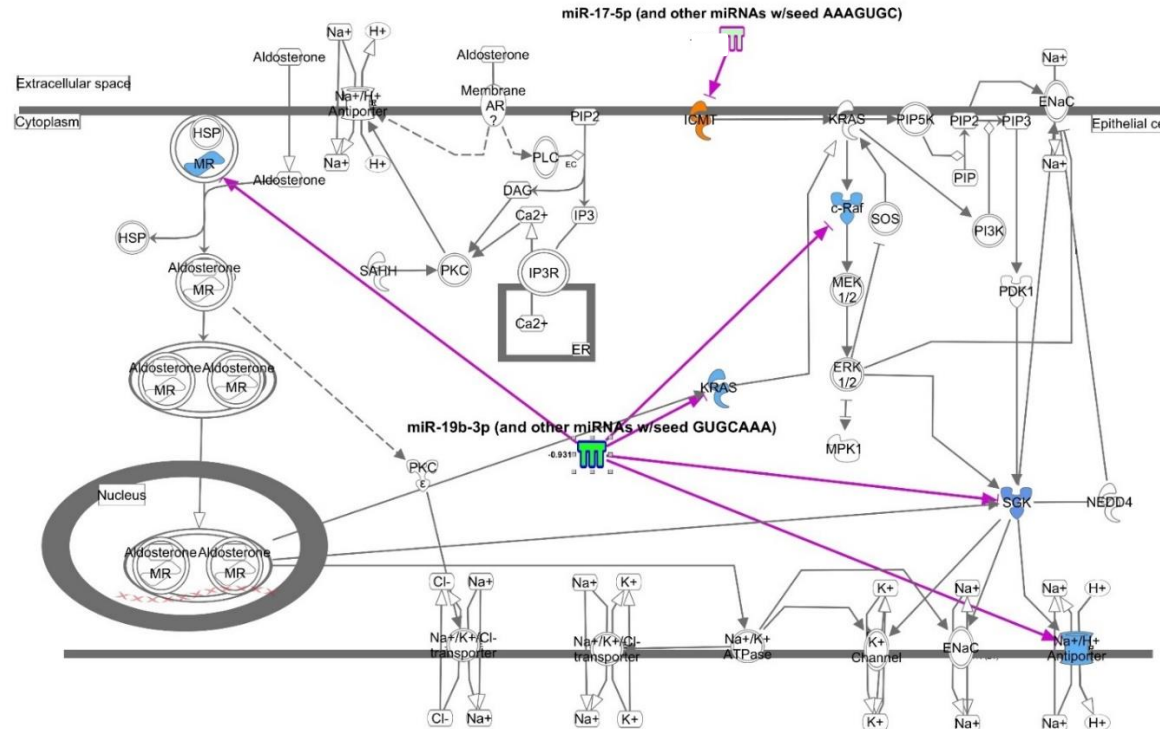
Both miR-17 and miR-19 target RUNX3, SMAD4, SMURF1 and ZFYVE9/SARA. The RUNX3 (runx-related transcription factor 3) gene encodes a member of the runx domain-containing family of transcription factors. By forming a complex with the

DNA sequence, 5'-PYGPYGGT-3' core (found in some promoters and enhancers), it can stimulate or inhibit transcription. The protein acts as a tumour suppressor and silencer of this gene, which is often related to cancer. The SMAD4 (SMAD family member 4) gene encodes a member of the SMAD family of signal transduction proteins. Mutations occur in pancreatic cancer and hereditary haemorrhagic telangiectasia syndrome. SMAD proteins are activated in response to TGF-Beta signalling and are subjected to post-transcriptional modification. The SMURF1 (SMAD specific E3 ubiquitin protein ligase 1) gene encodes a specific receptor-regulated SMAD protein (ubiquitin ligase) in the bone morphogenetic protein (BMP) pathway. This protein plays an essential role in cell motility, cell signalling and cell polarity. The ZFYVE9 (zinc finger, FYVE domain containing 9) gene encodes a double zinc finger motif-containing protein involved in the transforming growth factor-beta (TGFB) signalling pathway. The protein interacts with SMAD2 and SMAD3 and recruits SMAD2 to the TGFB receptor. The ZFYVE9 gene encodes a double zinc finger motif-containing protein involved in transforming growth factor-beta (TGFB) signalling pathway. The protein interacts with SMAD2 and SMAD3 and recruits SMAD2 to the TGFB receptor.

miR-19b-3p/miR-19a-3p (and other mature microRNA with seed GUGCAA) are predicted to target ARKADIA/RNF111, CRAF, GSC, PAI-1/SERPINE, TMEPAI/PMEPA1 and TGIF. RNF111 (ring finger protein 111) plays a critical role in embryonic mesoderm development; CRAF is involved in the cell cycle, migration, differentiation and apoptosis; GSC (goosecoid homeobox) encodes proteins of the bicoid subfamily of the paired (PRD) homeobox family. The protein acts as a TF; in mice it is involved in craniofacial and rib cage development during embryogenesis. SERPINE1 (serpin peptidase inhibitor, clade E (nexin, plasminogen activator inhibitor type 1), member 1) encodes the serine proteinase inhibitor (serpin) superfamily. The protein is an inhibitor of fibrinolysis (tissue plasminogen activator (tPA) and urokinase (uPA) inhibitor). High expression of the gene is associated with thrombophilia. TMEPAI/PMEPA1 (prostate transmembrane protein, androgen induced 1) overexpression is involved in many types of cancer. TGIF1 (TGFB-induced factor homeobox 1) encodes a protein that is active as a transcriptional co-repressor of SMAD2 and may be involved in nuclear signal transmission.

miR-17-5p (and other mature microRNA with seed AAAGUGC) is predicted to target BCL2, SKI, SMAD6 and SMAD7. The SKI (SKI proto-oncogene) gene encodes the nuclear protooncogene protein. This protein represses TGF-beta signalling which may contribute to neural tube development and muscle differentiation. The SMAD6 (SMAD family member 6) gene encodes a protein that negatively regulates TGF-beta/activin-signalling. The SMAD7 (SMAD family member 7) gene encodes a nuclear protein that binds the E3 ubiquitin ligase SMURF2. It interacts with TGF-beta receptor type-1 (TGFB1), leading to the receptor degradation. The gene is involved in colorectal cancer. BCL involves in inhibiting lymphocyte apoptosis.

Path Designer Aldosterone Signaling in Epithelial Cells

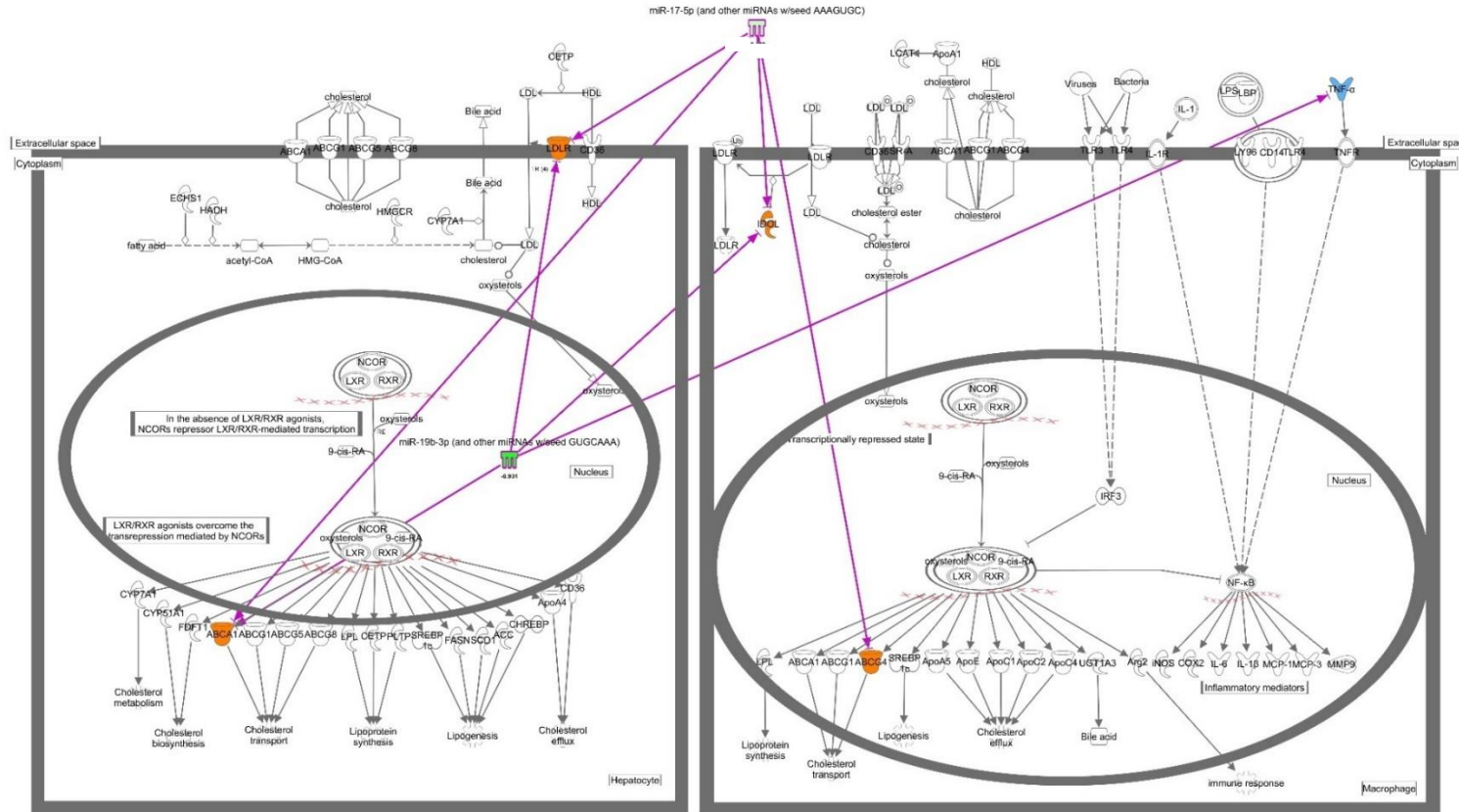


© 2000-2015 QIAGEN. All rights reserved.

### Figure 6-23: Aldosterone Signalling in the Epithelial Cellular Pathway.

miR-17-5p (and other miRNAs with seed AAAGUGC) targets ICMT while miR-19b-3p/miR-19a-3p (and other miRNAs with seed GUGCAAA) targets MR, cRaf, KRAS, SGK and SLC9A1 (Na<sup>+</sup>/H<sup>+</sup> Antiporter).

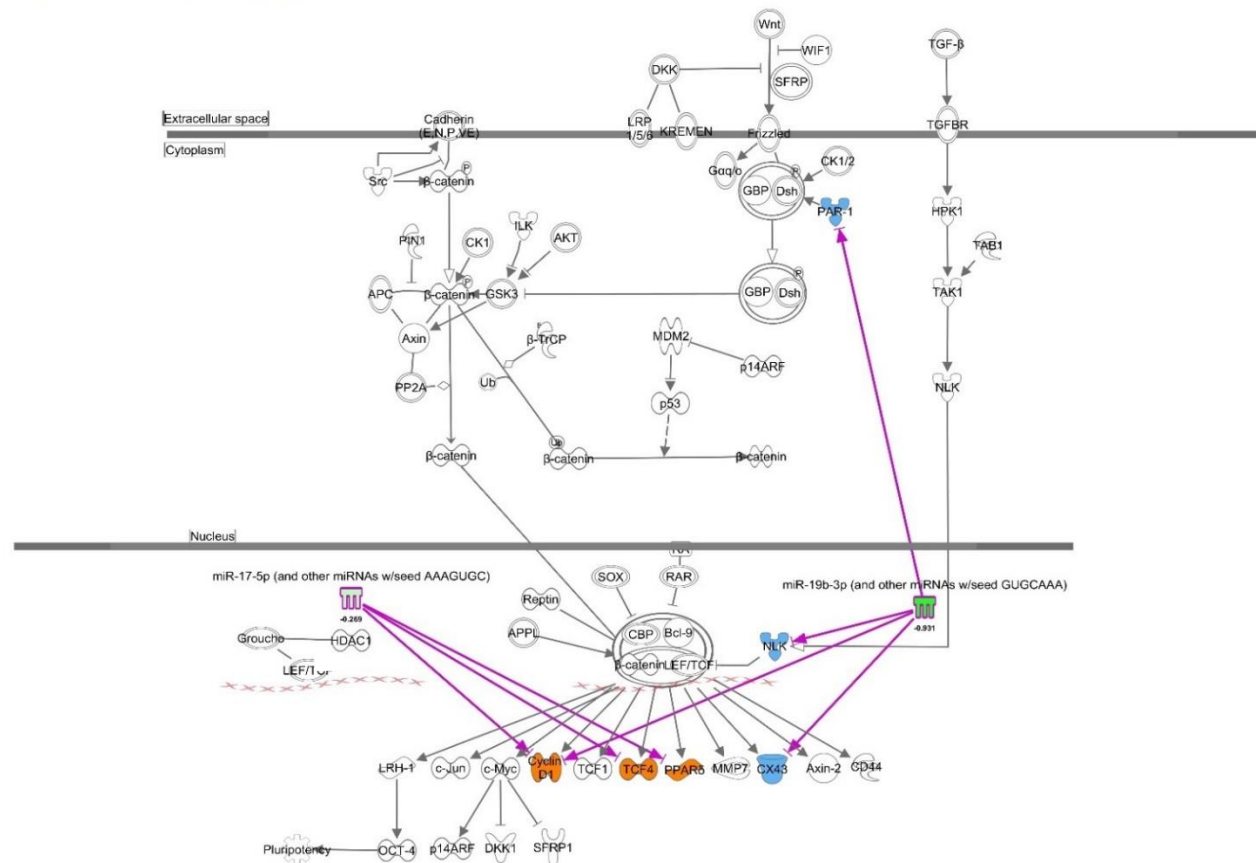
Path Designer LXR/RXR Activation



© 2000-2010 QIAGEN. All rights reserved.

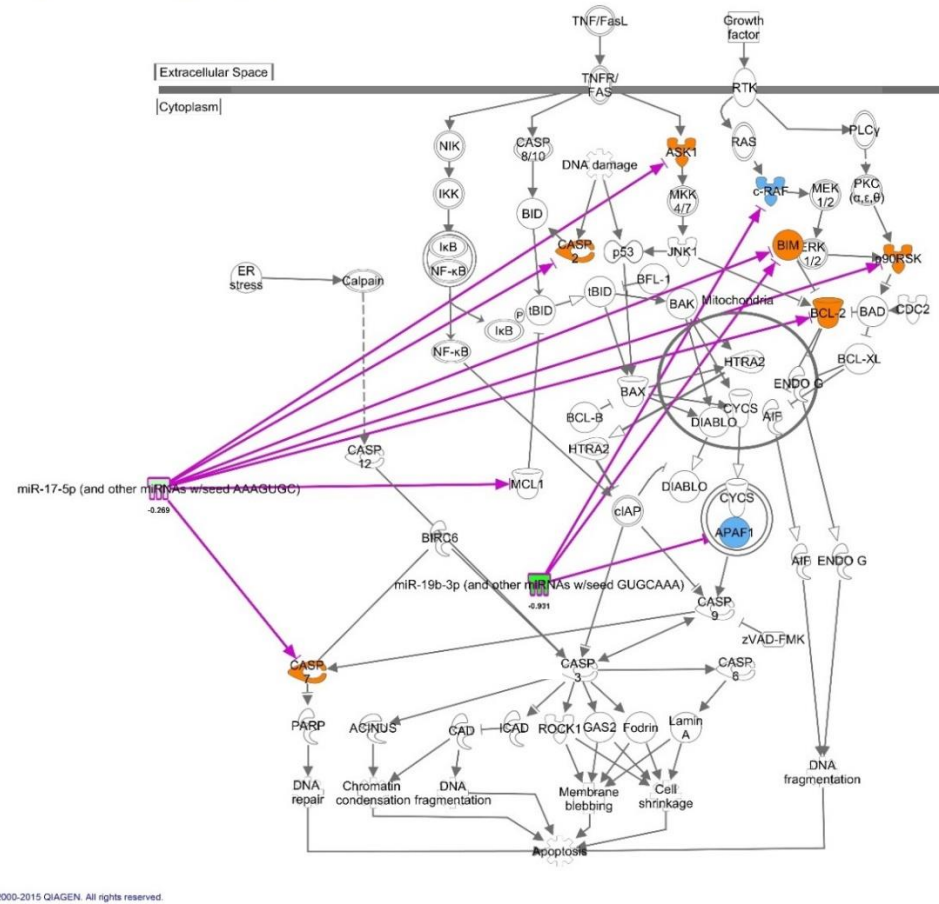
**Figure 6-24: The LXR/RXR Activation pathway.**

miR-17-5p (and other miRNAs with seed AAAGUGC) targets LDLR, ABCA1, IDOL and ABCG4 while miR-19b-3p/miR-19a-3p (and other miRNAs with seed GUGCAA) targets ABCA1, LDLR, IDOL and TNF-α.



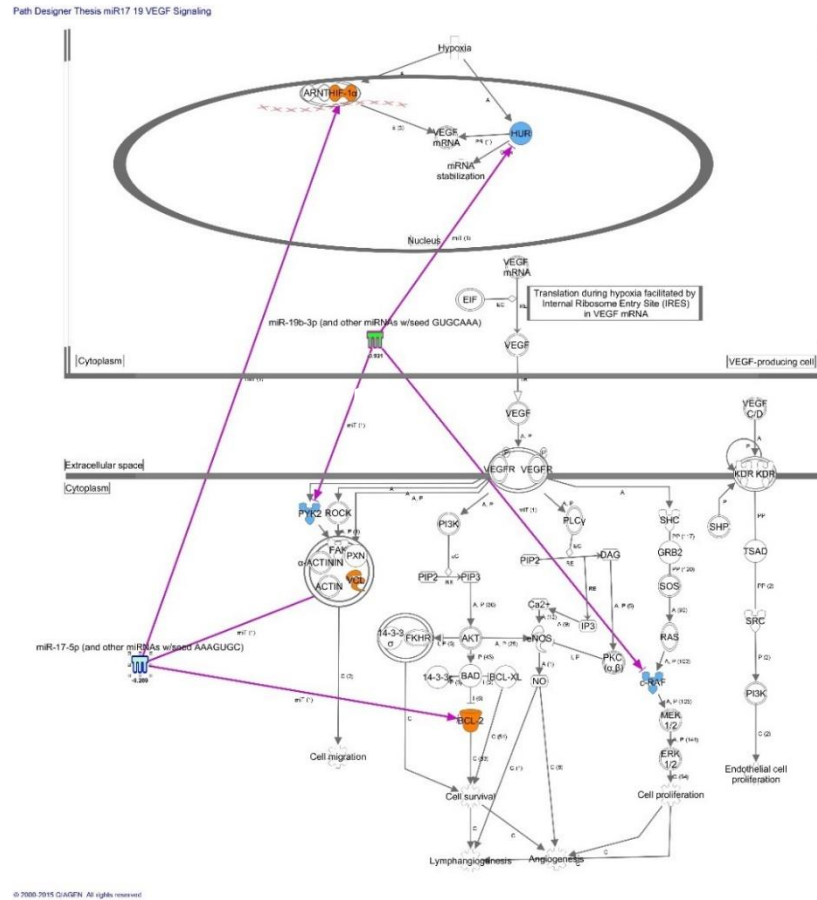
### Figure 6-25: The WNT/ $\beta$ -catenin Signalling Pathway.

miR-17-5p (and other miRNAs with seed AAAGUGC) targets Cyclin D1, TCF4 and PPAR $\delta$  while miR-19b-3p/miR-19a-3p (and other miRNAs with seed GUGCAA) targets PAR-1, NLK, Cyclin D1 and CX43.



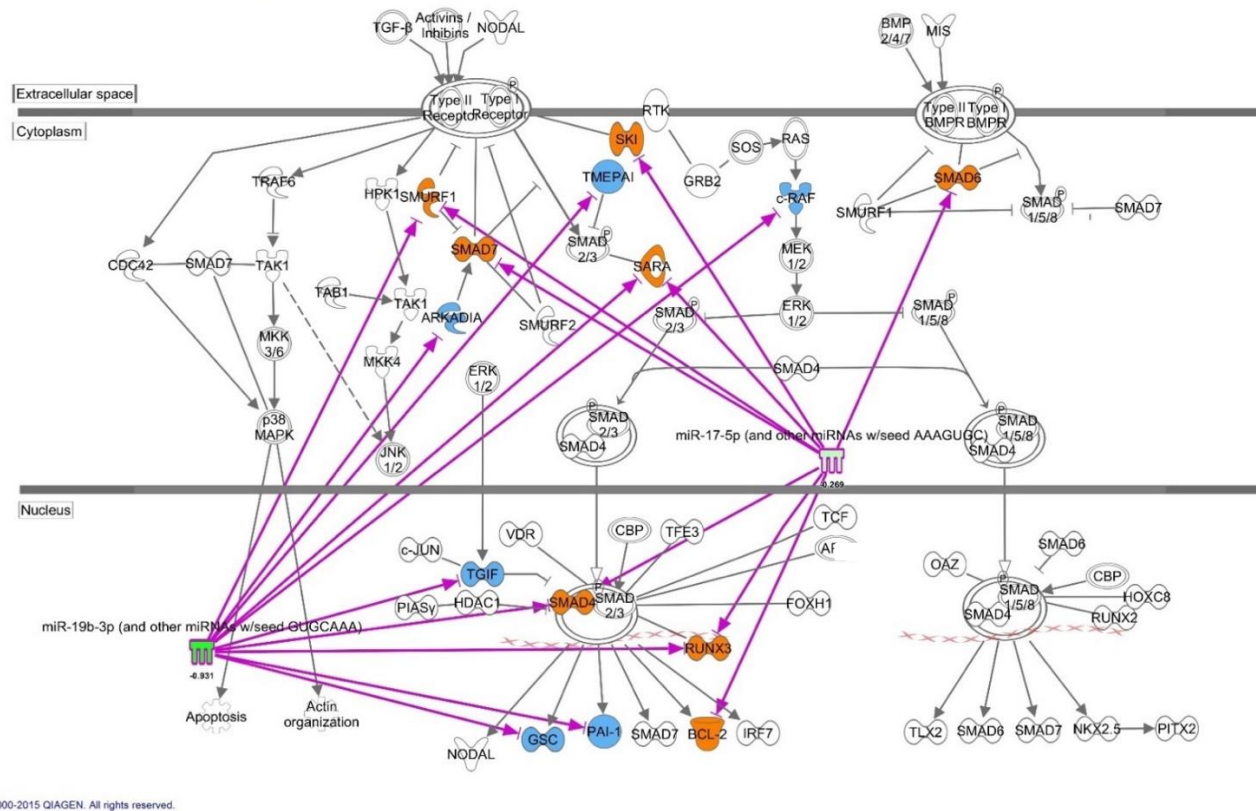
**Figure 6-26: The Apoptosis Signalling pathway.**

miR-17-5p (and other miRNAs with seed AAAGUGC) targets ASK1, CASP2, BIM, p90RSK, BCL-2, MCL and CASP7 while miR-19b-3p/miR-19a-3p (and other miRNAs with seed GUGCAAA) targets c-RAF, BIM and APAF1.



### Figure 6-27: The VEGF Signalling Pathway.

miR-17-5p (and other miRNAs with seed AAAGUGC) targets HIF-1 $\alpha$  (HIF1A), VCL and BCL-2 while miR-19b-3p/miR-19a-3p (and other miRNAs with seed GUGCAAA) targets HUR (ELAVL1), c-RAF (RAF1) and PYK2 (PTK2B).

Path Designer Thesis miR-17 19 TGF- $\beta$  Signaling

### Figure 6-28: The TGF- $\beta$ Signalling Pathway.

miR-17-5p (and other miRNAs with seed AAAGUGC) targets SMAD6, SKI, SARA (ZFYE9), SMURF1, SMAD7, SMAD4, RUNX3 and BCL2 while miR-19b-3p/miR-19a-3p (and other miRNAs with seed GUGCAA) targets SMURF1, ARKADIA (RNF111), TMEPAI (PMEPA1), SARA (ZFYE9), c-RAF (RAF1), TGIF (TGIF1), SMAD4, RUNX3, PAI-1 (SERPINE1) and GSC.

## 6.8 Result: Validation of microarray and bioinformatics study of miR-17-5p

### 6.8.1 miR-17-5p

#### 6.8.1.1 miR-17-5p in Angio II-Stimulated Cells

miR-17-5p expression was found by microarray to be significantly decreased in Angio II-stimulated cells (Figure 6-29 A). Quantitative validation of this effect was conducted by realtime qRT-PCR which, although showing a similar pattern of downregulation, did not achieve significance (Figure 6-29 B; Table 6-1).

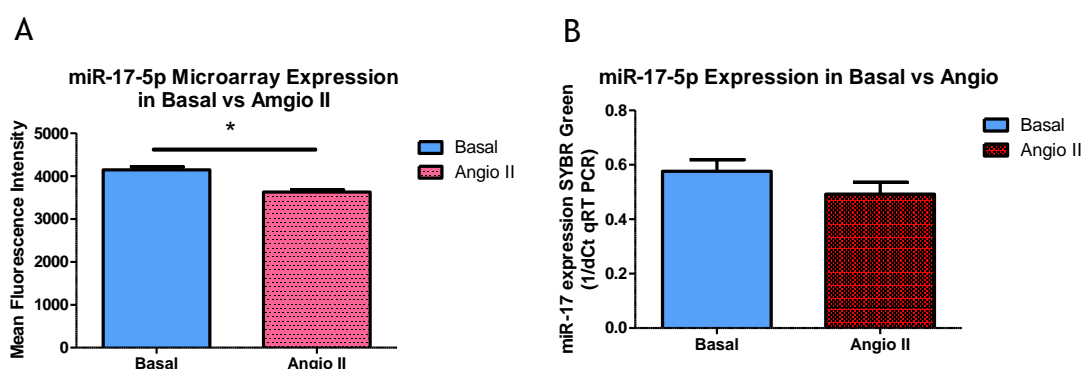


**Figure 6-29: Levels of miR-17-5p as in basal vs. Angio II-stimulated cells, as detected by (A) microarray (n= 3) and (B) realtime qRT-PCR (n= 5).**

\* indicates  $p < 0.05$ .

**Table 6-1: miRNA expression in Basal vs Angio II-stimulated H295R cells (Strain 1), analysed by realtime qRT-PCR.**

Ct= cycle threshold; ddCt= delta delta Ct; n= biological sample number; SD= standard deviation.

miRNA	n	Basal Mean Ct (SD)	Angio II Mean Ct (SD)	ddCt	Fold Change (Relative to basal= 1)	p-value
miR-17-5p	5	23.63 (0.01)	24.06 (0.31)	0.33	0.80	0.20

### 6.8.1.2 miR-17-5p in dbcAMP Stimulated Cells

Similarly, in dbcAMP-stimulated cells, a significant reduction of miR-17-5p had been observed by microarray but was not observed using realtime qRT-PCR (Figure 6-30; Table 6-2).

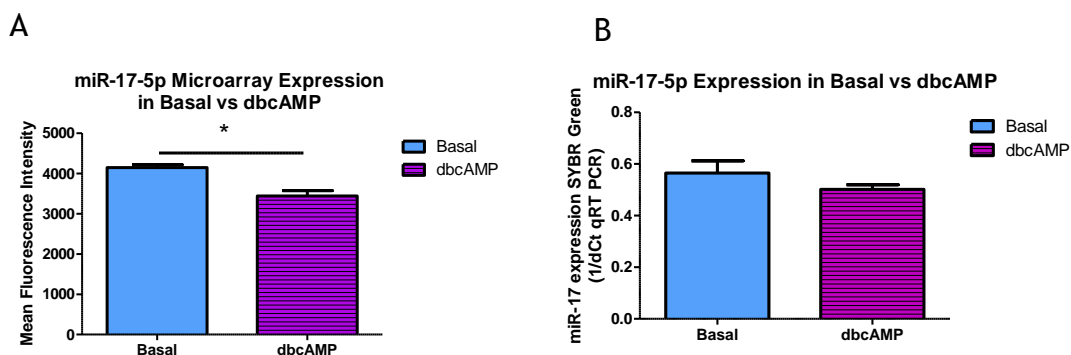


**Figure 6-30: Microarray expression of miR-17-5p (A) (n= 3) in Basal vs dbcAMP and the validation in qRT PCR (B) (n= 5) in Basal vs dbcAMP stimulated cells.**

\* indicates  $p < 0.05$ .

**Table 6-2: miRNA expression in Basal vs dbcAMP-stimulated H295R cells (Strain 1), analysed by realtime qRT-PCR.**

Ct= cycle threshold; ddCt= delta delta Ct; n= biological sample number; SD= standard deviation.

miRNA	n	Basal Mean Ct (SD)	dbcAMP Mean Ct (SD)	ddCt	Fold Change (Relative to basal= 1)	p-value
miR-17-5p	5	23.63 (0.34)	23.69 (0.23)	0.23	0.85	0.18

### 6.8.1.3 miR-17-5p in KCl Stimulated Cells

However, the significant reduction in miR-17-5p observed by microarray in KCl-stimulated cells was validated by realtime qRT PCR (Figure 6-31 and Table 6-3).

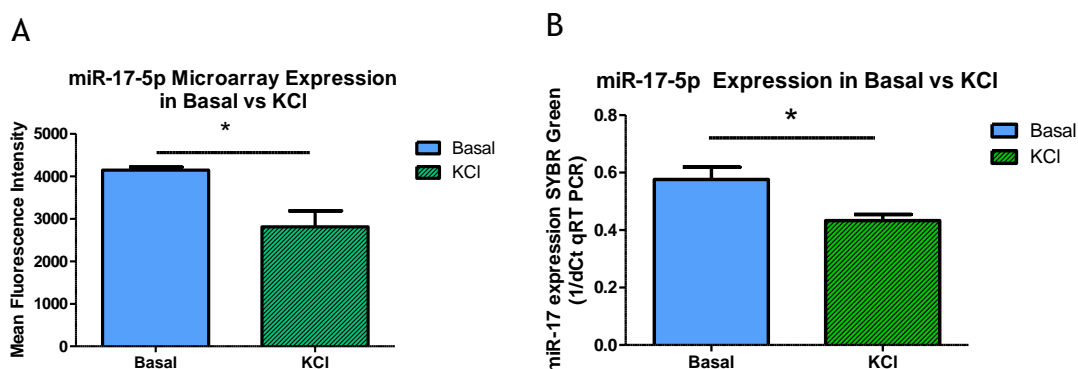


**Figure 6-31: Microarray expression of miR-17-5p (A) (n= 3) and validation by qRT PCR (B) (n= 5) of Basal vs KCl-stimulated cells.**

\* indicates  $p < 0.05$ .

**Table 6-3: miRNA expression in Basal vs KCl-stimulated H295R cells (Strain 1), analysed by realtime qRT-PCR.**

Ct= cycle threshold; ddCt= delta delta Ct; n= biological sample number; SD= standard deviation.

miRNA	n	Basal Mean Ct (SD)	KCl Mean Ct (SD)	ddCt	Fold Change (Relative to basal= 1)	p- value
miR-17-5p	5	23.63 (0.34)	24.02 (0.21)	0.56	0.68	0.01

## 6.8.2 miR-20b-5p

### 6.8.2.1 miR-20b-5p in Angio II Stimulated Cells

Microarray had identified significant downregulation of miR-20b-5p in Angio II-stimulated cells (Figure 6-32 A), but realtime qRT-PCR did not identify this reduction as significant (Figure 6-32 B).

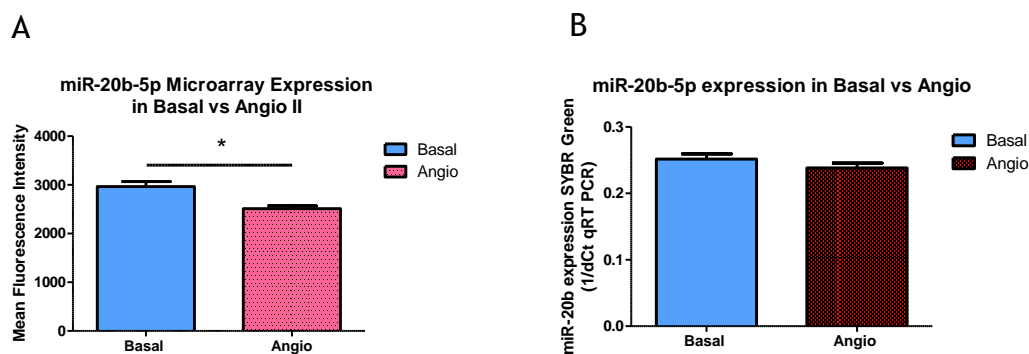


**Figure 6-32: Microarray expression of miR-20b-5p (A) (n= 3) in Basal vs Angio II-treated cells and its validation by qRT PCR (B) (n= 6).**

\* indicates  $p < 0.05$ .

**Table 6-4: miRNA expression in Basal vs Angio II-stimulated H295R cells (Strain 1), analysed by realtime qRT-PCR.**

Ct=cycle threshold; ddCt= delta delta Ct; n= biological sample number; SD= standard deviation.

miRNA	n	Basal Mean Ct (SD)	Angio II Mean Ct (SD)	ddCt	Fold Change (Relative to basal= 1)	p-value
miR-20b-3p	6	25.88 (0.28)	26.11 (0.41)	0.22	0.86	0.25

### 6.8.2.2 miR-20b-5p in dbcAMP Stimulated Cells

The reduction in miR-20b-5p observed by microarray in dbcAMP-stimulated cells (Figure 6-33 A) also was not found to be significant under realtime qRT-PCR (Figure 6-33 and Figure 6-34 B).

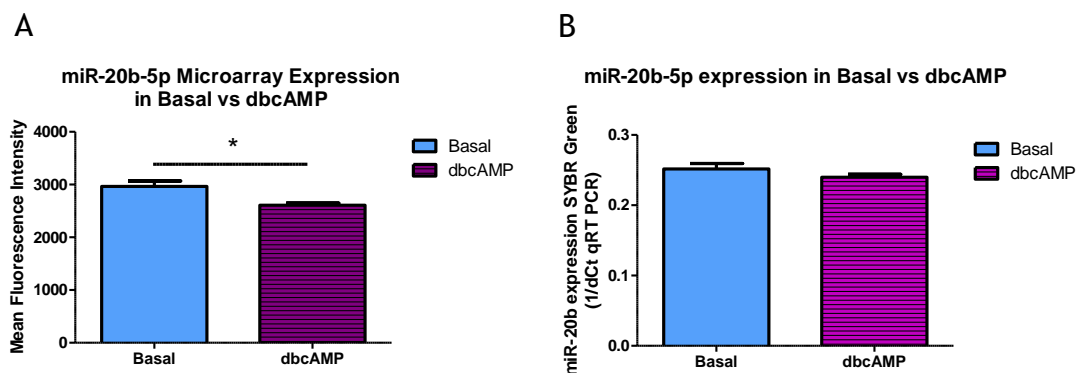


**Figure 6-33: Levels of miR-20b-5p in Basal vs dbcAMP-stimulated H295R cells (Strain 1), as measured by (A) microarray (n= 3) and (B) realtime qRT-PCR (n= 5).**

\* indicates  $p < 0.05$ .

**Table 6-5: miRNA expression in Basal vs dbcAMP-stimulated H295R cells (Strain 1), analysed by realtime qRT-PCR.**

Ct= cycle threshold; ddCt= delta delta Ct; n= biological sample number; SD= standard deviation.

miRNA	n	Basal Mean Ct (SD)	dbcAMP Mean Ct (SD)	ddCt	Fold Change (Relative to basal= 1)	p-value
miR-20b-3p	6	25.88 (0.28)	25.98 (0.30)	0.18	0.88	0.24

### 6.8.2.3 miR-20b-5p in KCl Stimulated Cells

The reduction in miR-20b-5p observed by microarray following KCl stimulation (Figure 6-34 A) was validated by realtime qRT-PCR (Figure 6-34 B and Table 6-6).

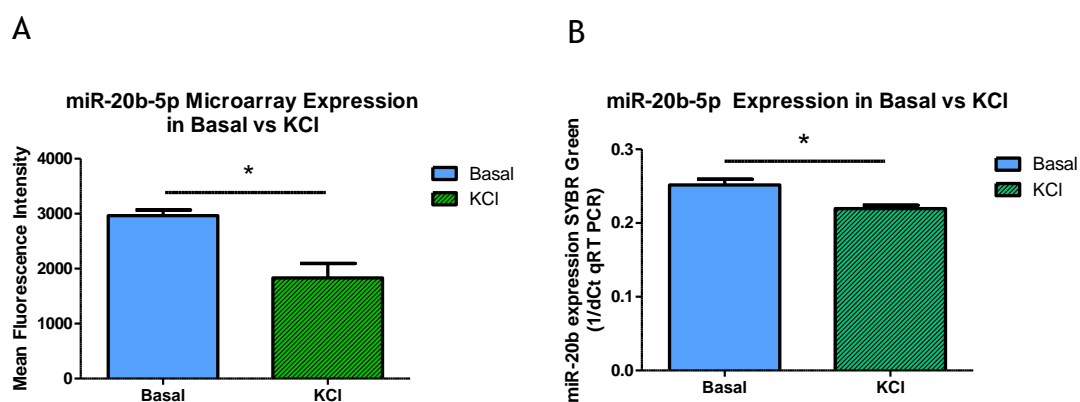


**Figure 6-34: Levels of miR-20b-5p following KCl stimulation of H295R cells (Strain 1) as measured by (A) microarray (n= 3) and (B) qRT-PCR (n= 6).**

\* indicates  $p < 0.05$ .

**Table 6-6: miR-20b-3p levels in Basal vs KCl-stimulated H295R cells (Strain 1) , analysed by realtime qRT-PCR.**

Ct=cycle threshold; ddCt= delta delta Ct; n= biological sample number; SD= standard deviation.

miRNA	n	Basal Mean Ct (SD)	KCl Mean Ct (SD)	ddCt	Fold Change (Relative to basal=1)	p- value
miR-20b-3p	6	25.88 (0.28)	26.26 (0.24)	0.57	0.67	<0.01

### 6.8.3 miR-766-3p

miR-766-3p was reported to be significantly upregulated in Angio II-stimulated cells analysed by microarray. The result was validated by realtime qRT PCR, which also identified significant upregulation of miR-766-3p (Figure 6-35 B and Table 6-7).

#### 6.8.3.1 miR-766-3p in Angio II Stimulated Cells

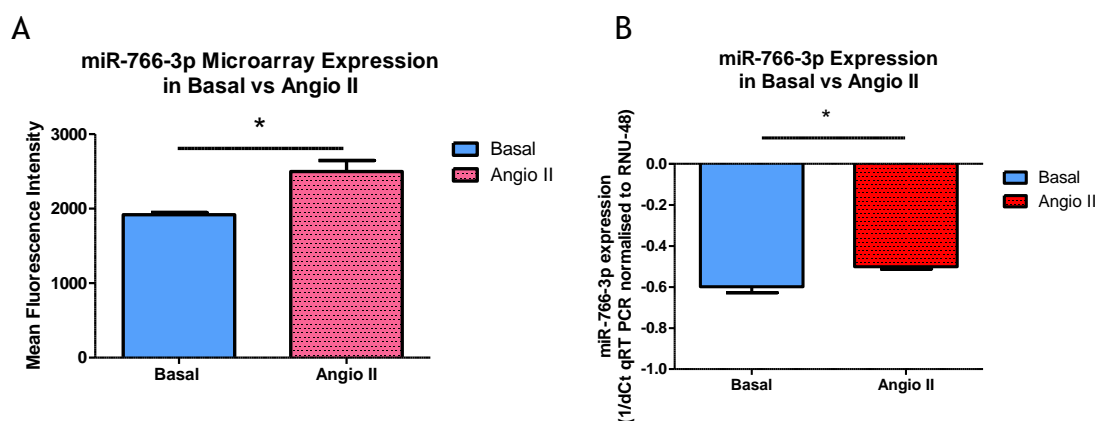


**Figure 6-35: Levels of miR-766-3p in basal vs Angio II-stimulated H295R cells (Strain 1) measured by (A) microarray (n= 3) and (B) realtime qRT-PCR (n= 5).**

\* indicates  $p < 0.05$ .

**Table 6-7: miRNA levels in Basal vs Angio II-stimulated H295R cells (Strain 1), analysed by realtime qRT-PCR.**

Ct= cycle threshold; ddCt= delta delta Ct; n= biological sample number; SD= standard deviation.

miRNA	n	Basal Mean Ct (SD)	Angio II Mean Ct (SD)	ddCt	Fold Change (Relative to basal= 1)	p-value
miR-766-3p	5	20.13 (0.14)	19.99 (0.26)	-0.31	1.24	0.01

### 6.8.3.2 miR-766-3p in dbcAMP Stimulated Cells

The upregulation of miR-766-3p in dbcAMP-stimulated cells could not be validated by realtime qRT-PCR (Figure 6-36; Table 6-8).

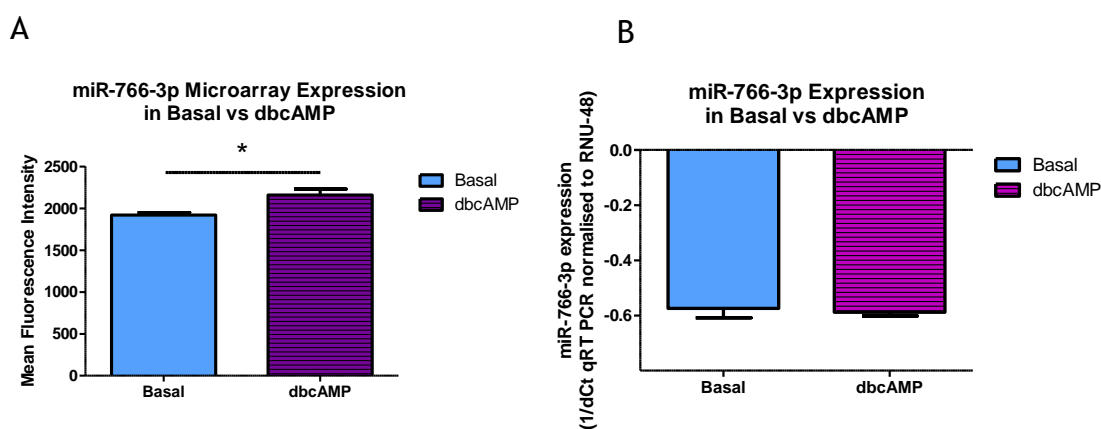


**Figure 6-36: Levels of miR-766-3p in Basal vs dbcAMP-stimulated H295R cells (Strain 1), as analysed by (A) microarray (n= 3) and (B) realtime qRT-PCR (n= 6).**  
\* indicates  $p < 0.05$ .

**Table 6-8: miRNA levels in basal vs dbcAMP-stimulated H295R cells (Strain 1), analysed by realtime qRT-PCR.**

Ct= cycle threshold; ddCt= delta delta Ct; n= biological sample number; SD= standard deviation.

miRNA	n	Basal Mean Ct (SD)	dbcAMP Mean Ct (SD)	ddCt	Fold Change (Relative to basal= 1)	p-value
miR-766-3p	6	20.09 (0.16)	20.08 (0.03)	0.07	0.95	0.56

### 6.8.3.3 miR-766-3p in KCl-Stimulated Cells

Levels of miR-766-3p also saw a significant increase following KCl stimulation when analysed by microarray (Figure 6-37 A) but, despite a trend towards increased levels when analysed by realtime RT-PCR, this change could not be validated by this method (Figure 6-37 B; Table 6-9).

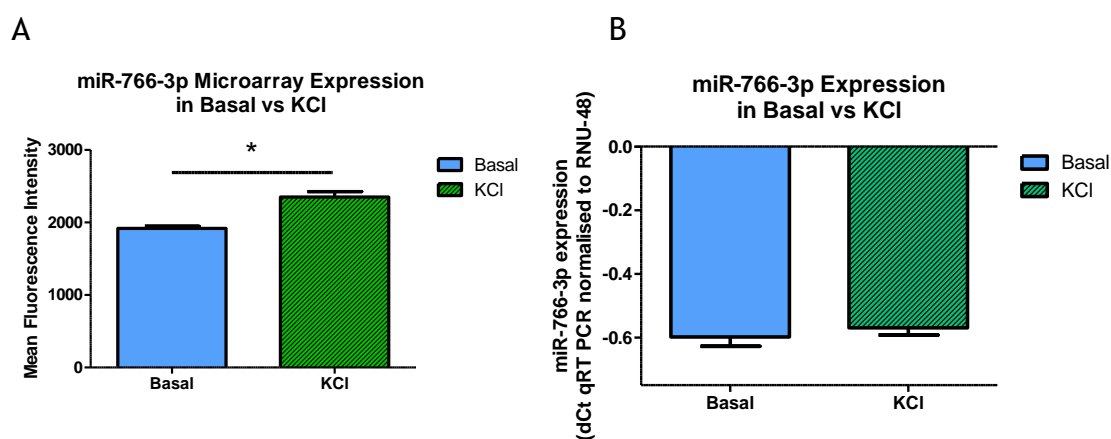


**Figure 6-37:** Levels of miR-766-3p in Basal vs KCl-stimulated H295R cells (Strain 1), as analysed by (A) microarray (n= 3) and (B) realtime RT-PCR (n= 6).

\* indicates p<0.05

**Table 6-9:** miRNA levels in Basal vs KCl-stimulated H295R cells (Strain 1), as analysed by realtime qRT-PCR.

Ct= cycle threshold; ddCt= delta delta Ct; n= biological sample number; SD= standard deviation.

miRNA	n	Basal Mean Ct (SD)	KCl Mean Ct (SD)	ddCt	Fold Change (Relative to basal=1)	p-value
miR-766-3p	6	20.09 (0.16)	20.08 (0.03)	0.07	0.95	0.56

#### 6.8.3.4 Validation of other miRNAs in Stimulated H295R Cells

miR-125a-5p as described previously, was significantly downregulated in dbcAMP-stimulated cells (Table 6-11) but not in other groups (Table 6-10 and Table 6-12). Other validated expressed miRNAs in the cells are miR-154-3p and miR-19a-3p, however no significant difference of these miRNAs was observed in basal vs stimulated cells, as shown in Table 6-10 and Table 6-12.

**Table 6-10: miRNA expression in Basal vs Angio II-stimulated cells (Strain 1).**

Ct= cycle threshold; ddCt= delta delta Ct; n= biological sample number; SD= standard deviation.

miRNA	n	Basal Mean Ct (SD)	Angio II Mean Ct (SD)	ddCt	Fold Change (Relative to basal= 1)	p- value
miR-125a-5p	6	19.87 (0.19)	20.01 (0.27)	0.06	0.96	0.62
mir-154-3p	6	25.66 (0.39)	25.74 (0.28)	-0.01	1.01	0.93
miR-19a-3p	6	25.43 (0.61)	25.60 (0.34)	0.03	0.98	0.76

**Table 6-11: miRNA expression in Basal vs dbcAMP-stimulated cells (Strain 1).**

Ct= cycle threshold; ddCt= delta delta Ct; n= biological sample number; SD= standard deviation.

miRNA	n	Basal Mean Ct (SD)	dbcAMP Mean Ct (SD)	ddCt	Fold Change (Relative to basal= 1)	p- value
miR-125a-5p	6	19.87 (0.19)	20.35 (0.10)	0.57	0.68	<0.01
mir-154-3p	6	25.66 (0.39)	25.65 (0.31)	0.07	0.95	0.66
miR-19a-3p	5	25.41 (0.64)	25.38(0.28)	0.03	0.98	0.92

**Table 6-12: miRNA expression in Basal vs KCl-stimulated cells (Strain 1).**

Ct= cycle threshold; ddCt= delta delta Ct; n= biological sample number; SD= standard deviation.

miRNA	n	Basal Mean Ct (SD)	KCl Mean Ct (SD)	ddCt	Fold Change (Relative to basal= 1)	p- value
miR-125a-5p	6	19.87 (0.19)	19.78 (0.18)	0.00	1.00	0.99
mir-154-3p	6	25.66 (0.39)	25.49 (0.13)	-0.09	1.07	0.62
miR-19a-3p	5	25.41 (0.64)	25.57 (0.21)	0.34	0.79	0.08

### 6.8.3.5 LDLR expression following miR-17 Transfection

In order to assess the effects of this significantly-altered miRNA on predicted target genes, H295R Strain 1 was transfected with pre-miR-17 for 24 hours, as described in Chapter 2, Section 2.3. A direct interaction between miR-17-5p and LDLR mRNA had been predicted by IPA. Following pre-miR-17 transfection, levels of this mRNA were found to be significantly reduced as shown in Figure 6-38 and Table 6-13.

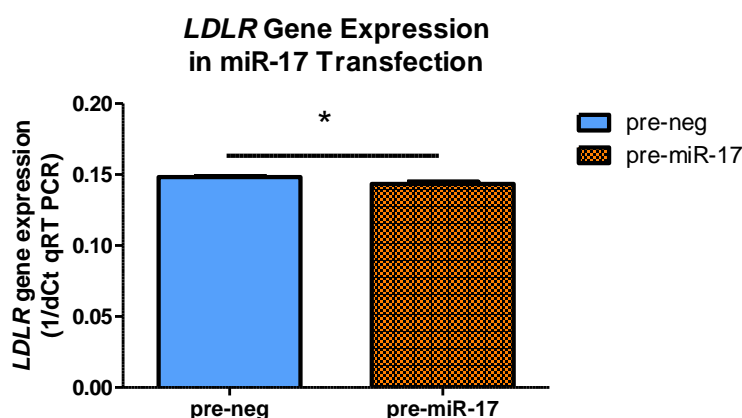


Figure 6-38: *LDLR* gene expression of H295R Strain 1 in pre-miR-17 transfection (n= 3). \* indicates p<0.05.

Table 6-13: *LDLR* mRNA levels following pre-miR-17 transfection of H295R cells (Strain 1), analysed by realtime qRT-PCR.

Ct= cycle threshold; ddCt= delta delta Ct; n= biological sample number; SD= standard deviation.

Gene	n	Pre-Neg Mean Ct (SD)	Pre-miRNA-17 Mean Ct (SD)	ddCt	Fold Change (Relative to basal= 1)	p-value
<i>LDLR</i>	3	26.08 (0.30)	26.46 (0.24)	0.23	0.85	0.04

## 6.9 Discussion

This chapter combined microarray, IPA analysis and further in vitro experimental work to analyse differences in miRNA expression between basal and stimulated cells (Angio II, dbcAMP and KCl), as measured by microarray analysis. This generated 3 lists of miRNAs significantly differentially expressed as a result of each type of stimulation (Figure 6-8 to Figure 6-10). Based on these patterns of expression, 7 miRNAs were found to be consistently altered throughout the 3 treatments. These 7 miRNAs were assembled into 2 main clusters as shown in Figure 6-11 and Figure 6-12. The 2 clusters were then cross-referenced with IPA analysis in order to construct a list of relevant mRNA targets and pathways that are predicted to be affected. Some of these miRNAs were validated by qRT PCR.

### 6.9.1 Microarray

Cross-referencing of miRNAs to mRNAs enabled identification of several predicted regulatory targets. IPA employs three levels of filter in its prediction of target: experimentally-validated target, high-confidence target and moderate-confidence target. These 3 levels of confidence are based on TargetScan, TarBase, miRecords, and the Ingenuity® Knowledge Base. The predicted targets are obtained by utilising the TargetScan algorithm which recognises the presence of conserved 8mers and 7mers that match the seed sequence of each miRNA. TarBase content identifies the target by miRNA/mRNA matching from Tarbase itself and miRBase identifiers. For experimentally-validated interactions, miRecords is used to ascertain identify these from published articles. Lastly, the Ingenuity® Knowledge Base is derived from thousands of manually-curated published articles by Ingenuity's own scientific experts.

miRNAs predicted to target *CYP11B2* include:

- miR-1275 and miR-4323 (basal vs Angio group, Figure 6-16)
- miR-125b-5p/miR-125a-5p, miR-1275, miR-647 and miR-766-3p (basal vs dbcAMP, Figure 6-17) miR-125b-5p/miR-125a-5p, miR-708-5p, miR-766-3p

miR-874-3p are predicted to bind to CYP11B2 (basal vs KCl group, Figure 6-18).

Of these, miR-125b-5p/miR-125a-5p and miR-766-3p are consistently expressed in a similar pattern across the 3 stimulations (i.e. downregulated in each stimulated group). Only miRNAs in the KCl group are predicted to target CYP11B1 (miR-874-3p) and CYP17A1 (miR-4730). CYP11B2 & CYP11B1 encode members of the cytochrome P450 superfamily of enzymes: namely aldosterone synthase and 11- $\beta$ -hydroxylase. They are the monooxygenase cytochrome P450 proteins located at the inner mitochondrial membrane, which catalyse various processes including cholesterol and steroid metabolism and drug metabolism. Mutation of CYP11B2 will cause corticosterone methyl oxidase deficiency and mutation of CYP11B1 will lead to congenital adrenal hyperplasia (due to 11- $\beta$ -hydroxylase deficiency). Another important gene in steroidogenesis is CYP17A1, which encodes 17 $\alpha$ -hydroxylase, important for the synthesis of mineralocorticoids, glucocorticoids, androgens, oestrogens and progestin. Mutation of this gene is associated with adrenal hyperplasia and 17- $\alpha$ -hydroxylase/17,20-lyase deficiency. In an experimentally validated study, miR-24 was shown to directly target the 3'UTR of CYP11B2 (Robertson, MacKenzie et al. 2013). In another study, miR-766 was shown to bind the 735G-allele at the 3'UTR of human CYP11B2; the transfection of miR-766 reduces human aldosterone synthase mRNA and protein level in adrenocortical cell lines. As there is known linkage disequilibrium between the A/G polymorphism at the 735 position and the single nucleotide polymorphism at -344, this might suggest that miR-766 downregulates human aldosterone synthase gene expression and reduces blood pressure in human subjects carrying the -344T allele (Maharjan, Mopidevi et al. 2014). miR-125a-5p and miR-125b-5p also has been shown to downregulate aldosterone synthase expression in pEZXR-reporter plasmid experiments (Stacy Wood 2011).

In the dbcAMP- and KCl-stimulated groups, 2 miRNAs are predicted to target HMGCR: miR-125b-5p/miR-125a-5p and miR-29b-3p. HMGCR is a rate-limiting enzyme for cholesterol synthesis regulated via a negative feedback mechanism controlled by sterols, the product of the reaction that it

catalyses. HMGCR is suppressed by cholesterol derived from the influx and degradation of low density lipoprotein (LDL) via the LDL receptor (LDLR). Competitive inhibitors of HMGCR increase liver LDLR, which in turn escalate the LDL plasma catabolism and decrease cholesterol concentration in circulation, a key factor of atherosclerosis. HMGCR aberrations may lead to cardiovascular disorder (e.g. coronary artery disease, myocardial infarction due to atherosclerosis formation) and stroke. It has been reported that mesangial cells produced aldosterone locally. Atorvastation, an HMGCR inhibitor intensely impaired the glucose, Angio II and LDL to aldosterone production. It is suggested that this mesangial endocrine system that produce local aldosterone might have therapeutic effect for diabetic nephropathy by the action of HMGCR inhibitor (Nishikawa, Matsuzawa et al. 2010). Therefore, inhibiting of HMGCR by miRNAs might have therapeutic effect on the abnormal aldosterone level.

There are a number of miRNAs that putatively bind *ABCA1*, in particular, miR-17-5p and miR-19b-3p/miR-19a-3p. Both of these miRNAs are derived from the same cluster. *ABCA1* (ATP-binding cassette, sub-family A, member 1) is from the superfamily of ATP-binding cassette (ABC) transporters. The protein transports cholesterol efflux in the cellular lipid removal pathway. The family of *ABC* genes is divided into seven distinct subfamilies (*ABCA1*, *MDR/TAP*, *MRP*, *ALD*, *OABP*, *GCN20* and *White*). Abnormalities in the *ABCA1* gene are associated with Tangier's disease and familial high-density lipoprotein deficiency. In an animal experimental study, it was shown that mouse *ABCA1* protein increased expression of *HMGCR* mRNA in the liver (Basso, Freeman et al. 2003).

miR-19a-3p and miR-17-5p are predicted to target *LDLR*. The *LDLR* (low density lipoprotein receptor) gene encodes cell surface proteins for receptor-mediated endocytosis. Low density lipoprotein (LDL) is normally bound to the receptor and taken into the cell. The protein is degraded by the lysosome and free cholesterol is made available for downregulation of the microsomal enzyme HMGCR, the rate-limiting step in cholesterol synthesis. Simultaneously, a reciprocal upregulation of cholesterol ester synthesis occurs. *LDLR* mutation is related to familial hypercholesterolemia.

LDLR abnormalities have been associated with atherosclerosis, obesity, hypercholesterolemia, hyperglycaemia, and insulin resistance.

## 6.9.2 Validation

**Table 6-14: miRNA expression in microarray and qRT PCR.**

Down= downregulated, Up= upregulated, \*= p value < 0.05.

miRNA	Microarray			qRT PCR		
	Angio II	dbcAMP	KCl	Angio II	dbcAMP	KCl
miR-17-5p	Down*	Down*	Down*	Down	Down	Down*
miR-154-3p	Down*	Down*	Down*	Down	Down	Down
miR-19a-3p	Down*	Down*	Down*	Down	Down	Down
miR-20b-5p	Down*	Down*	Down*	Down	Down	Down*
miR-766-3p	Up*	Up*	Up*	Up*	Down	Down

Validation of miRNAs of interest identified in the microarray study (Basal vs stimulated cells) was done by qRT PCR. These miRNAs were: miR-17-5p, miR-154, miR19a-3p, miR-20b-3p and miR-766-3p. miR-17-5p; each was consistently downregulated throughout the stimulation in microarray analysis. The expression was validated and only KCl caused a significant difference of expression. miR-17-5p belongs to Cluster 17-92. The primer for SYBR Green assay of miR-17-5p is similar to miR-106a-5p. Therefore, further analysis should be carried out to determine the real effect of gene expression by miR-17-5p. Interestingly, IPA analysis revealed that both miR-17-5p and miR-20a-5p shared the same seed sequence in target mRNA (see Table 8-11, Appendix). This is not so surprising as cluster mir-17/miR-19a (located at chr 13q31.3) is a paralogue cluster to miR-106a/ miR-20b (chr Xq26.2) (Mogilyansky 2013).

miR-17-5p is predicted by IPA to target LDLR and this effect was confirmed by qRT-PCR. LDLR is a vital transport mechanism for intracellular cholesterol homeostasis. Cholesterol is the main substrate of steroidogenesis, so targeting LDLR may reduce the level of cholesterol in the cytoplasm leading

to an effect on steroid secretion. No previous study has established the effect of LDLR level on aldosterone production intracellularly. However, miR-17-92 is widely expressed in various cancers and is known as the first 'oncomir' (He, Thomson et al. 2005). miR-17 and its cluster are also known for their role in suppressing proapoptotic genes E2F1 (O'Donnell, Wentzel et al. 2005, Petrocca, Visone et al. 2008). Interestingly, in studying miRNA expression in human aging, miR-17, miR-106, miR-19b and miR-20a were each reported to be downregulated in cell aging models (CD8(+) T cells, renal proximal tubular epithelial cells and fibroblast of skin) (Hackl, Brunner et al. 2010). miR-17-p and mir-106a also were reported to be involved in promoting adipogenesis and inhibiting osteogenesis by targeting BMP2 (Li, Li et al. 2013).

miR-20b-5p, like miR-17-5p, was consistently downregulated by all 3 stimulations of H295R cells *in vitro*, but qRT-PCR validation only achieved significance during KCl stimulation. From the IPA database, mir-20b-5p shares a similar seed sequence with mir-17-5p, miR-106a-5p and other miRNAs, as shown in Table 8-11 (Despite sharing similar seed sequences, the PCR primers used for amplification of mir-20b-5p differs from that for miR-17-5p). In human oral squamous carcinoma cells (clone E10), exogenous miR-20b downregulated cell proliferation by 50% (Khuu, Jevnaker et al. 2014). Interestingly, miR-20b, along with miR-21 and miR-24, has been found to be downregulated in the plasma of patients with Type 2 Diabetes Mellitus (Zampetaki, Kiechl et al. 2010). In LCC9 cells, mir-20b is upregulated compared to LCC1 and MCF7 (Mulrane, Terrile et al. 2013). LCC9 is derived from LCC1 (which is derived from MCF7), is completely oestrogen independent and exhibits resistance to fulvestrant and tamoxifen. However, LCC1 and MCF7 (derived from breast cancer cell line) are sensitive to tamoxifen (block oestrogen action) and fulvestrant (selective oestrogen receptor degrader) (Skerry Benjamin James Oliver 2013).

Again, miR-766-3p was consistently upregulated by all three stimulations according to microarray analysis (Basal vs stimulated cells). The upregulation pattern was confirmed by qRT-PCR for Angio II ( $p < 0.05$ ) but not dbcAMP or KCl treatment. In another study, expression of miR-766 was downregulated

in tumour-associated macrophage gastrointestinal cancer compared to normal gastrointestinal cells (Sugihara, Ishimoto et al. 2013). A study on microarray expression comparing a normal bladder cell line (SV-HUC-1) and bladder cancer cell lines revealed that miR-766 was downregulated in cancer cell lines ((Ueno, Hirata et al. 2012).

Microarray is known for its sensitivity and fast generation of large amounts of data, requiring minimal RNA relative to other techniques e.g. Northern Blotting. As microarray is not a 'gold standard' quantitative method, qRT-PCR is extensively employed to validate its key findings with greater confidence (Klein 2002). Many of the significant changes observed by microarray in the previous chapter could not be subsequently validated by qRT-PCR. There are several possible reasons for this, one of which may be insufficient power in the replication study i.e. a greater number of experimental replicates may have been required to identify significant changes between the basal and treatment groups for a qRT-PCR study. Although power calculations may have helped to identify this problem in advance, this would have required prior knowledge of the true size of expression change (if any), which was the aim of the experiment itself. The decision to use the group size employed here was based on previous studies which had been able to identify significant changes in this cell type. Another possible reason for the disparity between microarray and qRT-PCR results involves the RNA samples used. Although subjected to the same experimental conditions, the RNA samples analysed for microarray were different to those used for qRT-PCR, and were sourced from a different batch of H295R cells. The use of different batches of cells, or carry-over of contaminating factors from RNA isolation (e.g phenol, alcohol, airborne contamination) can cause adverse effect to RNA analyses (Freeman, Walker et al. 1999). Moreover, it has been reported that different efficiencies of cDNA production via reverse transcriptase method can also affect findings between qRT-PCR and microarray experiments (Freeman, Walker et al. 1999). On the other hand, qRT-PCR may also give rise to spurious results through the introduction of exponential amplification error (Freeman, Walker et al. 1999), mispriming and formation of primers dimers (Bustin 2002). However, it should be noted that primer dimers were excluded from

any realtime qRT-PCR analysis in the present study and good laboratory method aimed to reduce and, where possible, identify other errors through the use of control reactions, etc.

## 6.10 Conclusions

The microarray data presented in this chapter provide the first analysis of miRNA profiles in H295R cells following 3 types of stimulation (Angio II, dbcAMP and KCl). This revealed two main clusters, miR-17/19b and miR-106a/20b, to be consistently downregulated during all 3 stimulations. Many previous studies have linked miR-17/19b with tumour formation but this is the first study relating this cluster to the adrenal cortex. Using IPA, it also presents evidence and possible mechanisms by which the two miRNAs might act in several relevant canonical pathways.

Regardless of the reasons for inconsistent findings between the microarray and realtime qRT-PCR analyses (which are widely recognised and largely attributable to the semi-quantitative nature of microarray analysis), this study has validated certain key effects. This includes the fact that certain miRNAs are consistently altered across all 3 stimulations, and that one such miRNA inhibits the expression of *LDLR*, a gene relevant to steroidogenesis through its participation in cholesterol biosynthesis. The remaining 3 miRNAs showed no significant changes in quantity with the exception, of miR-125a-5p, which responded to dbcAMP, as shown in the previous chapter.

## **7 General Discussion**

Hypertension is the key risk factor for cardiovascular morbidity and mortality around the world. Abnormal levels of both systolic and diastolic blood pressure can cause adverse effects to heart, brain, kidney and other vital organs although most hypertensive cases are absent of symptoms. Despite the unknown aetiology of primary hypertension (PH), secondary hypertension offers a more definite causative root. Primary aldosteronism (PA) is the main cause of secondary hypertension (Scholl and Lifton 2013), with studies showing patients with PA have increased rates of cardiovascular events relative to PH patients of the same blood pressure (Milliez, Girerd et al. 2005). Approximately 15% of PA cases result from unilateral aldosterone producing adenoma (APA) (Ye, Mariniello et al. 2007). Therefore, I conducted studies into APA and the mechanisms by which microRNA might regulate its pathology. This involved miRNA profiling of APA and normal adrenal tissue followed by bioinformatic prediction of possible effects, several of which were validated by in vitro experiment. A similar study was then conducted that examined changes to the miRNA profile of H295R adrenocortical cells following stimulation of aldosterone production.

Microarray is a powerful tool for molecular study, capable of analysing expression of thousands of RNAs from multiple samples simultaneously. Many microarray studies have been implemented for cancer profiling (i.e. cancer vs non cancer), cancer stratification (i.e. carcinoma vs benign) or evaluation of tumour progression (i.e. early stage carcinoma vs late stage carcinoma) and assessment of tumour post-treatment (Giuseppe Russo 2003).

In this study, total RNA samples from APA and NA were collected from formalin-fixed paraffin-embedded (FFPE) and frozen tissue (Wood, M.MacKenzie et al. 2011). Frozen tissue samples have been described as having better RNA and protein integrity compared to FFPE and many antibodies that work in frozen tissues do not respond well in FFPE (Giuseppe Russo 2003). Furthermore, utilising small specimen for microarray analysis has raised questions whether the sample truly represents the entire tumour's gene expression. However, this technique can be improved by including multiple tissues punches for every sample in the microarray studies (Sallinen, Sallinen et al. 2000, Hoos, Urist et al. 2001). In my study, the adrenal and APA samples contain non-homogenous cell populations, therefore the miRNA detected in microarray studies are unlikely to represent

zone-specific expression. However, this can be improved by having zone-specific dissection and further qRT-PCR validation for the miRNA and mRNA expression. The quantitative limitations of microarray are well known, hence the need to validate significant changes in miRNA quantity by other methods, such as qRT-PCR. It should be noted that several such changes identified by microarray did not emerge as significant when a more accurate quantitative method was used, so such findings should always be treated with caution. It may be that microarray has now been overtaken as the prime method for such analysis by RNA sequencing (RNAseq), which has the advantage of being more truly quantitative and of being able to identify novel transcripts, unlike microarray which is limited to known molecules represented on the chip. As the previously prohibitive costs of RNAseq continue to fall, it will probably become the main method employed for such studies.

In spite of its limitations, in this study microarray was able to identify several significant changes in miRNA levels that were verified by qRT-PCR validation. It is also striking that certain changes in miRNA levels between APA and NA were also apparent in H295R cells following stimulation of aldosterone secretion (Figure 7-1). This may point to common mechanisms between the pathology of APA, with its raised aldosterone secretion, and the normal physiology of aldosterone regulation. It also points to a regulatory role for microRNAs in these mechanisms. In light of these findings, it seemed logical to investigate plausible targets of these dysregulated miRNAs that could be relevant to aldosterone biosynthesis and/or APA pathology.

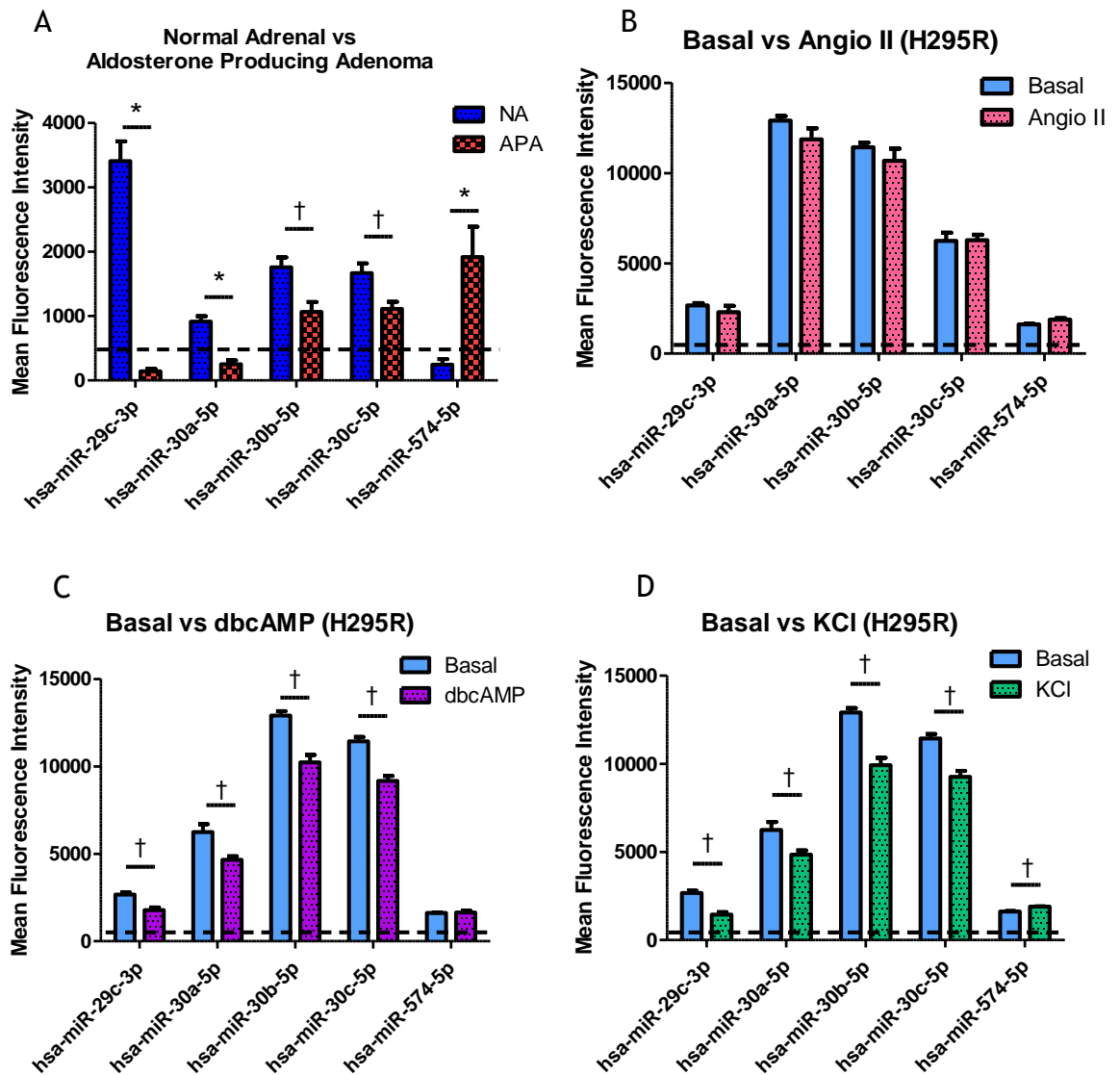


**Figure 7-1: Consistent miRNA expression in adrenal tissues; NA vs APA (A) and in H295R cell line; basal vs Angio II (B), basal vs dbcAMP (C) and basal vs KCl (D).**

The dotted line indicates the detection cut-off point of 500 AU ( $n=4$  in adrenal tissues and  $n=3$  in each group of stimulation of H295R cell line). \*miRNAs > 500 AU in NA or APA; †miRNAs present in both tissues/ both basal and stimulated cells ( $p<0.05$ ).

Within the evolving field of miRNA research, which depends on various quantitative techniques and predictive tools for target identification, a strong and reliable apparatus is needed to identify the most relevant biological target and pathways. Ingenuity Pathway Analysis supports such research by providing several tools e.g. miRNA Target Filter, which prioritises relevant miRNAs and mRNA targets. Furthermore, IPA is able to identify significant network and canonical pathways associated with the differentially expressed miRNA and targeted mRNA (Jiménez-Marín, Collado-Romero et al. 2009). IPA uses a manually curated non-public bibliographic database, which confers the ability to classify genes implicated in specific functions or diseases. For example, in this

study, it linked differentially-expressed miRNAs in stimulated H295R cells to the *LDLR* and *HMGCR* genes involved in cholesterol regulation. However, a downside of IPA is its bias towards cardiovascular and cancer mechanisms and pathways relative to other areas, such as endocrine disorders; this is a reflection of the overall bias in the research literature. Its manually-curated method for journal selection also limits its ability to deliver truly up to date findings, with an inevitable lag between publication of findings and its inclusion in the IPA database. For these reasons, IPA must be used with caution and a great deal of effort must be taken by the user to ensure that findings are properly filtered, are of physiological relevance and have a better than random level of actually occurring in a biological system. Nevertheless, IPA has provided several interesting findings for further study, in addition to the more obvious pathways.

Clearly, the most obvious initial place to examine the impact of miRNAs in APA is the steroidogenic pathway. The *CYP11B2* gene, encoding aldosterone synthase, is at the endpoint of this pathway. miR-125a-5p is upregulated in NA compared to APA and it is hypothesised that miR-125a-5p inhibits expression of *CYP11B2*, according to IPA. This finding is further supported by downregulation of *CYP11B2* following transfection of H295R cells with miR-125a-5p precursor mimic. Moreover, in a previous pEZX-reporter plasmid study, miR-125a-5p repressed *CYP11B2* by directly targeting the 3'UTR (Stacy Wood 2011), providing the first direct evidence that miRNA may have a significant role in aldosterone biosynthesis.

Using IPA to identify other pathways, cholesterol handling emerged as one of the key systems likely to be regulated at various points and by several of the differentially-expressed miRNAs. A high level of LDL is an established risk factor for atherosclerosis, the underlying aetiology of cerebrovascular disease and coronary heart syndrome. Statins are the most effective drugs in reducing circulating LDL, decreasing risk of stroke and cardiac events (Grundy 1998) by inhibiting *HMGCR*, the rate-limiting enzyme in production of cholesterol. This decreases intracellular sterol levels and reduces transport of the SCAP-SREB complex from endoplasmic reticulum (ER) to Golgi. Subsequently, it increases *LDLR* expression, transporting circulating LDL into cells (hepatocytes) and thereby downregulating blood LDL levels. One study characterized a new class

of compound that reduces cholesterol level *in vivo* by upregulating *LDLR* through direct action on the SCAP-SREB complex in a hamster model (Grand-Perret, Bouillot et al. 2001). The compound reduced LDL and triglycerides by up to 80% and increased *LDLR* mRNA in the liver. From the perspective of the current study, it is interesting to note the interplay of *LDLR* and *HMGCR* expression in determining circulating cholesterol levels.

If cholesterol levels can be regulated in this way, does this necessarily translate into significant changes in steroid biosynthesis? It has been assumed for many years that cholesterol supply was unimportant in determining steroid secretion as the rate-limiting stages of the process occurred further down the chain, either with the supply of cholesterol by StAR, or with the catalytic turnover of such enzymes as aldosterone synthase. Now, however, a different story is emerging. Baudrand et al recently reported that the HMGCR blockers statins effectively reduce aldosterone levels in hypertensive and diabetic subjects; interestingly, no similar cortisol suppression was observed (Baudrand, Pojoga et al. 2015). This finding is supported by a previous study showing that simvastatin treatment in hyperlipidaemic postmenopausal women also results in significant plasma aldosterone suppression but no changes in cortisol (Ide, Fujiya et al. 1990). Furthermore, Dahl rats fed with a high salt diet and treated with simvastatin showed significant suppression of aldosterone (Bayorh, Ganafa et al. 2005). A placebo-control study has also been conducted on men with hypercholesterolemia, with one group being treated with a high dose of simvastatin (80 mg). After 12 weeks, no changes in cortisol were observed in treated patients (Dobs, Schrott et al. 2000). Therefore, these studies appear to support the idea that changes in the handling and supply of cholesterol - through a pathway involving HMGCR - can result in significant effects on aldosterone secretion.

If miRNAs are significant regulators of cholesterol, could their clinical actions be countered directly *in vivo*? Results from clinical trials of miRNA-related therapies suggest this is a possibility. miR-122 antagonist (Miravirsen) was introduced for phase II clinical trial in hepatitis C patients in an attempt to counter the properties of miR-122, which binds the HCV genome and protects it from degradation. Miravirsen act as specific miR-122 blocker and was shown to

effectively reduce HCV replication in vivo (Lanford, Hildebrandt-Eriksen et al. 2010, Janssen, Reesink et al. 2013). Another clinical trial involved miRNA-related treatment of liver carcinoma (Christoph 2013). MRX-34, a miR-34a mimic has a tumour suppressor function, increasing G1 cell cycle arrest and participating in the p53 tumour suppressor pathway. Such studies suggest miRNAs could have a promising therapeutic future.

Future studies should explore the miRNA-mediated effects identified here, in order to verify that these result in actual changes to the proteins themselves, and to confirm their mechanism and physiological impact. It would also be valuable to repeat the H295R studies (possibly using the now-cheaper RNAseq rather than microarray), but this time simultaneously measuring mRNA levels as well as miRNA. This direct comparison of miRNA and mRNA in the same samples would be far more powerful than simply analysing miRNA alone, and would allow much more powerful analytical functions of the IPA software to be used.

To conclude, in this thesis I have presented several novel findings demonstrating differential expression of certain adrenocortical miRNAs in physiological and pathophysiological conditions. Furthermore, with the aid of bioinformatic prediction and in vitro validation, I have shown that certain of these miRNAs have direct regulatory effects on key genes relevant to these systems, including *CYP11B2* and *HMGCR*. Key miRNAs are significantly downregulated in APA tissues. It is hypothesized that reduced levels of these miRNAs may 'de-repress' expression of *HMGCR*, resulting in increased cholesterol synthesis which, in turn, would feed through into increased steroidogenesis.

So, while these findings add to the small but growing body of evidence that miRNAs have a significant regulatory effect on corticosteroidogenesis through direct targeting of steroidogenic mRNAs, the influence of these miRNAs on availability of cholesterol - the vital substrate for all steroid production - is also apparent. Given that cholesterol supply is emerging as an important regulatory factor in corticosteroidogenesis, it may be that this study has uncovered a key mechanism that could be exploited in order to treat the consequences of dysregulated corticosteroid production.

## **8 Appendix**

**Table 8-1: Highly expressed miRNAs in NA (mir-10a to miR-195).**  
Based on miRBase Database Release 21: June 2014.

microRNA (previous ID)	microRNA (latest ID)	Sequence	Chromosome Location	Cluster	Other microRNA within cluster	Start Co- ordinates	End Co- ordinates
<b>hsa-mir-10a</b>	hsa-miR-10a- 5p	UACCCUGUAGAUCCGAAUUUGUG	17	No		48579838	48579947
<b>hsa-miR-125a</b>	hsa-miR-125a- 5p	UCCCUGAGACCCUUUAACCUGUGA	19	Yes	hsa-miR-125a	51693254	51693339
					hsa-let-7e	51692786	51692864
					hsa-miR-99b	51692612	51692681
<b>hsa-miR-126</b>	hsa-miR-126- 3p	UCGUACCGUGAGUAAUAAUGCG	9	No	-	136670602	136670686
<b>hsa-miR-139</b>	hsa-miR-139- 5p	UCUACAGUGCACGUGUCUCCAGU	11	No		72615063	72615130
<b>hsa-miR-148a</b>	hsa-miR-148a- 3p	UCAGUGCACUACAGAACUUUGU	7	No	-	25949919	25949986
<b>hsa-miR-15a</b>	hsa-miR-15a- 5p	UAGCAGCACAUAAUGGUUUGUG	13	Yes	hsa-miR-15a	50049119	50049201
					hsa-mir-16-1	50048973	50049061
<b>hsa-miR-195</b>	hsa-miR-195- 5p	UAGCAGCACAGAAAUAUUGGC	17	Yes	hsa-miR-195	7017615	7017701
					hsa-mir-497	7017911	7018022

**Table 8-2: Highly expressed miRNAs in NA (mir-202\* to miR-29c).**  
Based on miRBase Database Release 21: June 2014.

microRNA (previous ID)	microRNA (latest ID)	Sequence	Chromosome Location	Cluster	Other microRNA within cluster	Start Co-ordinates	End Co-ordinates
<b>hsa-miR-202*</b>	hsa-miR-202-5p	UUCCUAUGCAUUAUCUUCUUUG	10	No	-	133247511	133247620
<b>hsa-miR-21</b>	hsa-miR-21-5p	UAGCUUAUCAGACUGAUGUUGA	17	No	-	59841266	59841337
<b>hsa-miR-24</b>	hsa-miR-24-3p	UGGCUCAGUUCAGCAGGAACAG	19	Yes	hsa-mir-24-2 loop	13836287	13836359
					hsa-mir-23a	13836587	13836659
					hsa-mir-27a	13836440	13836517
			9	Yes	hsa-mir-24-1 loop	95086021	95086088
					hsa-mir-23b	95085208	95085304
					hsa-mir-27b	95085445	95085541
					hsa-mir-3074	95086014	95086094
<b>hsa-miR-26b</b>	hsa-miR-26b-5p	UUCAAGUAAUUCAGGAUAGGU	2	No	-	218402646	218402722
<b>hsa-miR-27a</b>	hsa-miR-27a-3p	UUCACAGUGGCUAAGUCCGC	19	Yes	hsa-miR-27a	13836440	13836517
					hsa-mir-23a	13836587	13836659
					hsa-mir-24-2	13836287	13836359
<b>hsa-miR-27b</b>	hsa-miR-27b-3p	UUCACAGUGGCUAAGUUCUGC	9	Yes	hsa-miR-27b	95085445	95085541
					hsa-mir-23b	95085208	95085304
					hsa-mir-24-1	95086021	95086088
					hsa-mir-3074	95086014	95086094
<b>hsa-miR-29a</b>	hsa-miR-29a-3p	UAGCACCAUCUGAAAUCGGUUA	7	Yes	hsa-miR-29a	130876747	130876810
					hsa-mir-29b-1	130877459	130877539
<b>hsa-miR-29b</b>	hsa-miR-29b-3p	UAGCACCAUUUGAAAUCAGUGUU	7	Yes	hsa-mir-29b-1 loop	130877459	130877539
					hsa-mir-29a	130876747	130876810
			1	Yes	hsa-mir-29b-2 loop	207802443	207802523
					hsa-mir-29c	207801852	207801939
<b>hsa-miR-29c</b>	hsa-miR-29c-3p	UAGCACCAUUUGAAAUCGGUUA	1	Yes	hsa-miR-29c	207801852	207801939
					hsa-mir-29b-2	207802443	207802523

**Table 8-3: Highly expressed miRNAs in NA (mir-30a to miR-376c).**  
Based on miRBase Database Release 21: June 2014.

microRNA (previous ID)	microRNA (latest ID)	Sequence	Chromosome Location	Cluster	Other microRNA within cluster	Start Co-ordinates	End Co-ordinates
<b>hsa-miR-30a</b>	hsa-miR-30a-5p	UGUAAACAUCCUCGACUGGAAG	6	No	-	71403551	71403621
<b>hsa-miR-30b</b>	hsa-miR-30b-5p	UGUAAACAUCCUACACUCAGCU	8	Yes	hsa-miR-30b	134800520	134800607
					hsa-miR-30d	134804876	134804945
<b>hsa-miR-30c</b>	hsa-miR-30c-5p	UGUAAACAUCCUACACUCAGC	6	No	hsa-mir-30c-2 loop	71376960	71377031
			1	Yes	hsa-mir-30c-1 loop	40757284	40757372
					hsa-mir-30e	40754355	40754446
<b>hsa-miR-335</b>	hsa-miR-335-5p	UCAAGAGCAAUACGAAAAAUGU	7	No	-	130496111	130496204
<b>hsa-mir-376c</b>	hsa-miR-376c-3p	AACAUAGAGGAAAUUCCACGU	14	Yes	hsa-mir-376c	101039690	101039755
					hsa-mir-1193	101030052-	101030129
					hsa-mir-1185-1	101042977	101043062
					hsa-mir-1185-2	101044198	101044283
					hsa-mir-300	101041363	101041445
					hsa-mir-376a-1	101040782	101040849
					hsa-mir-376a-2	101040069	101040148
					hsa-mir-376b	101040436-	101040535
					hsa-mir-381	101045920	101045994
					hsa-mir-487b	101046455	101046538
					hsa-mir-495	101033755	101033836
					hsa-mir-539	101047321	101047398
					hsa-mir-543	101031987	101032064
					hsa-mir-544a	101048658	101048748
					hsa-mir-654	101040219-	101040299
					hsa-mir-655	101049550	101049646
					hsa-mir-889	101047901	101047979

**Table 8-4: Highly expressed miRNAs in NA (mir-376 to miR-424).**  
Based on miRBase Database Release 21: June 2014.

microRNA (previous ID)	microRNA (latest ID)	Sequence	Chromosome Location	Cluster	Other microRNA within cluster	Start Co- ordinates	End Co- ordinates
<b>hsa-miR-379</b>	hsa-miR-379-5p	UGGUAGACUAUGGAACGUAGG	14	Yes	hsa-miR-379	101022066	101022132
					hsa-mir-1193	101030052	101030129
					hsa-mir-1197	101025564	101025651
					hsa-mir-299	101023794	101023856
					hsa-mir-323a	101025732	101025817
					hsa-mir-329-1	101026785	101026864
					hsa-mir-329-2	101027100	101027183
					hsa-mir-380	101025017	101025077
					hsa-mir-411	101023325	101023420
					hsa-mir-494	101029634	101029714
<b>hsa-miR-424</b>	hsa-miR-424-5p	CAGCAGCAAUUCAUGUUUUGAA	X	Yes	hsa-miR-424	134546614	134546711
					hsa-mir-450a-1	134540341	134540431
					hsa-mir-450a-2	134540508	134540607
					hsa-mir-450b	134540185	134540262
					hsa-mir-503	134546328	134546398
					hsa-mir-542	134541341	134541437

**Table 8-5: Highly expressed miRNAs in APA (let-7a to let-7d).**  
Based on miRBase Database Release 21: June 2014.

microRNA (previous ID)	microRNA (latest ID)	Sequence	Chromosome Location	Cluster	Other microRNA within cluster	Start Co-ordinates	End Co-ordinates
<b>hsa-let-7a</b>	hsa-let-7a-5p	UGAGGUAGUAGGUUGUAUAGUU	9	Yes	hsa-let-7a-1 loop	94175957	94176036
					hsa-let-7d	94178834	94178920
					hsa-let-7f-1	94176347	94176433
			11	Yes	hsa-let-7a-2 loop	122146522	122146593
					hsa-mir-100	122152229	122152308
					22	Yes	hsa-let-7a-3 loop
hsa-let-7b	46113686	46113768					
hsa-mir-4763	46113566	46113657					
<b>hsa-let-7b</b>	hsa-let-7b-5p	UGAGGUAGUAGGUUGUGUGGUU	22	Yes	hsa-let-7b	46113686	46113768
					hsa-let-7a-3	46112749	46112822
					hsa-mir-4763	46113566	46113657
<b>hsa-let-7c</b>	hsa-let-7c	UGAGGUAGUAGGUUGUAUGGUU	21	Yes	hsa-mir-99a	16539828-	16539911
					hsa-mir-99a	16539089-	16539169
<b>hsa-let-7d</b>	hsa-let-7d-5p	AGAGGUAGUAGGUUGCAUAGUU	9	Yes	hsa-let-7a-1	94175957	94176036
					hsa-let-7f-1	94176347	94176433

**Table 8-6: Highly expressed miRNAs in APA (miR-103 to miR-149\*).**  
Based on miRBase Database Release 21: June 2014.

microRNA (previous ID)	microRNA (latest ID)	Sequence	Chromosome Location	Cluster	Other microRNA within cluster	Start Co-ordinates	End Co-ordinates
<b>hsa-miR-103</b>	hsa-miR-103a-3p	AGCAGCAUUGUACAGGGCUAUGA	20	Yes	hsa-mir-103a-2 loop	3917494	3917571
						hsa-mir-103b-2	3917502
			5	Yes	hsa-mir-103a-1 loop	168560896	168560973
						hsa-mir-103b-1	168560904
<b>hsa-miR-107</b>	hsa-miR-107	AGCAGCAUUGUACAGGGCUAUGA	10	No	-	89592747	89592827
<b>hsa-miR-122</b>	hsa-miR-122-5p	UGGAGUGUGACAAUGGUGUUUG	18	Yes	hsa-miR-122	58451074	58451158
<b>hsa-miR-134</b>	hsa-miR-134-5p	UGUGACUGGUUGACCAGAGGGG	14	Yes	hsa-mir-3591	58451080-	58451152
					hsa-miR-134	101054687	101054759
					hsa-mir-154	101059755	101059838
					hsa-mir-323b	101056219	101056300
					hsa-mir-377	101062050	101062118
					hsa-mir-381	101045920	101045994
					hsa-mir-382	101054306	101054381
					hsa-mir-485	101055419	101055491
					hsa-mir-487a	101052446	101052525
					hsa-mir-487b	101046455	101046538
					hsa-mir-496	101060573-	101060674
					hsa-mir-539	101047321	101047398
					hsa-mir-541	101064495	101064578
					hsa-mir-544a	101048658	101048748
hsa-mir-655	101049550	101049646					
hsa-mir-668	101055258	101055323					
hsa-mir-889	101047901	101047979					
<b>hsa-miR-140</b>	hsa-miR-140-3p	UACCACAGGGUAGAACCACGG	16	No		69933081	69933180
<b>hsa-miR-149*</b>	hsa-miR-149-3p	AGGGAGGGACGGGGCUGUGC	2	No		240456001	240456089

**Table 8-7: Highly expressed miRNAs in APA (miR-320a to miR-382).**  
Based on miRBase Database Release 21: June 2014.

microRNA (previous ID)	microRNA (latest ID)	Sequence	Chromosome Location	Cluster	Other microRNA within cluster	Start Co-ordinates	End Co-ordinates
<b>hsa-miR-320</b>	hsa-miR-320a	AAAAGCUGGGUUGAGAGGGCGA	8	No		22244962	22245043
<b>hsa-miR-34a</b>	hsa-miR-34a-5p	UGGCAGUGUCUUAGCUGGUUGU	1	No		9151668	9151777
<b>hsa-miR-34c-3p</b>	hsa-miR-34c-3p	AAUCACUAACCACACGGCCAGG	11	Yes	hsa-miR-34c-3p	111513439	111513515
					hsa-mir-34b	111512938	111513021
<b>hsa-miR-361</b>	hsa-miR-361-5p	UUAUCAGAAUCUCCAGGGGUAC	X	No		85903636	85903707
<b>hsa-miR-375</b>	hsa-mir-375	UUUGUUCGUUCGGCUCGCGUGA	2	No		219001645	219001708
<b>hsa-miR-382</b>	hsa-miR-382-5p	GAAGUUGUUCGUGGUGGAUUCG	14	Yes	hsa-miR-382	101054306-	101054381
					hsa-miR-134	101054687	101054759
					hsa-mir-154	101059755	101059838
					hsa-mir-323b	101056219	101056300
					hsa-mir-377	101062050	101062118
					hsa-mir-381	101045920	101045994
					hsa-mir-382	101054306	101054381
					hsa-mir-485	101055419	101055491
					hsa-mir-487a	101052446	101052525
					hsa-mir-487b	101046455	101046538
					hsa-mir-496	101060573-	101060674
					hsa-mir-539	101047321	101047398
					hsa-mir-544a	101048658	101048748
					hsa-mir-655	101049550	101049646
					hsa-mir-668	101055258	101055323
					hsa-mir-889	101047901	101047979

**Table 8-8: Highly expressed miRNAs in APA (miR-432 to miR-483-5p).**  
Based on miRBase Database Release 21: June 2014.

microRNA (previous ID)	microRNA (latest ID)	Sequence	Chromosome Location	Cluster	Other microRNA within cluster	Start Co- ordinates	End Co- ordinates
<b>hsa-miR-432</b>		UCUUGGAGUAGGUCAUUGGGU GG	14	Yes	hsa-miR-432	100884483	100884576
					hsa-mir-337	100874493	100874585
					hsa-mir-665	100875033	100875104
					hsa-mir-431	100881007	100881120
					hsa-mir-433	100881886	100881978
					hsa-mir-127	100882979	100883075
					hsa-mir-136	100884702	100884783
<b>hsa-miR-451</b>	hsa-miR-451a	AAACCGUUACCAUUCUGAGUU	17	Yes	hsa-miR-451	28861369	28861440
					hsa-mir-144	28861533	28861618
					hsa-mir-451b	28861371	28861438
					hsa-mir-4732	28861655	28861730
<b>hsa-miR-483-5p</b>	hsa-miR-483-5p	AAGACGGGAGGAAAGAAGGGA G	11	No		2134134	2134209

**Table 8-9: Highly expressed miRNAs in APA (miR-509 to miR-574-5p).**

Based on miRBase Database Release 21: June 2014.

microRNA (previous ID)	microRNA (latest ID)	Sequence	Chromosome Location	Cluster	Other microRNA within cluster	Start Co-ordinates	End Co-ordinates
<b>hsa-miR-509</b>	hsa-miR-509-3p	UGAUUGGUACGUCUGUGGGUAG	X	Yes	hsa-miR-509-1 loop	147260532	147260625
					hsa-mir-509-2	147258760	147258850
					hsa-mir-509-3	147259652-	147259726
					hsa-mir-509-2 loop	147258760	147258850
					hsa-miR-509-1	147260532	147260625
					hsa-mir-509-3	147259652-	147259726
					hsa-mir-514b	147250151-	147250230
					hsa-mir-509-3 loop	147259652-	147259726
					hsa-miR-509-1	147260532	147260625
					hsa-mir-509-2	147258760	147258850
					hsa-mir-514b	147250151-	147250230
<b>hsa-miR-574</b>	hsa-miR-574-3p	CACGCUCAUGCACACACCCACA	4	No		38868032	38868127
<b>hsa-miR-574-5p</b>	hsa-miR-574-5p	UGAGUGUGUGUGUGAGUGU GU	4	No		38868032	38868127

**Table 8-10: Highly expressed miRNAs in APA (miR-92a to miR-92b).**  
Based on miRBase Database Release 21: June 2014.

microRNA (previous ID)	microRNA (latest ID)	Sequence	Chromosome Location	Cluster	Other microRNA within cluster	Start Co- ordinates	End Co- ordinates		
<b>hsa-miR-92a</b>	hsa-miR-92a- 3p	UAUUGCACUUGUCCCGGCCUGU	13	Yes	hsa-mir-92a-1 loop	91351314	91351391		
					hsa-mir-17	91350605	91350688		
					hsa-mir-18a	91350751	91350821		
					hsa-mir-19a	91350891	91350972		
					hsa-mir-20a	91351065	91351135		
					hsa-mir-19b-1	91351192	91351278		
					X	Yes	hsa-mir-92a-2 loop	134169538	134169612
					hsa-mir-106a	134170198	134170278		
					hsa-mir-18b	134170041	134170111		
					hsa-mir-19b-2	134169671	134169766		
<b>hsa-miR-92b</b>	hsa-miR-92b- 3p	UAUUGCACUCGUCCCGGCCUCC	1	No	hsa-mir-20b	134169809	134169877		
					hsa-mir-363	134169378	134169452		
						155195177	155195272		

**Table 8-11: miRNAs that are differentially expressed in Angio II-stimulated cells (>500 AU).**

Synonym means the miRNAs have similar seed sequence and share similar mRNA targets according to IPA analysis. Bold and underlined sequences are the seed sequence of the miRNA.

miRNA (miRBase Accession)	Synonym miRNAs/ Overlapped miRNAs (IPA)	Sequence	Chromosome	Number of targeted mRNA
hsa-miR-106a-5p	hsa-miR-17-5p, hsa-miR-20a-5p, hsa-miR-20b-5p	<u>AAAAGUGC</u> UUACAGUGCAGGUAG	x	1418
hsa-miR-1185-1-3p	-	-	-	No match miRNA in IPA
hsa-miR-126-3p	hsa-miR-126-3p	<u>UCGUACCG</u> UGAGUAAUAAUGCG	9	111
hsa-miR-1275	-	<u>GUGGGGGAG</u> AGGCUGUC	6	1870
hsa-miR-140-5p	-	<u>CAGUGGUU</u> UUACCCUAUGGUAG	16	751
hsa-miR-154-3p	-	<u>AAUCAUAC</u> ACGGUUGACCUAUU	14	309
hsa-miR-17-5p	hsa-miR-106a-5p, hsa-miR-20a-5p, hsa-miR-20b-5p	<u>CAAAGUGC</u> UUACAGUGCAGGUAG	13	1418
hsa-miR-196b-5p	hsa-miR-196a-5p	<u>UAGGUAGU</u> UUCUGUUGUUGGG	7	628
hsa-miR-19a-3p	hsa-miR-19b-3p	<u>UGUGCAA</u> AUCUAUGCAAACUGA	13	1448
hsa-miR-20a-3p	-	-	-	Not included in IPA Target Filter analysis
hsa-miR-20a-5p	hsa-miR-17-5p, hsa-miR-106a-5p, hsa-miR-20b-5p	<u>UAAAGUGC</u> UUUAGUGCAGGUAG	13	1418
hsa-miR-20b-5p	hsa-miR-17-5p, hsa-miR-106a-5p, hsa-miR-20a-5p	<u>CAAAGUGC</u> UCAUAGUGCAGGUAG	X	1418
hsa-miR-218-1-3p	-	-	-	Not included in IPA Target Filter analysis
hsa-miR-222-3p	hsa-miR-221-3p	<u>AGCUACA</u> UCUGGCUACUGGGU	X	807
hsa-miR-345-5p	-	<u>GCUGACU</u> CCUAGUCCAGGGCUC	14	476
hsa-miR-3613-5p	-	<u>UGUUGUAC</u> UUUUUUUUUGUUC	13	263
hsa-miR-376a-5p	-	<u>GUAGAUU</u> CCUUCUAUGAGUA	14	3
hsa-miR-4323	-	<u>CAGCCCCA</u> CAGCCUCAGA	19	1272

**Table 8-12: miRNAs that are differentially expressed in Angio II-stimulated cells (>500 AU).**

Synonym means the miRNAs have similar seed sequence and share similar mRNA targets according to IPA analysis. Bold and underlined sequences are the seed sequence of the miRNA.

miRNA (miRBase Acession)	Synonym miRNAs/ Overlapped miRNAs (IPA)	Sequence	Chromosome	Number of targeted mRNA
hsa-miR-4741	hsa-miR-4675	<u>CGGGCUGU</u> CCGGAGGGGUCGGCU	18	1188
hsa-miR-4743-5p	-	<u>UGGCCGGA</u> UGGGACAGGAGGCAU	18	699
hsa-miR-488-3p	-	<u>UUGAAAGG</u> CUAUUUUCUUGGUC	1	735
hsa-miR-493-5p	-	-	-	Not included in IPA Target Filter analysis
hsa-miR-5100	-	-	-	Not included in IPA Target Filter analysis
hsa-miR-5190	-	-	-	Not included in IPA Target Filter analysis
hsa-miR-539-3p	hsa-miR-485-3p	<u>AUCAUACA</u> AGGACAAUUUCUUU	14	557
hsa-miR-548v	-	<u>AGCUACAGU</u> UACUUUUGCACCA	8	627
hsa-miR-568	-	<u>AUGUAUAA</u> AUGUAUACACAC	3	319
hsa-miR-574-5p	-	<u>UGAGUGUG</u> UGUGUGAGUGUGU	4	564
hsa-miR-647	-	<u>GUGGCUGC</u> ACUCACUCCUUC	20	1034
hsa-miR-7-5p	hsa-miR-7a-5p	<u>UGGAAGAC</u> UAGUGAUUUUGUUGU (from precursor: hsa-mir-7-1)	9	916
		<u>UGGAAGAC</u> UAGUGAUUUUGUUGU (from precursor: hsa-mir-7-2)	15	
		<u>UGGAAGAC</u> UAGUGAUUUUGUUGU (from precursor: hsa-mir-7-3)	19	
hsa-miR-766-3p	-	<u>ACUCCAGC</u> CCCACAGCCUCAGC	X	1096
hsa-miR-937-5p	-	-	-	Not included in IPA Target Filter analysis

**Table 8-13: miRNAs that are differentially expressed in dbcAMP-stimulated cells (>500 AU).**

Synonym means the miRNAs have similar seed sequence and share similar mRNA targets according to IPA analysis. Bold and underlined sequences are the seed sequence of the miRNA.

miRNA (miRBase Acession)	Synonym miRNAs/ Overlapped miRNAs (IPA)	Sequence	Chromosome	Number of targeted mRNA
hsa-miR-100-5p	hsa-miR-99a-5p	<u>AACCCGUAG</u> AUCCGAACUUGUG	11	193
hsa-miR-106a-5p	hsa-miR-17-5p, hsa-miR-106b-5p, hsa-miR-20a-5p, hsa-miR-20b-5p hsa-miR-93-5p	<u>AAAAGUGCU</u> UACAGUGCAGGUAG	X	1418
hsa-miR-106b-5p	hsa-miR-17-5p, hsa-miR-106a-5p, hsa-miR-20a-5p, hsa-miR-20b-5p hsa-miR-93-5p	<u>UAAAGUGC</u> UGACAGUGCAGAU	7	1418
hsa-miR-107	hsa-miR-103a-3p	<u>AGCAGCAU</u> UGUACAGGGCUAUCA	10	1255
hsa-miR-1185-1-3p	-	-	-	Not included in IPA Target Filter analysis
hsa-miR-1224-5p	-	<u>GUGAGGAC</u> UCGGGAGGUGG	3	593
hsa-miR-125a-5p	hsa-miR-125b-5p	<u>UCCCUGAG</u> ACCCUUAACUGUGA	19	1530
hsa-miR-125b-5p	hsa-miR-125a-5p	<u>UCCCUGAG</u> ACCCUAACUUGUGA (from precursor: hsa-mir-125b-1) <u>UCCCUGAG</u> ACCCUAACUUGUGA (from precursor: hsa-mir-125b-2)	11 21	1530
hsa-miR-126-3p	hsa-miR-126a-3p	<u>UCGUACCG</u> UGAGUAAUAAUGCG	9	111
hsa-miR-1275	-	<u>GUGGGGGA</u> GAGGCUGUC	6	1870
hsa-miR-132-3p	-	<u>UAACAGUC</u> UACAGCCAUGGUCG	17	767
hsa-miR-136-3p	-	-	-	Not included in IPA Target Filter analysis
hsa-miR-140-5p	-	<u>CAGUGGUU</u> UUACCCUAUGGUAG	16	751
hsa-miR-145-5p	-	<u>GUCCAGUU</u> UCCCAGGAUCCCU	5	1228
hsa-miR-146b-5p	hsa-miR-146a-5p	<u>UGAGAAC</u> UGAAUCCAUGGCU	10	650
hsa-miR-15a-5p	hsa-miR-16-5p	<u>UAGCAGCA</u> CAUAAUGGUUUGUG	13	2020

**Table 8-14: miRNAs that are differentially expressed in dbcAMP-stimulated cells (>500 AU).**

Synonym means the miRNAs have similar seed sequence and share similar mRNA targets according to IPA analysis. Bold and underlined sequences are the seed sequence of the miRNA.

miRNA (miRBase Acession)	Synonym miRNAs/ Overlapped miRNAs (IPA)	Sequence	Chromosome	Number of targeted mRNA
hsa-miR-154-3p	hsa-miR-487a-3p	<u>AAUCAUAC</u> ACGGUUGACCUAUU	14	309
hsa-miR-16-2-3p	-	-	-	Not included in IPA Target Filter analysis
hsa-miR-17-5p	hsa-miR-106a-5p, hsa-miR-106b-5p, hsa-miR-20a-5p, hsa-miR-20b-5p hsa-miR-93-5p	<u>CAAAGUGC</u> UUACAGUCAGGUAG	13	1418
hsa-miR-181b-5p	hsa-miR-181a-5p, hsa-miR-181c-5p	<u>AACAUUCA</u> UUGCUGUCGGUGGGU (from precursor: hsa-mir-181b-1)	1	1496
		<u>AACAUUCA</u> UUGCUGUCGGUGGGU (from precursor: hsa-mir-181b-2)	9	
hsa-miR-181c-5p	hsa-miR-181a-5p, hsa-miR-181b-5p	<u>AACAUUCA</u> ACCUGUCGGUGAGU	19	1496
hsa-miR-186-5p	-	<u>CAAAGAAU</u> UCUCCUUUUGGGCU	1	922
hsa-miR-194-5p	-	<u>UGUAACAG</u> CAACUCCAUGUGGA (from precursor: hsa-mir-194-1)	1	709
		<u>UGUAACAG</u> CAACUCCAUGUGGA (from precursor: hsa-mir-194-2)	11	
hsa-miR-196b-5p	hsa-miR-196a-5p	<u>UAGGUAGU</u> UUCUGUUGUUGGG	7	628
hsa-miR-197-5p	-	<u>CGGGUAGA</u> GAGGGCAGUGGGAGG	1	641
hsa-miR-19a-3p	hsa-miR-19b-3p	<u>UGUGCAA</u> AUCUAUGCAAACUGA	13	1448
hsa-miR-19b-3p	hsa-miR-19a-3p	<u>UGUGCAA</u> AUCCAUGCAAACUGA (from precursor: hsa-mir-19b-1)	13	1448
		<u>UGUGCAA</u> AUCCAUGCAAACUGA (from precursor: hsa-mir-19b-2)	X	

**Table 8-15: miRNAs that are differentially expressed in dbcAMP-stimulated cells (>500 AU).**

Synonym means the miRNAs have similar seed sequence and share similar mRNA targets according to IPA analysis. Bold and underlined sequences are the seed sequence of the miRNA.

miRNA (miRBase Acession)	Synonym miRNAs/ Overlapped miRNAs (IPA)	Sequence	Chromosome	Number of targeted mRNA
hsa-miR-20a-5p	hsa-miR-17-5p, hsa-miR-106a-5p, hsa-miR-106b-5p, hsa-miR-20b-5p, hsa-miR-93-5p	<u>UAAAGUGC</u> UUAUAGUGCAGGUAG	13	1418
hsa-miR-20b-5p	hsa-miR-17-5p, hsa-miR-106a-5p, hsa-miR-106b-5p, hsa-miR-20a-5p, hsa-miR-93-5p	<u>CAAAGUGC</u> UCAUAGUGCAGGUAG	X	1418
hsa-miR-21-5p	-	<u>UAGCUUAU</u> CAGACUGAUGUUGA	17	615
hsa-miR-222-3p	hsa-miR-221-3p	<u>AGCUACAUC</u> UGGCUACUGGGU	X	807
hsa-miR-23a-3p	hsa-miR-23b-3p, hsa-miR-23c-3p	<u>AUCACAUU</u> GCCAGGGAUUUC	19	807
hsa-miR-23b-3p	hsa-miR-23a-3p, hsa-miR-23c-3p	<u>AUCACAUU</u> GCCAGGGAUUACC	9	807
hsa-miR-23c	hsa-miR-23a-3p, hsa-miR-23b-3p	<u>AUCACAUU</u> GCCAGUGAUUACCC	X	807
hsa-miR-24-3p	-	<u>UGGCUCAGU</u> UCAGCAGGAACAG (from precursor: hsa-mir-24-1)	9	1505
		<u>UGGCUCAGU</u> UCAGCAGGAACAG (from precursor: hsa-mir-24-2)	19	
hsa-miR-29a-3p	hsa-miR-29b-3p, hsa-miR-29c-3p	<u>UAGCACCAU</u> UCUGAAAUCGGUUA	7	1492
hsa-miR-29c-3p	hsa-miR-29b-3p, hsa-miR-29a-3p	<u>UAGCACCAU</u> UUGAAAUCGGUUA	1	1492
hsa-miR-30a-5p	hsa-miR-30c-5p, hsa-miR-30b-5p, hsa-miR-30e-5p	<u>UGUAAACA</u> UCCUCGACUGGAAG	6	1592
hsa-miR-30b-5p	hsa-miR-30c-5p, hsa-miR-30a-5p, hsa-miR-30e-5p	<u>UGUAAACA</u> UCCUACACUCAGCU	8	1592

**Table 8-16: miRNAs that are differentially expressed in dbcAMP-stimulated cells (>500 AU).**

Synonym means the miRNAs have similar seed sequence and share similar mRNA targets according to IPA analysis. Bold and underlined sequences are the seed sequence of the miRNA.

miRNA (miRBase Acession)	Synonym miRNAs/ Overlapped miRNAs (IPA)	Sequence	Chromosome	Number of targeted mRNA
hsa-miR-30c-5p	hsa-miR-30a-5p, hsa-miR-30b-5p, hsa-miR-30e-5p	<u>UGUAAACA</u> UCCUACACUCUCAGC (from precursor: hsa-mir-30c-1) UGUAAACA <u>UCCUACACUCUCAGC</u> (from precursor: hsa-mir-30c-2)	1 6	1592
hsa-miR-30e-5p	hsa-miR-30c-5p, hsa-miR-30a-5p, hsa-miR-30b-5p	<u>UGUAAACA</u> UCCUUGACUGGAAG	1	1592
hsa-miR-329-3p	-	<u>AACACACC</u> UGGUUAAACCUCUUU (from precursor: hsa-mir-329-1) <u>AACACACC</u> UGGUUAAACCUCUUU (from precursor: hsa-mir-329-2)	14 14	913
hsa-miR-335-3p	-	-	-	Not included in IPA Target Filter analysis
hsa-miR-337-3p	-	<u>CUCCUAUA</u> UGAUGCCUUUCUUC	14	373
hsa-miR-337-5p	-	<u>GAACGGCU</u> UCAUACAGGAGUU	14	249
hsa-miR-3613-5p	-	<u>UGUUGUAC</u> UUUUUUUUUGUUC	13	263
hsa-miR-3620-5p	hsa-miR-1587	<u>GUGGGCUG</u> GGCUGGGCUGGGCC	1	994
hsa-miR-365a-3p	-	<u>UAAUGCCC</u> UAAAAUCCUUAU	16	715
hsa-miR-369-5p	-	<u>AGAUCGAC</u> CGUGUUUAUUCGC	14	107
hsa-miR-370-3p	-	<u>GCCUGCUG</u> GGGUGGAACCUUGU	14	1217
hsa-miR-376a-5p	-	<u>GUAGAUUC</u> UCCUUCUAUGAGUA	14	3
hsa-miR-376b-3p	hsa-miR-376a-3p	<u>AUCAUAGAG</u> GAAAAUCCAUGUU	14	581
hsa-miR-376b-5p	-	-	-	Not included in IPA Target Filter analysis
hsa-miR-376c-3p	-	<u>AACAUAGAG</u> GAAAAUCCACGU	14	667

**Table 8-17: miRNAs that are differentially expressed in dbcAMP-stimulated cells (>500 AU).**

Synonym means the miRNAs have similar seed sequence and share similar mRNA targets according to IPA analysis. Bold and underlined sequences are the seed sequence of the miRNA.

miRNA (miRBase Acession)	Synonym miRNAs/ Overlapped miRNAs (IPA)	Sequence	Chromosome	Number of targeted mRNA
hsa-miR-376c-5p	hsa-miR-376b-5p	-	-	Not included in IPA Target Filter analysis
hsa-miR-377-3p	-	AUCACACAAAGGCAACUUUUGU	14	1227
hsa-miR-409-3p	-	<u>GAAUGUUG</u> CUCGGUGAACCCCU	14	188
hsa-miR-410-3p	mmu-miR-344d-3p	<u>AAUAUAAC</u> ACAGAUGGCCUGU	14	733
hsa-miR-411-5p	-	<u>UAGUAGAC</u> CGUAUAGCGUACG	14	337
hsa-miR-424-3p	-	<u>CAAAACGUG</u> AGGGCGUGCUAU	X	3
hsa-miR-4270	-	<u>UCAGGGAGU</u> CAGGGGAGGGC	3	1302
hsa-miR-4284	-	<u>GGGCUACA</u> AUCACCCCAU	7	1253
hsa-miR-4286	-	<u>ACCCACUC</u> CCUGGUACC	8	1195
hsa-miR-4324	-	<u>CCCUGAGA</u> CCCUAACCUUAA	19	757
hsa-miR-433-3p	-	<u>AUCAUGAU</u> GGGCUCCUGGUGU	14	584
hsa-miR-4444	-	<u>CUCGAGUU</u> GGAAGAGGCG (from precursor: hsa-mir-4444-1)	2	164
		<u>CUCGAGUU</u> GGAAGAGGCG (from precursor: hsa-mir-4444-2)	3	
hsa-miR-4454	-	<u>GGAUCCGA</u> GUCACGGCACCA	4	111
hsa-miR-454-3p	hsa-miR-130a-3p	<u>UAGUGCAA</u> UAUUGCUUAUAGGGU	17	1252
hsa-miR-4727-5p	mmu-miR-3084-3p	<u>UUCUGCCA</u> GUCUCCUUCAGAC	17	948
hsa-miR-4732-5p	-	<u>UGUAGAGC</u> AGGGAGCAGGAAGCU	17	322
hsa-miR-4741	hsa-miR-4675	<u>CGGGCUGU</u> CCGGAGGGGUCGGCU	18	1188
hsa-miR-4743-5p	-	<u>UGGCCGGA</u> UGGGACAGGAGGCAU	18	699
hsa-miR-487a	hsa-miR-154-3p	<u>AAUCAUAC</u> AGGGACAUCAGUU	14	309

**Table 8-18: miRNAs that are differentially expressed in dbcAMP-stimulated cells (>500 AU).**

Synonym means the miRNAs have similar seed sequence and share similar mRNA targets according to IPA analysis. Bold and underlined sequences are the seed sequence of the miRNA.

miRNA (miRBase Acession)	Synonym miRNAs/ Overlapped miRNAs (IPA)	Sequence	Chromosome	Number of targeted mRNA
hsa-miR-488-3p	-	<u>UUGAAAGG</u> CUAUUUCUUGGUC	1	735
hsa-miR-494	-	<u>UGAAACA</u> UACACGGGAAACCUC	14	789
hsa-miR-539-3p	-	-	-	Not included in IPA Target Filter analysis
hsa-miR-542-3p	-	<u>UGUGACAG</u> AUUGAUACUGAAA	X	795
hsa-miR-6076	-	-	-	Not included in IPA Target Filter analysis
hsa-miR-647	-	<u>GUGGCUG</u> CACUCACUCCUUC	20	1034
hsa-miR-758-3p	-	<u>UUUGUGAC</u> CUGGUCCACUAACC	14	542
hsa-miR-766-3p	-	<u>ACUCCAGC</u> CCCACAGCCUCAGC	X	1096
hsa-miR-889	-	<u>UUAUAUC</u> GGAACCAUUGU	14	140
hsa-miR-93-5p	hsa-miR-17-5p, hsa-miR-106a-5p, hsa-miR-106b-5p, hsa-miR-20a-5p hsa-miR-20b-5p	<u>CAAAGUC</u> UGUUCGUGCAGGUAG	7	1418
hsa-miR-99a-5p	hsa-miR-100-5p	<u>AACCCGU</u> AGAUCGGAACUUGUG	21	193

**Table 8-19: miRNAs that are differentially expressed in KCI-stimulated cells (>500 AU).**

Synonym means the miRNAs have similar seed sequence and share similar mRNA targets according to IPA analysis. Bold and underlined sequences are the seed sequence of the miRNA.

miRNA (miRBase Accession)	Synonym miRNAs/ Overlapped miRNAs (IPA)	Sequence	Chromosome	Number of targeted mRNA
hsa-let-7g-5p	hsa-let-7a-5p	<u>UGAGGUAGU</u> AGUUUGUACAGUU	3	1396
hsa-miR-100-5p	hsa-miR-99a-5p	<u>AACCCGUAG</u> AUCCGAACUUGUG	11	193
hsa-miR-106a-5p	hsa-miR-17-5p, hsa-miR-106b-5p, hsa-miR-20a-5p, hsa-miR-20b-5p, hsa-miR-93-5p	<u>AAAAGUGC</u> UUACAGUGCAGGUAG	X	1418
hsa-miR-10b-5p	hsa-miR-10a-5p	U <u>ACCCUGU</u> AGAACCGAAUUUGUG	2	780
hsa-miR-125a-5p	hsa-miR-125b-5p	<u>UCCUGAG</u> ACCCUUUAACCUUGUGA	19	1530
hsa-miR-1271-5p	hsa-miR-96-5p	<u>CUUGGCACCU</u> AGCAAGCACUCA	5	1394
hsa-miR-128-3p	-	<u>UCACAGUG</u> AACCGGUCUCUUU (from precursor: hsa-mir-128-1) <u>UCACAGUG</u> AACCGGUCUCUUU (from precursor: hsa-mir-128-2)	2 3	1461
hsa-miR-139-3p	-	-	-	Not included in IPA Target Filter analysis
hsa-miR-15b-5p	hsa-miR-16-5p	<u>UAGCAGCA</u> CAUAAUGGUUUGUG	13	2020
hsa-miR-154-3p	hsa-miR-487a-3p	<u>AAUCAUAC</u> ACGGUUGACCUAUU	14	309
hsa-miR-16-2-3p	-	-	-	Not included in IPA Target Filter analysis
hsa-miR-17-5p	hsa-miR-17-5p, hsa-miR-106b-5p, hsa-miR-20a-5p, hsa-miR-20b-5p, hsa-miR-93-5p	<u>CAAAGUGC</u> UUACAGUGCAGGUAG	13	1418
hsa-miR-186-5p	-	<u>CAAAGAAU</u> UCUCCUUUUGGGCU	1	922
hsa-miR-195-5p	hsa-miR-16-5p		17	2020
hsa-miR-196b-5p	hsa-miR-196a-5p	UAGGUAGUUUCAUGUUGUUGGG	7	628

**Table 8-20: miRNAs that are differentially expressed in KCI-stimulated cells (>500 AU).**

Synonym means the miRNAs have similar seed sequence and share similar mRNA targets according to IPA analysis. Bold and underlined sequences are the seed sequence of the miRNA.

miRNA (miRBase Acession)	Synonym miRNAs/ Overlapped miRNAs (IPA)	Sequence	Chromosome	Number of targeted mRNA
hsa-miR-19a-3p	hsa-miR-19b-3p	<u>UGUGCAAA</u> UCUAUGCAAAACUGA	13	1448
hsa-miR-19b-3p	hsa-miR-19a-3p	<u>UGUGCAAA</u> UCCAUGCAAAACUGA (from precursor: hsa-mir-19b-1)	13	1448
		<u>UGUGCAAA</u> UCCAUGCAAAACUGA (from precursor: hsa-mir-19b-2)	X	
hsa-miR-20a-3p	-	-	-	Not included in IPA Target Filter analysis
hsa-miR-20b-5p	hsa-miR-17-5p, hsa-miR-106a-5p, hsa-miR-106b-5p, hsa-miR-20a-5p hsa-miR-93-5p	<u>CAAAGUGC</u> UCAUAGUGCAGGUAG	X	1418
hsa-miR-21-5p	-	<u>UAGCUUAU</u> CAGACUGAUGUUGA	17	615
hsa-miR-23a-3p	hsa-miR-23b-3p, hsa-miR-23c	<u>AUCACAUU</u> GCCAGGGAUUUCC	19	807
hsa-miR-23b-3p	hsa-miR-23a-3p, hsa-miR-23c	<u>AUCACAUU</u> GCCAGGGAUUACC	9	807
hsa-miR-23c	hsa-miR-23a-3p, hsa-miR-23b-3p	<u>AUCACAUU</u> GCCAGUGAUUACCC	X	807
hsa-miR-28-5p	hsa-miR-708-5p	<u>AAGGAGCU</u> CACAGUCUAUUGAG	3	874
hsa-miR-29c-3p	hsa-miR-29b-3p, hsa-miR-29a-3p	<u>UAGCACCA</u> UUUGAAAUCGGUUA	1	1492

**Table 8-21: miRNAs that are differentially expressed in KCI-stimulated cells (>500 AU).**

Synonym means the miRNAs have similar seed sequence and share similar mRNA targets according to IPA analysis. Bold and underlined sequences are the seed sequence of the miRNA.

miRNA (miRBase Acession)	Synonym miRNAs/ Overlapped miRNAs (IPA)	Sequence	Chromosome	Number of targeted mRNA
hsa-miR-30a-5p	hsa-miR-30c-5p, hsa-miR-30b-5p, hsa-miR-30e-5p	<u>UGUAAACA</u> UCCUCGACUGGAAG	6	1592
hsa-miR-30b-5p	hsa-miR-30c-5p, hsa-miR-30a-5p, hsa-miR-30e-5p	<u>UGUAAACA</u> UCCUACACUCAGCU	8	1592
hsa-miR-30c-5p	hsa-miR-30a-5p, hsa-miR-30b-5p, hsa-miR-30e-5p	<u>UGUAAACA</u> UCCUACACUCAGC (from precursor: hsa-mir-30c-2)	1	1592
		UGUAAACAUCCUACACUCAGC (from precursor: hsa-mir-30c-1)	6	
hsa-miR-30e-5p	hsa-miR-30c-5p, hsa-miR-30a-5p, hsa-miR-30b-5p	<u>UGUAAACA</u> UCCUUGACUGGAAG	1	1592
hsa-miR-3120-3p	-	<u>CACAGCAA</u> GUGUAGACAGGCA	1	869
hsa-miR-3178	-	<u>GGGGCGCG</u> GCCGGAUCG	16	529
hsa-miR-3195	-	<u>CGCGCCGG</u> CCCGGGUU	20	241
hsa-miR-329	-	<u>AACACACC</u> UGGUUAACCUCUUU (from precursor: hsa-mir-329-1)	14	913
		<u>AACACACC</u> UGGUUAACCUCUUU (from precursor: hsa-mir-329-2)	14	913
hsa-miR-335-3p	-	-	-	Not included in IPA Target Filter analysis
hsa-miR-337-3p	-	<u>CUCCUAUA</u> UGAUGCCUUCUUC	14	373
hsa-miR-3617-3p	-	-	-	Not included in IPA Target Filter analysis
hsa-miR-376b-3p	hsa-miR-376a-3p	<u>AUCAUAGAGG</u> AAAAUCAUGUU	14	581
hsa-miR-376b-5p	hsa-miR-376c-5p	-	-	Not included in IPA Target Filter analysis
hsa-miR-376c-5p	hsa-miR-376b-5p	-	-	Not included in IPA Target Filter analysis

**Table 8-22: miRNAs that are differentially expressed in KCl-stimulated cells (>500 AU).**

Synonym means the miRNAs have similar seed sequence and share similar mRNA targets according to IPA analysis. Bold and underlined sequences are the seed sequence of the miRNA.

miRNA (miRBase Acession)	Synonym miRNAs/ Overlapped miRNAs (IPA)	Sequence	Chromosome	Number of targeted mRNA
hsa-miR-3922-5p	-	<u>UCAAGGCC</u> CAGAGGUCCCACAGCA	12	834
hsa-miR-409-3p	-	<u>GAAUGUUG</u> CUCGGUGAACCCCU	14	188
hsa-miR-424-3p	-	<u>CAAACGUG</u> GAGGCGCUGCUAU	X	3
hsa-miR-4284	-	<u>GGGCUCAC</u> AUCACCCCAU	7	1253
hsa-miR-4288	-	<u>UUGUCUGC</u> UGAGUUUCC	8	666
hsa-miR-4497	-	<u>CUCCGGG</u> ACGGCUGGGC	12	414
hsa-miR-454-3p	hsa-miR-130a-3p	<u>UAGUGCAA</u> UAUUGCUUAUAGGGU	17	1252
hsa-miR-4730	-	<u>CUGGCGG</u> AGCCAUUCCAUGCCA	17	301
hsa-miR-4732-5p	-	<u>UGUAGAGC</u> AGGGAGCAGGAAGCU	17	322
hsa-miR-483-3p	-	<u>UCACUCCU</u> CUCCUCCGUCUU	11	615
hsa-miR-487a-3p	hsa-miR-154-3p	<u>AAUCAUAC</u> AGGGACAUCAGUU	14	309
hsa-miR-489-3p	-	GUGACAUCACAUAUACGGCAGC	11	410
hsa-miR-494	-	<u>UGAAACAU</u> ACACGGGAAACCUC	14	789

**Table 8-23: miRNAs that are differentially expressed in KCl-stimulated cells (>500 AU).**

Synonym means the miRNAs have similar seed sequence and share similar mRNA targets according to IPA analysis. Bold and underlined sequences are the seed sequence of the miRNA.

miRNA (miRBase Acession)	Synonym miRNAs/ Overlapped miRNAs (IPA)	Sequence	Chromosome	Number of targeted mRNA
hsa-miR-542-3p	-	<u>UGUGACAG</u> AUUGAUAAACUGAAA	X	795
hsa-miR-543	-	AA <u>ACAUUC</u> GCGGUGCACUUCUU	14	916
hsa-miR-568	-	<u>AUGUAUAAA</u> AUGUAUACACAC	3	319
hsa-miR-574-5p	-	<u>UGAGUGUG</u> UGUGUGUGAGUGUGU	4	564
hsa-miR-7-1-3p	-	-	-	Not included in IPA Target Filter analysis
hsa-miR-766-3p	-	<u>ACUCCAG</u> CCCCACAGCCUCAGC	X	1096
hsa-miR-874-3p	-	<u>CUGCCCU</u> GCCCCGAGGGACCGA	5	1069
hsa-miR-92a-3p	hsa-miR-92b-3p	UAUUGCACUUGUCCCGGCCUGU (from precursor: hsa-mir-92a-1) UAUUGCACUUGUCCCGGCCUGU (from precursor: hsa-mir-92a-2)	13  X	1138
hsa-miR-92b-3p	hsa-miR-92a-3p	<u>UAUUGCAC</u> UCGUCCCGGCCUCC	1	1138

## References

- Abdullah-Sayani, A., J. M. Bueno-de-Mesquita and M. J. van de Vijver (2006). "Technology Insight: tuning into the genetic orchestra using microarrays limitations of DNA microarrays in clinical practice." Nat Clin Pract Oncol 3(9): 501-516.
- Abe-Dohmae, S., S. Suzuki, Y. Wada, H. Aburatani, D. E. Vance and S. Yokoyama (2000). "Characterization of Apolipoprotein-Mediated HDL Generation Induced by cAMP in a Murine Macrophage Cell Line." Biochemistry 39(36): 11092-11099.
- Aburto, N. J., A. Ziolkovska, L. Hooper, P. Elliott, F. P. Cappuccio and J. J. Meerpohl (2013). "Effect of lower sodium intake on health: systematic review and meta-analyses." BMJ 346: 1-20.
- Akingbemi, B. T., R. Ge, C. S. Rosenfeld, L. G. Newton, D. O. Hardy, J. F. Catterall, D. B. Lubahn, K. S. Korach and M. P. Hardy (2003). "Estrogen Receptor- $\alpha$  Gene Deficiency Enhances Androgen Biosynthesis in the Mouse Leydig Cell." Endocrinology 144(1): 84-93.
- Altuvia, Y., P. Landgraf, G. Lithwick, N. Elefant, S. Pfeffer, A. Aravin, M. Brownstein, T. Tuschl and H. Margalit (2005). "Clustering and conservation patterns of human microRNAs." Nucleic Acids Res 33: 2697 - 2706.
- Ambros, V., B. Bartel, D. P. Bartel, C. B. Burge, J. C. Carrington, X. Chen, G. Dreyfuss, S. R. Eddy, S. Griffiths-Jones, M. Marshall, M. Matzke, G. Ruvkun and T. Tuschl (2003). "A uniform system for microRNA annotation." RNA 9(3): 277-279.
- Anand, K., A. N. Mooss and S. M. Mohiuddin (2006). "Review: Aldosterone Inhibition Reduces the Risk of Sudden Cardiac Death in Patients with Heart Failure." Journal of Renin-Angiotensin-Aldosterone System 7(1): 15-19.
- Anastas, J. N. and R. T. Moon (2013). "WNT signalling pathways as therapeutic targets in cancer." Nat Rev Cancer 13(1): 11-26.
- Arce, L., N. N. Yokoyama and M. L. Waterman (2006). "Diversity of LEF//TCF action in development and disease." Oncogene 25(57): 7492-7504.
- Arnaldi, G., V. Mancini, C. Costantini, M. Giovagnetti, M. Petrelli, A. Masini, X. Bertagna and F. Mantero (1998). "ACTH receptor mRNA in human adrenocortical tumors: overexpression in aldosteronomas." Endocrine research 24(3-4): 845-849.
- Aucott, L., A. Poobalan, W. C. S. Smith, A. Avenell, R. Jung and J. Broom (2005). "Effects of Weight Loss in Overweight/Obese Individuals and Long-Term Hypertension Outcomes: A Systematic Review." Hypertension 45(6): 1035-1041.
- Azhar, S. and E. Reaven (2002). "Scavenger receptor class BI and selective cholesteryl ester uptake: partners in the regulation of steroidogenesis." Molecular and Cellular Endocrinology 195(1-2): 1-26.
- Barlaskar, F. M., A. C. Spalding, J. H. Heaton, R. Kuick, A. C. Kim, D. G. Thomas, T. J. Giordano, E. Ben-Josef and G. D. Hammer (2009). "Preclinical Targeting of the Type I Insulin-Like Growth Factor Receptor in Adrenocortical Carcinoma." The Journal of Clinical Endocrinology & Metabolism 94(1): 204-212.
- Bartel, D. (2004). "MicroRNAs: genomics, biogenesis, mechanism, and function." Cell 116(2): 281 - 297.

- Bartel, D. P. (2009). "MicroRNAs: Target Recognition and Regulatory Functions." Cell **136**(2): 215-233.
- Baskerville, S. and D. Bartel (2005). "Microarray profiling of microRNAs reveals frequent coexpression with neighboring miRNAs and host genes." RNA **11**: 241 - 247.
- Bassett, M., Y. Zhang, C. Clyne, P. White and W. Rainey (2002). "Differential regulation of aldosterone synthase and 11beta-hydroxylase transcription by steroidogenic factor-1." Journal of Molecular Endocrinology **28**(2): 125-135.
- Bassett, M. H., T. Suzuki, H. Sasano, P. C. White and W. E. Rainey (2004). "The Orphan Nuclear Receptors NURR1 and NGFIB Regulate Adrenal Aldosterone Production." Molecular Endocrinology **18**(2): 279-290.
- Basso, F., L. Freeman, C. L. Knapper, A. Remaley, J. Stonik, E. B. Neufeld, T. Tansey, M. J. A. Amar, J. Fruchart-Najib, N. Duverger, S. Santamarina-Fojo and H. B. Brewer (2003). "Role of the hepatic ABCA1 transporter in modulating intrahepatic cholesterol and plasma HDL cholesterol concentrations." Journal of Lipid Research **44**(2): 296-302.
- Batuman, V. (2013). "Salt and hypertension: why is there still a debate?" Kidney International Supplements **3**(4): 316-320.
- Baudrand, R., L. H. Pojoga, A. Vaidya, A. E. Garza, P. A. Vöhringer, X. Jeunemaitre, P. N. Hopkins, T. M. Yao, J. Williams, G. K. Adler and G. H. Williams (2015). "Statin Use and Adrenal Aldosterone Production in Hypertensive and Diabetic Subjects." Circulation **132**(19): 1825-1833.
- Baxter, J. D., M. Schambelan, D. T. Matulich, B. J. Spindler, A. A. Taylor and F. C. Bartter (1976). "Aldosterone receptors and the evaluation of plasma mineralocorticoid activity in normal and hypertensive states." Journal of Clinical Investigation **58**(3): 579-589.
- Bayascas, J. R. and D. R. Alessi "Regulation of Akt/PKB Ser473 Phosphorylation." Molecular Cell **18**(2): 143-145.
- Bayorh, M. A., A. A. Ganafa, D. Eatman, M. Walton and G. Z. Feuerstein (2005). "Simvastatin and Losartan Enhance Nitric Oxide and Reduce Oxidative Stress in Salt-Induced Hypertension\*." American Journal of Hypertension **18**(11): 1496-1502.
- Beg, M. S., M. Borad, J. Sachdev, D. S. Hong, S. Smith, A. Bader, J. Stoudemire, S. Kim and A. Brenner (2014). "Abstract CT327: Multicenter phase I study of MRX34, a first-in-class microRNA miR-34 mimic liposomal injection." Cancer Research **74**(19 Supplement): CT327.
- Behm-Ansmant, I., J. Rehwinkel, T. Doerks, A. Stark, P. Bork and E. Izaurralde (2006). "mRNA degradation by miRNAs and GW182 requires both CCR4:NOT deadenylase and DCP1:DCP2 decapping complexes." Genes & Development **20**(14): 1885-1898.
- Bertherat, J. and X. Bertagna (2009). "Pathogenesis of adrenocortical cancer." Best Practice & Research Clinical Endocrinology & Metabolism **23**(2): 261-271.
- Berthon, A., C. Drelon, B. Ragazzon, S. Boulkroun, F. Tissier, L. Amar, B. Samson-Couterie, M.-C. Zennaro, P.-F. Plouin, S. Skah, M. Plateroti, H. Lefèbvre, I. Sahut-Barnola, M. Batisse-Lignier, G. Assié, A.-M. Lefrançois-Martinez, J. Bertherat, A. Martinez and P. Val (2014). "WNT/ $\beta$ -catenin signalling is activated in aldosterone-producing adenomas and controls aldosterone production." Human Molecular Genetics **23**(4): 889-905.

- Berthon, A., I. Sahut-Barnola, S. Lambert-Langlais, C. de Jousineau, C. Damon-Soubeyrand, E. Louiset, M. M. Taketo, F. Tissier, J. Bertherat, A.-M. Lefrançois-Martinez, A. Martinez and P. Val (2010). "Constitutive  $\beta$ -catenin activation induces adrenal hyperplasia and promotes adrenal cancer development." Human Molecular Genetics **19**(8): 1561-1576.
- Binart, N., M. Lombes, M. E. Rafestin-Oblin and E. E. Baulieu (1991). "Characterization of human mineralocorticosteroid receptor expressed in the baculovirus system." Proceedings of the National Academy of Sciences of the United States of America **88**(23): 10681-10685.
- Bird, I. M., N. A. Hanley, R. A. Word, J. M. Mathis, J. L. McCarthy, J. I. Mason and W. E. Rainey (1993). "Human NCI-H295 adrenocortical carcinoma cells: a model for angiotensin-II-responsive aldosterone secretion." Endocrinology **133**(4): 1555-1561.
- Black, S. M., J. A. Harikrishna, G. D. Szklarz and W. L. Miller (1994). "The mitochondrial environment is required for activity of the cholesterol side-chain cleavage enzyme, cytochrome P450<sub>sc</sub>." Proceedings of the National Academy of Sciences of the United States of America **91**(15): 7247-7251.
- Blahna, M. T. and A. Hata (2012). "Smad-mediated regulation of microRNA biosynthesis." FEBS Letters **586**(14): 1906-1912.
- Blanchard, N., D. Lankar, F. Faure, A. Regnault, C. Dumont, G. Raposo and C. Hivroz (2002). "TCR Activation of Human T Cells Induces the Production of Exosomes Bearing the TCR/CD3/ $\zeta$  Complex." The Journal of Immunology **168**(7): 3235-3241.
- Blankenhorn, D. H., S. P. Azen, D. M. Krams, W. J. Mack, L. Cashin-Hemphill, H. N. Hodis, L. W. V. DeBoer, P. R. Mahrer, M. J. Masteller, L. I. Vailas, P. Alaupovic and L. J. Hirsch (1993). "Coronary Angiographic Changes with Lovastatin Therapy: The Monitored Atherosclerosis Regression Study (MARS)." Annals of Internal Medicine **119**(10): 969-976.
- Bochar DA, F. J., Stauffacher CV, Rodwell VW (1999). Biosynthesis of mevalonic acid from acetyl-CoA. In Isoprenoids Including Carotenoids and Steroids. C. D. New York, Pergamon Press: 15-44.
- Bodzioch, M., E. Orso, J. Klucken, T. Langmann, A. Bottcher, W. Diederich, W. Drobnik, S. Barlage, C. Buchler, M. Porsch-Ozcurumez, W. E. Kaminski, H. W. Hahmann, K. Oette, G. Rothe, C. Aslanidis, K. J. Lackner and G. Schmitz (1999). "The gene encoding ATP-binding cassette transporter 1 is mutated in Tangier disease." Nat Genet **22**(4): 347-351.
- Bollag, W. B., P. Q. Barrett, C. M. Isales, M. Liscovitch and H. Rasmussen (1990). "A Potential Role for Phospholipase-D in the Angiotensin-II-Induced Stimulation of Aldosterone Secretion from Bovine Adrenal Glomerulosa Cells." Endocrinology **127**(3): 1436-1443.
- Boon, R. A., T. Seeger, S. Heydt, A. Fischer, E. Hergenreider, A. J. G. Horrevoets, M. Vinciguerra, N. Rosenthal, S. Sciacca, M. Pilato, P. van Heijningen, J. Essers, R. P. Brandes, A. M. Zeiher and S. Dimmeler (2011). "MicroRNA-29 in Aortic Dilatation: Implications for Aneurysm Formation." Circulation Research **109**(10): 1115-1119.
- Borchert, G. M., W. Lanier and B. L. Davidson (2006). "RNA polymerase III transcribes human microRNAs." Nat Struct Mol Biol **13**(12): 1097-1101.
- Borkowski, A. J., S. Levin, C. Delcroix, A. Mahler and V. Verhas (1967). "Blood Cholesterol and Hydrocortisone Production in Man: Quantitative Aspects of the

- Utilization of Circulating Cholesterol by the Adrenals at Rest and under Adrenocorticotropin Stimulation." Journal of Clinical Investigation **46**(5): 797-811.
- Bouchie, A. (2013). "First microRNA mimic enters clinic." Nat Biotech **31**(7): 577-577.
- Bouizar, Z., B. Ragazzon, L. Viou, M. Hortane, J. Bertherat and M. Rizk-Rabin (2010). "8Cl-cAMP modifies the balance between PKAR1 and PKAR2 and modulates the cell cycle, growth and apoptosis in human adrenocortical H295R cells." Journal of Molecular Endocrinology **44**(6): 331-347.
- Boutillier, A. L., D. Monnier, D. Lorang, J. R. Lundblad, J. L. Roberts and J. P. Loeffler (1995). "Corticotropin-releasing hormone stimulates proopiomelanocortin transcription by cFos-dependent and -independent pathways: characterization of an AP1 site in exon 1." Mol Endocrinol **9**(6): 745-755.
- Brunham, L. R., J. K. Kruit, T. D. Pape, J. M. Timmins, A. Q. Reuwer, Z. Vasanji, B. J. Marsh, B. Rodrigues, J. D. Johnson, J. S. Parks, C. B. Verchere and M. R. Hayden (2007). "[beta]-cell ABCA1 influences insulin secretion, glucose homeostasis and response to thiazolidinedione treatment." Nat Med **13**(3): 340-347.
- Bueno, M. J., M. Gómez de Cedrón, U. Laresgoiti, J. Fernández-Piqueras, A. M. Zubiaga and M. Malumbres (2010). "Multiple E2F-Induced MicroRNAs Prevent Replicative Stress in Response to Mitogenic Signaling." Molecular and Cellular Biology **30**(12): 2983-2995.
- Bustin, S. A. (2002). "Quantification of mRNA using real-time reverse transcription PCR (RT-PCR): trends and problems." J Mol Endocrinol **29**(1): 23-39.
- Cai, X., C. Hagedorn and B. Cullen (2004). "Human microRNAs are processed from capped, polyadenylated transcripts that can also function as mRNAs." RNA **10**: 1957 - 1966.
- Calhoun, D. A. and K. Sharma (2010). "The Role of Aldosteronism in Causing Obesity-Related Cardiovascular Risk." Cardiology clinics **28**(3): 517-527.
- Cao, G., L. Zhao, H. Stangl, T. Hasegawa, J. A. Richardson, K. L. Parker and H. H. Hobbs (1999). "Developmental and Hormonal Regulation of Murine Scavenger Receptor, Class B, Type 1." Molecular Endocrinology **13**(9): 1460-1473.
- Caron, K. M., Y. Ikeda, S.-C. Soo, D. M. Stocco, K. L. Parker and B. J. Clark (1997). "Characterization of the Promoter Region of the Mouse Gene Encoding the Steroidogenic Acute Regulatory Protein." Molecular Endocrinology **11**(2): 138-147.
- Carr, B. R. and E. R. Simpson (1981). "Lipoprotein Utilization and Cholesterol Synthesis by the Human Fetal Adrenal Gland." Endocrine Reviews **2**(3): 306-326.
- Carthew, R. and E. Sontheimer (2009). "Origins and mechanisms of miRNAs and siRNAs." Cell **136**: 642 - 655.
- Caulfield, M., P. Munroe, J. Pembroke, N. Samani, A. Dominiczak, M. Brown, J. Webster, P. Ratcliffe, S. O'Shea, J. Papp, E. Taylor, R. Dobson, J. Knight, S. Newhouse, J. Hooper, W. Lee, N. Brain, D. Clayton, G. M. Lathrop, M. Farrall, J. Connell and N. Benjamin (2003). "Genome-wide mapping of human loci for essential hypertension." The Lancet **361**(9375): 2118-2123.
- Cederbaum, A. I. (2015). "Molecular mechanisms of the microsomal mixed function oxidases and biological and pathological implications." Redox Biology **4**: 60-73.

- Chabre, O., R. Libé, G. Assie, O. Barreau, J. Bertherat, X. Bertagna, J.-J. Feige and N. Cherradi (2013). "Serum miR-483-5p and miR-195 are predictive of recurrence risk in adrenocortical cancer patients." Endocrine-Related Cancer **20**(4): 579-594.
- Chendrimada, T. P., R. I. Gregory, E. Kumaraswamy, J. Norman, N. Cooch, K. Nishikura and R. Shiekhattar (2005). "TRBP recruits the Dicer complex to Ago2 for microRNA processing and gene silencing." Nature **436**(7051): 740-744.
- Chobanian AV, B. G., Black HR (2003). The seventh report of the Joint National Committee on Prevention, Detection, Evaluation, and Treatment of High Blood Pressure: the JNC 7 report. **289**(19): 2560-2572.
- Choi, M., U. I. Scholl, P. Yue, P. Bjorklund, B. Zhao, C. Nelson-Williams, W. Ji, Y. Cho, A. Patel, C. J. Men, E. Lolis, M. V. Wisgerhof, D. S. Geller, S. Mane, P. Hellman, G. Westin, G. Akerstrom, W. Wang, T. Carling and R. P. Lifton (2011). "K<sup>+</sup> Channel Mutations in Adrenal Aldosterone-Producing Adenomas and Hereditary Hypertension." Science **331**(6018): 768-772.
- Christiansen-Weber, T. A., J. R. Voland, Y. Wu, K. Ngo, B. L. Roland, S. Nguyen, P. A. Peterson and W.-P. Fung-Leung (2000). "Functional Loss of ABCA1 in Mice Causes Severe Placental Malformation, Aberrant Lipid Distribution, and Kidney Glomerulonephritis As Well As High-Density Lipoprotein Cholesterol Deficiency." The American Journal of Pathology **157**(3): 1017-1029.
- Christoph (2013). "Mirna Therapeutics is First to Advance MicroRNA into the Clinic for Cancer." mirnablog <http://mirnablog.com/mirna-therapeutics-is-first-to-advance-microrna-into-the-clinic-for-cancer/>.
- Clyne, C. D., Y. Zhang, L. Slutsker, J. M. Mathis, P. C. White and W. E. Rainey (1997). "Angiotensin II and Potassium Regulate Human CYP11B2 Transcription through Common cis-Elements." Molecular Endocrinology **11**(5): 638-649.
- Connell, J. M. C. and E. Davies (2005). "The new biology of aldosterone." Journal of Endocrinology **186**(1): 1-20.
- Corbetta, S., V. Vaira, V. Guarnieri, A. Scillitani, C. Eller-Vainicher, S. Ferrero, L. Vicentini, I. Chiodini, M. Bisceglia, P. Beck-Peccoz, S. Bosari and A. Spada (2010). "Differential expression of microRNAs in human parathyroid carcinomas compared with normal parathyroid tissue." Endocrine-Related Cancer **17**(1): 135-146.
- Cornelissen, V. A. and N. A. Smart (2013). "Exercise Training for Blood Pressure: A Systematic Review and Meta-analysis." Journal of the American Heart Association **2**(1): 1-68.
- Côté, M., M. D. Payet, E. Rousseau, G. Guillon and N. Gallo-Payet (1999). "Comparative Involvement of Cyclic Nucleotide Phosphodiesterases and Adenylyl Cyclase on Adrenocorticotropin-Induced Increase of Cyclic Adenosine Monophosphate in Rat and Human Glomerulosa Cells." Endocrinology **140**(8): 3594-3601.
- Cullen, B. R. (2004). "Transcription and Processing of Human microRNA Precursors." Molecular Cell **16**(6): 861-865.
- Curnow, K. M., M.-T. Tusie-Luna, L. Pascoe, R. Natarajan, J.-L. Gu, J. L. Nadler and P. C. White (1991). "The Product of the CYP11B2 Gene Is Required for Aldosterone Biosynthesis in the Human Adrenal Cortex." Molecular Endocrinology **5**(10): 1513-1522.

- Dalby, B., S. Cates, A. Harris, E. C. Ohki, M. L. Tilkins, P. J. Price and V. C. Ciccarone (2004). "Advanced transfection with Lipofectamine 2000 reagent: primary neurons, siRNA, and high-throughput applications." Methods **33**(2): 95-103.
- Davies, E., C. D. Holloway, M. C. Ingram, G. C. Inglis, E. C. Friel, C. Morrison, N. H. Anderson, R. Fraser and J. M. C. Connell (1999). "Aldosterone Excretion Rate and Blood Pressure in Essential Hypertension Are Related to Polymorphic Differences in the Aldosterone Synthase Gene CYP11B2." Hypertension **33**(2): 703-707.
- Delcayre, C. and J.-S. Silvestre (1999). "Aldosterone and the heart: towards a physiological function?" Cardiovascular Research **43**(1): 7-12.
- Denli, A. M., B. B. J. Tops, R. H. A. Plasterk, R. F. Ketting and G. J. Hannon (2004). "Processing of primary microRNAs by the Microprocessor complex." Nature **432**(7014): 231-235.
- Deshpande, A., A. Pastore, A. J. Deshpande, Y. Zimmermann, G. Hutter, M. Weinkauff, C. Buske, W. Hiddemann and M. Dreyling (2009). "3'UTR mediated regulation of the cyclin D1 proto-oncogene." Cell Cycle **8**(21): 3592-3600.
- Di Leva, F., T. Domi, L. Fedrizzi, D. Lim and E. Carafoli (2008). "The plasma membrane Ca<sup>2+</sup> ATPase of animal cells: Structure, function and regulation." Archives of Biochemistry and Biophysics **476**(1): 65-74.
- Dibb, K. M., T. Rose, S. Y. Makary, T. W. Claydon, D. Enkvetchakul, R. Leach, C. G. Nichols and M. R. Boyett (2003). "Molecular Basis of Ion Selectivity, Block, and Rectification of the Inward Rectifier Kir3.1/Kir3.4 K<sup>+</sup> Channel." Journal of Biological Chemistry **278**(49): 49537-49548.
- Diehl, P., A. Fricke, L. Sander, J. Stamm, N. Bassler, N. Htun, T. Helbing, A. El-Osta, J. B. M. Jowett and K. Peter (2012). "Microparticles: major transport vehicles for distinct miRNAs in circulation." Cardiovascular Research **4**: 633-644.
- Dittmar, K. D., M. Banach, M. D. Galigniana and W. B. Pratt (1998). "The Role of DnaJ-like Proteins in Glucocorticoid Receptor·hsp90 Heterocomplex Assembly by the Reconstituted hsp90·p60·hsp70 Foldosome Complex." Journal of Biological Chemistry **273**(13): 7358-7366.
- Diver, L. A., S. M. MacKenzie, R. Fraser, F. McManus, E. M. Freel, S. Alvarez-Madrazo, J. D. McClure, E. C. Friel, N. A. Hanley, A. F. Dominiczak, M. J. Caulfield, P. B. Munroe, J. M. Connell and E. Davies (2016). "Common Polymorphisms at the CYP17A1 Locus Associate With Steroid Phenotype: Support for Blood Pressure Genome-Wide Association Study Signals at This Locus." Hypertension **67**(4): 724-732.
- Dobs, A. S., H. Schrott, M. H. Davidson, H. Bays, E. A. Stein, D. Kush, M. Wu, Y. Mitchel and R. D. Illingworth (2000). "Effects of high-dose simvastatin on adrenal and gonadal steroidogenesis in men with hypercholesterolemia." Metabolism **49**(9): 1234-1238.
- Doebele, C., A. Bonauer, A. Fischer, A. Scholz, Y. Reiss, C. Urbich, W.-K. Hofmann, A. M. Zeiher and S. Dimmeler (2010). "Members of the microRNA-17-92 cluster exhibit a cell-intrinsic antiangiogenic function in endothelial cells." Blood **115**(23): 4944-4950.
- Doghman, M., J. Cazareth and E. Lalli (2008). "The T cell factor/β-Catenin Antagonist PKF115-584 Inhibits Proliferation of Adrenocortical Carcinoma Cells." The Journal of Clinical Endocrinology & Metabolism **93**(8): 3222-3225.

Doyle, M., L. Badertscher, L. Jaskiewicz, S. Güttinger, S. Jurado, T. Hugenschmidt, U. Kutay and W. Filipowicz (2013). "The double-stranded RNA binding domain of human Dicer functions as a nuclear localization signal." RNA **19**(9): 1238-1252.

Droual, R. (2015). Chapter 6- Endocrine System. Courses Taught by Dr. Robert Droual.

Eckel, R. H., J. M. Jakicic, J. D. Ard, J. M. de Jesus, N. H. Miller, V. S. Hubbard, I.-M. Lee, A. H. Lichtenstein, C. M. Loria, B. E. Millen, C. A. Nonas, F. M. Sacks, S. C. Smith, L. P. Svetkey, T. A. Wadden and S. Z. Yanovski (2014). "2013 AHA/ACC Guideline on Lifestyle Management to Reduce Cardiovascular Risk." A Report of the American College of Cardiology/American Heart Association Task Force on Practice Guidelines **129**(25 suppl 2): 76-99.

Edinger, R. S., C. Coronello, A. J. Bodnar, W. A. LaFramboise, P. V. Benos, J. Ho, J. P. Johnson and M. B. Butterworth (2014). "Aldosterone Regulates MicroRNAs in the Cortical Collecting Duct to Alter Sodium Transport." Journal of the American Society of Nephrology: 2445-2457.

Ehret, G. B. and M. J. Caulfield (2013). "Genes for blood pressure: an opportunity to understand hypertension." **34**(13): 951-961.

Ehrhart-Bornstein, M., V. Lamounier-Zepter, A. Schraven, J. Langenbach, H. S. Willenberg, A. Barthel, H. Hauner, S. M. McCann, W. A. Scherbaum and S. R. Bornstein (2003). "Human adipocytes secrete mineralocorticoid-releasing factors." Proc Natl Acad Sci U S A **100**(24): 14211-14216.

Eldh, M., R. Olofsson Bagge, C. Lasser, J. Svanvik, M. Sjostrand, J. Mattsson, P. Lindner, D.-S. Choi, Y. Gho and J. Lotvall (2014). "MicroRNA in exosomes isolated directly from the liver circulation in patients with metastatic uveal melanoma." BMC Cancer **14**(1): 1-10.

Ender, C. and G. Meister (2010). "Argonaute proteins at a glance." Journal of Cell Science **123**(11): 1819-1823.

F. Beuschlein, S. B., A. Osswald, T. Wieland, H.N. Nielsen, U.D. Lichtenauer, D. Penton, V.R. Schack, L. Amar, E. Fischer, A. Walther, P. Tauber, T. Schwarzmayr, S. Diener, E. Graf, B. Allolio, B. Samson-Couterie, A. Benecke, M. Quinkler, F. Fallo, P.F. Plouin, F. Mantero, T. Meitinger, P. Mulatero, X. Jeunemaitre, R. Warth, B. Vilsen, M.C. Zennaro, T.M. Strom, M. Reincke (2013). "Somatic mutations in ATP1A1 and ATP2B3 lead to aldosterone-producing adenomas and secondary hypertension." Nature. Genetics **45**: 440-444.

Fan, X., Y. Liu, J. Jiang, Z. Ma, H. Wu, T. Liu, M. Liu, X. Li and H. Tang (2010). "miR-20a promotes proliferation and invasion by targeting APP in human ovarian cancer cells." Acta Biochimica et Biophysica Sinica **42**(5): 318-324.

Faselis, C., M. Dumas, J. P. Kokkinos, D. Panagiotakos, R. Kheirbek, H. M. Sheriff, K. Hare, V. Papademetriou, R. Fletcher and P. Kokkinos (2012). "Exercise Capacity and Progression From Prehypertension to Hypertension." Hypertension **60**(2): 333-338.

Filipowicz, W., S. Bhattacharyya and N. Sonenberg (2008). "Mechanisms of post-transcriptional regulation by microRNAs: are the answers in sight?" Nat Rev Genet **9**: 102 - 114.

Francke, U., M. S. Brown and J. L. Goldstein (1984). "Assignment of the human gene for the low density lipoprotein receptor to chromosome 19: synteny of a receptor, a ligand, and a genetic disease." Proceedings of the National Academy of Sciences of the United States of America **81**(9): 2826-2830.

- Freel, E. M. and J. M. C. Connell (2005). "Diagnosis of adenomatous primary aldosteronism in a patient with severe hypertension." Nat Clin Pract End Met 1(2): 111-115.
- Freeman, W. M., S. J. Walker and K. E. Vrana (1999). "Quantitative RT-PCR: pitfalls and potential." Biotechniques 26(1): 112-122, 124-115.
- Friedlander, M., E. Lizano, A. Houben, D. Bezdán, M. Banez-Coronel, G. Kudla, E. Mateu-Huertas, B. Kagerbauer, J. Gonzalez, K. Chen, E. LeProust, E. Marti and X. Estivill (2014). "Evidence for the biogenesis of more than 1,000 novel human microRNAs." Genome Biology 15(4): 1-17.
- Friedman, R., K. Farh, C. Burge and D. Bartel (2009). "Most mammalian mRNAs are conserved targets of microRNAs." Genome Res 19: 92 - 105.
- Fukuda, T., K. Yamagata, S. Fujiyama, T. Matsumoto, I. Koshida, K. Yoshimura, M. Mihara, M. Naitou, H. Endoh, T. Nakamura, C. Akimoto, Y. Yamamoto, T. Katagiri, C. Foulds, S. Takezawa, H. Kitagawa, K.-i. Takeyama, B. W. O'Malley and S. Kato (2007). "DEAD-box RNA helicase subunits of the Drosha complex are required for processing of rRNA and a subset of microRNAs." Nat Cell Biol 9(5): 604-611.
- Funder, J. (2005). "Mineralocorticoid Receptors: Distribution and Activation." Heart Failure Reviews 10(1): 15-22.
- Funder, J., P. Pearce, R. Smith and A. Smith (1988). "Mineralocorticoid action: target tissue specificity is enzyme, not receptor, mediated." Science 242(4878): 583-585.
- Funder, J. W. (2004). "Aldosterone, mineralocorticoid receptors and vascular inflammation." Molecular and Cellular Endocrinology 217(1-2): 263-269.
- Ganguly, A., S. Chiou and J. S. Davis (1990). "Intracellular mediators of potassium-induced aldosterone secretion." Life Sciences 46(3): 173-180.
- Garovic, V. D., A. A. Hilliard and S. T. Turner (2006). "Monogenic forms of low-renin hypertension." Nat Clin Pract Neph 2(11): 624-630.
- Gazdar, A. F., H. K. Oie, C. H. Shackleton, T. R. Chen, T. J. Triche, C. E. Myers, G. P. Chrousos, M. F. Brennan, C. A. Stein and R. V. La Rocca (1990). "Establishment and Characterization of a Human Adrenocortical Carcinoma Cell Line That Expresses Multiple Pathways of Steroid Biosynthesis." Cancer Research 50(17): 5488-5496.
- Gebert, L. F. R., M. A. E. Rebhan, S. E. M. Crivelli, R. Denzler, M. Stoffel and J. Hall (2014). "Miravirsen (SPC3649) can inhibit the biogenesis of miR-122." Nucleic Acids Research 42(1): 609-621.
- Gent, J. and I. Braakman (2004). "Low-density lipoprotein receptor structure and folding." Cellular and Molecular Life Sciences CMLS 61(19-20): 2461-2470.
- Gerin, I., V. W. Dolinsky, J. G. Shackman, R. T. Kennedy, S.-H. Chiang, C. F. Burant, K. R. Steffensen, J.-Å. Gustafsson and O. A. MacDougald (2005). "LXRβ Is Required for Adipocyte Growth, Glucose Homeostasis, and B Cell Function." Journal of Biological Chemistry 280(24): 23024-23031.
- Gimm, O., C. DeMicco, A. Perren, F. Giammarile, M. Walz and L. Brunaud (2012). "Malignant pheochromocytomas and paragangliomas: a diagnostic challenge." Langenbeck's Archives of Surgery 397(2): 155-177.

- Giuseppe Russo, C. Z., Antonio Giordano (2003). "Advantages and limitations of microarray technology in human cancer." Oncogene(22): 6497-6507.
- Go, G.-w. and A. Mani (2012). "Low-Density Lipoprotein Receptor (LDLR) Family Orchestrates Cholesterol Homeostasis." The Yale Journal of Biology and Medicine **85**(1): 19-28.
- Goldsmith, O., D. H. Solomon and R. Horton (1967). "Hypogonadism and Mineralocorticoid Excess." New England Journal of Medicine **277**(13): 673-677.
- Goldstein, J. L. and M. S. Brown (1990). "Regulation of the mevalonate pathway." Nature **343**(6257): 425-430.
- Gomez-Sanchez, C. E. and K. Oki (2013). "Minireview: Potassium Channels and Aldosterone Dysregulation: Is Primary Aldosteronism a Potassium Channelopathy?" Endocrinology **155**(1): 47-55.
- Goodfriend, T. L., D. L. Ball, H. Raff, E. D. Bruder, H. W. Gardner and G. Spiteller (2002). "OXIDIZED PRODUCTS OF LINOLEIC ACID STIMULATE ADRENAL STEROIDOGENESIS." Endocrine Research **28**(4): 325-330.
- Gould, A. L., J. E. Rossouw, N. C. Santanello, J. F. Heyse and C. D. Furberg (1998). "Cholesterol reduction yields clinical benefit: impact of statin trials." Circulation **97**(10): 946-952.
- Grand-Perret, T., A. Bouillot, A. Perrot, S. Commans, M. Walker and M. Issandou (2001). "SCAP ligands are potent new lipid-lowering drugs." Nat Med **7**(12): 1332-1338.
- Gregory, R. I., K.-p. Yan, G. Amuthan, T. Chendrimada, B. Doratotaj, N. Cooch and R. Shiekhattar (2004). "The Microprocessor complex mediates the genesis of microRNAs." Nature **432**(7014): 235-240.
- Griekspoor, A., W. Zwart, J. Neefjes and R. Michalides (2007). "Visualizing the action of steroid hormone receptors in living cells." Nuclear Receptor Signaling **5**: 1-9.
- Grün, D., Y.-L. Wang, D. Langenberger, K. C. Gunsalus and N. Rajewsky (2005). "microRNA Target Predictions across Seven Drosophila Species and Comparison to Mammalian Targets." PLoS Computational Biology **1**(1): 1-16.
- Grundy, S. M. (1998). "Statin Trials and Goals of Cholesterol-Lowering Therapy." Circulation **97**(15): 1436-1439.
- Gu, S. and M. Kay (2010). "How do miRNAs mediate translational repression?" Silence **1**(1): 1-5.
- Guagliardo, N. A., J. Yao, C. Hu and P. Q. Barrett (2012). "Minireview: Aldosterone Biosynthesis: Electrically Gated for Our Protection." Endocrinology **153**(8): 3579-3586.
- Guo, D. F., Y. L. Sun, P. Hamet and T. Inagami (2001). "The angiotensin II type 1 receptor and receptor-associated proteins." Cell Res **11**(3): 165-180.
- Gwizdek, C., B. Ossareh-Nazari, A. M. Brownawell, S. Evers, I. G. Macara and C. Dargemont (2004). "Minihelix-containing RNAs Mediate Exportin-5-dependent Nuclear Export of the Double-stranded RNA-binding Protein ILF3." Journal of Biological Chemistry **279**(2): 884-891.
- Gwynne, J. T. and J. F. Strauss (1982). "The Role of Lipoproteins in Steroidogenesis and Cholesterol Metabolism in Steroidogenic Glands." Endocrine Reviews **3**(3): 299-329.

- Hackl, M., S. Brunner, K. Fortschegger, C. Schreiner, L. Micutkova, C. Muck, G. T. Laschober, G. Lepperdinger, N. Sampson, P. Berger, D. Herndler-Brandstetter, M. Wieser, H. Kuhnel, A. Strasser, M. Rinnerthaler, M. Breitenbach, M. Mildner, L. Eckhart, E. Tschachler, A. Trost, J. W. Bauer, C. Papak, Z. Trajanoski, M. Scheideler, R. Grillari-Voglauer, B. Grubeck-Loebenstein, P. Jansen-Durr and J. Grillari (2010). "miR-17, miR-19b, miR-20a, and miR-106a are down-regulated in human aging." *Aging Cell* **9**(2): 291-296.
- Han, J., Y. Lee, K.-H. Yeom, Y.-K. Kim, H. Jin and V. N. Kim (2004). "The Drosha-DGCR8 complex in primary microRNA processing." *Genes & Development* **18**(24): 3016-3027.
- Han, J., Y. Lee, K.-H. Yeom, J.-W. Nam, I. Heo, J.-K. Rhee, S. Y. Sohn, Y. Cho, B.-T. Zhang and V. N. Kim (2006). "Molecular Basis for the Recognition of Primary microRNAs by the Drosha-DGCR8 Complex." *Cell* **125**(5): 887-901.
- Harding, C., J. Heuser and P. Stahl (1984). "Endocytosis and intracellular processing of transferrin and colloidal gold-transferrin in rat reticulocytes: demonstration of a pathway for receptor shedding." *European journal of cell biology* **35**(2): 256-263.
- Hattangady, N., L. Olala, W. B. Bollag and W. E. Rainey (2012). "Acute and Chronic Regulation of Aldosterone Production." *Molecular and Cellular Endocrinology* **350**(2): 151-162.
- Hayashita, Y., H. Osada, Y. Tatematsu, H. Yamada, K. Yanagisawa, S. Tomida, Y. Yatabe, K. Kawahara, Y. Sekido and T. Takahashi (2005). "A Polycistronic MicroRNA Cluster, miR-17-92, Is Overexpressed in Human Lung Cancers and Enhances Cell Proliferation." *Cancer Research* **65**(21): 9628-9632.
- He, A., L. Zhu, N. Gupta, Y. Chang and F. Fang (2007). "Overexpression of Micro Ribonucleic Acid 29, Highly Up-Regulated in Diabetic Rats, Leads to Insulin Resistance in 3T3-L1 Adipocytes." *Molecular Endocrinology* **21**(11): 2785-2794.
- He, J., Y. Cao, T. Su, Y. Jiang, L. Jiang, W. Zhou, C. Zhang, W. Wang and G. Ning (2015). "Downregulation of miR-375 in aldosterone-producing adenomas promotes tumour cell growth via MTDH." *Clinical Endocrinology* **83**(4): 581-589.
- He, J., Y. Cao, T. Su, Y. Jiang, L. Jiang, W. Zhou, C. Zhang, W. Wang and G. Ning (2015). "Downregulation of miR-375 in aldosterone-producing adenomas promotes tumour cell growth via MTDH." *Clinical Endocrinology*: 581-589.
- He, L., J. M. Thomson, M. T. Hemann, E. Hernando-Monge, D. Mu, S. Goodson, S. Powers, C. Cordon-Cardo, S. W. Lowe, G. J. Hannon and S. M. Hammond (2005). "A microRNA polycistron as a potential human oncogene." *Nature* **435**(7043): 828-833.
- Heginbotham, L., Z. Lu, T. Abramson and R. MacKinnon (1994). "Mutations in the K<sup>+</sup> channel signature sequence." *Biophysical Journal* **66**(4): 1061-1067.
- Heinrichs, S. C. and G. F. Koob (2004). "Corticotropin-Releasing Factor in Brain: A Role in Activation, Arousal, and Affect Regulation." *Journal of Pharmacology and Experimental Therapeutics* **311**(2): 427-440.
- Helen H. Hobbs, M. S. B., Joseph L. Goldstein (1992). "Molecular Genetics of the LDL Receptor Genet in Familial Hypercholesterolemia " *Human Mutation* **1**: 445-466.
- Henke, J. I., D. Goergen, J. Zheng, Y. Song, C. G. Schüttler, C. Fehr, C. Jünemann and M. Niepmann (2008). "microRNA-122 stimulates translation of hepatitis C virus RNA." *Journal of Virology* **82**(24): 3300-3310.

- Herrera, B. M., H. E. Lockstone, J. M. Taylor, Q. F. Wills, P. J. Kaisaki, A. Barrett, C. Camps, C. Fernandez, J. Ragoussis, D. Gauguier, M. I. McCarthy and C. M. Lindgren (2009). "MicroRNA-125a is over-expressed in insulin target tissues in a spontaneous rat model of Type 2 Diabetes." BMC Medical Genomics **2**(1): 1-11.
- Heyn, H., M. Engelmann, S. Schreek, P. Ahrens, U. Lehmann, H. Kreipe, B. Schlegelberger and C. Beger (2011). "MicroRNA miR-335 is crucial for the BRCA1 regulatory cascade in breast cancer development." International Journal of Cancer **129**(12): 2797-2806.
- Hille, U. E., Q. Hu, M. A. E. Pinto-Bazurco Mendieta, M. Bartels, C. A. Vock, T. Lauterbach and R. W. Hartmann (2009). "Steroidogenic cytochrome P450 (CYP) enzymes as drug targets: Combining substructures of known CYP inhibitors leads to compounds with different inhibitory profile." Comptes Rendus Chimie **12**(10-11): 1117-1126.
- Himathongkam, T., R. G. Dluhy and G. H. Williams (1975). "Potassium-Aldosterone-Renin Interrelationships." The Journal of Clinical Endocrinology & Metabolism **41**(1): 153-159.
- Holgate, S. T. and R. Polosa (2008). "Treatment strategies for allergy and asthma." Nat Rev Immunol **8**(3): 218-230.
- Hong, L., J. Yang, Y. Han, Q. Lu, J. Cao and L. Syed (2012). "High expression of miR-210 predicts poor survival in patients with breast cancer: A meta-analysis." Gene **507**(2): 135-138.
- Hoos, A., M. J. Urist, A. Stojadinovic, S. Mastorides, M. E. Dudas, D. H. Leung, D. Kuo, M. F. Brennan, J. J. Lewis and C. Cordon-Cardo (2001). "Validation of tissue microarrays for immunohistochemical profiling of cancer specimens using the example of human fibroblastic tumors." Am J Pathol **158**(4): 1245-1251.
- Hornsby, P. J., M. J. O'Hare and A. Munro Neville (1974). "Functional and Morphological Observations on Rat Adrenal Zona Glomerulosa Cells in Monolayer Culture." Endocrinology **95**(5): 1240-1251.
- Huang, J. and D. Chen (2014). "miRNAs in Circulation: Mirroring Bone Conditions?" Journal of Bone and Mineral Research **29**(8): 1715-1717.
- Huang, L., J. Luo, Q. Cai, Q. Pan, H. Zeng, Z. Guo, W. Dong, J. Huang and T. Lin (2011). "MicroRNA-125b suppresses the development of bladder cancer by targeting E2F3." International Journal of Cancer **128**(8): 1758-1769.
- Huby, A. C., G. Antonova, J. Groenendyk, C. E. Gomez-Sanchez, W. B. Bollag, J. A. Filosa and E. J. Belin de Chantemele (2015). "Adipocyte-Derived Hormone Leptin Is a Direct Regulator of Aldosterone Secretion, Which Promotes Endothelial Dysfunction and Cardiac Fibrosis." Circulation **132**(22): 2134-2145.
- Hutvagner, G. and M. J. Simard (2008). "Argonaute proteins: key players in RNA silencing." Nat Rev Mol Cell Biol **9**(1): 22-32.
- Ide, H., S. Fujiya, Y. Aanuma and Y. Agishi (1990). "Effects of simvastatin, an HMG-CoA reductase inhibitor, on plasma lipids and steroid hormones." Clinical therapeutics **12**(5): 410-420.
- Igaz, P., I. Igaz, Z. Nagy, G. Nyíró, P. Szabó, A. Falus, A. Patócs and K. Rácz (2015). "MicroRNAs in adrenal tumors: relevance for pathogenesis, diagnosis, and therapy." Cellular and Molecular Life Sciences **72**(3): 417-428.

- Ikonen, E. (2008). "Cellular cholesterol trafficking and compartmentalization." Nat Rev Mol Cell Biol **9**(2): 125-138.
- Imamichi, Y., T. Mizutani, Y. Ju, T. Matsumura, S. Kawabe, M. Kanno, T. Yazawa and K. Miyamoto (2014). "Transcriptional regulation of human ferredoxin reductase through an intronic enhancer in steroidogenic cells." Biochimica et Biophysica Acta (BBA) - Gene Regulatory Mechanisms **1839**(1): 33-42.
- IPA (2016). "MicroRNA Target Filter."
- Ishibashi, S., M. S. Brown, J. L. Goldstein, R. D. Gerard, R. E. Hammer and J. Herz (1993). "Hypercholesterolemia in low density lipoprotein receptor knockout mice and its reversal by adenovirus-mediated gene delivery." Journal of Clinical Investigation **92**(2): 883-893.
- Ishihara, K., T. Yamamoto and Y. Kubo (2009). "Heteromeric assembly of inward rectifier channel subunit Kir2.1 with Kir3.1 and with Kir3.4." Biochemical and Biophysical Research Communications **380**(4): 832-837.
- Israelow, B., G. Mullokandov, J. Agudo, M. Sourisseau, A. Bashir, A. Y. Maldonado, A. C. Dar, B. D. Brown and M. J. Evans (2014). "Hepatitis C virus genetics affects miR-122 requirements and response to miR-122 inhibitors." Nat Commun **5**: 1-11.
- Jacob, A. L. and J. Lund (1998). "Mutations in the Activation Function-2 Core Domain of Steroidogenic Factor-1 Dominantly Suppresses PKA-dependent Transactivation of the Bovine CYP17 Gene." Journal of Biological Chemistry **273**(22): 13391-13394.
- James, P. A., S. Oparil, B. L. Carter and et al. (2014). "2014 evidence-based guideline for the management of high blood pressure in adults: Report from the panel members appointed to the eighth joint national committee (jnc 8)." JAMA **311**(5): 507-520.
- Janssen, H. L. A., H. W. Reesink, E. J. Lawitz, S. Zeuzem, M. Rodriguez-Torres, K. Patel, A. J. van der Meer, A. K. Patick, A. Chen, Y. Zhou, R. Persson, B. D. King, S. Kauppinen, A. A. Levin and M. R. Hodges (2013). "Treatment of HCV Infection by Targeting MicroRNA." New England Journal of Medicine **368**(18): 1685-1694.
- Jeansok J. Kim, H. J. L., Jung-Soo Han, Mark G. Packard (2001). "Amygdala Is Critical for Stress-Induced Modulation of Hippocampal Long-Term Potentiation and Learning." The Journal of Neuroscience **21**(14): 5222-5228.
- Jeffrey, S. S. (2008). "Cancer biomarker profiling with microRNAs." Nat Biotech **26**(4): 400-401.
- Jeniël Parmar, R. E. K., William E. Rainey (2008). "Development of an Adrenocorticotropin-Responsive Human Adrenocortical Carcinoma Cell Line." The Journal of Clinical Endocrinology & Metabolism **93**(11): 4542-4546.
- Jensen, M. D., D. H. Ryan, C. M. Apovian, J. D. Ard, A. G. Comuzzie, K. A. Donato, F. B. Hu, V. S. Hubbard, J. M. Jakicic, R. F. Kushner, C. M. Loria, B. E. Millen, C. A. Nonas, F. X. Pi-Sunyer, J. Stevens, V. J. Stevens, T. A. Wadden, B. M. Wolfe and S. Z. Yanovski (2014). "2013 AHA/ACC/TOS Guideline for the Management of Overweight and Obesity in Adults: A Report of the American College of Cardiology/American Heart Association Task Force on Practice Guidelines and The Obesity Society." Journal of the American College of Cardiology **63**(25\_PA): 1-12.
- Jiang, S., C. Li, V. Olive, E. Lykken, F. Feng, J. Sevilla, Y. Wan, L. He and Q.-J. Li (2011). "Molecular dissection of the miR-17-92 cluster's critical dual roles in promoting Th1 responses and preventing inducible Treg differentiation." Blood **118**(20): 5487-5497.

- Jiménez-Marín, Á., M. Collado-Romero, M. Ramirez-Boo, C. Arce and J. J. Garrido (2009). "Biological pathway analysis by ArrayUnlock and Ingenuity Pathway Analysis." BMC Proceedings **3**(4): 1-6.
- Johnson, M. S. C., P.-A. Svensson, K. Helou, H. Billig, G. Levan, L. M. S. Carlsson and B. Carlsson (1998). "Characterization and Chromosomal Localization of Rat Scavenger Receptor Class B Type I, a High Density Lipoprotein Receptor with a Putative Leucine Zipper Domain and Peroxisomal Targeting Sequence." Endocrinology **139**(1): 72-80.
- Jukema, J. W., A. V. G. Brusckhe, A. J. van Boven, J. H. C. Reiber, E. T. Bal, A. H. Zwinderman, H. Jansen, G. J. M. Boerma, F. M. van Rappard, K. I. Lie and o. b. o. t. R. S. G. I. C. I. U. Netherlands (1995). "Effects of Lipid Lowering by Pravastatin on Progression and Regression of Coronary Artery Disease in Symptomatic Men With Normal to Moderately Elevated Serum Cholesterol Levels: The Regression Growth Evaluation Statin Study (REGRESS)." Circulation **91**(10): 2528-2540.
- Kapas, S., A. Purbrick and J. P. Hinson (1995). "Role of tyrosine kinase and protein kinase C in the steroidogenic actions of angiotensin II, alpha-melanocyte-stimulating hormone and corticotropin in the rat adrenal cortex." Biochemical Journal **305**(Pt 2): 433-438.
- Kaplan, J. H. (2002). "BIOCHEMISTRY OF NA,K-ATPASE." Annual Review of Biochemistry **71**(1): 511-535.
- Kappelmann, M., S. Kuphal, G. Meister, L. Vardimon and A. K. Bosserhoff (2013). "MicroRNA miR-125b controls melanoma progression by direct regulation of c-Jun protein expression." Oncogene **32**(24): 2984-2991.
- Kawahara, Y., M. Megraw, E. Kreider, H. Iizasa, L. Valente, A. G. Hatzigeorgiou and K. Nishikura (2008). "Frequency and fate of microRNA editing in human brain." Nucleic Acids Research **36**(16): 5270-5280.
- Kellendonk, C., F. Tronche, H. M. Reichardt, A. Bauer, E. Greiner, W. Schmid and G. Schütz (2002). Analysis of Glucocorticoid Receptor Function in the Mouse by Gene Targeting. Recent Advances in Glucocorticoid Receptor Action. A. C. B. Cato, H. Schäcke and K. Asadullah, Springer Berlin Heidelberg. **40**: 305-318.
- Khuu, C., A. M. Jevnaker, M. Bryne and H. Osmundsen (2014). "An investigation into anti-proliferative effects of microRNAs encoded by the miR-106a-363 cluster on human carcinoma cells and keratinocytes using microarray profiling of miRNA transcriptomes." Front Genet **5**: 1-14.
- Kim, H.-J., M. Miyazaki, W. C. Man and J. M. Ntambi (2002). "Sterol Regulatory Element-Binding Proteins (SREBPs) as Regulators of Lipid Metabolism." Annals of the New York Academy of Sciences **967**(1): 34-42.
- Kim, S. and H. Iwao (2000). "Molecular and Cellular Mechanisms of Angiotensin II-Mediated Cardiovascular and Renal Diseases." Pharmacological Reviews **52**(1): 11-34.
- Kiriakidou, M., G. S. Tan, S. Lamprinaki, M. De Planell-Saguer, P. T. Nelson and Z. Mourelatos (2007). "An mRNA m7G Cap Binding-like Motif within Human Ago2 Represses Translation." Cell **129**(6): 1141-1151.
- Klein, D. (2002). "Quantification using real-time PCR technology: applications and limitations." Trends in Molecular Medicine **8**(6): 257-260.

- Kloosterman, W. P., E. Wienholds, R. F. Ketting and R. H. Plasterk (2004). "Substrate requirements for let-7 function in the developing zebrafish embryo." Nucleic Acids Res. **32**: 6284-6291.
- Kobori, H., M. Nangaku, L. G. Navar and A. Nishiyama (2007). "The Intrarenal Renin-Angiotensin System: From Physiology to the Pathobiology of Hypertension and Kidney Disease." Pharmacological Reviews **59**(3): 251-287.
- Koivukoski, L., S. A. Fisher, T. Kanninen, C. M. Lewis, F. von Wöern, S. Hunt, S. L. R. Kardia, D. Levy, M. Perola, T. Rankinen, D. C. Rao, T. Rice, B. A. Thiel and O. Melander (2004). "Meta-analysis of genome-wide scans for hypertension and blood pressure in Caucasians shows evidence of susceptibility regions on chromosomes 2 and 3." Human Molecular Genetics **13**(19): 2325-2332.
- Kokkinos, P., A. Manolis, A. Pittaras, M. Doulas, A. Giannelou, D. B. Panagiotakos, C. Faselis, P. Narayan, S. Singh and J. Myers (2009). "Exercise Capacity and Mortality in Hypertensive Men With and Without Additional Risk Factors." Hypertension **53**(3): 494-499.
- Kokkinos, P., J. Myers, M. Doulas, C. Faselis, A. Manolis, A. Pittaras, J. P. Kokkinos, S. Singh and R. D. Fletcher (2009). "Exercise Capacity and All-Cause Mortality in Prehypertensive Men." American Journal of Hypertension **22**(7): 735-741.
- Kokkinos, P., J. Myers, J. P. Kokkinos, A. Pittaras, P. Narayan, A. Manolis, P. Karasik, M. Greenberg, V. Papademetriou and S. Singh (2008). "Exercise Capacity and Mortality in Black and White Men." Circulation **117**(5): 614-622.
- Kokkinos, P., J. Myers, E. Nylen, D. B. Panagiotakos, A. Manolis, A. Pittaras, M. R. Blackman, R. Jacob-Issac, C. Faselis, J. Abella and S. Singh (2009). "Exercise Capacity and All-Cause Mortality in African American and Caucasian Men With Type 2 Diabetes." Diabetes Care **32**(4): 623-628.
- Krotkiewski, M., K. Mandroukas, L. Sjöström, L. Sullivan, H. Wetterqvist and P. Björntorp (1979). "Effects of long-term physical training on body fat, metabolism, and blood pressure in obesity." Metabolism **28**(6): 650-658.
- Kypreos, K. E. and V. I. Zannis (2006). "LDL receptor deficiency or apoE mutations prevent remnant clearance and induce hypertriglyceridemia in mice." Journal of Lipid Research **47**(3): 521-529.
- Landais, S., S. Landry, P. Legault and E. Rassart (2007). "Oncogenic Potential of the miR-106-363 Cluster and Its Implication in Human T-Cell Leukemia." Cancer Research **67**(12): 5699-5707.
- Lanford, R. E., E. S. Hildebrandt-Eriksen, A. Petri, R. Persson, M. Lindow, M. E. Munk, S. Kauppinen and H. Ørum (2010). "Therapeutic Silencing of MicroRNA-122 in Primates with Chronic Hepatitis C Virus Infection." Science **327**(5962): 198-201.
- Laudet, V., C. Hänni, J. Coll, F. Catzeflis and D. Stéhelin (1992). "Evolution of the nuclear receptor gene superfamily." The EMBO Journal **11**(3): 1003-1013.
- Lauzier, B., S. Delemasure, B. Collin, L. Duvillard, F. Menetrier, C. Vergely, J. L. Connat and L. Rochette (2011). "Effect of a Chronic Cholesterol-rich Diet on Vascular Structure and Oxidative Stress in LDLR Mice." Cellular Physiology and Biochemistry **27**(1): 31-36.
- Le, T. D., L. Liu, A. Tsykin, G. J. Goodall, B. Liu, B.-Y. Sun and J. Li (2013). "Inferring microRNA-mRNA causal regulatory relationships from expression data." Bioinformatics **29**(6): 765-771.

- Lee, Y., M. Kim, J. Han, K. H. Yeom, S. Lee, S. H. Baek and V. N. Kim (2004). "MicroRNA genes are transcribed by RNA polymerase II." *23*(20): 4051-4060.
- Lei, E. P. and P. A. Silver (2002). "Protein and RNA Export from the Nucleus." *Developmental Cell* **2**(3): 261-272.
- Levy, D., G. B. Ehret, K. Rice, G. C. Verwoert, L. J. Launer, A. Dehghan, N. L. Glazer, A. C. Morrison, A. D. Johnson, T. Aspelund, Y. Aulchenko, T. Lumley, A. Kottgen, R. S. Vasan, F. Rivadeneira, G. Eiriksdottir, X. Guo, D. E. Arking, G. F. Mitchell, F. U. S. Mattace-Raso, A. V. Smith, K. Taylor, R. B. Scharpf, S.-J. Hwang, E. J. G. Sijbrands, J. Bis, T. B. Harris, S. K. Ganesh, C. J. O'Donnell, A. Hofman, J. I. Rotter, J. Coresh, E. J. Benjamin, A. G. Uitterlinden, G. Heiss, C. S. Fox, J. C. M. Witteman, E. Boerwinkle, T. J. Wang, V. Gudnason, M. G. Larson, A. Chakravarti, B. M. Psaty and C. M. van Duijn (2009). "Genome-wide association study of blood pressure and hypertension." *Nat Genet* **41**(6): 677-687.
- Lewis-Tuffin, L. J., C. M. Jewell, R. J. Bienstock, J. B. Collins and J. A. Cidlowski (2007). "Human Glucocorticoid Receptor  $\beta$  Binds RU-486 and Is Transcriptionally Active." *Molecular and Cellular Biology* **27**(6): 2266-2282.
- Li, H., C. Bian, L. Liao, J. Li and R. Zhao (2011). "miR-17-5p promotes human breast cancer cell migration and invasion through suppression of HBP1." *Breast Cancer Research and Treatment* **126**(3): 565-575.
- Li, H., T. Li, S. Wang, J. Wei, J. Fan, J. Li, Q. Han, L. Liao, C. Shao and R. C. Zhao (2013). "miR-17-5p and miR-106a are involved in the balance between osteogenic and adipogenic differentiation of adipose-derived mesenchymal stem cells." *Stem Cell Research* **10**(3): 313-324.
- Li, J., N. Zhang, L.-B. Song, W.-T. Liao, L.-L. Jiang, L.-Y. Gong, J. Wu, J. Yuan, H.-Z. Zhang, M.-S. Zeng and M. Li (2008). "Astrocyte Elevated Gene-1 is a Novel Prognostic Marker for Breast Cancer Progression and Overall Patient Survival." *Clinical Cancer Research* **14**(11): 3319-3326.
- Li, W.-F., G. Wang, Z.-B. Zhao and C.-A. Liu (2014). "High expression of metadherin correlates with malignant pathological features and poor prognostic significance in papillary thyroid carcinoma." *Clinical Endocrinology*: 572-580.
- Lima, R. T., S. Busacca, G. M. Almeida, G. Gaudino, D. A. Fennell and M. H. Vasconcelos (2011). "MicroRNA regulation of core apoptosis pathways in cancer." *European Journal of Cancer* **47**(2): 163-174.
- Linda Jacobsen, P. H. (2007). "Effects of Passage Number on Cell Line Transfection." *Biochemical and Biophysical Research Communications* **3**: 32.
- Lisurek, M. and R. Bernhardt (2004). "Modulation of aldosterone and cortisol synthesis on the molecular level." *Molecular and Cellular Endocrinology* **215**(1-2): 149-159.
- Liu, H., W. Li, C. Chen, Y. Pei and X. Long (2015). "MiR-335 acts as a potential tumor suppressor miRNA via downregulating ROCK1 expression in hepatocellular carcinoma." *Tumor Biology*: 1-7.
- Liu, J. (2004). "Argonaute2 is the catalytic engine of mammalian RNAi." *Science* **305**: 1437-1441.
- Lodygin, D., V. Tarasov, A. Epanchintsev, C. Berking, T. Knyazeva, H. Körner, P. Knyazev, J. Diebold and H. Hermeking (2008). "Inactivation of miR-34a by aberrant CpG methylation in multiple types of cancer." *Cell Cycle* **7**(16): 2591-2600.

- Louis-Dit-Picard, H., J. Barc, D. Trujillano, S. Miserey-Lenkei, N. Bouatia-Naji, O. Pylypenko, G. Beaurain, A. Bonnefond, O. Sand, C. Simian, E. Vidal-Petiot, C. Soukaseum, C. Mandet, F. Broux, O. Chabre, M. Delahousse, V. Esnault, B. Fiquet, P. Houillier, C. I. Bagnis, J. Koenig, M. Konrad, P. Landais, C. Mourani, P. Niaudet, V. Probst, C. Thauvin, R. J. Unwin, S. D. Soroka, G. Ehret, S. Ossowski, M. Caulfield, P. Bruneval, X. Estivill, P. Froguel, J. Hadchouel, J.-J. Schott and X. Jeunemaitre (2012). "KLHL3 mutations cause familial hyperkalemic hypertension by impairing ion transport in the distal nephron." Nat Genet **44**(4): 456-460.
- Lu, M., Q. Zhang, M. Deng, J. Miao, Y. Guo, W. Gao and Q. Cui (2008). "An Analysis of Human MicroRNA and Disease Associations." PLoS ONE **3**(10): 1-5.
- Luciano, D. J., H. Mirsky, N. J. Vendetti and S. Maas (2004). "RNA editing of a miRNA precursor." RNA **10**(8): 1174-1177.
- Luo, X., Y. Ikeda and K. L. Parker (1994). "A cell-specific nuclear receptor is essential for adrenal and gonadal development and sexual differentiation." Cell **77**(4): 481-490.
- Ma, E., I. J. MacRae, J. F. Kirsch and J. A. Doudna (2008). "Autoinhibition of Human Dicer by Its Internal Helicase Domain." Journal of Molecular Biology **380**(1): 237-243.
- Maegdefessel, L., J. Azuma, R. Toh, D. R. Merk, A. Deng, J. T. Chin, U. Raaz, A. M. Schoelmerich, A. Raiesdana, N. J. Leeper, M. V. McConnell, R. L. Dalman, J. M. Spin and P. S. Tsao (2012). "Inhibition of microRNA-29b reduces murine abdominal aortic aneurysm development." The Journal of Clinical Investigation **122**(2): 497-506.
- Maharjan, S., B. Mopidevi, M. K. Kaw, N. Puri and A. Kumar (2014). "Human aldosterone synthase gene polymorphism promotes miRNA binding and regulates gene expression." Physiological Genomics **46**(24): 860-865.
- Manna, P. R. and D. M. Stocco (2007). "Crosstalk of CREB and Fos/Jun on a single cis-element: transcriptional repression of the steroidogenic acute regulatory protein gene." Journal of Molecular Endocrinology **39**(4): 261-277.
- Mathieu, A., A. Fleury, L. Ducharme, P. Lavigne and J. LeHoux (2002). "Insights into steroidogenic acute regulatory protein (StAR)-dependent cholesterol transfer in mitochondria: evidence from molecular modeling and structure-based thermodynamics supporting the existence of partially unfolded states of StAR." Journal of Molecular Endocrinology **29**(3): 327-345.
- May, P., H. H. Bock and J. Herz (2003). "Integration of Endocytosis and Signal Transduction by Lipoprotein Receptors." Science Signaling **2003**(176): 1-6.
- McMaster, A. and D. W. Ray (2008). "Drug Insight: selective agonists and antagonists of the glucocorticoid receptor." Nat Clin Pract End Met **4**(2): 91-101.
- Meijsing, S. H., C. Elbi, H. F. Luecke, G. L. Hager and K. R. Yamamoto (2007). "The Ligand Binding Domain Controls Glucocorticoid Receptor Dynamics Independent of Ligand Release." Molecular and Cellular Biology **27**(7): 2442-2451.
- Melo, Sonia A., H. Sugimoto, Joyce T. O'Connell, N. Kato, A. Villanueva, A. Vidal, L. Qiu, E. Vitkin, Lev T. Perelman, Carlos A. Melo, A. Lucci, C. Ivan, George A. Calin and R. Kalluri (2014). "Cancer Exosomes Perform Cell-Independent MicroRNA Biogenesis and Promote Tumorigenesis." Cancer Cell **26**(5): 707-721.
- Miall, W. E. and P. D. Oldham (1963). "The Hereditary Factor in Arterial Blood-pressure." British Medical Journal **1**(5323): 75-80.

Miller, W. L. (1988). "Molecular Biology of Steroid Hormone Synthesis." Endocrine Reviews **9**(3): 295-318.

Miller, W. L. (2007). "Steroidogenic acute regulatory protein (StAR), a novel mitochondrial cholesterol transporter." Biochimica et Biophysica Acta (BBA) - Molecular and Cell Biology of Lipids **1771**(6): 663-676.

Miller, W. L. and R. J. Auchus (2011). "The Molecular Biology, Biochemistry, and Physiology of Human Steroidogenesis and Its Disorders." Endocrine Reviews **32**(1): 81-151.

Milliez, P., X. Girerd, P.-F. o. Plouin, J. Blacher, M. E. Safar and J.-J. Mourad (2005). "Evidence for an increased rate of cardiovascular events in patients with primary aldosteronism." Journal of the American College of Cardiology **45**(8): 1243-1248.

miRBase. (2014). "miRBase Release 21: June 2014." from <http://www.mirbase.org/index.shtml>.

Mitra, D., P. M. Das, F. C. Huynh and F. E. Jones (2011). "Jumonji/ARID1 B (JARID1B) Protein Promotes Breast Tumor Cell Cycle Progression through Epigenetic Repression of MicroRNA let-7e." Journal of Biological Chemistry **286**(47): 40531-40535.

MM Grumbach, I. H., FA Conte, Ed. (2003). Disorder of sex differentiation. In: Larsen PR, Kronenberg HM, Melmed S, editors. Williams Textbook of Endocrinology, Philadelphia: Saunders.

Mogilyansky, E. R. (2013). "The miR-17/92 cluster: a comprehensive update on its genomics, genetics, functions and increasingly important and numerous roles in health and disease." Cell Death Differ **20**(12): 1603-1614.

Mornet, E., J. Dupont, A. Vitek and P. C. White (1989). "Characterization of two genes encoding human steroid 11 beta-hydroxylase (P-450(11) beta)." Journal of Biological Chemistry **264**(35): 20961-20967.

Morton, N. E. (1996). "Logarithm of odds (lods) for linkage in complex inheritance." Proceedings of the National Academy of Sciences of the United States of America **93**(8): 3471-3476.

Moseley, A. E., J. P. Huddleson, C. S. Bohanan, P. F. James, J. N. Lorenz, B. J. Aronow and J. B. Lingrel (2005). "Genetic Profiling Reveals Global Changes in Multiple Biological Pathways in the Hearts of Na, K-ATPase Alpha 1 Isoform Haploinsufficient Mice." Cellular Physiology and Biochemistry **15**(1-4): 145-158.

MS Brown, J. G. (1986). "A receptor-mediated pathway for cholesterol homeostasis." Science **232**: 34-47.

Mulrane, L., M. Terrile, K. Bryan, R. L. Stallings, R. Clarke, J. P. Crown, W. M. Gallagher and D. P. O'Connor (2013). "Abstract B049: An integrated approach to study miRNA involvement in anti-endocrine resistance in breast cancer." Molecular Cancer Research **11**(10 Supplement): B049.

Muto, S. (1995). "Action of aldosterone on renal collecting tubule cells." Current Opinion in Nephrology and Hypertension **4**(1): 31-40.

Myers, J. (2003). "Exercise and Cardiovascular Health." Circulation **107**(1): 1-5.

NCBI. (2014). "Ideogram of human chromosome 8." GRCh38.p2 (Genome Reference Consortium Human Build 38 patch release 2 (2014)), from

[https://en.wikipedia.org/wiki/Chromosome\\_8\\_\(human\)#/media/File:Human\\_chromosome\\_08\\_-\\_550\\_bphs.png](https://en.wikipedia.org/wiki/Chromosome_8_(human)#/media/File:Human_chromosome_08_-_550_bphs.png).

Newton-Cheh, C., T. Johnson, V. Gateva, M. D. Tobin, M. Bochud, L. Coin, S. S. Najjar, J. H. Zhao, S. C. Heath, S. Eyheramendy, K. Papadakis, B. F. Voight, L. J. Scott, F. Zhang, M. Farrall, T. Tanaka, C. Wallace, J. C. Chambers, K.-T. Khaw, P. Nilsson, P. van der Harst, S. Polidoro, D. E. Grobbee, N. C. Onland-Moret, M. L. Bots, L. V. Wain, K. S. Elliott, A. Teumer, J. a. Luan, G. Lucas, J. Kuusisto, P. R. Burton, D. Hadley, W. L. McArdle, M. Brown, A. Dominiczak, S. J. Newhouse, N. J. Samani, J. Webster, E. Zeggini, J. S. Beckmann, S. Bergmann, N. Lim, K. Song, P. Vollenweider, G. Waeber, D. M. Waterworth, X. Yuan, L. Groop, M. Orho-Melander, A. Allione, A. Di Gregorio, S. Guarrera, S. Panico, F. Ricceri, V. Romanazzi, C. Sacerdote, P. Vineis, I. Barroso, M. S. Sandhu, R. N. Luben, G. J. Crawford, P. Jousilahti, M. Perola, M. Boehnke, L. L. Bonnycastle, F. S. Collins, A. U. Jackson, K. L. Mohlke, H. M. Stringham, T. T. Valle, C. J. Willer, R. N. Bergman, M. A. Morken, A. Doring, C. Gieger, T. Illig, T. Meitinger, E. Org, A. Pfeufer, H. E. Wichmann, S. Kathiresan, J. Marrugat, C. J. O'Donnell, S. M. Schwartz, D. S. Siscovick, I. Subirana, N. B. Freimer, A.-L. Hartikainen, M. I. McCarthy, P. F. O'Reilly, L. Peltonen, A. Pouta, P. E. de Jong, H. Snieder, W. H. van Gilst, R. Clarke, A. Goel, A. Hamsten, J. F. Peden, U. Seedorf, A.-C. Syvanen, G. Tognoni, E. G. Lakatta, S. Sanna, P. Scheet, D. Schlessinger, A. Scuteri, M. Dorr, F. Ernst, S. B. Felix, G. Homuth, R. Lorbeer, T. Reffelmann, R. Rettig, U. Volker, P. Galan, I. G. Gut, S. Hercberg, G. M. Lathrop, D. Zelenika, P. Deloukas, N. Soranzo, F. M. Williams, G. Zhai, V. Salomaa, M. Laakso, R. Elosua, N. G. Forouhi, H. Volzke, C. S. Uiterwaal, Y. T. van der Schouw, M. E. Numans, G. Matullo, G. Navis, G. Berglund, S. A. Bingham, J. S. Kooner, J. M. Connell, S. Bandinelli, L. Ferrucci, H. Watkins, T. D. Spector, J. Tuomilehto, D. Altshuler, D. P. Strachan, M. Laan, P. Meneton, N. J. Wareham, M. Uda, M.-R. Jarvelin, V. Mooser, O. Melander, R. J. F. Loos, P. Elliott, G. R. Abecasis, M. Caulfield and P. B. Munroe (2009). "Genome-wide association study identifies eight loci associated with blood pressure." *Nat Genet* **41**(6): 666-676.

Nishikawa, T., Y. Matsuzawa, S. Suematsu, J. Saito, M. Omura and T. Kino (2010). "Effect of atorvastatin on aldosterone production induced by glucose, LDL or angiotensin II in human renal mesangial cells." *Arzneimittelforschung* **60**(07): 445-451.

Niu, W. Q., S. J. Guo, Y. Zhang, P. J. Gao and D. L. Zhu (2010). "Genetic and functional analyses of aldosterone synthase gene C-344T polymorphism with essential hypertension." *J Hum Hypertens* **24**(6): 427-429.

Nogueira, E. F. and W. E. Rainey (2010). "Regulation of Aldosterone Synthase by Activator Transcription Factor/cAMP Response Element-Binding Protein Family Members." *Endocrinology* **151**(3): 1060-1070.

Nogueira, E. F., Y. Xing, C. A. V. Morris and W. E. Rainey (2009). "Role of angiotensin II-induced rapid response genes in the regulation of enzymes needed for aldosterone synthesis." *Journal of Molecular Endocrinology* **42**(4): 319-330.

Nusse, R. and H. E. Varmus (1982). "Many tumors induced by the mouse mammary tumor virus contain a provirus integrated in the same region of the host genome." *Cell* **31**(1): 99-109.

O'Donnell, K. A., E. A. Wentzel, K. I. Zeller, C. V. Dang and J. T. Mendell (2005). "c-Myc-regulated microRNAs modulate E2F1 expression." *Nature* **435**(7043): 839-843.

O'Driscoll, L., P. Gammell, E. McKiernan, E. Ryan, P. B. Jeppesen, S. Rani and M. Clynes (2006). "Phenotypic and global gene expression profile changes between low passage and high passage MIN-6 cells." *Journal of Endocrinology* **191**(3): 665-676.

- Ogawa, T., M. Iizuka, Y. Sekiya, K. Yoshizato, K. Ikeda and N. Kawada (2010). "Suppression of type I collagen production by microRNA-29b in cultured human stellate cells." Biochemical and Biophysical Research Communications **391**(1): 316-321.
- Olive, V., M. J. Bennett, J. C. Walker, C. Ma, I. Jiang, C. Cordon-Cardo, Q.-J. Li, S. W. Lowe, G. J. Hannon and L. He (2009). "miR-19 is a key oncogenic component of mir-17-92." Genes & Development **23**(24): 2839-2849.
- Oram, J. F. and R. M. Lawn (2001). "ABCA1: the gatekeeper for eliminating excess tissue cholesterol." Journal of Lipid Research **42**(8): 1173-1179.
- Ott, J., J. Wang and S. M. Leal (2015). "Genetic linkage analysis in the age of whole-genome sequencing." Nat Rev Genet **16**(5): 275-284.
- Ou, Q., J.-F. Mouillet, X. Yan, C. Dorn, P. A. Crawford and Y. Sadovsky (2001). "The DEAD Box Protein DP103 Is a Regulator of Steroidogenic Factor-1." Molecular Endocrinology **15**(1): 69-79.
- Özata, D. M., S. Caramuta, D. Velázquez-Fernández, P. Akçakaya, H. Xie, A. Höög, J. Zedenius, M. Bäckdahl, C. Larsson and W.-O. Lui (2011). "The role of microRNA deregulation in the pathogenesis of adrenocortical carcinoma." Endocrine-Related Cancer **18**(6): 643-655.
- Padmanabhan, S., M. Caulfield and A. F. Dominiczak (2015). "Genetic and Molecular Aspects of Hypertension." Circulation Research **116**(6): 937-959.
- Padmanabhan, S., O. Melander, T. Johnson, A. M. Di Blasio, W. K. Lee, D. Gentilini, C. E. Hastie, C. Menni, M. C. Monti, C. Delles, S. Laing, B. Corso, G. Navis, A. J. Kwakernaak, P. van der Harst, M. Bochud, M. Maillard, M. Burnier, T. Hedner, S. Kjeldsen, B. Wahlstrand, M. Sjögren, C. Fava, M. Montagnana, E. Danese, O. Torffvit, B. Hedblad, H. Snieder, J. M. C. Connell, M. Brown, N. J. Samani, M. Farrall, G. Cesana, G. Mancina, S. Signorini, G. Grassi, S. Eyheramendy, H. E. Wichmann, M. Laan, D. P. Strachan, P. Sever, D. C. Shields, A. Stanton, P. Vollenweider, A. Teumer, H. Völzke, R. Rettig, C. Newton-Cheh, P. Arora, F. Zhang, N. Soranzo, T. D. Spector, G. Lucas, S. Kathiresan, D. S. Siscovick, J. a. Luan, R. J. F. Loos, N. J. Wareham, B. W. Penninx, I. M. Nolte, M. McBride, W. H. Miller, S. A. Nicklin, A. H. Baker, D. Graham, R. A. McDonald, J. P. Pell, N. Sattar, P. Welsh, P. Munroe, M. J. Caulfield, A. Zanchetti, A. F. Dominiczak and B. C. Global (2010). "Genome-Wide Association Study of Blood Pressure Extremes Identifies Variant near UMOD Associated with Hypertension." PLoS Genet **6**(10): 1-11.
- Padmanabhan, S., C. Newton-Cheh and A. F. Dominiczak (2012). "Genetic basis of blood pressure and hypertension." Trends in Genetics **28**(8): 397-408.
- Pan, W.-H., J.-W. Chen, C. Fann, Y.-S. Jou and S.-Y. Wu (2000). "Linkage analysis with candidate genes: the Taiwan young-onset hypertension genetic study." Human Genetics **107**(3): 210-215.
- Patel, D., M. Boufraquech, M. Jain, L. Zhang, M. He, K. Gesuwan, N. Gulati, N. Nilubol, T. Fojo and E. Kebebew (2013). "MiR-34a and miR-483-5p are candidate serum biomarkers for adrenocortical tumors." Surgery **154**(6): 1224-1229.
- Patterson, E. E., A. K. Holloway, J. Weng, T. Fojo and E. Kebebew (2011). "MicroRNA profiling of adrenocortical tumors reveals miR-483 as a marker of malignancy." Cancer **117**(8): 1630-1639.
- Payne, A. H. and D. B. Hales (2004). "Overview of Steroidogenic Enzymes in the Pathway from Cholesterol to Active Steroid Hormones." Endocrine Reviews **25**(6): 947-970.

- Pecci, A., E. N. Cozza, M. Devlin, C. E. Gomez-Sanchez and E. P. Gomez-Sanchez (1994). "Endothelin-1 stimulation of aldosterone and zona glomerulosa ouabain-sensitive sodium/potassium-ATPase." The Journal of Steroid Biochemistry and Molecular Biology **50**(1-2): 49-53.
- Pedersen, T. R., K. Berg, T. J. Cook and et al. (1996). "SAfety and tolerability of cholesterol lowering with simvastatin during 5 years in the scandinavian simvastatin survival study." Archives of Internal Medicine **156**(18): 2085-2092.
- Pegtel, D. M., K. Cosmopoulos, D. A. Thorley-Lawson, M. A. J. van Eijndhoven, E. S. Hopmans, J. L. Lindenberg, T. D. de Gruijl, T. Würdinger and J. M. Middeldorp (2010). "Functional delivery of viral miRNAs via exosomes." Proceedings of the National Academy of Sciences **107**(14): 6328-6333.
- Peng, Y., J. Laser, G. Shi, K. Mittal, J. Melamed, P. Lee and J.-J. Wei (2008). "Antiproliferative Effects by Let-7 Repression of High-Mobility Group A2 in Uterine Leiomyoma." Molecular Cancer Research **6**(4): 663-673.
- Perico, N., A. Benigni and G. Remuzzi (2008). "Present and future drug treatments for chronic kidney diseases: evolving targets in renoprotection." Nat Rev Drug Discov **7**(11): 936-953.
- Petersen, C. P., M. E. Bordeleau, J. Pelletier and P. A. Sharp (2006). "Short RNAs repress translation after initiation in mammalian cells." Mol. Cell **21**: 533-542.
- Petrocca, F., R. Visone, M. Onelli, M. Shah, M. Nicoloso, I. de Martino, D. Iliopoulos, E. Pilozi, C. Liu, M. Negrini, L. Cavazzini, S. Volinia, H. Alder, L. Ruco, G. Baldassarre, C. Croce and A. Vecchione (2008). "E2F1-regulated microRNAs impair TGFbeta-dependent cell-cycle arrest and apoptosis in gastric cancer." Cancer Cell **13**: 272 - 286.
- Petrocca, F., R. Visone, M. R. Onelli, M. H. Shah, M. S. Nicoloso, I. de Martino, D. Iliopoulos, E. Pilozi, C.-G. Liu, M. Negrini, L. Cavazzini, S. Volinia, H. Alder, L. P. Ruco, G. Baldassarre, C. M. Croce and A. Vecchione (2008). "E2F1-Regulated MicroRNAs Impair TGFβ-Dependent Cell-Cycle Arrest and Apoptosis in Gastric Cancer." Cancer Cell **13**(3): 272-286.
- Pickering, M. T., B. M. Stadler and T. F. Kowalik (2008). "miR-17 and miR-20a temper an E2F1-induced G1 checkpoint to regulate cell cycle progression." Oncogene **28**(1): 140-145.
- Pillai, R. S., S. N. Bhattacharyya and W. Filipowicz (2007). "Repression of protein synthesis by miRNAs: how many mechanisms?" Trends in Cell Biology **17**(3): 118-126.
- Png, K. J., M. Yoshida, X. H.-F. Zhang, W. Shu, H. Lee, A. Rimner, T. A. Chan, E. Comen, V. P. Andrade, S. W. Kim, T. A. King, C. A. Hudis, L. Norton, J. Hicks, J. Massagué and S. F. Tavazoie (2011). "MicroRNA-335 inhibits tumor reinitiation and is silenced through genetic and epigenetic mechanisms in human breast cancer." Genes & Development **25**(3): 226-231.
- Portrat, S., P. Mulatero, K. M. Curnow, J.-L. Chaussain, Y. Morel and L. Pascoe (2001). "Deletion Hybrid Genes, due to Unequal Crossing Over between CYP11B1 (11β-Hydroxylase) and CYP11B2(Aldosterone Synthase) Cause Steroid 11β-Hydroxylase Deficiency and Congenital Adrenal Hyperplasia." The Journal of Clinical Endocrinology & Metabolism **86**(7): 3197-3201.
- Province, M. A., S. L. R. Kardia, K. Ranade, D. C. Rao, B. A. Thiel, R. S. Cooper, N. Risch, S. T. Turner, D. R. Cox, S. C. Hunt, A. B. Weder and E. Boerwinkle (2003). "A meta-analysis of genome-wide linkage scans for hypertension: The National Heart, Lung

and Blood Institute Family Blood Pressure Program\*." American Journal of Hypertension **16**(2): 144-147.

Qiagen. "LDLR Biosynthesis and Transport." from <https://www.qiagen.com/us/shop/genes-and-pathways/pathway-details/?pwid=268>.

Qin, X., X. Wang, Y. Wang, Z. Tang, Q. Cui, J. Xi, Y.-S. J. Li, S. Chien and N. Wang (2010). "MicroRNA-19a mediates the suppressive effect of laminar flow on cyclin D1 expression in human umbilical vein endothelial cells." Proceedings of the National Academy of Sciences **107**(7): 3240-3244.

Rainey, W. E., I. M. Bird and J. I. Mason (1994). "The NCI-H295 cell line: a pluripotent model for human adrenocortical studies." Molecular and Cellular Endocrinology **100**(1): 45-50.

Rao, D. C., M. A. Province, M. F. Leppert, A. Oberman, G. Heiss, R. C. Ellison, D. K. Arnett, J. H. Eckfeldt, K. Schwander, S. C. Mockrin and S. C. Hunt (2003). "A genome-wide affected sibpair linkage analysis of hypertension: the HyperGEN network\*." American Journal of Hypertension **16**(2): 148-150.

Raposo, G., H. W. Nijman, W. Stoorvogel, R. Liejendekker, C. V. Harding, C. J. Melief and H. J. Geuze (1996). "B lymphocytes secrete antigen-presenting vesicles." The Journal of Experimental Medicine **183**(3): 1161-1172.

Raposo, G. and W. Stoorvogel (2013). "Extracellular vesicles: Exosomes, microvesicles, and friends." The Journal of Cell Biology **200**(4): 373-383.

Raposo, G., D. Tenza, S. Mecheri, R. Peronet, C. Bonnerot and C. Desaynard (1997). "Accumulation of Major Histocompatibility Complex Class II Molecules in Mast Cell Secretory Granules and Their Release upon Degranulation." Molecular Biology of the Cell **8**(12): 2631-2645.

Reinhart, A. J., S. C. Williams and D. M. Stocco (1999). "Transcriptional regulation of the StAR gene." Molecular and Cellular Endocrinology **151**(1-2): 161-169.

Renoir, J. M., C. Mercier-Bodard, K. Hoffmann, S. Le Bihan, Y. M. Ning, E. R. Sanchez, R. E. Handschumacher and E. E. Baulieu (1995). "Cyclosporin A potentiates the dexamethasone-induced mouse mammary tumor virus-chloramphenicol acetyltransferase activity in LMCAT cells: a possible role for different heat shock protein-binding immunophilins in glucocorticosteroid receptor-mediated gene expression." Proceedings of the National Academy of Sciences of the United States of America **92**(11): 4977-4981.

Riegelhaupt, J. J., M. P. Waase, J. Garbarino, D. E. Cruz and J. L. Breslow (2010). "Targeted disruption of steroidogenic acute regulatory protein D4 leads to modest weight reduction and minor alterations in lipid metabolism." Journal of Lipid Research **51**(5): 1134-1143.

Robertson, S., S. M. MacKenzie, S. Alvarez-Madrazo, L. A. Diver, J. Lin, P. M. Stewart, R. Fraser, J. M. Connell and E. Davies (2013). "MicroRNA-24 Is a Novel Regulator of Aldosterone and Cortisol Production in the Human Adrenal Cortex." Hypertension: 1-14.

Rodríguez-Rodríguez, E., I. Mateo, J. Infante, J. Llorca, I. García-Gorostiaga, J. L. Vázquez-Higuera, P. Sánchez-Juan, J. Berciano and O. Combarros (2009). "Interaction between HMGCR and ABCA1 cholesterol-related genes modulates Alzheimer's disease risk." Brain Research **1280**: 166-171.

- Rodriguez, A., S. Griffiths-Jones, J. Ashurst and A. Bradley (2004). "Identification of mammalian microRNA host genes and transcription units." Genome Res **14**: 1902 - 1910.
- Romero, D. G., E. P. Gomez-Sanchez and C. E. Gomez-Sanchez (2010). "Angiotensin II-regulated transcription regulatory genes in adrenal steroidogenesis." Physiological Genomics **42A**(4): 259-266.
- Romero, D. G., M. W. Plonczynski, C. A. Carvajal, E. P. Gomez-Sanchez and C. E. Gomez-Sanchez (2008). "Microribonucleic Acid-21 Increases Aldosterone Secretion and Proliferation in H295R Human Adrenocortical Cells." Endocrinology **149**(5): 2477-2483.
- Ronconi, V., F. Turchi, G. Appolloni, V. di Tizio, M. Boscaro and G. Giacchetti (2012). "Aldosterone, mineralocorticoid receptor and the metabolic syndrome: role of the mineralocorticoid receptor antagonists." Curr Vasc Pharmacol **10**(2): 238-246.
- Rossi, G. P., G. Bernini, G. Desideri, B. Fabris, C. Ferri, G. Giacchetti, C. Letizia, M. Maccario, M. Mannelli, M.-J. Matterello, D. Montemurro, G. Palumbo, D. Rizzoni, E. Rossi, A. C. Pessina, F. Mantero and f. t. P. S. Participants (2006). "Renal Damage in Primary Aldosteronism: Results of the PAPY Study." Hypertension **48**(2): 232-238.
- Ruvkun, G. (2001). "Glimpses of a Tiny RNA World." Science **294**(5543): 797-799.
- Sacks, F. M., L. P. Svetkey, W. M. Vollmer, L. J. Appel, G. A. Bray, D. Harsha, E. Obarzanek, P. R. Conlin, E. R. Miller, D. G. Simons-Morton, N. Karanja, P.-H. Lin, M. Aickin, M. M. Most-Windhauser, T. J. Moore, M. A. Proschan and J. A. Cutler (2001). "Effects on Blood Pressure of Reduced Dietary Sodium and the Dietary Approaches to Stop Hypertension (DASH) Diet." New England Journal of Medicine **344**(1): 3-10.
- Sahay, M. and R. K. Sahay (2012). "Low renin hypertension." Indian Journal of Endocrinology and Metabolism **16**(5): 728-739.
- Sallinen, S.-L., P. K. Sallinen, H. K. Haapasalo, H. J. Helin, P. T. Helén, P. Schraml, O.-P. Kallioniemi and J. Kononen (2000). "Identification of Differentially Expressed Genes in Human Gliomas by DNA Microarray and Tissue Chip Techniques." Cancer Research **60**(23): 6617-6622.
- Salonen, R., K. Nyyssönen, E. Porkkala, J. Rummukainen, R. Belder, J.-S. Park and J. T. Salonen (1995). "Kuopio Atherosclerosis Prevention Study (KAPS): A Population-Based Primary Preventive Trial of the Effect of LDL Lowering on Atherosclerotic Progression in Carotid and Femoral Arteries." Circulation **92**(7): 1758-1764.
- Sampath, D., G. A. Calin, V. K. Pudevalli, G. Gopisetty, C. Taccioli, C.-G. Liu, B. Ewald, C. Liu, M. J. Keating and W. Plunkett (2009). "Specific activation of microRNA106b enables the p73 apoptotic response in chronic lymphocytic leukemia by targeting the ubiquitin ligase Itch for degradation." Blood **113**(16): 3744-3753.
- Sánchez-Castillo, C. P., O. Velásquez-Monroy, A. Lara-Esqueda, A. Berber, J. Sepulveda, R. Tapia-Conyer and W. P. T James (2005). "Diabetes and hypertension increases in a society with abdominal obesity: results of the Mexican National Health Survey 2000." Public Health Nutrition **8**(01): 53-60.
- Saruta, T., T. Okuno, T. Eguchi, R. Nakamura, I. Saito, K. Kondo, M. Oka and S. Matsuki (1979). "RESPONSES OF ALDOSTERONE-PRODUCING ADENOMAS TO ACTH AND ANGIOTENSINS." Acta Endocrinologica **92**(4): 702-709.
- Sato, T., T. Yamamoto and A. Sehara-Fujisawa (2014). "miR-195/497 induce postnatal quiescence of skeletal muscle stem cells." Nat Commun **5**.

- Sawh, A. N. and T. F. Duchaine (2012). "Turning Dicer on its head." Nat Struct Mol Biol **19**(4): 365-366.
- Scadden, A. D. J. (2005). "The RISC subunit Tudor-SN binds to hyper-edited double-stranded RNA and promotes its cleavage." Nat Struct Mol Biol **12**(6): 489-496.
- Schmitz, K. J., J. Helwig, S. Bertram, S. Y. Sheu, A. C. Suttorp, J. Seggewiß, E. Willscher, M. K. Walz, K. Worm and K. W. Schmid (2011). "Differential expression of microRNA-675, microRNA-139-3p and microRNA-335 in benign and malignant adrenocortical tumours." Journal of Clinical Pathology **64**(6): 529-535.
- Schneider, W. J. and J. Nimpf (2003). "LDL receptor relatives at the crossroad of endocytosis and signaling." Cellular and Molecular Life Sciences CMLS **60**(5): 892-903.
- Scholl, U. I. and R. P. Lifton (2013). "New insights into aldosterone-producing adenomas and hereditary aldosteronism: mutations in the K<sup>+</sup> channel KCNJ5." Current Opinion in Nephrology and Hypertension **22**(2): 141-147.
- Schultz, J., P. Lorenz, G. Gross, S. Ibrahim and M. Kunz (2008). "MicroRNA let-7b targets important cell cycle molecules in malignant melanoma cells and interferes with anchorage-independent growth." Cell Res **18**(5): 549-557.
- Schwartz, K., R. M. Lawn and D. P. Wade (2000). "ABC1 Gene Expression and ApoA-I-Mediated Cholesterol Efflux Are Regulated by LXR." Biochemical and Biophysical Research Communications **274**(3): 794-802.
- Schwarzenbach, H., N. Nishida, G. A. Calin and K. Pantel (2014). "Clinical relevance of circulating cell-free microRNAs in cancer." Nat Rev Clin Oncol **11**(3): 145-156.
- Scotti, E., C. Hong, Y. Yoshinaga, Y. Tu, Y. Hu, N. Zelcer, R. Boyadjian, P. J. de Jong, S. G. Young, L. G. Fong and P. Tontonoz (2011). "Targeted Disruption of the Idol Gene Alters Cellular Regulation of the Low-Density Lipoprotein Receptor by Sterols and Liver X Receptor Agonists." Molecular and Cellular Biology **31**(9): 1885-1893.
- Sengupta, S., J. A. den Boon, I.-H. Chen, M. A. Newton, S. A. Stanhope, Y.-J. Cheng, C.-J. Chen, A. Hildesheim, B. Sugden and P. Ahlquist (2008). "MicroRNA 29c is down-regulated in nasopharyngeal carcinomas, up-regulating mRNAs encoding extracellular matrix proteins." Proceedings of the National Academy of Sciences **105**(15): 5874-5878.
- Sethi, A., N. Kulkarni, S. Sonar and G. Lal (2013). "Role of miRNAs in CD4 T cell plasticity during inflammation and tolerance." Front Genet **4**: 1-13.
- Shang, C., Y. Hong, Y. Guo, Y.-h. Liu and Y.-x. Xue (2014). "MiR-210 Up-Regulation Inhibits Proliferation and Induces Apoptosis in Glioma Cells by Targeting SIN3A." Medical Science Monitor : International Medical Journal of Experimental and Clinical Research **20**: 2571-2577.
- Shell, S., S.-M. Park, A. R. Radjabi, R. Schickel, E. O. Kistner, D. A. Jewell, C. Feig, E. Lengyel and M. E. Peter (2007). "Let-7 expression defines two differentiation stages of cancer." Proceedings of the National Academy of Sciences **104**(27): 11400-11405.
- Shenker, Y., M. D. Gross and R. J. Grekin (1985). "Central serotonergic stimulation of aldosterone secretion." The Journal of Clinical Investigation **76**(4): 1485-1490.
- Shigehiro, K. and Y. Tohru (1982). "A binding-protein for aldosterone in human plasma." Journal of Steroid Biochemistry **16**(2): 185-192.

Shimomura, I., Y. Bashmakov, H. Shimano, J. D. Horton, J. L. Goldstein and M. S. Brown (1997). "Cholesterol feeding reduces nuclear forms of sterol regulatory element binding proteins in hamster liver." Proceedings of the National Academy of Sciences of the United States of America **94**(23): 12354-12359.

Shmulewitz, D., S. C. Heath, M. L. Blundell, Z. Han, R. Sharma, J. Salit, S. B. Auerbach, S. Signorini, J. L. Breslow, M. Stoffel and J. M. Friedman (2006). "Linkage analysis of quantitative traits for obesity, diabetes, hypertension, and dyslipidemia on the island of Kosrae, Federated States of Micronesia." Proceedings of the National Academy of Sciences of the United States of America **103**(10): 3502-3509.

Sicard, F., M. Gayral, H. Lulka, L. Buscail and P. Cordelier (2013). "Targeting miR-21 for the Therapy of Pancreatic Cancer." Mol Ther **21**(5): 986-994.

Simonetti, G., M. Mohaupt and M. Bianchetti (2012). "Monogenic forms of hypertension." European Journal of Pediatrics **171**(10): 1433-1439.

Singh, R., V. Yadav, S. kumar and N. Saini (2015). "MicroRNA-195 inhibits proliferation, invasion and metastasis in breast cancer cells by targeting FASN, HMGCR, ACACA and CYP27B1." Scientific Reports **5**: 1-15.

Skerry Benjamin James Oliver (2013). Investigating epigenetic mechanisms of acquired endocrine resistance in an in vitro model of breast cancer. PhD, University of Edinburgh.

Slaby, O., M. Svoboda, J. Michalek and R. Vyzula (2009). "MicroRNAs in colorectal cancer: translation of molecular biology into clinical application." Molecular Cancer **8**(1): 1-13.

Sluijter, J. P. G. and E. van Rooij (2015). "Exosomal MicroRNA Clusters Are Important for the Therapeutic Effect of Cardiac Progenitor Cells." Circulation Research **116**(2): 219-221.

Smoak, K. A. and J. A. Cidlowski (2007). Glucocorticoid Signaling in Health and Disease. NeuroImmune Biology, Elsevier. **Volume 7**: 33-53.

So, A. Y.-L., C. Chaivorapol, E. C. Bolton, H. Li and K. R. Yamamoto (2007). "Determinants of Cell- and Gene-Specific Transcriptional Regulation by the Glucocorticoid Receptor." PLoS Genetics **3**(6): 1-12.

Soccio, R. E., R. M. Adams, K. N. Maxwell and J. L. Breslow (2005). "Differential Gene Regulation of StarD4 and StarD5 Cholesterol Transfer Proteins: ACTIVATION OF StarD4 BY STEROL REGULATORY ELEMENT-BINDING PROTEIN-2 AND StarD5 BY ENDOPLASMIC RETICULUM STRESS." Journal of Biological Chemistry **280**(19): 19410-19418.

Soccio, R. E. and J. L. Breslow (2003). "StAR-related Lipid Transfer (START) Proteins: Mediators of Intracellular Lipid Metabolism." Journal of Biological Chemistry **278**(25): 22183-22186.

Sokalska, A., S. D. Stanley, J. A. Villanueva, I. Ortega and A. J. Duleba (2014). "Comparison of Effects of Different Statins on Growth and Steroidogenesis of Rat Ovarian Theca-Interstitial Cells." Biology of Reproduction **90**(2): 44-44.

Song, H., X. Li, C. Zhu and M. Wei (2000). "Glomerulosclerosis in Adriamycin-induced nephrosis is accelerated by a lipid-rich diet." Pediatric Nephrology **15**(3-4): 196-200.

Soon, P. S. H., L. J. Tacon, A. J. Gill, C. P. Bambach, M. S. Sywak, P. R. Campbell, M. W. Yeh, S. G. Wong, R. J. Clifton-Bligh, B. G. Robinson and S. B. Sidhu (2009). "miR-195

and miR-483-5p Identified as Predictors of Poor Prognosis in Adrenocortical Cancer." Clinical Cancer Research **15**(24): 7684-7692.

Sorrentino, V., L. Scheer, A. Santos, E. Reits, B. Bleijlevens and N. Zelcer (2011). "Distinct Functional Domains Contribute to Degradation of the Low Density Lipoprotein Receptor (LDLR) by the E3 Ubiquitin Ligase Inducible Degradator of the LDLR (IDOL)." Journal of Biological Chemistry **286**(34): 30190-30199.

Spät, A. and L. Hunyady (2004). "Control of Aldosterone Secretion: A Model for Convergence in Cellular Signaling Pathways." Physiological Reviews **84**(2): 489-539.

Stacy Wood, A. E., Craig Livie, Scott MacKenzie, John Connell, Eleanor Davies (2011). Altered miR-125 and miR-134 expression in aldosterone-producing adenoma and post-transcriptional regulation of the CYP11B2 gene. Society for Endocrinology BES 2011. Birmingham, UK, Endocrine Abstracts

Suárez, Y., C. Fernández-Hernando, J. Yu, S. A. Gerber, K. D. Harrison, J. S. Pober, M. L. Iruela-Arispe, M. Merckenschlager and W. C. Sessa (2008). "Dicer-dependent endothelial microRNAs are necessary for postnatal angiogenesis." Proceedings of the National Academy of Sciences **105**(37): 14082-14087.

Sugihara, H., T. Ishimoto, M. Watanabe, H. Sawayama, M. Iwatsuki, Y. Baba, Y. Komohara, M. Takeya and H. Baba (2013). "Identification of miR-30e\* regulation of Bmi1 expression mediated by tumor-associated macrophages in gastrointestinal cancer." PLoS One **8**(11): 1-13.

Sukata, T., K. Sumida, M. Kushida, K. Ogata, K. Miyata, S. Yabushita and S. Uwagawa (2011). "Circulating microRNAs, possible indicators of progress of rat hepatocarcinogenesis from early stages." Toxicology Letters **200**(1-2): 46-52.

Szabo, D. R., M. Luconi, P. M. Szabo, M. Toth, N. Szucs, J. Horanyi, Z. Nagy, M. Mannelli, A. Patocs, K. Racz and P. Igaz (2014). "Analysis of circulating microRNAs in adrenocortical tumors." Lab Invest **94**(3): 331-339.

Tadjine, M., A. Lampron, L. Ouadi and I. Bourdeau (2008). "Frequent mutations of  $\beta$ -catenin gene in sporadic secreting adrenocortical adenomas\*." Clinical Endocrinology **68**(2): 264-270.

Takeda, K. and S. Akira (2005). "Toll-like receptors in innate immunity." International Immunology **17**(1): 1-14.

Tamura, S. and I. Shimomura (2005). "Contribution of adipose tissue and de novo lipogenesis to nonalcoholic fatty liver disease." Journal of Clinical Investigation **115**(5): 1139-1142.

Tang, H. A. O., R.-P. Li, P. Liang, Y.-L. Zhou and G.-W. Wang (2015). "miR-125a inhibits the migration and invasion of liver cancer cells via suppression of the PI3K/AKT/mTOR signaling pathway." Oncology Letters **10**(2): 681-686.

Tanzer, A. and P. F. Stadler (2004). "Molecular Evolution of a MicroRNA Cluster." Journal of Molecular Biology **339**(2): 327-335.

Tili, E., J.-J. Michaille, Z. Luo, S. Volinia, L. Z. Rassenti, T. J. Kipps and C. M. Croce (2012). "The down-regulation of miR-125b in chronic lymphocytic leukemias leads to metabolic adaptation of cells to a transformed state." Blood **120**(13): 2631-2638.

Tissier, F., C. Cavard, L. Groussin, K. Perlemoine, G. Fumey, A.-M. Hagneré, F. René-Corail, E. Jullian, C. Gicquel, X. Bertagna, M.-C. Vacher-Lavenu, C. Perret and J.

- Bertherat (2005). "Mutations of  $\beta$ -Catenin in Adrenocortical Tumors: Activation of the Wnt Signaling Pathway Is a Frequent Event in both Benign and Malignant Adrenocortical Tumors." Cancer Research **65**(17): 7622-7627.
- Tobert, J. A. (2003). "Lovastatin and beyond: the history of the HMG-CoA reductase inhibitors." Nat Rev Drug Discov **2**(7): 517-526.
- Tokumaru, S., M. Suzuki, H. Yamada, M. Nagino and T. Takahashi (2008). "let-7 regulates Dicer expression and constitutes a negative feedback loop." Carcinogenesis **29**(11): 2073-2077.
- Tömböl, Z., P. M. Szabó, V. Molnár, Z. Wiener, G. Tölgyesi, J. Horányi, P. Riesz, P. Reismann, A. Patócs, I. Likó, R.-C. Gaillard, A. Falus, K. Rácz and P. Igaz (2009). "Integrative molecular bioinformatics study of human adrenocortical tumors: microRNA, tissue-specific target prediction, and pathway analysis." Endocrine-Related Cancer **16**(3): 895-906.
- Tome, M., P. Lopez-Romero, C. Albo, J. C. Sepulveda, B. Fernandez-Gutierrez, A. Dopazo, A. Bernad and M. A. Gonzalez (2011). "miR-335 orchestrates cell proliferation, migration and differentiation in human mesenchymal stem cells." Cell Death Differ **18**(6): 985-995.
- Tong, Z., N. Liu, L. Lin, X. Guo, D. Yang and Q. Zhang (2015). "miR-125a-5p inhibits cell proliferation and induces apoptosis in colon cancer via targeting BCL2, BCL2L12 and MCL1." Biomedicine & Pharmacotherapy **75**: 129-136.
- Tsai, Z.-Y., S. Singh, S.-L. Yu, L.-P. Kao, B.-Z. Chen, B.-C. Ho, P.-C. Yang and S. S.-L. Li (2010). "Identification of microRNAs regulated by activin A in human embryonic stem cells." Journal of Cellular Biochemistry **109**(1): 93-102.
- Tsuchida, A., S. Ohno, W. Wu, N. Borjigin, K. Fujita, T. Aoki, S. Ueda, M. Takanashi and M. Kuroda (2011). "miR-92 is a key oncogenic component of the miR-17-92 cluster in colon cancer." Cancer Science **102**(12): 2264-2271.
- Udhane, S. S., A. V. Pandey, G. Hofer, P. E. Mullis and C. E. Flück (2015). "Retinoic acid receptor beta and angiopoietin-like protein 1 are involved in the regulation of human androgen biosynthesis." Scientific Reports **5**: 1-16.
- Ueno, K., H. Hirata, S. Majid, S. Yamamura, V. Shahryari, Z. L. Tabatabai, Y. Hinoda and R. Dahiya (2012). "Tumor Suppressor MicroRNA-493 Decreases Cell Motility and Migration Ability in Human Bladder Cancer Cells by Downregulating RhoC and FZD4." Molecular Cancer Therapeutics **11**(1): 244-253.
- Unger, R. H. (1995). "Lipotoxicity in the Pathogenesis of Obesity-Dependent NIDDM: Genetic and Clinical Implications." Diabetes **44**(8): 863-870.
- Val, P., A.-M. Lefrançois-Martinez, G. Veyssière and A. Martinez (2003). "SF-1 a key player in the development and differentiation of steroidogenic tissues." Nuclear Receptor **1**(1): 1-23.
- Valadi, H. (2007). "Exosome-mediated transfer of mRNAs and microRNAs is a novel mechanism of genetic exchange between cells." Nature Cell Biol. **9**: 654-659.
- Van Doren, M., H. T. Broihier, L. A. Moore and R. Lehmann (1998). "HMG-CoA reductase guides migrating primordial germ cells." Nature **396**(6710): 466-469.
- Vedder, H. (2007). Physiology of the Hypothalamic-Pituitary-Adrenocortical Axis. NeuroImmune Biology, Elsevier. **Volume 7**: 17-31.

- Velázquez-Fernández, D., S. Caramuta, D. M. Özata, M. Lu, A. Höög, M. Bäckdahl, C. Larsson, W.-O. Lui and J. Zedenius (2014). "MicroRNA expression patterns associated with hyperfunctioning and non-hyperfunctioning phenotypes in adrenocortical adenomas." European Journal of Endocrinology **170**(4): 583-591.
- Veronese, A., L. Lupini, J. Consiglio, R. Visone, M. Ferracin, F. Fornari, N. Zanesi, H. Alder, G. D'Elia, L. Gramantieri, L. Bolondi, G. Lanza, P. Querzoli, A. Angioni, C. M. Croce and M. Negrini (2010). "Oncogenic Role of miR-483-3p at the IGF2/483 Locus." Cancer Research **70**(8): 3140-3149.
- Viengchareun, S., D. Le Menuet, L. Martinerie, M. Munier, L. Pascual-Le Tallec and M. Lombès (2007). "The mineralocorticoid receptor: insights into its molecular and pathophysiological biology." Nuclear Receptor Signaling **5**: 1-16.
- Volinia, S., M. Galasso, M. E. Sana, T. F. Wise, J. Palatini, K. Huebner and C. M. Croce (2012). "Breast cancer signatures for invasiveness and prognosis defined by deep sequencing of microRNA." Proceedings of the National Academy of Sciences **109**(8): 3024-3029.
- Wang, G., W. Mao, S. Zheng and J. Ye (2009). "Epidermal growth factor receptor-regulated miR-125a-5p - a metastatic inhibitor of lung cancer." FEBS Journal **276**(19): 5571-5578.
- Wang, H., J. Liu, Y. Zong, Y. Xu, W. Deng, H. Zhu, Y. Liu, C. Ma, L. Huang, L. Zhang and C. Qin (2010). "miR-106b aberrantly expressed in a double transgenic mouse model for Alzheimer's disease targets TGF- $\beta$  type II receptor." Brain Research **1357**: 166-174.
- Wang, T. and W. E. Rainey (2012). "Human Adrenocortical Carcinoma Cell Lines." Molecular and Cellular Endocrinology **351**(1): 58-65.
- Wang, T., J. G. Rowland, J. Parmar, M. Nesterova, T. Seki and W. E. Rainey (2012). "Comparison of Aldosterone Production Among Human Adrenocortical Cell Lines." Horm Metab Res **44**(EFirst): 245-250.
- Wang, X.-L., M. Bassett, Y. Zhang, S. Yin, C. Clyne, P. C. White and W. E. Rainey (2000). "Transcriptional Regulation of Human 11 $\beta$ -Hydroxylase (hCYP11B1)." Endocrinology **141**(10): 3587-3594.
- Wang, Y., X. Li and H. Hu (2011). "Transcriptional regulation of co-expressed microRNA target genes." Genomics **98**(6): 445-452.
- Wang, Y., Y. Liang and Q. Lu (2008). "MicroRNA epigenetic alterations: predicting biomarkers and therapeutic targets in human diseases." Clinical Genetics **74**(4): 307-315.
- Wang, Z., Y.-B. Wei, Y.-L. Gao, B. I. N. Yan, J.-R. Yang and Q. Guo (2014). "Metadherin in prostate, bladder, and kidney cancer: A systematic review." Molecular and Clinical Oncology **2**(6): 1139-1144.
- Warf, M. B., W. E. Johnson and B. L. Bass (2011). "Improved annotation of *C. elegans* microRNAs by deep sequencing reveals structures associated with processing by Drosha and Dicer." RNA **17**(4): 563-577.
- Weber, M. M., P. Michl, C. J. Auernhammer and D. Engelhardt (1997). "Interleukin-3 and Interleukin-6 Stimulate Cortisol Secretion from Adult Human Adrenocortical Cells." Endocrinology **138**(5): 2207-2207.

Weitz, S. H., M. Gong, I. Barr, S. Weiss and F. Guo (2014). "Processing of microRNA primary transcripts requires heme in mammalian cells." Proceedings of the National Academy of Sciences **111**(5): 1861-1866.

White, P. C. and L. Slutsker (1995). "Haplotype analysis of CYP11B2." Endocrine Research **21**(1-2): 437-442.

WHO (2002). World Health Report 2002: Reducing risks, promoting healthy life. . Geneva, Switzerland, World Health Organization 2002.

Williams, G. (2005). "Aldosterone Biosynthesis, Regulation, and Classical Mechanism of Action." Heart Failure Reviews **10**(1): 7-13.

Williams, T. A., S. Monticone, V. R. Schack, J. Stindl, J. Burrello, F. Buffolo, L. Annaratone, I. Castellano, F. Beuschlein, M. Reincke, B. Lucatello, V. Ronconi, F. Fallo, G. Bernini, M. Maccario, G. Giacchetti, F. Veglio, R. Warth, B. Vilsen and P. Mulatero (2014). "Somatic ATP1A1, ATP2B3, and KCNJ5 Mutations in Aldosterone-Producing Adenomas." Hypertension **63**(1): 188-195.

Willnow, T. E., A. Nykjaer and J. Herz (1999). "Lipoprotein receptors: new roles for ancient proteins." Nat Cell Biol **1**(6): E157-E162.

Wood, S., S. M. MacKenzie, S. Alvarez-Madrazo, R. Fraser and E. Davies (2011). Thesis: Regulation of adrenal corticosteroidogenesis: the role of microRNAs in the control of aldosterone synthase and 11 $\beta$ -hydroxylase expression. Doctoral,

Woods, K., J. Thomson and S. Hammond (2007). "Direct regulation of an oncogenic micro-RNA cluster by E2F transcription factors." J Biol Chem **282**: 2130 - 2134.

Woods, K., J. M. Thomson and S. M. Hammond (2007). "Direct Regulation of an Oncogenic Micro-RNA Cluster by E2F Transcription Factors." Journal of Biological Chemistry **282**(4): 2130-2134.

Wostenberg, C., J. W. Lary, D. Sahu, R. Acevedo, K. A. Quarles, J. L. Cole and S. A. Showalter (2012). "The Role of Human Dicer-dsRBD in Processing Small Regulatory RNAs." PLoS ONE **7**(12): 1-12.

Wu, L., J. Fan and J. G. Belasco (2006). "MicroRNAs direct rapid deadenylation of mRNA." Proceedings of the National Academy of Sciences of the United States of America **103**(11): 4034-4039.

Wu, S.-J., F.-T. Chiang, W. J. Chen, P.-H. Liu, K.-L. Hsu, J.-J. Hwang, L.-P. Lai, J.-L. Lin, C.-D. Tseng and Y.-Z. Tseng (2004). "Three single-nucleotide polymorphisms of the angiotensinogen gene and susceptibility to hypertension: single locus genotype vs. haplotype analysis." **17**(2): 79-86.

Xing, Y., M. A. Edwards, C. Ahlem, M. Kennedy, A. Cohen, C. E. Gomez-Sanchez and W. E. Rainey (2011). "The Effects of Adrenocorticotrophic Hormone on Steroid Metabolomic Profiles in Human Adrenal Cells." The Journal of endocrinology **209**(3): 327-335.

Xu, J., T. Wang, Z. Cao, H. Huang, J. Li, W. Liu, S. Liu, L. You, L. Zhou, T. Zhang and Y. Zhao (2014). "MiR-497 downregulation contributes to the malignancy of pancreatic cancer and associates with a poor prognosis." Oncotarget **5**(16): 6983-6993.

Xu, T., Y. Zhu, Y. Xiong, Y.-Y. Ge, J.-P. Yun and S.-M. Zhuang (2009). "MicroRNA-195 suppresses tumorigenicity and regulates G1/S transition of human hepatocellular carcinoma cells." Hepatology **50**(1): 113-121.

- Yanase, T., E. R. Simpson and M. R. Waterman (1991). "17 $\alpha$ -Hydroxylase/17,20-Lyase Deficiency: From Clinical Investigation to Molecular Definition." Endocrine Reviews **12**(1): 91-108.
- Ye, P., B. Mariniello, F. Mantero, H. Shibata and W. E. Rainey (2007). "G-protein-coupled receptors in aldosterone-producing adenomas: a potential cause of hyperaldosteronism." Journal of Endocrinology **195**(1): 39-48.
- Yeom, K.-H., Y. Lee, J. Han, M. R. Suh and V. N. Kim (2006). "Characterization of DGCR8/Pasha, the essential cofactor for Drosha in primary miRNA processing." Nucleic Acids Research **34**(16): 4622-4629.
- Yingst, D. R., J. Davis, S. Krenz and R. J. Schiebinger (1999). "Insights into the mechanism by which inhibition of Na,K-ATPase stimulates aldosterone production." Metabolism **48**(9): 1167-1171.
- Yu, Z., C. Wang, M. Wang, Z. Li, M. C. Casimiro, M. Liu, K. Wu, J. Whittle, X. Ju, T. Hyslop, P. McCue and R. G. Pestell (2008). "A cyclin D1/microRNA 17/20 regulatory feedback loop in control of breast cancer cell proliferation." The Journal of Cell Biology **182**(3): 509-517.
- Zampetaki, A., S. Kiechl, I. Drozdov, P. Willeit, U. Mayr, M. Prokopi, A. Mayr, S. Weger, F. Oberhollenzer, E. Bonora, A. Shah, J. Willeit and M. Mayr (2010). "Plasma MicroRNA Profiling Reveals Loss of Endothelial MiR-126 and Other MicroRNAs in Type 2 Diabetes." Circulation Research **107**(6): 810-817.
- Zeng, L., X. He, Y. Wang, Y. Tang, C. Zheng, H. Cai, J. Liu, Y. Wang, Y. Fu and G. Y. Yang (2014). "MicroRNA-210 overexpression induces angiogenesis and neurogenesis in the normal adult mouse brain." Gene Ther **21**(1): 37-43.
- Zennaro, M.-C. (1998). "Syndromes of glucocorticoid and mineralocorticoid resistance." European Journal of Endocrinology **139**: 127-138.
- Zennaro, M.-C. and X. Jeunemaitre (2011). "Mutations in KCNJ5 Gene Cause Hyperaldosteronism." Circulation Research **108**(12): 1417-1418.
- Zhang, H., F. A. Kolb, L. Jaskiewicz, E. Westhof and W. Filipowicz (2004). "Single Processing Center Models for Human Dicer and Bacterial RNase III." Cell **118**(1): 57-68.
- Zhang, L., Y. Ge and E. Fuchs (2014). "miR-125b can enhance skin tumor initiation and promote malignant progression by repressing differentiation and prolonging cell survival." Genes & Development **28**(22): 2532-2546.
- Zhang, P., A. Huang, J. Ferruzzi, R. P. Mecham, B. C. Starcher, G. Tellides, J. D. Humphrey, F. J. Giordano, L. E. Niklason and W. C. Sessa (2012). "Inhibition of MicroRNA-29 Enhances Elastin Levels in Cells Haploinsufficient for Elastin and in Bioengineered Vessels—Brief Report." Arteriosclerosis, Thrombosis, and Vascular Biology **32**(3): 756-759.
- Zhang, X., G. Azhar and J. Y. Wei (2012). "The Expression of microRNA and microRNA Clusters in the Aging Heart." PLoS One **7**(4): 1-13.
- Zhang, X. and Y. Zeng (2010). "The terminal loop region controls microRNA processing by Drosha and Dicer." Nucleic Acids Research **38**(21): 7689-7697.
- Zhao, J.-J., J. Yang, J. Lin, N. Yao, Y. Zhu, J. Zheng, J. Xu, J. Cheng, J.-Y. Lin and X. Ma (2009). "Identification of miRNAs associated with tumorigenesis of retinoblastoma by miRNA microarray analysis." Child's Nervous System **25**(1): 13-20.

Zhong, Y. Q., J. Wei, Y. R. Fu, J. Shao, Y. W. Liang, Y. H. Lin, J. Liu and Z. H. Zhu (2008). "Toxicity of cationic liposome Lipofectamine 2000 in human pancreatic cancer Capan-2 cells." Nan Fang Yi Ke Da Xue Xue Bao **28**(11): 1981-1984.

Zuo, J., M. Wen, M. Lei, X. Peng, X. Yang and Z. Liu (2015). "MiR-210 Links Hypoxia With Cell Proliferation Regulation in Human Laryngocarcinoma Cancer." Journal of Cellular Biochemistry **116**(6): 1039-1049.